DECIPHERING THE KYNURENINE-3-MONOOXYGENASE INTERACTOME

A thesis submitted for the degree of

Doctor of Philosophy

by

Mathuravani Aaditiyaa Thevandavakkam
Department of Genetics
University of Leicester

June 2011

DECIPHERING THE KYNURENINE-3-MONOOXYGENASE INTERACTOME

Mathuravani Aaditiyaa Thevandavakkam

Department of Genetics, University of Leicester

Thesis submitted for the degree of Doctor of Philosophy, June 2011

ABSTRACT

Kynurenine-3-monooxygenase (KMO) is a mitochondrial enzyme in the kynurenine pathway (KP) through which tryptophan is degraded to NAD^+. The central KP is altered in neurodegenerative diseases and other CNS disorders. The causative role of KP metabolites has been particularly well studied in the neurodegenerative disorder Huntington's disease (HD), a fatal adult onset condition inherited in an autosomal dominant manner. In HD, flux in the KP is perturbed such that neurotoxic metabolites (3-hydroxykynurenine and quinolinic acid) of the pathway are increased relative to a neuroprotective metabolite (kynurenic acid). KMO lies at a critical branching point in the KP such that inhibition of KMO activity ameliorates this metabolic perturbation. Consequently, several recent studies have found that KMO inhibition is protective in models of HD. These findings have widespread implications in treating several neurodegenerative diseases such as Alzheimer's disease and Parkinson's disease where the KP is implicated in pathogenesis. The focus of this project was to better understand the cellular role(s) and interactions of KMO. To this end, a novel membrane yeast two hybrid approach was established and optimised to identify protein interaction partners for outer mitochondrial membrane proteins. This approach was implemented to identify protein interaction partners of human KMO and its yeast orthologue Bna4, which were confirmed by biochemical approaches. Additionally, genetic interaction partners of *BNA4* identified by systematic genetic screens were individually validated by classic genetic manipulations. Bioinformatic tools were then used to identify enriched interaction networks for KMO using this novel interaction data. These analyses suggested possible roles for KMO in many processes, including energy metabolism, cytoskeleton organisation and response to infection and inflammation, providing evidence that KMO plays roles in diverse cellular pathways in addition to the KP.

ACKNOWLEDGEMENTS

I would like to thank Dr. Flaviano Giorgini for providing me with the opportunity to work on this PhD project under him. His friendliness, guidance and support have been wonderful over the four years. Last but not the least, thank you for all the thesis proofreading, I would not be at this stage without your feedback and encouragement.

Thanks to our collaborators Dr. Charlie Boone (University of Toronto), Dr. Paul Muchowski (University of California, San Francisco) and Wanda Kwan (University of California, San Francisco) and especially to Dr. Igor Stagljar (University of Toronto) for his valuable suggestions.

I would also like to give a special thank you to Leonor Miller Fleming who initiated the early stages of this project. Many thanks for all the coffee time discussions and troubleshooting when things were not working.

I'd like to extend my gratitude to Dr. Rob Mason for his ideas and suggestions throughout the course of the PhD, Dr. Kees Straatman for all the help with the microscopy work and Joshua Smalley for all the help with the bioinformatics. I have been privileged to work with a fantastic group of people who have been wonderful source of moral support when things have not been going well and also provided some timely relief from the rigours of lab work- thanks to Amit, Shanow, Christian, Daniel, Mariaelena, Angie, Janine, Gurdeep, Mahdieh, Max, Carlo, Ed, Susie, Nicky, Rebecca, Maryam, Rally, Alex, Rhona, Raff, Gary and other past members of the lab.

Last but not the least this journey would not have been possible if not for the support of my parents and family, whose love, guidance and well wishes have enabled me reach this stage without losing perspective of what's important. Thank You.

ABBREVIATIONS

3-AT	3-Aminotriazole
3-HK	3-Hydroxykynurenine
3-NP	3-Nitropropionic acid
µl	Microlitre
AD	Activating domain
ADE2	Adenine 2
AGE	Advanced glycation endproducts
AIDS	Acquired immunodeficiency syndrome
Amp	Ampicillin
AMPA	2-amino-3-(5-methyl-3-oxo-1,2- oxazol-4-yl)propanoic acid
ATP	Adenosine triphosphate
BD	Binding Domain
BiFC	Bimolecular fluorescent complementation
BIND	Bimolecular interaction network database
BIPs	Bna4 interacting proteins
Bna4	Biosynthesis of nicotinic acid 4
BSA	Bovine serum albumin
CFL1	Cofilin1
CNS	Central nervous system
Co-IP	Co-Immunoprecipitation
Cub	C-terminal Ubiquitin
DAPI	4',6-diamidino-2-phenylindole
DCTN2	Dynactin 2
DHAP	Dihydroxyacetone phosphate
DIP	Database of interacting proteins
DNA	Deoxyribonucleic acid
DYNC1H1	Dynein heavy chain 1
E. coli	Escherichia coli
ECL	Electrogenerated chemiluminescence
ER	Endoplasmic reticulum
ERMES	ER-Mitochondria tethering complex
FAD	Flavin adenine dinucleotide
G3P	Glyceraldehyde 3-phosphate
G418	Geneticin
GABA	Gamma amino butyric acid
GAL4	Galactose 4
GAPDH	Glyceraldehyde-3-phosphate dehydrogenasae
GO	Gene ontology
GSN	Gelsolin
GTP	Guanosine triphosphate
HAP1	Huntingtin Associated protein 1
HD	Huntington's Disease
HDAC	Histone deacetylase
HIS3	Histidine 3
HIV	Human immunodeficiency virus

Htt	Huntingtin
HUGO	Human Genome Organisation
IDO	Indoleamine 2,3-dioxygenase
INDOL1	Indoleamine-pyrrole 2,3 dioxygenase-like 1
IFNγ	Interferon gamma
IL-6	Interleukin 6
iNOS	Inducible nitric oxide synthetase
IPA	Ingenuity pathway analysis
Kan	Kanamycin
KAT	Kynurenine Aminotransferase
Kb	Kilo base
KEGG	Kyoto Encyclopaedia of Genes and Genomes
KIPs	KMO interacting proteins
KMO	Kynurenine 3-monooxygenase
KP	Kynurenine pathway
KYN	Kynurenine
KYNA	Kynurenic acid
LB	Luria Bertani medium
LiAc	Lithium Acetate
LTD	Long term depression
LTP	Long term potentiation
MAPK	Mitogen activated protein kinase
M	Moles
mHtt	Mutant huntingtin
MitAAT	Mitochondrial KAT
MINT	Molecular interaction database
ml	millilitre
MPTP	Mitochondrial permeability transition pore
MSN	Medium spiny neurons
MYTH	Membrane yeast two hybrid
NAD+	Nicotinamide adenine dinucleotide
NADP	Nicotinamide adenine dinucleotide phosphate
NADPH	Nicotinamide adenine dinucleotide phosphate (reduced)
Nat	Nourseothricin
nM	Nanomoles
NMDA	N-methyl D-Aspartate
NMDAR	N-methyl D-Aspartate receptor
NubG	N-terminal Ubiquitin (mutated)
NubI	N-terminal Ubiquitin (wildtype)
OMM-MYTH	Outer mitochondrial membrane membrane yeast two hybrid
ONPG	Ortho-Nitrophenyl-β-galactoside
ORF	Open reading frame
PBS	Phosphate buffered Saline
PEG	Polyethylene glycol
PET	Positron emission tomography
psi	pounds per square inch
PVDF	Polyvinylidene Fluoride
QTL	Quantitative trait loci

QUIN	Quinolinic acid
RAGE	Receptor for advanced glycation endproducts
RFP	Red fluorescent protein
RNS	Reactive nitrogen species
ROS	Reactive oxygen species
Rpm	Revolutions per minute
rRRS	Reverse RAS recruitment system
SD	Synthetic dropout
SDS	Sodium dodecyl sulphate
SDS-PAGE	Sodium dodecyl sulfate polyacrylamide gel electrophoresis
SGA	Synthetic Genetic Array
SGD	Saccharomyces cerevisiae genome database
SNP	Single nucleotide polymorphism
SP1	Specific protein 1
SPS	Supplemented pre-sporulation medium
ssDNA	Single stranded Deoxyribonucleic acid
TBE	Tris Borate EDTA
TBST	Tris- buffered saline Tween 20
TCA	Tricarboxylic acid cycle
TDO	Tryptophan 2,3-dioxygenase
TE	Tris-HCl EDTA
TIM	Translocating protein of inner mitochondrial membrane
TNFα	Tumor necrosis factor-alpha
TOM	Translocating protein of outer mitochondrial membrane
Tris-HCl	Tris-Hydrochloride
UBP	Ubiquitin specific proteases
UV	Ultraviolet light
VEGF	Vascular endothelial growth factor
Y2H	Yeast two hybrid
YEPD	Yeast extract, peptone, dextrose medium
YEPEG	Yeast extract, peptone, ethanol, glycerol medium

CONTENTS

CHAPTER 1 KYNURENINE PATHWAY AND HUNTINGTON'S DISEASE

1.1 INTRODUCTION

Kynurenine-3-monooxygenase (KMO) is an enzyme in the kynurenine pathway (KP) through which tryptophan is degraded to produce NAD^+. Alterations in this pathway play a crucial role in development and disease. Upregulation of the central KP has been implicated in neuropathological features observed in neurodegenerative diseases such as Huntington's disease (HD), Alzheimer's disease, Parkinson's disease, as well as other brain disorders. KP associated alterations in HD, a fatal adult onset neurodegenerative disorder, have been studied in detail and therapeutic targeting of the pathway via KMO has been found to alleviate HD phenotypes in model systems. This chapter reviews relevant literature and provides a brief introduction to the kynurenine pathway, KMO, and HD, and then gives an overview of the central aims of the completed studies.

1.2 THE KYNURENINE PATHWAY

The kynurenine pathway is a major metabolic pathway through which > 95% of tryptophan is digested in humans; the rest of tryptophan is metabolised via the seratonergic pathway and during protein synthesis (Stone, 1993). The pathway is also vital since it is responsible for conversion of tryptophan into nicotinamide dinucleotide (NAD^+). NAD^+ is one of the most important co-enzymes involved in oxido-reductive reactions in mitochondria and is required for formation of ATP, apart from which it also functions as a precursor for cell regulatory molecules (Rongvaux et al., 2003).The KP has been implicated in the pathology of several diseases (see Table 1-1) and has been postulated to play an important role in neurodegenerative disease and disorders of the immune system (Schwarcz, 2004).

Table 1-1: Levels of Kynurenine pathway metabolites in various diseases.

Pathology	KP metabolite	References
HIV	↓ TRP;↑KYN;↓TRP/KYN ratio; ↑↑QUIN;↑IFN-γ	(Werner et al., 1988, Fuchs et al., 1991)
Cancer:		
Colorectal cancer	↓TRP;↑KYN/TRP ratio	(Huang et al., 2002)
Lung cancer	↑TRP	(Cascino et al., 1991)
Malaria	↑QUIN	(Medana et al., 2002)
Epilepsy	↑↑KYN;↑KYNA;↓QUIN	(Heyes et al., 1994)
Anxiety and Depression	↑KYN;↑KYN/TRP ratio	(Orlikov et al., 1994)
Schizophrenia	↑KYN;↓KYNA	(Erhardt et al., 2001, Nilsson et al., 2005)
Amyotrophic lateral sclerosis	↓KYNA	(Ilzecka et al., 2003)
Huntington's disease	↑QUIN;↑3-HK;↓KYNA ↓KYNA/QUIN ratio	(Beal et al., 1992, Pearson and Reynolds, 1992, Guidetti et al., 2006)
Alzheimer's disease	↓KYNA	(Hartai et al., 2007)
Chronic brain injury	↑KYN;↓KYNA;↓3-HK ↑KYN/TRP ratio	(Mackay et al., 2006)
Stroke	↓TRP;↑KYN;↑KYN/TRP ratio	(Darlington et al., 2007)
Coronary heart disease	↑KYN/TRP ratio	(Wirleitner et al., 2003)

The table lists alterations in KP metabolites in various disease states. The arrow indicates changes in levels of the respective KP metabolite. TRP=Tryptophan; KYN=Kynurenine; KYNA=Kynurenic acid; QUIN=Quinolinic acid; 3-HK=3-Hydroxykynurenine

1.2.1 Overview of kynurenine pathway biochemistry

The first step in the kynurenine pathway (Figure 1-1) is conversion of L-tryptophan into N-formylkynurenine. The indole ring of tryptophan can potentially be cleaved by three independent enzymes: tryptophan 2, 3-dioxygenase (TDO) (predominantly liver and brain), indoleamine 2, 3-dioxygenase (IDO) (non-hepatic tissues, brain and macrophages) and indoleamine-pyrrole 2, 3 dioxygenase-like 1 (INDOL1) (kidney, epididymis and liver) (Schutz et al., 1972, Schutz and Feigelson, 1972, Yamazaki et al., 1985). The action of TDO is dependent on substrate availability and acts as a rate-limiting step (Bender and McCreanor, 1982) while IDO activity is induced in response to inflammation (Takikawa et al., 1999, Chiarugi et al., 2001a). Activation of IDO is seen in several diseases of the brain characterised by inflammation including AIDS (Heyes et al., 1993, Sardar and Reynolds, 1995). Interferon Gamma (IFNγ), a cytokine that plays a vital role in innate and adaptive immune response, prevents proliferation of mammalian and microbial cells by upregulating IDO activity leading to reduced tryptophan levels in the immediate cellular environment (Takikawa et al., 1999). Reduction of tryptophan levels by IFNγ also alters immune response by suppressing T lymphocyte activity (Takikawa et al., 1999, Chiarugi et al., 2001b). INDOL1, found in mammals, is the third enzyme that catalyses the first step of the KP and shares ~43% similarity with IDO. The *INDOL1* gene is located next to *IDO* gene and is thought to have arisen from gene duplication events of the IDO gene; however it is functionally distinct from IDO and its activity is not increased in infectious diseases (Ball et al., 2007). Although the overlapping activity of the enzymes may suggest some redundancy, the differential expression pattern and regulation of the enzymes indicates functional divergence, and also highlights the key role of the kynurenine pathway in physiology and disease.

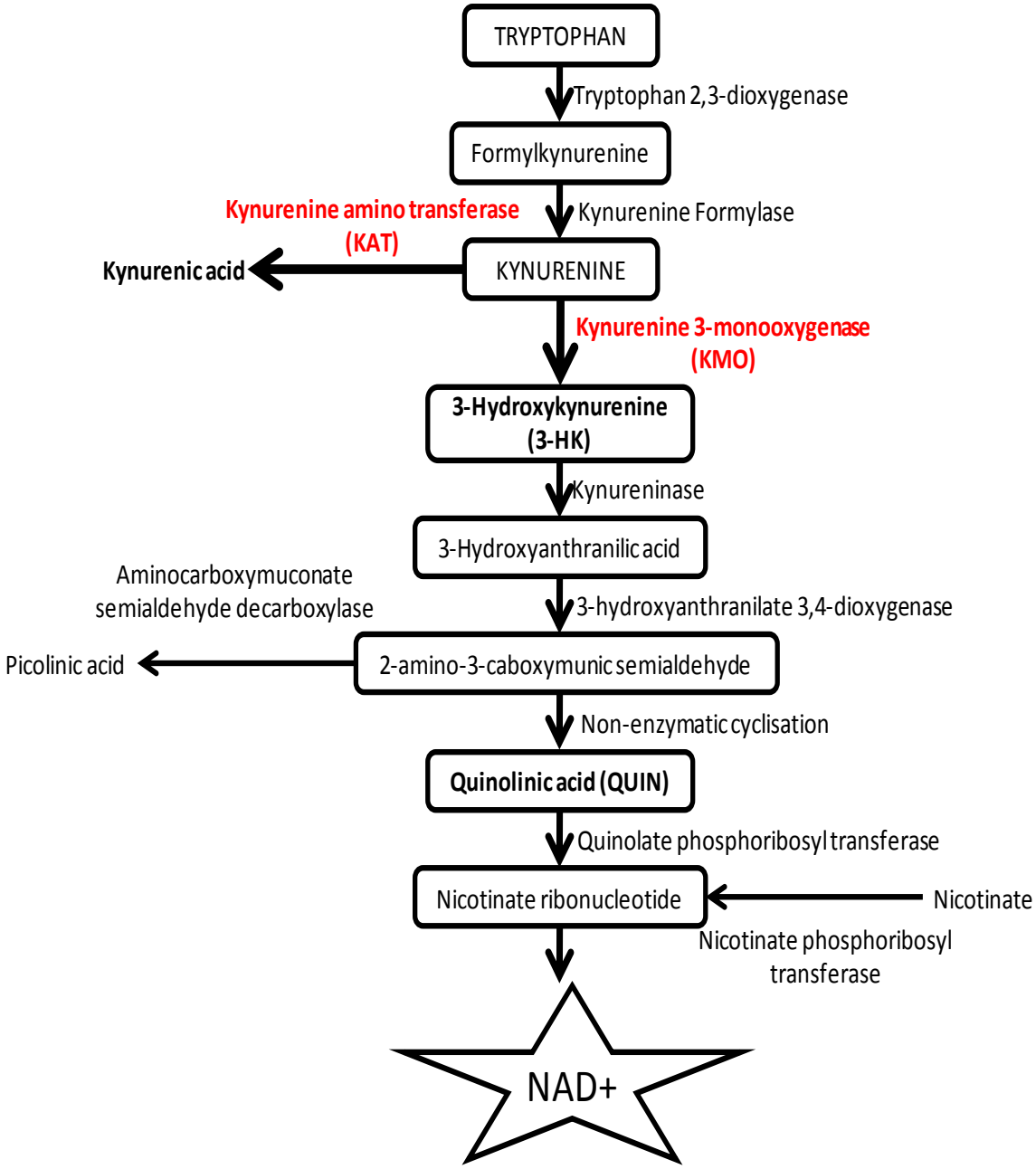

Figure 1-1: Overview of the Kynurenine pathway metabolism of tryptophan

KP is the major route of tryptophan degradation in the cell. KP has three neuroactive components in KYNA, 3-HK and QUIN. The substrate L-kynurenine can be acted upon by two enzymes: Kynurenine aminotransferase (KAT) and kynurenine-3-monooxygenase (KMO). KAT converts kynurenine to KYNA which is neuroprotective while KMO converts kynurenine to 3-HK and further downstream to QUIN which are neurotoxic. Increase in neurotoxic metabolites of the pathway relative to neuroprotective metabolite KYNA is implicated in pathology of neurodegenerative disorders.

Another key metabolite in the KP is L-kynunrenine (KYN), which can also be acted upon by several enzymes. In the presence of KMO, KYN is converted to 3-hydroxykynurenine (3-HK) whilst in the presence of kynurenine amino transferase (KATI, KATII and mitAAT), KYN is converted to kynurenic acid (Uemura and Hirai, 1998, Guidetti et al., 2007). In the CNS, KAT activity is found to be highly expressed in astrocytes, but with very little activity being observed in microglia or neurons (Thevandavakkam et al., 2010). KMO activity, on the other hand, is predominantly localized to microglia in the CNS (Kita et al., 2002, Giorgini et al., 2008). 3-HK is metabolised by kynureninase to 3-hydroxyxanthranilic acid (3-HANA), which is subsequently metabolised by 3-hydroxyxanthranilate 3, 4-dioxygenase to 2-amino-3-carboxymuconic acid. Upon non-enzymatic cyclisation, this metabolite produces quinolinic acid (QUIN). QUIN is acted upon by a specific ribosyl transferase enzyme - quinolate phosphoribosyl transferase - resulting in the formation of NAD^+ via the Preiss-Handler pathway (Sas et al., 2007).

1.2.1.1 KMO- a key modulator of the KP

The catalysis of KYN to 3-HK by KMO requires the presence of flavin-adenine dinucleotide (FAD)(Alberati-Giani et al., 1997, Uemura and Hirai, 1998). KMO is an outer mitochondrial membrane protein and has a molecular weight of 49KDa; it is functional only in its dimeric state and is not active as a monomer (Uemura and Hirai, 1998). The enzyme, an NADPH dependent monooxygenase, exists as an apoenzyme and upon interaction with FAD forms a holoenzyme, the flavin moiety of the enzyme being required during hydroxylation reactions, since it acts as an electron donor (Nisimoto et al., 1977).

In humans, *KMO* is located on chromosome 1q42-q44 and is comprised of 15 exons (Alberati-Giani et al., 1997). There are five predicted isoforms of the protein that differ at the C-terminus (496aa, 452aa, 473aa, 486aa and 407aa) and are thought to be splice variants (Alberati-Giani et al., 1997). The 496aa and 486aa KMO isoforms contain two

transmembrane loops while the other proteins have only a single membrane spanning region (Alberati-Giani et al., 1997). KP is well characterised in yeast and the enzymes of the pathway are conserved between humans and yeast, with the yeast orthologue of KMO encoded by *BNA4* (biosynthesis of nicotinic acid protein 4) (Panozzo et al., 2002).

KMO activity plays a vital role regulating the flux through the 3-HK/QUIN branch of the pathway towards production of NAD+ such that inhibition of KMO increases the flux through the neuroprotective KYNA branch of the pathway, thereby resulting in increased production of KYNA and reduced levels of 3-HK and QUIN (Guidetti et al., 2004). Since 3-HK/QUIN are neurotoxic and KYNA is neuroprotective, KMO inhibitors are considered as a potential therapeutic target in neurodegenerative diseases (see section 1.3.3).

1.2.2 Neuroactive components of the KP

Several metabolites of the KP have shown to be neuroactive; this Section provides a brief overview of these metabolites: QUIN, 3-HK and KYNA.

1.2.2.1 Quinolinic acid (QUIN)

QUIN was the first KP metabolite implicated to play a role in neurodegeneration when striatal injections of QUIN in rodents reproduced some of the characteristic features of HD (Schwarcz and Kohler, 1983, Schwarcz et al., 1983). QUIN induced striatal lesions are also associated with abnormalities in movement (Storey et al., 1994) and spatial abnormalities (Tatter et al., 1995) in rodents, similar to symptoms observed in early stage HD patients. QUIN is an N-methyl D-Aspartate receptor (NMDAR) agonist and causes neuronal damage by both excitotoxic mechanisms (Schwarcz et al., 1983) and by generating free radicals (Chiarugi et al., 2001a).

Excitotoxicity refers to increased stimulation of neuroreceptors by excitatory amino acids (EAA) such as glutamate, resulting in cell stress and death (Fan and Raymond, 2007). EAAs alter the membrane potential of neuronal membrane accompanied by influx of sodium, calcium and water. Glutamate dependent excitotoxicity is mediated by ionotrophic receptors where stimulation by glutamate is due to ion exchange between synapses, thereby altering the membrane potential. Ionotrophic receptors are of three types: α-amino-3-hydroxy-5-methyl-4-isoxazolepropionic acid (AMPA), kainite and NMDA receptors (NMDAR). NMDAR play a major role in excitotoxicity because of the number of NMDAR present and their distribution in the brain and due to their role in calcium permeability, conductance and desensitization (reviewed in (Dingledine et al., 1999)). The CNS is differentially sensitive to QUIN mediated excitotoxicity with the hippocampus, cerebral cortex and striatum being most sensitive due to the presence of NMDAR subtype NR2, the requisite receptor required for NMDAR excitotoxicity (Perkins and Stone, 1983).

Activation of NMDAR also leads to increased production of reactive nitrogen species (RNS)(i.e. nitric oxide and superoxide produced by the enzymatic activity of inducible nitric oxide synthetase) which damages double stranded DNA, ultimately culminating in necrosis (Chiarugi et al., 2001a). Reactive oxygen species (ROS) produced by QUIN can be attenuated by antioxidant therapy in rat models of HD (Santamaria et al., 2003) indicating that QUIN dependent oxidative damage may contribute to neurodegenerative disorders such as HD.

1.2.2.2 3-Hydroxykynurenine (3-HK)

3-HK is a neurotoxic metabolite of KP and can act as an oxidant via production of free radicals (Okuda et al., 1996). Slight increases in 3-HK levels cause neurotoxicity in primary neuronal cell cultures from rat striatum. After about 48 hours of exposure of primary neurons to 1μm (at concentration slightly higher than endogenous levels) of 3-HK,

approximately 50% of the striatal neurones showed degeneration and interestingly, the NADPH diaphorase neurons that are spared in HD also are spared in 3-HK induced neurotoxicity.

3-HK is also able to potentiate QUIN mediated neurotoxicity (Guidetti and Schwarcz, 1999). Striatal co-injections of QUIN and 3-HK at otherwise tolerable doses (i.e. doses that does not cause neurodegeneration) cause neuronal loss resulting in a pattern of neurotoxicity similar to that of NMDA-dependent excitotoxicity. This shows that a slight increase in 3-HK levels in combination with altered QUIN levels may duplicate the cardinal features of HD.

Neuronal cell death due to 3-HK has been shown to be associated with apoptosis (Chiarugi et al., 2001a). In this work, it was found that increased caspase 3 activity due to 3-HK mediated cell death can be reversed by anti-apoptotic factors such as Bcl2. Increased ATP usage and opening of the mitochondrial permeability transition pore complex (MPTP) is also a part of the apoptosis execution pathway mediated by 3-HK (Chiarugi et al., 2001a).

1.2.2.3 Kynurenic acid (KYNA)

KYNA is a neuroprotective glutamate receptor antagonist and is antagonistic to all three subtypes of ionotrophic receptors discussed earlier (Foster et al., 1984b, Bertolino et al., 1989). KYNA has a high affinity for the glycine binding site of NMDAR in comparison to the glutamate binding site (Birch et al., 1988, Bertolino et al., 1989) and also binds to α7-nicotinic acetylcholine receptors (Hilmas et al., 2001). While it has been hypothesised that KYNA may play a role in glutamatergic transmission, KYNA regulation of glutamate release may be indirectly mediated by inhibition of acetylcholine receptors (Carpenedo et al., 2001).

KYNA at high concentrations is known to possess anti-convulsant and neuroprotective properties (Foster et al., 1984b). Dose-dependent administration of KYNA results in behavioural changes mimicking properties of chemicals that block open channels of NMDAR, further supporting its role in modulation of these receptors (Vecsei and Beal, 1990). KYNA is protective against neurotoxicity caused by both QUIN and kainite and can inhibit release of glutamate by reduction of receptor activation (Foster et al., 1984a, Carpenedo et al., 2001). It has been shown that reduction of kynurenic acid levels due to deletion of KATII increases the size of QUIN-induced lesions compared to control littermates (Yu et al., 2004, Sapko et al., 2006). This is a clear indication that even a small reduction in KYNA can amplify the effect of NMDA mediated excitotoxicity. Furthermore, on administration of dopamerigic drugs that temporarily decrease KYNA levels, striatal QUIN induced lesions are enlarged (Poeggeler et al., 2007) clearly underscoring the neuroprotective properties of KYNA.

1.3 KYNURENINE PATHWAY AND NEURODEGENERATION

The first disease in which KP dysfunction was implicated was HD, where intrastriatal injections of excitotoxin QUIN in rodents was found to mimic the cardinal features of this disease (Schwarcz et al., 1983). As described above, it has subsequently been found that the pathway has additional neuroactive components. It is therefore possible that the kynurenine pathway may be a key and early pathway perturbed in neurodegenerative disease pathogenesis.

1.3.1 Huntington's disease: A brief overview of pathology

HD is a progressive disorder characterised by abnormal movements, cognitive dysfunction and psychiatric disturbances. The primary involuntary movement disorder observed in HD is involuntary jerking of muscles (chorea) affecting the limbs, trunk and face, which occurs in almost 90% of HD patients. Other symptoms include bradykinesia (slow movement),

rigidity and dystonia (muscular spasms) (Kirkwood et al., 2001). HD is caused by a CAG triplet nucleotide repeat expansion in the HD gene (*IT-15*), which encodes a 348KD protein, known as huntingtin (Htt) (H.D.C.R.G, 1993). This CAG repeat encodes a polyglutamine (polyQ) expansion, which leads to misfolding and aggregation of Htt. The size of the polyQ expansion is inversely proportional to the age of onset (Duyao et al., 1993) and directly proportional to aggregation kinetics (Scherzinger et al., 1999, Chen et al., 2001). Protein misfolding and aggregate formation caused by polyQ expansion is likely to play an important role in HD pathogenesis, however it remains unclear whether oligomers or aggregates are causative (Bates, 2003). The normal allele has between 4-35 repeats while repeat sizes ≥40 are fully penetrant and result in HD. In individuals carrying ≥60 repeats, juvenile HD is observed. Alleles with 35-39 repeats are incompletely penetrant; although the carriers of this allele may be non-symptomatic, instability of the allele during meiosis can result in CAG repeat expansion leading to HD in the offspring (known as anticipation) (Landles and Bates, 2004). However a great variation exists in the age of onset in individuals containing an identical number of repeats, and as much as ~30-40% of variation in the age of onset may be attributed to other genetic or environmental modifiers (Wexler et al., 2004). An example for genetic contribution to variation in age of onset includes single nucleotide polymorphisms (SNPs) in huntingtin associated protein-1 (*HAP1*) that has high affinity for mHtt. A SNP (M441) compared to another SNP (T441) causes HAP1 to bind mHtt with higher affinity reducing degeneration of mHtt fragments and thereby delaying the age of onset in HD by 8 years (Metzger et al., 2008). A variety of genes involved in energy metabolism, stress response, transcription, protein degradation have all been implicated to have a role in modifying the age of onset of motor symptoms (reviewed in (Gusella and MacDonald, 2009)). The function of Htt is not clear, and it has been suggested to play a role in a myriad of cellular processes, including: (a) Vesicle transport and maintenance of cytoskeleton structure- due to interactions with components

of the cytoskeleton complex such as dynactin, microtubules and β-tubulin; (b) clathrin mediated endocytosis; (c) neuronal transport and post synaptic signalling; (d) cell survival via anti-apoptotic functions & (e) embryonic development (Landles and Bates, 2004) .

The region of brain most affected in HD is the striatum with up to a 30% decrease in brain mass being observed due to neuronal cell loss associated with loss of GABAergic (i.e. associated with the neurotransmitter gamma aminobutyric acid (GABA)) medium spiny neurons (MSN) and is characterised by axon-sparing lesions (Figure 1-2) (Gutekunst et al., 2002). Apart from atrophy of the basal ganglia, widespread atrophy of the gyrus (ridge of the cerebral cortex) and reduction in number of pyramidal neurons in the prefrontal and parietal cortex is also observed (Gutekunst et al., 2002). The levels of GABA, the enzyme glutamate decarboxylase (which synthesises GABA), acetylcholine, the enzyme choline-acetyl transferase and other associated neurotransmitters such as enkephalins and substance P have been observed to be decreased in HD (Faull et al., 1993, Storey et al., 1994). In addition, a reduction in the number of NMDA receptors has also been observed in HD (Gutekunst et al., 2002) leading to the hypothesis that glutamate associated/induced excitotoxicity may be responsible for the HD pathology at a cellular level. Additionally, microglial stimulation and activation (reactive gliosis) has also been described in striatum and cortex of HD patient brains (Sapp et al., 2001, Pavese et al., 2006, Tai et al., 2007b) indicating a role for non-neuronal cells in HD pathology.

Cell death in HD is attributed to mHtt affecting various cellular processes through both gain-of-function and loss-of-function mechanisms, including: transcription dysregulation, impairment of chaperone activity, impairment of ubiquitin proteasome system, excitotoxicity, mitochondrial impairment and microglial activation (Zuhlke et al., 1993, Wellington, 2003, Landles and Bates, 2004). Based on the predicted role(s) of the kynurenine pathway and KMO in HD pathogenesis, in this chapter we focus specifically on

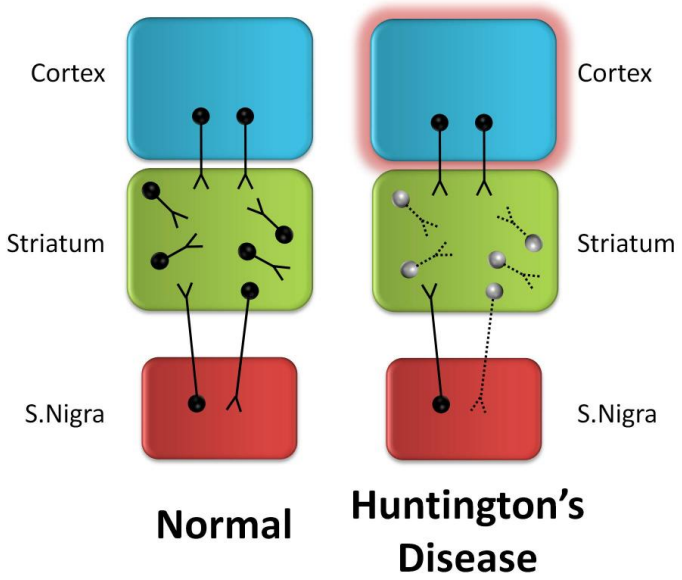

Figure 1-2: Schematic model showing axon-sparing lesions in HD striatum.

Striatum containing the medium spiny neurons is the major region of the brain affected in HD primarily due to excitotoxic insults; however a selective sparing of dopaminergic afferent fibres is observed even in later stages of the disease. The dashed lines indicate degenerating neurons and highlighted in red "aura" is the damage to the cortex (Thevandavakkam et al., 2010).

the role of excitotoxicity, mitochondrial impairment and microglial activation in HD pathogenesis.

1.3.1.1 Role of excitotoxicity in HD pathology

As discussed earlier, QUIN an excitotoxin was found to be implicated in HD pathology when striatal injection of QUIN in rodents replicated the HD phenotype suggesting a role for excitotoxicity in HD pathology (Schwarcz and Kohler, 1983). Further, removal of the corticostriatal glutamatergic cortical afferents was also found to be further protective against QUIN induced lesions (McGeer and McGeer, 1978, Orlando et al., 2001) suggesting a role for glutamate released by the cortex in activating the metabotrophic receptors in the striatum. Altered glutamate release (Cepeda et al., 2003) and altered KP (Guidetti et al., 2004, Guidetti et al., 2006) observed in pre-symptomatic and early stage HD mice suggests that increased glutamate release accompanied by increase in QUIN and oxidative metabolites plays an important role in NMDAR activation and MSN stress. Excitotoxicity caused by NMDAR activation is associated with aberrant calcium homeostasis (Berliocchi et al., 2005), mitochondrial dysfunction and oxidative stress (Nicholls and Ward, 2000) which are discussed later.

Activation of NMDAR has been implicated to play a vital role in mediating excitotoxic response in general and in HD in particular (Zeron et al., 2002). In striatal neurons, NMDAR mediated excitotoxicity is associated with increased glutamate release at the synapse and subsequently reduced uptake of glutamate after synaptic release, increased NMDAR sensitivity to glutamate, and reduced ability of mitochondria to neutralize excess Ca^{2+}. Elevated NMDAR levels associated with increased levels of intracellular calcium in the MSN have been observed in HD mouse models (Zeron *et al.*, 2002 and Zeron *et al.*, 2004). Subsequent influx of Ca^{2+} following NMDAR activation activates proteolytic enzymes such as calpains and proteases, leading to increased levels of ROS and RNS.

Increased Ca^{2+} also mediates apoptosis and necrosis in positive feedback loop (Rami *et al.*, 1997). Additionally, induction of proteases following NMDAR activation can also lead to cleavage of mHtt, increase in nuclear expression of cleaved mHtt fragments and transcriptional dysregulation (reviewed in (Martinez-Vicente et al., 2005)).

As discussed earlier, variation in NMDAR number and composition have also been observed in HD mice with SNPs in NMDAR subtypes contributing to 4.5%-12.5% variation in the age of onset in HD (Arning et al., 2005) underscoring the importance of NMDAR mediated excitotoxicity in HD pathology.

1.3.1.2 Energy metabolism and oxidative stress in HD

Mitochondria are essential for synthesis of ATP, regulation of glucose metabolism and maintenance of intracellular calcium levels. ATP required for cellular processes is synthesised via the electron transport chain (Chen 1988). Deficient energy metabolism has been implicated in HD due to experimental evidence showing that glucose metabolism is impaired in HD patient brains, especially in the basal ganglia (Mazziotta et al., 1987, Powers et al., 2007). Also, the drastic weight loss observed in HD patients indicates a potential role for defective metabolic pathway(s) in HD (O'Brien et al., 1990). Studies with fungal toxin 3-nitropropionic acid (3NP) in rodents that inhibits succinate dehydrogenase complex activity of the electron transport chain and TCA cycle mimics the symptoms seen in HD patients (Gould and Gustine, 1982, Hamilton and Gould, 1987). Finally, mitochondrial impairment has also been associated with excitotoxicity (Beal et al., 1991). The opening and closing of NMDA receptor channels is voltage dependent (Ca^{2+}/Mg^{2+} concentration) and studies in rodents using the compound: aminooxyacetic acid that inhibits energy metabolism and reduces ATP production, produces lesions in the brain mimicking HD in a manner similar to NMDA antagonists (Beal *et al.*, 1991 and Urbanska *et al.*, 1989).

In HD, both disruption of electron transport chain and NMDAR activation causes an increase in free radicals such as peroxynitrite ions and superoxide ions, as well as increased production of hydrogen peroxide that can cause nitration of proteins further impairing mitochondrial function and triggering the apoptotic pathway (Beckman et al., 1990, Balakirev et al., 1997, Chavez et al., 1997, Carreras et al., 2004).

Mitochondria are particularly sensitive to damage caused by ROS associated with the opening of the MPTP (Jacobson and Duchen, 2002). In HD rodents, mitochondrial membrane potential is lowered (Panov *et al.*, 2003) and mHtt has been shown to be associated with the outer mitochondrial membrane, specifically sensitising the MPTP to calcium, causing the opening of MPTP and cytochrome C induced apoptosis in the presence of low Ca^{2+} levels (Choo *et al.*, 2004). These processes have also been implicated in other neurodegenerative diseases such as Parkinson's disease and Alzheimer's disease (Zhang *et al.*, 2006). In a related note, work in our group has found that overexpression of mitochondrial import proteins is protective in HD model yeast, further supporting the role of mitochondrial dysfunction in HD pathogenesis (R. Mason and F. Giorgini, unpublished observations).

1.3.1.3 Role of microglia in HD toxicity

Microglia are non-neuronal cells associated with the CNS that are activated by CNS stress and/or injury such as inflammation, wherein they become phagocytic (Block et al., 2007). Microglia are of particular interest in KP biology as KMO is specifically expressed in these cells in the CNS (Guillemin et al., 2001, Kiss et al., 2003, Giorgini et al., 2008). Reactive gliosis and activation of microglia are observed in HD patient brains (Sapp *et al.*, 2001). Inflammation of the CNS/neuroinflammation also characterises both symptomatic and pre-symptomatic HD brains indicating that this process plays a very important role in HD (Sapp et al., 2001). Positron emission tomography (PET) studies have also shown that

there is a marked increase in microglial activation in the cortex and striatum of HD patients when compared to healthy control brains and there is a correlation between the severity of disease and levels of microglial activation (Tai et al., 2007a). Plasma levels of other components of the innate immune system such as α-2-macroglobulin, clusterin, components of the complement system such as C4, C7, C9 and interleukin-6 that are markers for microglial activation are also altered in HD indicating that microglial activation and subsequent neuroinflammation may play a vital role in HD (Dalrymple et al., 2007). Both in vivo and in vitro studies using HD mice show that levels of 3-HK is elevated in microglia and is associated with the mHtt expression in microglia (WT Htt is not expressed in the microglia) (Giorgini et al., 2008). The activation of microglia and levels of 3-HK were reduced on administering HDAC inhibitors or KMO inhibitors further underscoring the importance of microglial activation in HD pathology.

Furthermore, in transgenic mice, expression of mHtt in astrocytes causes age-dependent neurodegeneration akin to HD. Expression of mHtt in astrocytes also potentiates neurotoxicity in HD by impairing glutamate uptake into astrocytes, resulting in enhanced excitotoxicity and also inhibition of secretion of vital chemokine CCL5/RANTES required for trophic support to neurons (Shin et al., 2005, Chou et al., 2008). These studies collectively support the hypothesis that non-neuronal cells play a vital role in HD pathology.

1.3.2 Altered kynurenine pathway metabolites in HD

Much work suggests that imbalances between the KP neurotoxins QUIN/3-HK and neuroprotective metabolite KYNA could contribute to HD pathology (Chou et al., 2008). This was first supported by studies in HD patients that recorded an increase in the KP enzyme 3-hydroxyanthranilate (that acts upstream to QUIN formation) (Schwarcz et al., 1988), decreased KYNA levels in cerebrospinal fluid, and increased KYN/KYNA ratio in

putamen in HD patients (Beal et al., 1992). Unexpectedly, little or no changes were found in levels of QUIN and 3-HK (Reynolds et al., 1988, Heyes et al., 1991).

One of the major disadvantages in the above studies was the choice of material analysed. The HD brains that were analysed were from late stage HD patients. Late stage HD patients show a great deal of acute brain atrophy with only a thin layer of glial cells and few neurons (Myers et al., 1991, Ross et al., 1997). Recent studies show that QUIN is indeed elevated in the caudate nucleus and putamen a.k.a. neostriatum and cortex of early stage HD patients; work by Guidetti *et al.*, have shown that there is a 3-4 fold increase in QUIN and 5-10 fold increase in 3-HK in early stage HD patients (Vonsattel grade 0-1) while in later stage HD patients (Vonsattel grade 2, 3, 4) there was no significant alteration in QUIN or 3-HK levels. Furthermore, increases in QUIN and 3-HK levels were specific to the cortex and neostriatum and not cerebellum (Guidetti et al., 2000, Guidetti and Schwarcz, 2003).

No difference in KYNA levels were found between early/late stage HD samples and controls (Guidetti et al., 2004). However, there was an increase in 3-HK/KYNA and QUIN/KYNA ratios indicating an increase flux through the neurotoxic branch of the KP instead of the neuroprotective branch leading to KYNA formation (Guidetti et al., 2004).

These studies in humans have been backed up by studies in HD mouse models that also showed an increase in QUIN and 3-HK levels versus controls (Guidetti et al., 2006). In mouse models that expressed full length mHtt protein and developed striatal degeneration, there was a ~10-fold increase in 3-HK levels. In addition to this, three other HD mouse models showed similar increases in QUIN and 3-HK. In the R6/2 mice, the commonly used HD model that shows an early onset of disease phenotypes, high levels of 3-HK were observed in the cortex, striatum and cerebellum between 4-12 weeks. There was no increase in 3-HK observed in the hippocampus (Guidetti et al., 2006). In the YAC128

mouse model, that shows comparatively slower onset of HD symptoms (8-12 months), increased 3-HK was observed in cortex, striatum and cerebellum, with the highest increase seen in cortex. Increased QUIN levels were also observed but were restricted to striatum and cortex. There was no elevation of QUIN level in the cerebellum. The hippocampus showed no elevation in either 3-HK or QUIN levels (Guidetti et al., 2006). In HdhQ92/HdhQ111 knock-in mice, which exhibit intermediate phenotypes between the R6/2 mice and YAC128 mice, an increase in 3-HK and QUIN levels in cortex and striatum in mice aged 15-17 months was observed (Guidetti et al., 2006). This data taken in conjunction with the fact that KMO is expressed only in the microglia in the CNS further signifies that non-neuronal cell types causally contribute to mHtt mediated degeneration of neurons (Figure 1-3).

1.3.3 Kynurenine-3-monooxygenase (KMO) as a potential therapeutic target for HD

The results discussed above strongly support a role for the KP in HD pathogenesis. Thus, substances that inhibit KP enzymes at various points of the pathway are of great interest as potential therapeutic agents in HD. Amongst these enzymes, KMO is an interesting target, since inhibition of KMO is predicted to increase the flux through the neuroprotective KYNA branch of the pathway and reduces flux through the neurotoxic branch of the pathway.

Early work showed that inhibition of KMO using compounds such as *m*-nitrobenzoylalanine and UPF 648 can ameliorate HD-relevant phenotypes in rat and mice administered intrastriatal injections of QUIN. Specifically, studies with *m*-nitrobenzoylalanine have shown that the percentage of pyramidal neurons with lesions is

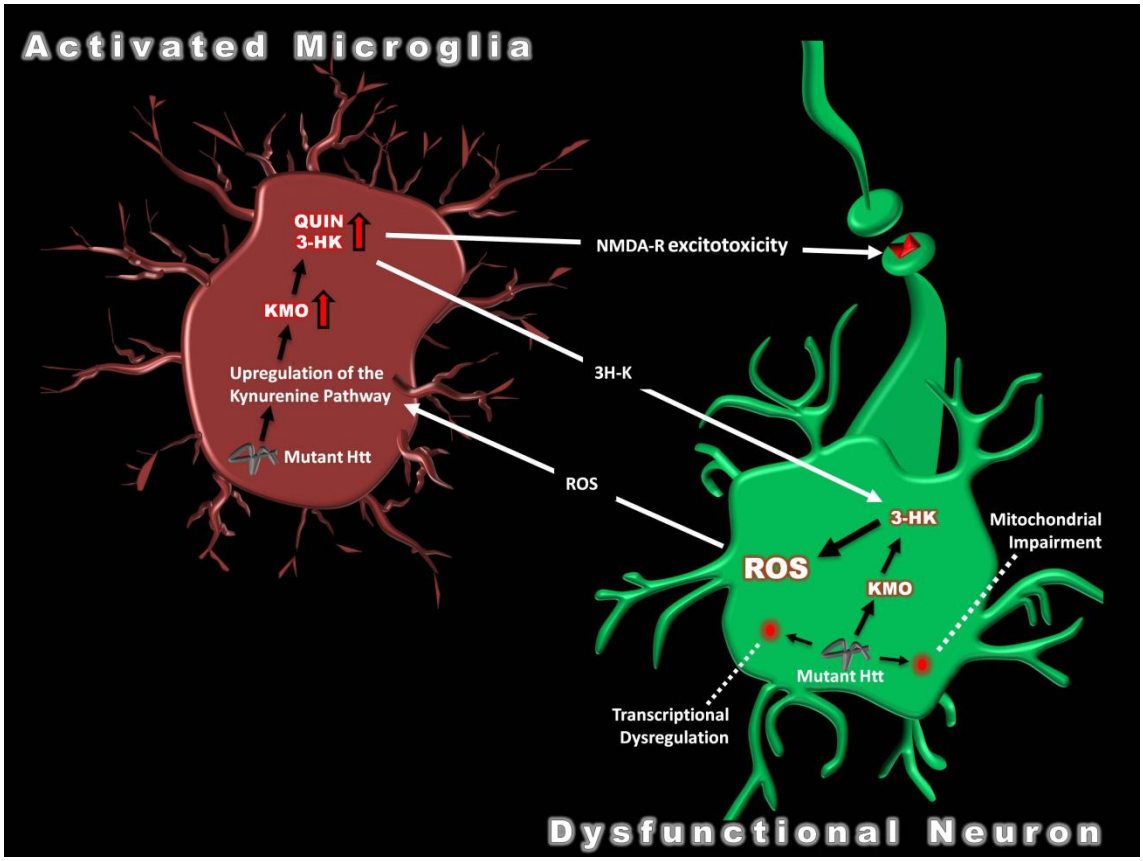

Figure 1-3: Role of KP and microglia in HD pathology.

Expression of mHtt in microglia causes an upregulation of KP resulting in increased production of QUIN and 3-HK resulting in increased ROS and NMDA mediated excitotoxicity that consequently results in degeneration and death of neurons expressing mHtt (Thevandavakkam et al., 2010).

reduced by 85% (Pellicciari et al., 1994, Chiarugi and Moroni, 1999). Similarly studies with UPF 648 have shown to be protective against QUIN lesions, even in models partially depleted for KAT activity (Ceresoli-Borroni et al., 2007).

The first genetic evidence supporting KMO inhibition as a therapeutic strategy for HD was obtained using a yeast model of HD. In a loss of function suppressor screen conducted by Giorgini *et al* for gene deletions that suppress mHtt toxicity in *Saccharomyces cerevisiae*, 28 suppressors were identified, including a gene deletion of *BNA4*, the human homologue of which is KMO (Giorgini et al., 2005). Levels of 3-HK and QUIN were found to be increased in HD yeast model and deletion of *BNA4* was found to eliminate the formation of these metabolites, supporting the hypothesis that the KP plays a vital role in HD. As yeast do not have NMDARs, toxicity by QUIN and 3-HK is most likely caused by generation of ROS and the resultant oxidative stress. To explore this possibility, oxidation sensitive dyes were used to measure ROS levels in yeast, and it was found that levels of ROS were significantly elevated in mHtt expressing yeast versus controls, and the deletion of *BNA4* reversed this effect (Giorgini et al., 2005). Thus in this model elevation of 3-HK and QUIN is correlated to increased ROS and cell death, and genetic inhibition of KMO reserves ameliorates all these effects, suggesting that ROS generated from 3-HK and QUIN is contributing to toxicity in this model.

This mHtt dependent upregulation of central KP flux in yeast is likely due to increased expression of *BNA2* (TDO) relative to controls (Giorgini et al., 2008). This process appears to be regulated via the yeast Rpd3 histone deacetylase (HDAC) complex, as either genetic impairment of Rpd3 or treatment with HDAC inhibitors decreased levels of 3-HK and QUIN, as well as expression of four central KP genes, in HD yeast. This observation was supported by work in primary microglia expressing mHtt and a mouse model of HD

showing that the HDAC inhibitor suberoylanilide hydroxamic acid abrogated mHtt dependent increases of KP metabolites (Giorgini et al., 2008).

Furthermore, studies in an HD fly model have validated KMO as a therapeutic target for HD and demonstrated a direct link between HD pathology and 3-HK mediated neurotoxicity and KYNA mediated neuroprotection (Campesan et al., *in press*). Deletion of KMO or treatment with a KMO inhibitor ameliorated neurodegeneration and was characterised by decreased 3-HK/KYNA ratio. Furthermore, administering 3-HK reversed the protective effects KMO inhibition in a dose dependent manner and was found to enhance neurotoxicity in HD flies (Campesan et al., *in press*). On the other hand, KYNA treatment reduced neurodegeneration in these flies.

Recent evidence to support the role of KMO as a potential therapeutic target for HD comes from Zwilling *et al.* who have shown that in HD model mice KMO inhibition rescued synaptic loss and reduced microglial activation (Zwilling et al., *in press*). The novel KMO inhibitor JM6 also increased the lifespan of these mice by ~30% and improved locomotor performance via the rotarod assay was also observed. Interestingly, studies with JM6 show that there is an increase in KYNA levels in both the blood plasma and brain and this is accompanied by reduction of extracellular glutamate (Zwilling *et al.*, *in press*). JM6 is pro-drug of Ro 61-8048, which also does not cross the blood-barrier, thus peripherally administering a KMO inhibitor is sufficient to increase flux through the KYNA branch of the pathway in the brain possibly via increased KYN transport into the brain, which is preferentially converted to KYNA

Apart from HD, KMO inhibition is also effective in ameliorating phenotypes in other neurodegenerative disorders such as Alzheimer's disease, where administering KMO inhibitors rescue key phenotypes such as synaptic loss and loss of spatial learning in AD model mice (Zwilling *et al*, *in press*). In infectious diseases such as cerebral malaria,

pretreating mice with KMO inhibitors makes them resistant to infection causing malaria and reduces CNS related symptoms (Miu et al., 2009). In another infectious disease-trypanosomiasis (African sleeping sickness), KMO inhibitors reduce inflammation of the CNS in late stages of the diseases (Rodgers et al., 2009). These studies clearly underscore the importance of KP and KMO in particular in various diseases affecting the CNS.

SPECIFIC AIMS:

As discussed above KMO is a potential therapeutic target for HD and other brain diseases, however, little is known about the cellular role of KMO apart from its function as an enzyme and key modulator of the KP. Indeed, to date no physical or genetic interactors of human KMO have been described in the literature. This project aims to elucidate the role of KMO in the cell. To this end, the aims of the project include:

1. Identifying protein interaction partners of human and yeast KMO:

a) Optimising the outer mitochondrial membrane-membrane yeast two hybrid approach (OMM-MYTH)(Chapter 3):

A novel membrane yeast two-hybrid approach was established and validated to enable identification of protein interactors of outer mitochondrial membrane proteins by high throughput screening in yeast.

b) Identifying protein interaction partners of yeast and human KMO using OMM-MYTH (Chapter 4):

The OMM-MYTH was then used to screen > 10 million clones from yeast ORF and human cDNA libraries to identify novel protein interactors of yeast and human KMO respectively.

c) Validation of protein interactors by biochemical approaches (Chapter 5):

A high false positive rate has been attributed to yeast two hybrid approaches. To overcome false positives from the screen, the protein interactors from the screen were re-confirmed by co-immunoprecipitation analysis.

2. Identifying genetic interaction partners of yeast KMO (Chapter 6):

Genetic interaction partners of yeast KMO previously identified in a systematic genetic screen were characterised and validated using tetrad analysis to confirm synthetic lethal interactions.

3. Elucidating the cellular role of KMO using bioinformatic tools (Chapter 7):

Bioinformatic tools were used to analyse interaction data so that enriched functional categories and networks involving KMO could be identified and used to clarify the cellular role of KMO.

CHAPTER 2 MATERIALS AND METHODS

2.1 MATERIALS

2.1.1 Plasmids and Strains used in this study

All plasmid constructs and amplifications were made using chemically competent *E. coli* DH5-α cells (*φ80lacZΔM15, recA1, endA1, gyrA96, thi-1, hsd*R17 (*K, $^{m}K^{+}$), *supE44, relA1, deo*R, Δ *(lacZYA-argF) U169*) (from Invitrogen). The *Saccharomyces cerevisiae* strain THY.AP4 [*MATa leu2-3, 112 ura3-52 trp1-289 lexA*::*ADE2* lexA:: *LacZ*] was used for all MYTH related procedures unless stated otherwise. This strain has *HIS3*, *ADE2* and *LacZ* reporter genes controlled by *LexA* promoter. Plasmid pCCW-STE, into which the bait was cloned, was obtained from Dualsystems Biotech Inc (San Pedro, USA). The libraries used for the screen were a human fetal cDNA library (X-NubG) and a yeast ORF library (X-NubG) (obtained from Dr. Igor Stagljar (University of Toronto)).

For genetic interaction studies YFG deletions were obtained from the yeast knockout collection library (*YFGΔ::Kan_MATa his3Δ leu2Δ met15Δ ura3Δ*) from Open Biosystems (Huntsville, USA). *bna4Δ* was created by deleting *BNA4* with a *NAT* cassette in a mutated S288C strain (*MATa his3Δ leu2Δ lys2Δ0 ura3Δ RME1(ins308A), TAO3(E1493Q) MKT1(Φ3ΦG)*) (Deutschbauer and Davis, 2005). Table 2-1, Table 2-2 & Table 2-3 lists all the yeast strains and plasmids used in this study.

Table 2-1: Strain Genotypes.

Strain	***Genotype***
THY.AP4	*MATa leu2-3, 112 ura3-52 trp1-289 lexA::ADE2 lexA:: LacZ*
pex3-RFP	*pex3-RFP MATa his3Δ leu2Δ met15Δ ura3Δ*
bna4::KanMX4	*bna4::KanMX4 MATa his3Δ leu2Δ met15Δ ura3Δ*
bna4::NatMX4-1	*bna4::NatMx4 can1Δ::MFA1pr-HIS3 mfa1Δ::MFa1pr-LEU2lyp1Δura3Δleu2Δhis3Δmet15Δlys2+*
bna4::NatMX4-2	*bna4::NatMX4 MATα his3Δ leu2Δ lys2Δ0 ura3Δ RME1(ins308A), TAO3(E1493Q) MKT1(Φ3ΦG)*
aro1::KanMX4	*aro1::KanMX4 MATa his3Δ leu2Δ met15Δ ura3Δ*
aro2::KanMX4	*aro2::KanMX4 MATa his3Δ leu2Δ met15Δ ura3Δ*
bem1::KanMX4	*bem1::KanMX4 MATa his3Δ leu2Δ met15Δ ura3Δ*
bsd2::KanMX4	*bsd2::KanMX4 MATa his3Δ leu2Δ met15Δ ura3Δ*
dep1::KanMX4	*dep1::KanMX4 MATa his3Δ leu2Δ met15Δ ura3Δ*
dst1::KanMX4	*dst1::KanMX4 MATa his3Δ leu2Δ met15Δ ura3Δ*
fyv4::KanMX4	*fyv4::KanMX4 MATa his3Δ leu2Δ met15Δ ura3Δ*
hos2::KanMX4	*hos2::KanMX4 MATa his3Δ leu2Δ met15Δ ura3Δ*
maf1::KanMX4	*maf1::KanMX4 MATa his3Δ leu2Δ met15Δ ura3Δ*
nhp10::KanMX4	*nhp10::KanMX4 MATa his3Δ leu2Δ met15Δ ura3Δ*
nkp2::KanMX4	*nkp2::KanMX4 MATa his3Δ leu2Δ met15Δ ura3Δ*
npt1::KanMX4	*npt1::KanMX4 MATa his3Δ leu2Δ met15Δ ura3Δ*
oar1::KanMX4	*oar1::KanMX4 MATa his3Δ leu2Δ met15Δ ura3Δ*
pmp3::KanMX4	*pmp3::KanMX4 MATa his3Δ leu2Δ met15Δ ura3Δ*
ptc1::KanMX4	*ptc1::KanMX4 MATa his3Δ leu2Δ met15Δ ura3Δ*
ric1::KanMX4	*ric1::KanMX4 MATa his3Δ leu2Δ met15Δ ura3Δ*
rom2::KanMX4	*rom2::KanMX4 MATa his3Δ leu2Δ met15Δ ura3Δ*
rpn4::KanMX4	*rpn4::KanMX4 MATa his3Δ leu2Δ met15Δ ura3Δ*

Strain	***Genotype***
sec66::KanMX4	*sec66::KanMX4 MATa his3Δ leu2Δ met15Δ ura3Δ*
tim18::KanMX4	*tim18::KanMX4 MATa his3Δ leu2Δ met15Δ ura3Δ*
tna1::KanMX4	*tna1::KanMX4 MATa his3Δ leu2Δ met15Δ ura3Δ*
utr1::KanMX4	*utr1::KanMX4 MATa his3Δ leu2Δ met15Δ ura3Δ*
ypt5::KanMX4	*ypt5::KanMX4 MATa his3Δ leu2Δ met15Δ ura3Δ*
ygl024w::KanMX4	*ygl024w::KanMX4 MATa his3Δ leu2Δ met15Δ ura3Δ*
ygr2259c::KanMX4	*ygr2259c::KanMX4 MATa his3Δ leu2Δ met15Δ ura3Δ*

Table 2-2: Double deletion strains with *bna4*Δ and deletion for candidate gene being tested.

Strain	**Genotype**
bna4::NatMX4	*bna4::NatMX4 MATα his3Δ leu2Δ ura3Δ lys2Δ0 RME1(ins308A), TAO3(E1493Q) MKT1(Φ3ΦG)*
aro1::KanMX4	*aro1::KanMX4 MATa his3Δ leu2Δ ura3Δ RME1, TAO3 MKT1*
bna4::NatMX4	*bna4Δ::NatMX4 MATα his3Δ leu2Δ ura3Δ lys2Δ0 RME1(ins308A), TAO3(E1493Q) MKT1(Φ3ΦG)*
aro2::KanMX4	*aro2::KanMX4 MATa his3Δ leu2Δ ura3Δ RME1, TAO3 MKT1*
bna4::NatMX4	*bna4Δ::NatMX4 can1Δ::MFA1pr-HIS3 mfa1Δ::MFa1pr-LEU2 lyp1 Δura3 Δleu2 Δhis3 Δmet15 Δlys2+*
*aro1::KanMX4**	*aro1::KanMX4 MATa Δura3 Δleu2 Δhis3 Δmet15*
bna4::NatMX4	*bna4Δ::NatMX4 can1Δ::MFA1pr-HIS3 mfa1Δ::MFa1pr-LEU2 lyp1 Δura3 Δleu2 Δhis3 Δmet15 Δlys2+*
*aro2::KanMX4**	*aro2::KanMX4 MATa Δura3 Δleu2 Δhis3 Δmet15*

The table shows the genotype for diploid carrying deletions of *BNA4* and *ARO1* and *BNA4* and *ARO2*. Similar diploid deletion strains were created carrying *bna4*Δ and deletion of one of the candidate genes:*BEM1, BSD2, DEP1, DST2, FYV4, HOS2, MAF1, NHP10, NKP2, NPT1, OAR1, PMP3, PTC1, RIC1, ROM2, RPN4, SEC66, TIM18, TNA1, UTR1, YPT5, YGLO24W, YGR2259C.*

*represents diploid created in the BY4741 background.

Table 2-3: List of plasmids used in this study.

Plasmid	Description	Reference
pCCW-Ste-Cub	Starter plasmid for cloning the baits (See Appendix 1)	(Iyer et al., 2005)
pFur4-NubI	Starter plasmid for cloning prey controls and prey control in MYTH screen	(Iyer et al., 2005)
pFur4-NubG	Starter plasmid for cloning prey controls and prey control in MYTH screen	(Iyer et al., 2005)
NubG (empty Vector)	Negative control in MYTH screen	(Iyer et al., 2005)
pCCW-Ste-KMO-Cub	Bait in MYTH screen	(this study)
pCCW-Ste-Bna4-Cub	Bait in MYTH screen	(this study)
pCCW-Δste-Bna4-Cub	Bait in MYTH screen	(this study)
pCCW-Ste-Mmm1-Cub	Control Bait in MYTH screen	(this study)
pMmm1-NubI	Prey control in MYTH screen	(this study)
pMmm1-NubG	Prey control in MYTH screen	(this study)
pMmm1-RFP-NubI	Prey control in MYTH screen and used for confocal microcopy	(this study)
pMmm1-RFP-NubG	Prey control in MYTH screen and used for confocal microcopy	(this study)
pTom20-NubI	Prey control in MYTH screen	(this study)
pTom20-NubG	Prey control in MYTH screen	(this study)
pOst1-NubI	Prey control in MYTH screen (See Appendix 1)	(this study)
pOst1-NubG	Prey control in MYTH screen	(this study)
pKMO-Myc	Used in pull-down experiments to confirm protein interactors of KMO	(this study)
pBna4-Myc	Used in pull-down experiments to confirm protein interactors of Bna4	(this study)
pKMO-TAP	Used in pull-down experiments to confirm protein interactors of KMO	(this study)
pBna4-TAP	Used in pull-down experiments to confirm protein interactors of Bna4	(this study)
pKMO-FLAG	Used in pull-down experiments to confirm protein interactors of KMO	(this study)
pBna4-FLAG	Used in pull-down experiments to confirm protein interactors of Bna4	(this study)
pAG25	Contains NATMX4 used to amplify NAT and delete *BNA4*	(Goldstein and McCusker, 1999)
mRFPmars	Contains RFP used to create Mmm1-RFP-NubI/G	(Fischer et al., 2004)

2.1.2 Yeast media and growth conditions

Yeast transformants were grown in synthetic drop out (SD) supplemented with the appropriate nutrients. The SD medium consisted of 2.7% w/v Difco yeast nitrogen base, 2% w/v Dextrose, the pH was adjusted to 6-6.5. 870 mg/l of the dropout mixture without the required amino acids (Table 2-4) was added to this mixture along with 3 ml/l 1% (w/v) lysine solution and autoclaved. Where required, 3-amino-triazole (3-AT) (Fulka, Sigma) stock solution (8.4 g in 100 ml H_20) was added to SD media at the required concentration (e.g. for a final concentration of 120 mM 3AT, 12 ml of 3-AT stock solution was added to 800 ml SD media). Yeast cultures were grown at 30°C with continuous agitation unless mentioned otherwise.

Yeast carrying gene deletions were grown in YEPD (Yeast Extract Peptone Dextrose) medium containing 1% (w/v) Bacto yeast extract, 2% (w/v) dextrose, 2% (w/v) Bacto peptone and 0.05% (w/v) adenine hemisulphate in 0.05 M hydrochloric acid. To test for petite mutants, the cells were subsequently grown on YEPEG (Yeast Extract, Peptone, Ethanol, Glycerol) medium containing 1% (w/v) succinic acid, 1% (w/v) Bacto yeast extract, 2% (w/v) Bacto peptone, 2% (v/v) glycerol and 0.5% (w/v) adenine hemisulphate in 0.05 M hydrochloric acid. The pH was adjusted to 5.5. 3% (v/v) 100% ethanol was added after autoclaving. The media were autoclaved for 20 min at 115°C at a pressure of 10 psi. For geneticin (200 μg/ml; Invitrogen) and nourseothricin (100 μg/ml; Werner Bioagents) containing media, the appropriate amount of the drug was added after autoclaving. Diploids were sporulated in liquid sporulation medium consisting of 2% (w/v) potassium acetate, pH 7.0 or solid media comprising synthetic complete potassium acetate containing 2% (w/v) potassium acetate, 0.22% (w/v) Bacto yeast extract, 0.05% (w/v) dextrose, 875 mg/l complete amino acid mix (Table 2-4) and 2.5% (w/v) Bacto agar. The medium was adjusted to pH 7.0.

Table 2-4: Components of Amino acid nutrient mixture.

Nutrient	Amount(mg)
Adenine	800
Arginine	800
Aspartic acid	4000
Histidine	800
Leucine	800
Lysine	800
Methionine	800
Phenylalanine	2000
Threonine	8000
Tryptophan	800
Tyrosine	1200
Uracil	800

To make dropout mixes, the appropriate amino acid was omitted from the mixture. 0.7 g of dropout mix was used per 800 ml of media.

To make solid media 2.5% (w/v) Bacto agar was added. Deionised water was used to make the media. All the stock solutions for amino acids mixtures and drugs were made with distilled water unless mentioned otherwise. The yeast media/chemicals were purchased from Sigma Aldrich unless otherwise stated. The required pH was obtained by adding either 1 M hydrochloric acid or 1 M sodium hydroxide. Yeast stocks were made in 15% glycerol (v/v) and stored at -80°C.

2.1.3 Bacterial media and growth conditions

E. coli containing plasmids were grown in Luria agar broth containing 1 % Bacto-tryptone, 0.5 % Bacto yeast extract, 0.5 % sodium chloride, pH 7.2. To ensure plasmids are not lost during propagation the LB media was suitably supplemented with kanamycin (50 μg/ml; Sigma) or ampicillin (100 mg/ml; Melford laboratories). *E. coli* were grown at 37°C with liquid *E. coli* cultures being grown at 37°C with agitation at 200 rpm. All media and protocols are as described in Iyer *et al.*, 2005 unless stated otherwise (Iyer et al., 2005).

2.1.4 Measuring Optical density of liquid bacterial and yeast cultures

To determine the cell density of liquid cultures, the optical density was measured at a wavelength of 600 nm using a spectrophotometer. The density was determined on the assumption that an OD_{600} of 1 equals ~$8x10^8$ cells/ml.

2.1.5 Oligonucleotides

Oligonucleotides were designed to have a melting temperature between 54°C-60°C with a GC content of 40-60%. Oligonucleotides were ordered from Invitrogen and are listed in (Table 2-5).

Table 2-5: List of oligonucleotides used in this study.

Primer name	Sequence	Application
pKMO-Cub Fw	GCAAACACAAATACACACACTAATCTAGAAAGAATCAAAAATGGACTCATCTGTCATTCA	Constructing KMO bait for MYTH
pKMO-Cub-Rv	AGGCGGCCTTAATTAAAGGCCTGGCCGTAATGGCCATTACCCTGCTAATGAGATTGGAAA	Constructing KMO bait for MYTH
KMO-F	CGATTATGCCATCGACCTTT	KMO bait sequencing primer
KMO-R	TTCAAGGCTTGTCGTCCTCT	KMO bait sequencing primer
pBna4-Cub-Fw	CGCCTCGGCCATCTGCAGGAATTCGATATCAAGCTTATCGATGTCTGAATCAGTGGCCAT	Constructing Bna4 bait for MYTH
pBna4delste-Fw	GCAAACACAAATACACACACTAATCTAGAAAGAATCAAAAATGTCTGAATCAGTGGCCAT	Constructing Ste2 deletedBna4 bait for MYTH
pBna4-Cub-Rv	TTTTGACAAGAGAACGTTCCATACCGTCGACCATGTCGGGGGGGGATCCCTCCAGATCAAC	Constructing Bna4 bait for MYTH
Bna4-F	GCGTGGATGGCCAGGCAACT	Bna4 bait sequencing primer
Bna4-R	GTCTGGCTGATGTGATCACG	Bna4 bait sequencing primer
pMMM1-Cub-Fw	ATGTCTGATGCGGCTCCTTCATTGAGCAATCTATTTTATATGACTGATAGTGAGAATGAA	Constructing Mmm1 Bait for MYTH
pMMM1-Cub-Rv	GTTGATCTGGAGGGATCCCCCCCGACATGGTCGACGGTATTAACTCTGTAGGCTTTTCTT	Constructing Mmm1 Bait for MYTH
Mmm1-F	CGTTTCGGTGGATTCATTCT	Mmm1 bait sequencing primer
Mmm1-R	CGTTTCGGTGGATTCATTCT	Mmm1 bait sequencing primer
Fur4-F	TTCTTCCCTGTACCTGGGTG	Fur4 bait sequencing primer
Fur4-R	CAATCTTTTTGAAGAGCCGC	Fur4 bait sequencing primer
pMmm1-I/G-Fw	ATACAATCAACTCATCTAGACGTCAGCGCTCCGCGGAAAAATGACTGATAGTGAGAATGA	Constructing Mmm1-NubI/G prey control for MYTH
pMmm1-I/G-Rv	CGGTCAAAGTCTTGACGAAAATCTGCATGGGACTGCAGCCTAACTCTGTAGGCTTTTCTT	Constructing Mmm1-NubI/G prey control for MYTH
pMmm1-I/G-RFP-Fw	CAACTTAAGTCGAAAATTCAAGACAAGGAATCCCTATGGCCTCCTCCGAGGAGGACGT	Constructing Mmm1-NubI/G-RFP prey control for MYTH
pMmm1-I/G-RFP-Rv	ATAAGAAATTCGCCCGGAATTAGCTTGGCTGCATGCGGCCTTAGGCGCCGGTGGAGTGGC	Constructing Mmm1-NubI/G-RFP prey control for MYTH
pTom20-I/G-Fw	ATACAATCAACTCATCTAGACGTCAGCGCTCCGCGGAAAAATGTCCCAGTCGAACCCTAT	Constructing Tom20-NubI/G prey control for MYTH
pTom20-I/G-Rv	CGGTCAAAGTCTTGACGAAAATCTGCATGGGACTGCAGCAGTCATCGATATCGTTAGCTT	Constructing Tom20-NubI/G prey control for MYTH
pOst1-I/G-Fw	ATACAATCAACTCATCTAGACGTCAGCGCTCCGCGGAAAAATGAGGCAGGTTTGGTTCTC	Constructing Ost1-NubI/G prey control for MYTH
pOst1-I/G-Rv	CGGTCAAAGTCTTGACGAAAATCTGCATGGGACTGCAGCGTTAGTTACGTTCATGTTCAA	Constructing Ost1-NubI/G prey control for MYTH

Primer name	Sequence	Application
Ost1-F	CCGGACAGTGTATATATGATAA	Ost1 bait sequencing primer
Ost1-R	TGGCTATTTAAAAAAGTTGC	Ost1 bait sequencing primer
Fetal-Seq	GGTATACGGCCTTCCTTCCA	Sequencing the fetal cDNA library
DSL-NubG-x	CCGATACCATCGACAACGTTAAGTCG	Sequencing the yeast cDNA library
YLibrary-F	GTCGAAAATTCAAGACAAGG	Sequencing for yeast cDNA Clone(s)
YLibrary-R	AAGCGTGACATAACTAATTAC	Sequencing for yeast cDNA Clone(s)
KMO-Myc-F	CAGAATAAGATACCATGAGGCTGTGCAGCGTTGGCATTGGCAAAAAAGGACGTACGCTGCAG GTCGAC	Constructing KMO-Myc tagged construct
Bna4-Myc-F	TATCTATTGGCGGTTACAAGCTTTTCAAATTTTTGACAAGAGAACGTTCCCGTACGCTGCAGGT CGAC	Constructing Bna4-Myc tagged construct
Common-Myc-R	ATCAATCTTTGTTGATCTGGAGGGATCCCCCCCGACATGGTCGACGGTATATCGATGAATTCG AGCTCG	Common primer for constructing KMO/Bna4-Myc tagged construct
KMO-TAP-F	GGGGACAAGTTTGTACAAAAAAGCAGGCAGAACCATGGACTCATCTGTCATTCAA	Constructing KMO-TAP tagged construct
KMO-TAP-R	GGGGACCACTTTGTACAAGAAAGCTGGGTCCCTTTTTTGCCAATGCCAACG	Constructing KMO-TAP tagged construct
Bna4-TAP-F	GGGGACAAGTTTGTACAAAAAAGCAGGCAGAACCATGTCTGAATCAGTGGCCATTA	Constructing Bna4-TAP tagged construct
Bna4-TAP-R	GGGGACCACTTTGTACAAGAAAGCTGGGTCGGAACGTTCTCTTGTCAAAAAT	Constructing Bna4-TAP tagged construct
KMO-FLAG-F	GGGGACAAGTTTGTACAAAAAAGCAGGCAGAACCATGGACTCATCTGTCATTCAA	Constructing KMO-FLAG tagged construct
KMO-FLAG-R	GGGGACCACTTTGTACAAGAAAGCTGGGTCTCAGCTTGTCATCGTCGTCCTTGTAGTCCCTTTT TTGCCAATGCCAACG	Constructing KMO-FLAG tagged construct
Bna4-FLAG-F	GGGGACAAGTTTGTACAAAAAAGCAGGCAGAACCATGTCTGAATCAGTGGCCATTA	Constructing Bna4-FLAG tagged construct
Bna4-FLAG-R	GGGGACCACTTTGTACAAGAAAGCTGGGTCTCAGCTTGTCATCGTCGTCCTTGTAGTCGGAAC GTTCTCTTGTCAAAAAT	Constructing Bna4-FLAG tagged construct
Bna4delNAT-F	TAAAATATTGAATGACAGTTAAAAAATCACGTAGTCAGTTAATCTGTTTAACTTGAAAATCGTA CGCTGCAGGTCGAC	Creating Bna4 deletion using a NATMX4 cassette
Bna4delNAT-R	TATATCACTTATTTTAATAATCCTCTCCTAGCGTACACGGATGGCAAGAATAAACTGGCTATCG ATGAATTCGAGCTCG	Creating Bna4 deletion using a NATMX4 cassette
delNAT-seq-F	AGGTCACCAACGTCAACGCA	Sequencing primer for confirming Bna4 deletion with NATMX4
delNAT-seq-R	GATTCGTCGTCCGATTCGTC	Sequencing primer for confirming Bna4 deletion with NATMX4

2.1.6 Molecular weight markers

Bacteriophage λ DNA digested with *BstE*II from New England Biolabs was used as a molecular weight standard during agarose gel electrophoresis at a concentration of 50 ng/μl. Alternatively, the 10Kb Hyperladder I from Bioline was used at a concentration of 50 ng/μl.

Precision plus protein dual colour marker from Biorad was used at a concentration of ~20 μg per well in western blotting.

2.1.7 Antibodies

For co-immunoprecipitation experiments: Sepharose–G (GE healthcare), anti-HA conjugated agarose beads (Santa Cruz), anti-Myc conjugated agarose beads (Santa Cruz), anti-FLAG coated dynabeads (Sigma) were used with standard protocols as applicable (See 2.2.16).

In co-immunoprecipitation/immunoblotting experiments involving prey proteins mouse anti-HA monoclonal antibody (1:4000 dilution, Santa Cruz) was used as the primary antibody and rabbit anti-mouse antibody (1:12000, Dianova) was used as the secondary. Mouse anti-MYC monoclonal antibody (1:3000 dilution, Santa Cruz) was used to detect expression of Myc tagged constructs.

2.2 METHODS

2.2.1 Cloning strategy

2.2.1.1 Plasmid cloning by homologous recombination

Homologous recombination in yeast is a powerful tool which enables cloning foreign DNA into a plasmid of choice. It makes use of the process where by nucleotide sequence is exchanged between similar or identical DNA molecules(Ma et al., 1987). Baits and prey controls used in the MYTH study were created by this method as described by Iyer et al

(Iyer et al., 2005). PCR primers were designed to have 40 basepair homology to the vector in which the cDNA of interest is to be cloned into and 20 basepair homology to the gene of interest to be cloned such that the cDNA remains inframe. The vector was digested with a suitable restriction enzyme, the digested vector and the PCR product were mixed in a 1:3 ratio in the yeast transformation mixture and transformed into yeast using high efficiency lithium acetate transformation (see section 2.2.9) (Figure 2-1). The clones were selected on appropriate SD media and following plasmid rescue in E.coli were verified by restriction digestion analysis and DNA sequencing.

A similar procedure was also used to tag KMO and Bna4 baits with Myc tag in the absence of appropriate restriction enzyme sites as described by Knop et al (Knop et al., 1999).

2.2.1.2 Gene knockout using homologous recombination

To knockout *BNA4* for genetic interaction studies, the NAT cassette was amplified with primers with 20 basepair homology to NAT and 60 basepair homology to regions immediately flanking the genomic *BNA4*. The PCR product was transformed into the host strain *(MATa his3*Δ *leu2*Δ *lys2*Δ*0 ura3*Δ *RME1(ins308A), TAO3(E1493Q) MKT1(Φ3ΦG))* by high efficiency lithium acetate transformation and selected on media supplemented with NAT. Following colony PCR the clones were verified by DNA sequencing.

2.2.1.3 Gateway cloning

Gateway cloning aids in shuttling the gene of interest into various expression systems (Alberti et al., 2007). Gateway cloning (Invitrogen) was carried out as per manufactures instructions. For the KMO/Bna4 TAP cloning, the cDNA of interest was amplified and cloned into the donor vector pDONR 221 in *E. coli* through recombinational cloning following which the clones were confirmed by sequencing to ensure that they contain the insert. The donor vector was then transformed along with the pAdvanced Gateway Destination vector containing TAP by high efficiency transformation into *E. coli.*

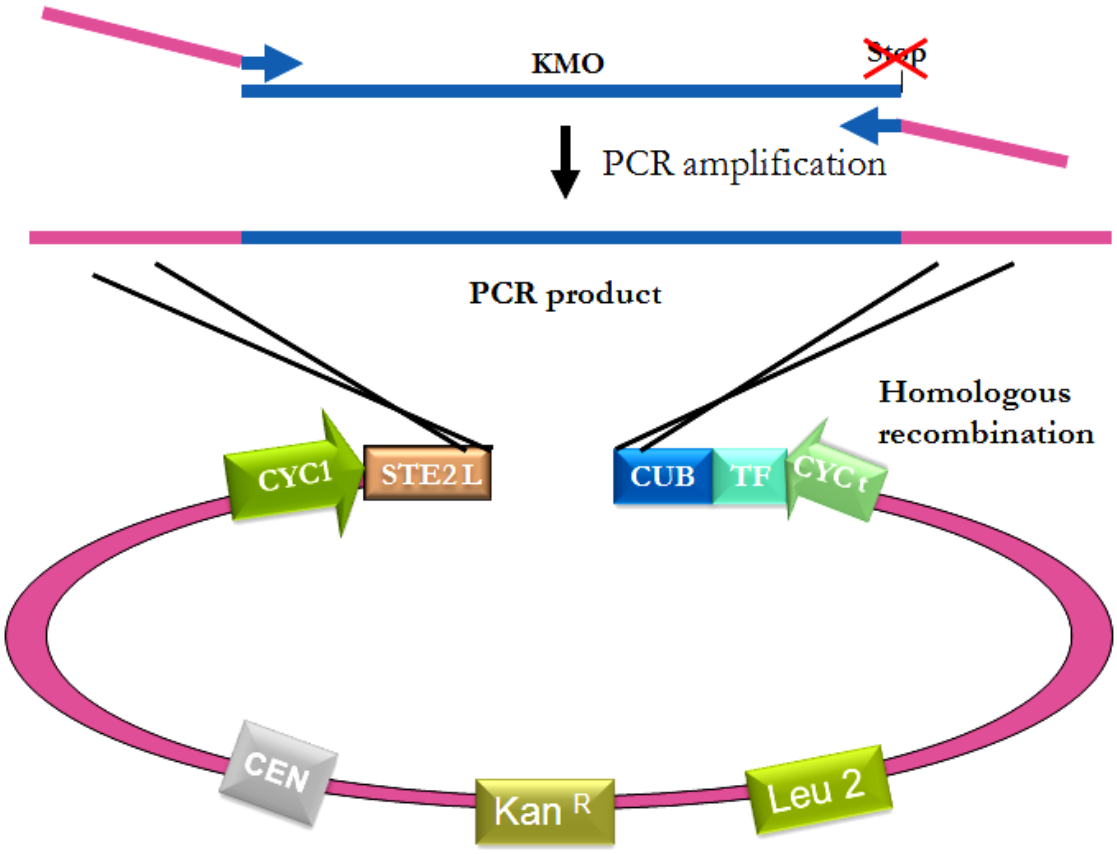

Figure 2-1: Overview of Cloning by homologous recombination in yeast

Homologous recombination is the process by which DNA containing identical sequences are exchanged. This system forms the basis for cloning by homologous recombination in yeast. To create the KMO bait for the MYTH screen, cDNA encoding KMOp was amplified by primers having 20 basepair homology to the cDNA and 40 basepair homology to the vector. The digested vector and PCR were transformed into yeast resulting in gap repair by homologous recombination.

KMO/Bna4 FLAG constructs were created by incorporating the FLAG sequence in the primers. The remaining procedure was carried out as above. The pAdvanced Gateway Destination Vector containing no tag was used.

2.2.2 Agarose gel electrophoresis

Agarose gel electrophoresis was performed with gels made using Seakem LE agarose from Lonza dissolved in 1xTBE (90 mM Tris base, 90 mM boric acid, 2 mM EDTA pH 8.0). The gels were supplemented with ethidium bromide (0.5 μg/ml) prior to casting the gel and the percentage of the gel was determined by the DNA fragment to be separated. DNA samples were mixed with 0.25X volume of 5X loading dye (10 % (w/v) Ficoll type 400, (w/v) 0.25 % bromophenol blue, 0.5% (w/v) SDS) and loaded into agarose gel to be separated by electric field through 1xTBE buffer. Appropriate DNA markers (section 2.1.6) were used to determine the size of the DNA fragment. Gels were visualised using a UV transilluminator and imaged using a Kodak 200L dark chamber and processed using the Kodak 1D Image analysis software.

2.2.3 Purification of DNA

Following agarose gel electrophoresis, the DNA band of interest was excised using a scalpel, to reduce nicking of DNA a dark reader was used. The samples were further processed using QIAGEN® MinElute Gel Extraction Kit as per manufacturer's instructions. When PCR products were purified before being used for transformation or sequencing, Qiagen PCR purification kit was used as per manufacturer's instructions.

2.2.4 Quantifying DNA

DNA samples were quantified by measuring the absorbance at 260 nm in a UV spectrophotometer. The absorbance value was converted to a concentration using the following constant: 1 OD_{260} unit = 50 μg of double stranded DNA.

2.2.5 Restriction digestion

Restriction enzymes and respective buffers were purchased from New England Biolabs and the restriction digests were set up as per manufacturer's instructions. A typical 10 µl reaction contained 200 ng DNA, 1 µl 10X buffer, 0.5 µl restriction enzyme and H_2O to 10 µl. Samples were incubated at the appropriate temperature for 1 hr before further processing.

2.2.6 Plasmid Preparation

2.2.6.1 Low throughput plasmid preparation

Plasmids from *E. coli* were extracted using Omega's E.Z.D.A. Plasmid Mini kit I as per manufacturer's instructions from 5ml overnight cultures. Plasmids from yeast were extracted similarly, however after addition of Solution I, 250 µl glass beads were added and the cell suspension was vortexed at high velocity using a Bead Beater. The rest of the protocol was as per manufacturer's instructions.

2.2.6.2 High throughput plasmid extraction

Putative hits from the MYTH screen were processed by this method. 1ml *E. coli* cultures supplemented with the suitable antibiotic were grown overnight in 1.5ml 96-well plates sealed with PCR film (Thermoscientific). A multichannel pipette was used for all manipulations. All solutions and equipments were used cold (4°C) unless otherwise mentioned. The samples were harvested at 4°C for 10 min at 5000 rpm and the cell pellet was resuspended in 100 µl of cold Solution I (50 mM glucose, 25 mM Tris-HCl (pH 8.0), 10 mM EDTA (pH 8.0)) and vortexed. To this suspension 200 µl of freshly made Solution II (0.2 N NaOH, 1% (w/v) SDS) was added and mixed thoroughly after which 150 µl of cold Solution III (3 M acetate, 5 M potassium, pH4.8) was added. After thorough mixing, the samples were incubated on ice for 5 min and the plates were centrifuged at 5000 rpm for 10 min and the supernatant (~400 µl) was transferred to a fresh 1.5 ml 96-well plate. 2X

volume of 100% ice-cold ethanol was added to the supernatant and the plate was then vortexed and allowed to stand for 2 min after which the samples were centrifuged as before. The supernatant was removed and the pellet was resuspended in 70% ice-cold ethanol and the sample was processed as before and centrifuged similarly. The supernatant was removed and the pellet was air-dried and resuspended in 20 µl 1xTE buffer (10 mM Tris-HCl (pH 8.0), 0.1 mM EDTA (pH 8.0)). The samples were used for high throughput transformation of yeast.

Plasmids from yeast cultures were extracted similarly. The solutions and equipment were used at room temperature except for solution III that was used cold. Solution I was supplemented with 10 mg/ml zymolase and the yeast cells resuspended in solution I were incubated at 37°C with shaking for 30 min (until they form spleroplasts). Following which the samples were processed as above. The samples were used for high throughput transformation of *E. coli*.

2.2.6.3 Large Scale plasmid DNA prep

E. coli were grown in 50ml LB supplemented with antibiotic media for 20-22 hr. The cells were pelleted and resuspended in 6ml of solution I (50 mM Glucose, 25 mM Tris-HCl pH 8.0, 10 mM EDTA pH 8.0). 12ml of solution II (0.2 M NaOH, 1% (w/v) SDS) was added and the solution was mixed by inverting the ultracentrifuge tube repeatedly. The samples were incubated on ice for 5 min following which 4.5 ml of 7.5 M NH_4Ac (pH 7.4) was added and the samples were mixed by inverting and incubated on ice for 5 min. The samples were centrifuged at 11000 rpm for 10 min. The supernatant was removed to a fresh tube and centrifuged again. The supernatant was transferred to a fresh tube and 0.6 volumes of isopropanol added. The samples were incubated at room temperature for 30 min and then centrifuged at 11000 rpm for 15 min, the pellet was resuspended in 2 ml of 2 M NH_4Ac (pH 7.4) and transferred to four microcentrifuge tubes and incubated on ice for

5 min. The samples were pelleted at 5000 rpm for 5 min and the supernatant was removed to a fresh microcentrifuge tube and incubated with equal volume of isopropanol at room temperature for 30 min. Following centrifugation at 13000 rpm for 15 min, the samples were rinsed with 500 µl 70% ethanol, the ethanol was removed and spun at 13000 rpm for 2 min and air dried. The pellet was resuspended in 245 µl 10 mM Tris with 5 µl RNase A (10mg ml^{-1}) and the samples were incubated for an hr at 37°C and mixed with 125 µl 7.5M NH_4Ac (pH 7.4) and 375 µl isopropanol and incubated at room temperature for 15 min. The samples were pelleted for 10 min and rinsed with 70% ethanol as before and air dried as before. The dry pellet was then resuspended in 400 µl of 10 mM Tris.

2.2.7 Polymerase Chain Reaction-associated procedures

2.2.7.1 Proofreading PCR

Proofreading PCR was carried out using Phusion HighFidelity polymerase enzyme from Finnzymes. A typical 30 µl reaction consisted of 50 ng template DNA, 0.2 µM of each primer, 2 U of Phusion polymerase and 2.7 µl of 11.1x buffer (450 mM Tris-HCl, pH 8.8; 110 mM ammonium sulphate; 45 mM magnesium chloride; 67 mM β-mercaptoethanol; 44 µM EDTA, pH 8.0; 10 mM dATP; 10 mM dGTP; 10 mM dTTP; 10 mM dCTP; 1.13 $mg.ml^{-1}$ BSA). Typical cycling conditions included an initial 98°C denaturation step for 1 min; 35 cycles of denaturation at 98°C for 30 s, 30 s of annealing at a primer-dependent temperature followed by extension at 72°C for time equalling 1 min/kb and a final extension step at 72°C for 10 min. Annealing temperatures were optimised for individual primer pairs as required. PCR was carried out using a PTC-225 Peltier Thermal Cycler (MJ Research).

2.2.7.2 Colony PCR

Colony PCR reactions were carried out as a preliminary screen to test if clones contain the gene of interest without having to prepare the DNA, enabling large scale screening of clones. *Taq* polymerase (Kappa Biosystems) was used for colony PCR. From the transformation plate, a small portion of the colony (= ~0.2 mm^2) was resuspended in 20 µl 0.02 M NaOH and incubated at 98°C for 10 min and then incubated on ice for 5 min. 3 µl of supernatant was used in Taq polymerase reaction as in section 2.2.7.1 comprising 5U Taq polymerase. The PCR cycling conditions were the same as in section 2.2.7.1 except that the denaturation step was carried out at a temperature of 95°C and the initial denaturation was extended to 3 min.

2.2.8 DNA sequencing

DNA sequencing was carried out using the BigDye® v3.1 Cycle Sequencing Kit, Applied Biosystems. Approximately 400 ng of plasmid DNA or 100 ng of purified PCR product was used in a 10 µl reaction in addition to 1 µl Big Dye ™, 3.2 pmole primers and 3 µl of sequencing buffer. Cycling conditions for sequencing reaction included an initial denaturation step at 96°C for 1 min followed by 25 cycles at 96°C, for 10 s, 5 s at 50°C and 4 min at 60°C. To purify the reaction after sequencing, 0.2% (w/v) SDS was added to the sequencing reaction and incubated at 95°C for 10 min. Excess dye was removed using Performa DTR gel filtration columns (Edge Biosystems) according to the manufacturer's instructions. Samples were analyzed using an Applied Biosystems 3730 sequencer at the Protein Nucleic Acid Chemistry Laboratory facility, University of Leicester.

2.2.9 Yeast transformation procedures

2.2.9.1 High efficiency lithium acetate (LiAc) transformation

High efficiency LiAc transformation was carried out as described by Iyer et al with slight modifications (Iyer et al., 2005). Cells were grown in 10ml YEPD media overnight at 30°C. The cells were washed twice with water, diluted to an OD_{600} of 0.2, and allowed to grow until they completed 2 doublings (~4 hr). The cells were then pelleted on a table top centrifuge at 3000 rpm for 5 min and washed twice with an equal volume of water. The cells were resuspended in 1ml of water and 0.5 µl of cell suspension was transferred into each of two 1.5 ml tubes. Cells were pelleted for 30 s at 3000 rpm and the supernatant was removed. The cells were resuspended in transformation mix containing 240 µl 50% (w/v) polyethylene glycol (MW 3350), 36 µl 1 M lithium acetate, 50 µl 2 mg/ml single-stranded salmon sperm DNA (denatured at 95°C for 10 min and snap chilled on ice) and 34 µl of DNA to be transformed. The cells were vortexed to mix the contents and heat shocked at 42°C for 40 min. After heat shock, the cells were pelleted by centrifugation at 3000 rpm for 5 min and washed once with water. If selecting for drug resistance such as NAT or G418, the pellet was resuspended in 1 ml of YEPD and incubated at 30°C with shaking for 3 hr. The cells were then plated on appropriate media and incubated at 30°C for 3-4 days.

2.2.9.2 Large scale high efficiency transformation

This transformation protocol was used to perform large scale transformations of cDNA libraries into plasmid bearing yeast for the MYTH screen. The protocol was carried out as described by Iyer et al (Iyer et al., 2005). Yeast cells were grown in 10 ml of the appropriate SD medium overnight. The 10 ml culture was inoculated into 100 ml of fresh SD medium and allowed to grow overnight. 30 OD_{600} units of culture was washed twice with water, resuspended 200 ml of YEPD to a final OD_{600} of 0.2, and grown for two doublings (OD_{600}=0.8). The culture was split into 4 x 50 ml falcon tubes, centrifuged at 3500 rpm for

5 min, and washed with equal volumes of water. The supernatant was removed and each pellet resuspended in 600 µl of water and transferred to 10 ml tube containing 2.5 ml transformation mix (see 0) and 5 µg of library plasmid. The cells were vortexed for ~1 min and heat shocked in a water bath at 42°C for 50 min. The contents were mixed every 15 min to ensure uniform heat shock. The cells were pelleted and resuspended in 3 ml of YPED. Cells from different falcon tubes were pooled together and incubated at 30°C for 90 min with shaking. The cells were washed and resuspended in 4.7 ml of water and 300 µl aliquots of the transformed yeast were plated onto the appropriate media (-trp-leu-ade-his+3AT) and incubated at 30°C for 7-10 days. Four 5 fold serial dilutions of the cells was plated on SD (-trp-leu) plate and incubated at 30°C for 2 days. The number of colonies on the control plate was used to calculate the transformation efficiency.

2.2.9.3 Short transformation of yeast

This method was used for the routine transformation of plasmids into yeast and was carried out as described by Chen et al (Chen et al., 1992) with slight modifications. Yeast cells were grown in the appropriate media for 1-2 days. 250 µl aliquots of were pelleted at 3000 rpm for 5 min and resuspended in 100 µl one step transformation mix (800 µl 40% (w/v) polyethylene glycol (MW 3350), 200 µl 1 M lithium acetate, 100 µl 1 M DTT), 5 µl 10 mg/ml single-stranded salmon sperm DNA (denatured at 95°C for 10 min and snap chilled on ice) and 50 ng - 1 µg plasmid. Cells were vortexed to completely mix the contents and heat-shocked at 42°C for 30 min. Cells were washed once with 1 ml of water, resuspended in 200 µl of water, and plated on appropriate media and incubated at 30°C for 2-3 days.

2.2.9.4 Yeast 96-well plate short transformation protocol

The protocol was used for propagate putative interactors from MYTH screen and was carried out as described by Giorgini and Muchowski (Giorgini and Muchowski, 2006) with

slight modifications. 50 ml cultures of yeast cells were grown in appropriate SD medium at 30°C until they reached a stationary phase. 100 µl of culture per well was aliquoted into a 96 well plate (U bottom) using a multichannel pipette. The plate was spun at 1200 rpm for 10 min and the supernatant was removed. 20 µl of transformation mix (see 0) and ~1 µg plasmid DNA was added per well and the plate sealed with PCR film. The plate was vortexed to ensure that the cell pellet was thoroughly suspended in the transformation mix and incubated at 42°C for 30 min. 5 µl of cells were spotted onto appropriate media and allowed to air dry before incubating them at 30°C for 2-3 days. As the growth spots represent a mixture of transformants the colonies were re-streaked before being used for further manipulations.

2.2.10 Transformation of chemically competent *E. coli*

Fresh *E. coli* was inoculated in 10 ml LB media overnight from which a 1/100 dilution was made. These subcultures were grown to an OD_{600}=0.4-0.7. The cells were harvested by centrifuging at 4000 rpm for 10 min at 4°C and washed with 0.5 volumes of ice-cold water. The cells were then washed thrice with 0.5 volumes of ice-cold 100 mM calcium chloride and incubated with 0.5 volume of 100 mM Calcium chloride for 1 hr on ice. The cells were either used immediately or stored in 100 µl aliquots as glycerol stocks at -80°C after the addition of glycerol to 15%.

To transform *E. coli*, 100 µl of competent *E. coli* were incubated with 500 ng of yeast plasmid or 100 ng of *E. coli* plasmid on ice for 30 min, heat shocked at 42°C for 45 s, and immediately incubated on ice for 2 min. 1ml of antibiotic free LB was added and the cells were incubated at 37°C with shaking for 1 hr. 100 µl of transformed *E. coli* was plated onto antibiotic supplemented LB media and incubated at 37°C overnight.

2.2.10.1 E. coli 96-well plate transformation

This protocol was used to propagate putative interactor plasmids obtained from the screen. 50 µl of chemically competent *Ecolab* was aliquoted into individual wells of a 96 well plate and incubated with 500 ng of yeast plasmid on ice for 30 min. The plate was heat shocked at 42°C for 60 s and immediately incubated on ice for 2 min. 100 µl of antibiotic free LB was added and the cells were incubated at 37°C with shaking for 1hr. The cells were harvested by centrifuging at 2000 rpm for 5 min. The supernatant was removed and the cell pellet was resuspended in 5 µl of water and either spotted or streaked on antibiotic supplemented LB media and incubated at 37°C overnight.

2.2.11 Quantitative β-galactosidase assay

LacZ activity was used to confirm protein interactions of putative protein interactors identified from the MYTH screen. The β-galactosidase assay used in this study was adapted from Griffith and Wolf (Griffith and Wolf, 2002). Yeast cells bearing bait and prey plasmids were grown overnight in suitable SD media. 800 µl of cells were washed twice with water and harvested by spinning the cells at 3500 rpm for 5 min and suspended in 1 ml of Z-buffer mix (10 ml Z-buffer (60 mM Na_2PO_4 , 40 mM Na_2HPO_4 , 10 mM KCl, 1 mM $MgSO_4$, 50 mM β-mercaptoethanol) , 400 µl 0.1% (w/v) SDS, 600 µl chloroform). The reaction was started by the addition of 200 µl of ONPG (4 mg ml^{-1} in Z-buffer without β-mercaptoethanol) and samples were incubated at 30°C until yellow colour developed. The reaction was stopped by the addition of 400 µl of 1 M sodium carbonate and the samples were spun at 3500 rpm for 5 min to pellet the cells. The OD_{420} and OD_{550} of the supernatant were measured in a spectrometer (Colowick et al., 2002, Griffith and Wolf, 2002). The assay was performed in triplicate and β-galactosidase activity was calculated using the formula:

$$\textbf{Activity} = 1000*(OD_{420}-(1.75*OD_{550})/(\text{time}*\text{volume assayed}*OD_{600})$$

2.2.11.1 High throughput β–galactosidase assay

Putative interactors from the MYTH screen were subjected to preliminary screening using a β-galactosidase assay to detect false positives. For the 96-well plate β-galactosidase assay yeast cells were grown overnight in 100 µl SD (-trp-leu) media in 96 well plates to a final OD_{600} of 1.0. The cells were harvested by centrifugation at 2700 rpm for 5 min and suspended in 100 µl of Z-buffer (see 0), 60 µl of chloroform and 40 µl of 0.1% (w/v) SDS per well. The plates were vortexed for 30 s, after which they were incubated at 30˚C for 5 min. The reaction was initiated by adding 20 µl ONPG and the samples were incubated at 30˚C till a yellow colour developed, after which the reaction was stopped by adding 50 µl of 1 M Na_2CO_3. The plates where centrifuged at 2700 rpm for 5 min, the supernatant was transferred to a fresh plate, and the OD_{420} and OD_{550} of the supernatant were measured in an Omega 96-well plate reader (Colowick et al., 2002, Griffith and Wolf, 2002). The assay was performed in triplicate and β-galactosidase activity was calculated using the formula:

$$\textbf{Activity} = 1000*(OD_{420}-(1.75*OD_{550}) / (\text{time}*\text{volume assayed}*OD_{600})$$

2.2.12 Spotting assay

The spotting assay was used to measure the reporter gene activity of *ADE2* and *HIS3* by growth assays. Yeast cells bearing both bait and prey were inoculated into 96-well plates containing SD media lacking tryptophan and leucine and grown overnight at 30˚C. Four 5-fold serial dilutions of the cultures were plated onto media lacking tryptophan, leucine, adenine and histidine supplemented with 3 AT and incubated at 30°C for 2-3 days. A putative interaction is confirmed when growth at 10^4 dilution is observed.

2.2.13 Formaldehyde Crosslinking

Crosslinking reactions were performed to stabilise protein-protein interactions before further manipulations. Yeast cells were grown as 5 ml cultures overnight at 30°C in appropriate SD medium. Cells were diluted to an OD_{600} of 0.2 in 50 ml of YEPD and grown until OD_{600}=1.0. 37% formaldehyde solution was added to the cultures to a final concentration of 1% and the cells were incubated at 37°C for 15 min, 30 min or 1 hr. The crosslinking was stopped by adding 1.25 M glycine to a final concentration of 125 mM for 5 min at room temperature and the cells were washed twice with 1X PBS and protein extracts were either prepared directly from the cell pellet or the cell pellet was stored -80°C until later use.

2.2.14 UV-Crosslinking

Crosslinking reactions were performed to stabilise protein-protein interactions before further manipulations. Yeast cells were grown as 5 ml cultures overnight at 30°C in appropriate SD medium. The cells were diluted with 50 ml of YEPD and allowed to grow until OD_{600}=1.0. Cells were harvested by spinning them at 3500 rpm for 5 min and resuspended in 15 ml of water. 5 ml cell suspension was spread evenly in a small 90 cm petri dish and crosslinked with 254 nm UV light for 2 min. The cells were pooled together after UV-crosslinking and washed with water once. Protein extracts were either prepared directly from the cell pellet or the cell pellet was stored at -80°C until later use.

2.2.15 Preparation of total protein extracts

To prepare total protein extracts, yeast colonies were grown overnight in 5 ml SD media. The cells were diluted with 50 ml of YEPD and allowed to grow until OD_{600}=1.0. Cells were harvested by spinning them at 3500 rpm for 5 min in a 50 ml falcon tube. All equipment and solutions were subsequently maintained at 4°C to avoid degradation of protein. The cell pellet was suspended in 400 µl of B60 buffer (50 mM Hepes-KOH pH

7.3, 60 mM K-Acetat, 5 mM Mg-Acetat, 0.1% (v/v) Triton X 100, 10% (v/v) glycerol, 1 mM NaF, 20 mM glycerophosphate, 1 mM DTT, 1X Roche complete protease inhibitor cocktail). 250 µl of glass beads were added and the cells were sheared using a bead beater at maximum speed for 1 min. The samples were centrifuged at 13000 rpm for 5 min and supernatant was transferred to a fresh tube after which the supernatant was centrifuged at 13000 rpm for 20 min and approximately 300 µl the cleared protein lysate transferred to a fresh tube. The protein concentration was measured using 1.5 µl of each sample on a NanoDrop™ ND-1000 spectrophotometer according to the manufacturer's instructions. The protein extracts were used directly for co-immunoprecipitation analysis or incubated with 0.2 volumes 5X Laemelli-buffer (60 mM Tris-Cl pH 6.8, 2% (w/v) SDS, 10% (v/v) glycerol, 5% (v/v) β-mercaptoethanol, 0.1% (w/v) bromophenol blue) at 95°C for 5 min prior to SDS-PAGE (see 2.2.1.7).

2.2.16 Co-Immunoprecipitation

When agarose/sepharose beads were used for Co-IP analysis, the agarose/sepharose beads were centrifuged and the supernatant solution was removed. Protein concentration for all the samples was normalised to be the same and the protein lysates were used to re-suspend agarose/sepharose beads. The samples were incubated on a rocker at 4°C for 90 min. The beads were washed with 1ml B60 buffer (see 2.2.15) thrice and resuspended with 50 µl 10% (w/v) SDS buffer and incubated at room temperature for 10 min. The mixture was loaded on top of the filter in a P200 tip and centrifuged at 1000 rpm for 1 min. The flow through was incubated with 0.2 volumes 5XLaemelli-buffer at 95°C for 5 min. When Dynabeads (Invitrogen) were used for pull down experiments, prior to incubation with the protein the beads were treated as per manufacturer's instructions. The rest of the procedure was followed as described, except that the washing steps were performed using 1 x TBS and

instead of centrifugation steps, a magnetic separator was used to separate the beads and supernatant.

2.2.17 Western blotting

Samples for western blotting were prepared as described in sections 2.2.15 & 2.2.16. Approximately 50 μg of protein was loaded per lane along with a suitable marker (see 0). Unless mentioned otherwise a standard 12% gel (5 ml Buffer A (0.75 M Tris.HCl (pH 8.8), 0.2% (w/v) SDS), 4 ml 30% (w/v) acrylamide/methylene bisacrylamide solution (ProtoGel), 750 μl H_2O, 250 μl 10% APS, 5 μl TEMED) was used for all western blotting experiments. Electrophoresis was carried out at 100 volts in running buffer (0.025 M Tris.HCl, 0.192 M glycine, 0.1% (w/v) SDS) until sufficient separation of protein bands was achieved. Following electrophoresis, the gel was transferred to blotting apparatus and layered with PVDF membrane (Millipore) treated with 100% methanol and blotted for 2 hr at 100 volts in blotting buffer (0.025 M Tris.HCl, 0.192 M glycine, 20% (v/v) methanol). Following blotting the PVDF membrane was incubated in blocking solution (5% (w/v) milk solution in 1XTBST) for 30 min. The membrane was then incubated in primary antibody diluted in blocking solution to the required concentration and was incubated overnight on a rocker at 4°C. The membrane was washed thrice for 15 min in 1XTBST and then incubated with secondary antibody diluted in blocking solution to the required concentration and incubated for 2 hr at room temperature. The membrane was washed thrice in 1XTBST for 15 min and drained. The bands were visualised with ECL reagent (Biological industries) and X-ray film (Fujifilm).

2.2.18 Confocal microscopy

2.2.18.1 MitoTracker staining

Yeast cells were grown overnight in 5 ml SD media and were diluted next day with 50ml of YEPD and allowed to grow until OD_{600}=1.0 (or until two doublings). MitoTracker Red

(Invitrogen) was added to a final concentration of 50 nm and cultures grown for a further 30 min at 30˚C with shaking. Cells were harvested at 1500 rpm for 5 min and washed thrice with water. 5 µl of cell suspension was mixed with 10 µl of warm 2 % low melting point agarose solution in water and sealed with a cover slip. Microscopic investigation of agarose-embedded cells was performed using Olympus confocal microscope FV1000.

2.2.18.2 Immunohistochemistry

Yeast cells were grown overnight in 5 ml SD media and were diluted the next day with 50 ml of YEPD and allowed to grow until OD_{600}=1.0 (or until two doublings). If applicable, the cells were stained with MitoTracker Red CMXRos (see 2.2.18.1). Cells were fixed with formaldehyde solution at a final concentration of 4% for 90 min. Cells were then washed with 0.1 M KPO4 and resuspended in 1 ml spheroplast solution (0.1 M KPO4, pH6.5/1.2 M sorbitol/0.5 mM β-mercaptoethanol/0.4 mg 20 T zymolase). The cells were incubated at 37˚C for 20 min (or until digestion is sufficient i.e. cells appear dark, translucent gray under a phase contrast microscope) to allow spheroplast formation. Cells were pelleted gently by centrifugation at 1200 rpm for 5 min at 4°C. The pellet was resuspended in 1 ml 0.1 M KPO_4, pH 6.5/1.2 M sorbitol solution and 20 µl of the cell suspension was placed on a lysine coated slide. After 5 min, the excess cells were aspirated and the cells were fixed in ice cold methanol (6 min) and acetone (30 s). The slides were then washed with 10 mg/ml BSA in 1xPBS. Cells were incubated with a 1 in 100 dilution of KMO antibody (Proteintech group) in BSA/PBS overnight at 4°C in a moist chamber. The cells were washed with BSA/PBS four times and were incubated with a 1 in 100 dilution of AlexaFluor 488 secondary antibody (Invitrogen) in BSA/PBS for 2 hr in a moist dark chamber to prevent bleaching of the secondary antibody. The cells were washed four times with BSA/PBS. Excess solution was aspirated and cover slip was mounted in Vectashield mounting medium with DAPI (Vectashield) and sealed with nail polish. Microscopic

investigation of fixed yeast was performed using an Olympus confocal microscope FV1000. Images of yeast cells were taken using a 100X objective.

2.2.19 Genetic procedures

2.2.19.1 Creating diploids

Yeast strains exist in two mating types *MATa* and *MAT*α. To create diploids, *MATa* and *MAT*α strains having complementary markers were crossed on YEPD plate and incubated for a minimum of 5 hr at 30°C. The diploids were selected by complementation by replicating the plate with the cross to a minimal media plate (supplemented with NAT and G418). The plate was incubated overnight at 30°C and the resulting colonies were streaked on YEPD plates.

2.2.19.2 Solid sporulation

Diploids were streaked on YEPEG media and allow to grow for 24 hr, replica plated onto complete sporulation media (2% potassium acetate), and allowed to sporulate for 7-10 days at 23°C and 30°C. Sporulation of yeast cells was confirmed using Zeiss Axiostar phase contrast microscope.

2.2.19.3 Liquid Sporulation

A single diploid colony was selected and used to inoculate 5 ml liquid YEPEG, which was grown overnight at 30°C with shaking. The following day, 150 ml SPS was inoculated with the required amount of the overnight YEPEG culture (1 in 400 dilution). When the SPS culture reached an OD_{600} of 2, the cells were pelleted at 1500 rpm for 2 min, washed in an equal volume of 2% (w/v) KAc and resuspended in 225 ml 2% (w/v) KAc. Cultures were transferred to a 1 L Erlenmeyer flask and incubated at 23°C with vigorous shaking.

2.2.19.4 Tetrad dissection

To prepare the tetrads for dissection, the cells were resuspended in 100 µl of dissecting buffer (1 M Sorbitol, 10 µm EDTA, 10 µm sodium phosphate and 5 µl of 5 mg/ml 20T zymolase) and incubated at 37°C to enable digestion of the ascal wall, following which a further 400 µl of dissection buffer was added and the prepared cells were stored at 4°C. The asci were separated by micromanipulation using a Zeiss dissecting microscope and needles were purchased from Singer Instruments and the procedure was carried out as described previously (Abdullah and Borts, 2001).

2.2.19.5 Mating type testing

To determine the mating type of selected spores, cells were mated on YEPD medium to *MAT*a and *MAT*α tester strains for at least 4 hr before replica plating to minimal media and incubation overnight at 30°C. The mating tester strains are auxotrophic for *ura2, tyr1* not present in the strains used for analysis. Therefore, after replicating onto minimal media, only cells that have mated and undergone complementation of auxotrophies will be able to grow. This should show a 2:2 segregation pattern.

2.2.19.6 Assessing synthetic lethality

Viability of spores was assessed by counting the number of spores visible to the naked eye. The dissected plate was replica plated to double drug media supplemented with Nat and G418. If the genes are synthetically lethal no spores would be observed on the double drug media. If spore growth is observed, the sporulation procedure was repeated and another 20 tetrads were dissected to reconfirm the results.

2.2.20 Bioinformatic analysis

2.2.20.1 Bioinformatic analysis using David gene ontology database(Huang da et al., 2009b)

Hugo gene symbols for all the human genes and *Saccharomyces cerevisiae* standard gene names were used for functional analysis by DAVID via HTML-based API and included the following annotation categories: GOTERM_BP_ALL, GOTERM_CC_ALL, GOTERM_MF_ALL, BIND, DIP and MINT. Generally a P-value less than 0.05 was considered significant.

2.2.20.2 Bioinformatic analysis using Ingenuity pathway analysis (IPA) tool (Ingenuity® systems, www.ingenuity.com)

The "core analysis" function included in IPA was used to interpret the protein interactors of KMO with respect to biological processes, pathways and networks. The human genes were inputted using their official HUGO gene symbols, a gene list was generated, and inputted into IPA. Following the analysis, biological processes and canonical pathways were tested by Fisher Exact test P-value. The networks were ordered by a "score" indicative of significance. The biological processes were grouped in: diseases and disorders, molecular and cellular function, physiological system development and function. Canonical pathways were also ordered by the ratio value which signifies the number of molecules in a given pathway from the inputted list that meet divided by the total number of molecules that make up the pathway. To create an integrated network of KMO interacting proteins and Htt interactions involving KMO interacting proteins the Ingenuity Knowledgebase was used.

CHAPTER 3 OPTIMISING THE MEMBRANE YEAST TWO HYBRID (MYTH) TO IDENTIFY PROTEIN INTERACTIONS INVOLVING MITOCHONDRIAL MEMBRANE PROTEINS

3.1 INTRODUCTION

The MYTH is a split-ubiquitin based approach modelled on the traditional yeast two hybrid (Y2H) system which allows protein interaction partners to be identified by genetic screens in the yeast *Saccharomyces cerevisiae* (Fields and Song, 1989, Iyer et al., 2005). The classic Y2H approach exploits the fact that transcription factors contain two independent functional domains: the DNA binding domain (BD) and the activation domain (AD) (Van Criekinge and Beyaert, 1999). The two domains are independent of one another and are functionally stable even when separated. In Y2H, the protein of interest ("the bait") is mostly fused to the BD, which is the BD of *E. coli* LexA, a library of proteins against which the bait interaction is to be tested is fused to the AD ("the prey"), the AD of yeast Gal4. When the bait and prey are expressed in a yeast cell, interactions between the bait and prey reconstitute a functional transcription factor which activates the reporter gene. Interaction between proteins is confirmed by testing for reporter gene activity (Phizicky and Fields, 1995, Van Criekinge and Beyaert, 1999). The system is dependent on the interaction between the proteins and reconstitution of transcription factor occurring in the nucleus. This feature is a limitation when testing for protein interactions involving membrane proteins (Iyer et al., 2005).

The MYTH, however, uses ubiquitin that can be split into two halves that are stable and reconstitute a functional ubiquitin when brought into close proximity and overcomes the

disadvantage of Y2H (as described below), making yeast-based physical interaction screens possible for membrane bound proteins.

In MYTH, the bait and prey are fused to two halves of ubiquitin instead of a transcription factor (Iyer et al., 2005). Under normal cellular conditions proteins to be degraded by the proteasome are tagged by ubiquitin, which is recognised and cleaved by ubiquitin specific proteases (UBP) (Kornitzer and Ciechanover, 2000). Ubiquitin can be split into two halves (a carboxy-terminal half (Cub) and an amino-terminal half (Nub)) which have high affinity for one another and can spontaneously recombine creating a functional ubiquitin tag (Figure 3-1A&B). To prevent spontaneous reconstitution of ubiquitin in MYTH, a mutation is introduced in the Nub half where isoleucine at position 13 (NubI) is replaced by glycine (NubG). NubG shows decreased affinity for Cub and hence does not spontaneously reconstitute with Cub to form a functional ubiquitin tag (Figure 3-1C). MYTH takes advantage of this property, fusing the Cub half to both a bait protein and a transcription factor, and fusing the NubG half to a prey protein. When a bait and prey protein interact the Cub and NubG halves are brought in close proximity, thereby overcoming the NubG block and forming functional ubiquitin. This reconstituted ubiquitin tag is recognized and cleaved by USPs, ultimately releasing the transcription factor fused to Cub which can now enter the nucleus and trigger activation of reporter genes (*ADE2*, *HIS3* and *LacZ*). When there is no interaction between the bait and prey, functional ubiquitin is not reconstituted and consequently, there is no reporter gene activity (Iyer et al., 2005) (Figure 3-1D&E).

Figure 3-1: Split ubiquitin system: The basic principles

The split ubiquitin system is based on the modular nature of ubiquitin. (A & B) Ubiquitin can be split into two halves: Cub and Nub (also referred to as NubI) that spontaneously recombine when in close proximity. When the bait and prey fused to Cub and Nub, respectively, occur in close proximity ubiquitin is reconstituted, and therefore cleavage by ubiquitin specific proteases (UBPs), culminating in the release of reporter protein. (C) When a mutation is introduced in Nub (NubG), the two halves of ubiquitin do not spontaneously recombine unless there is an interaction between bait and prey. Bait protein is fused to Cub and a transcription factor (comprising *E. Coli LexA* binding domain and herpes simplex *VP16* Activating Domain). The prey is fused to NubG. (D) When there is no interaction between bait and prey, the ubiquitin is not reconstituted and there is no UBP activity or reporter gene activity. (E) When the bait and prey interact, the Cub and Nub reconstitute ubiquitin which is recognised by UBPs and results in the cleavage of transcription factor, which enters the nucleus to activate reporter gene activity. Activation of *HIS3* and *ADE2* can be tested by growing cells in medium lacking adenine and histidine while LacZ activity can be tested by assaying for β-galactosidase activity.

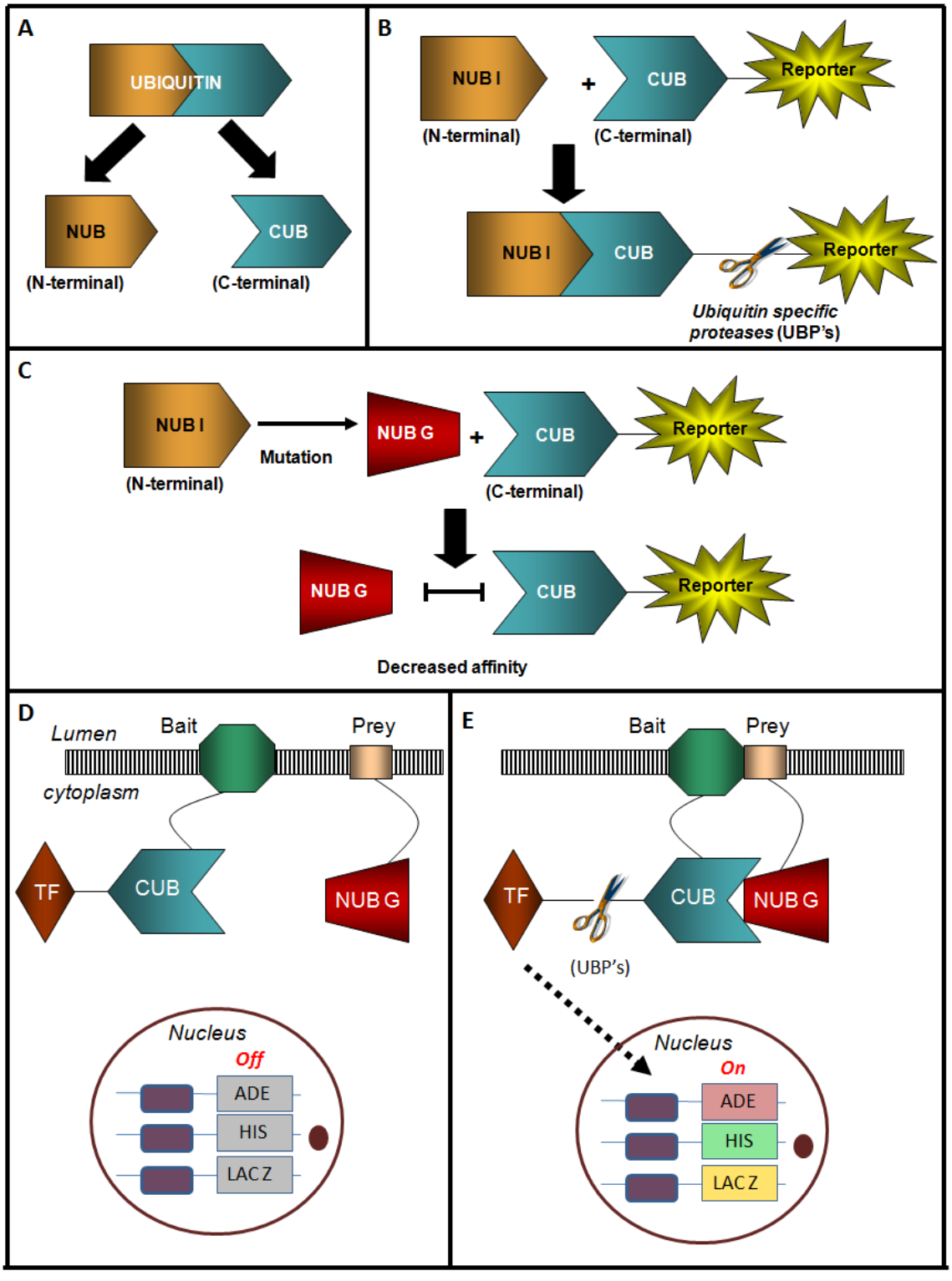
A
UBIQUITIN
NUB
(N-terminal)
CUB
(C-terminal)
B
NUB I
(N-terminal)
+
CUB
(C-terminal)
Reporter
NUB I
CUB
Reporter
Ubiquitin specific proteases (UBP's)
C
NUB I
(N-terminal)
Mutation
NUB G
+
CUB
(C-terminal)
Reporter
NUB G
CUB
Reporter
Decreased affinity
D
Lumen
Bait
Prey
cytoplasm
TF
CUB
NUB G
Nucleus
Off
ADE
HIS
LACZ
E
Bait
Prey
TF
CUB
NUB G
(UBP's)
Nucleus
On
ADE
HIS
LACZ

The MYTH system has permitted screening of NubG human cDNA and yeast open reading frame (ORF) libraries to identify protein interaction partners for several membrane proteins (Stagljar et al., 1998, Thaminy et al., 2003). However, to date MYTH has not been modified for use with outer mitochondrial membrane (OMM) proteins. We hypothesized that optimizing and applying the MYTH for use with mitochondrial membrane proteins would enable large scale screening of cDNA/ORF libraries to identify novel protein interaction partners of KMO. To this end, in this chapter we describe optimisation of MYTH for use with OMM proteins, in particular with yeast and human KMO.

3.2 RESULTS

3.2.1 A mitochondrial bait is functional in the MYTH system

As in any Y2H, it is essential in the MYTH that the bait is correctly expressed and that there is no self activation of the bait. In the MYTH system, it is also imperative to ensure that the bait localises to the correct membrane.

Membrane specificity in the MYTH system is determined via the NubG/NubI test, which ensures correct expression and localisation of the bait. The NubG/I test is based on the principle that if a bait fused to the Cub domain interacts with the prey control (i.e. a protein of known cellular localisation fused to wild type NubI), Nub and Cub are brought together to reconstitute functional ubiquitin because of their close proximity in the same membrane. For this to occur, the bait must be correctly expressed and localized in the same membrane as the prey fused to NubI, with the Cub domain and transcription factor in the cytosol (Figure 3-2).

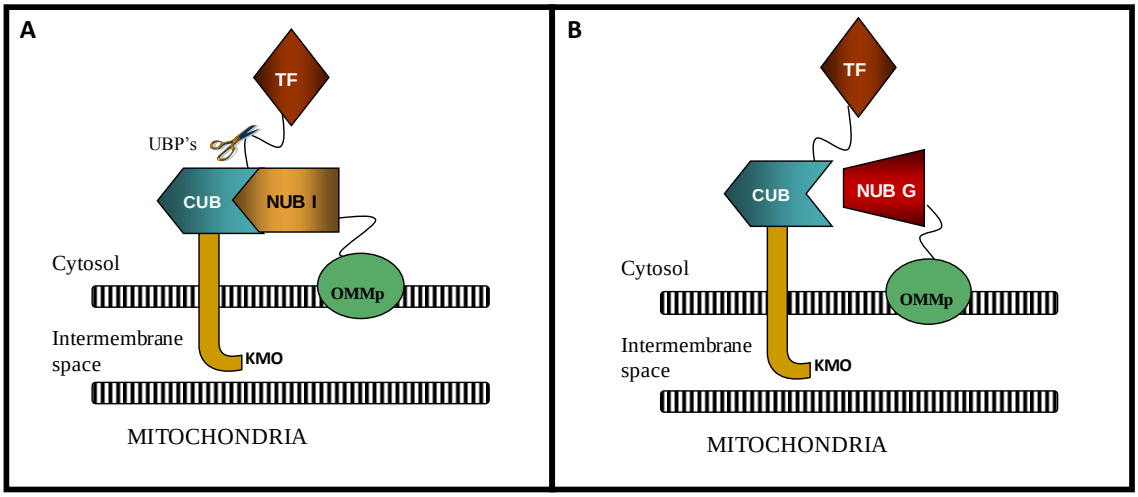

Figure 3-2: Overview of the NubG/I test

OMMp (a protein that localises to the outer mitochondrial membrane) is used as a prey control to illustrate the principle of the NubG/I test. OMMp localises to the outer mitochondrial membrane in yeast. (A)When OMMp-NubI and KMO-Cub bait are co-expressed, they are expected to interact if the bait - localises correctly to the mitochondria and is functional i.e. is oriented correctly with the Cub domain in the cytosol. (B) If there is no known interaction between OMMp and KMO, OMMp-NubG and KMO will not interact. Hence, if the bait is correctly localised and functional, reporter gene activity is expected only with OMMp-NubI and not with OMMp-NubG.

3.2.1.1 Designing prey controls for the NubG/I test

For the development of MYTH for OMM proteins, two OMM proteins: Mmm1 and Tom20 that localise to the outer mitochondrial membrane were chosen (Pfanner and Neupert, 1990, Burgess et al., 1994, Pfanner et al., 2004). Ost1, an endoplasmic reticulum protein (Pathak et al., 1995) and Fur4, a plasma membrane protein (Chevallier and Lacroute, 1982, Silve et al., 1991) previously used in MYTH studies (Stagljar et al., 1998, Iyer et al., 2005) were chosen as additional controls to ensure that there is no mislocalisation of the bait. Empty NubG vector was used as negative control to ensure that no self activation of the bait occurs.

The genes encoding the selected proteins were cloned into NubG and NubI vectors respectively to create the prey controls by standard approaches (see section 2.2.1.1). Yeast bearing KMO-Cub were transformed with the prey controls and assessed by growth assays (Figure 3-3A&B) and β-galactosidase assays (Figure 3-4) to measure reporter gene activity. Activity of the reporter genes *ADE2* and *HIS3* was measured by growth assays done on appropriate selective media lacking adenine and histidine supplemented with 3-aminotriazole (3-AT) (a competitive inhibitor of *HIS3* gene product) and β-galactosidase activity was measured by liquid LacZ assays as described in (see section 2.2.11 & 2.2.12).

Since Mmm1/Tom20 and KMO/Bna4 are predicted to localise to the same membrane, interaction between KMO-Cub with Mmm1-NubI/Tom20-NubI should result in the activation of reporter genes. As there is no known interaction between Mmm1/Tom20 and KMO/Bna4, we do not expect to see any reporter gene activity in yeast co-expressing KMO-Cub and Mmm1-NubG or Tom20-NubG. The findings from the growth assay (Figure 3-3A&B) and LacZ assay (Figure 3-4) were in accordance with this. Only background levels of reporter gene activity was observed between KMO/Bna4 and any of the prey controls tagged with NubG or with the empty NubG vector, indicating that there

Figure 3-3: Confirming functionality of KMO and Bna4 bait in MYTH using the NubG/I test

Growth assay for KMO bait (A) and Bna4 (B) with different prey controls were carried out to verify the expression of reporter genes *ADE2* and *HIS3*. Overnight cultures of yeast cells bearing the bait and the prey controls were serially diluted and plated on selective media lacking adenine and histidine supplemented with 3AT. The plates were incubated at 30°C for 2-3 days. The growth of colonies observed is directly proportional to the levels of reporter genes activated. As expected we see higher growth in yeast expressing KMO/Bna4 + Mmm1 NubI and KMO/Bna4 + Tom20 NubI which are mitochondrial controls. We also see reporter gene activity in yeast expressing ER protein: KMO/Bna4+Ost NubI. Very minimal growth is seen in yeast expressing KMO/Bna4+ Tom20/Mmm1/Ost1/Fur4 NubG or KMO/Bna4 + NubG (empty vector).

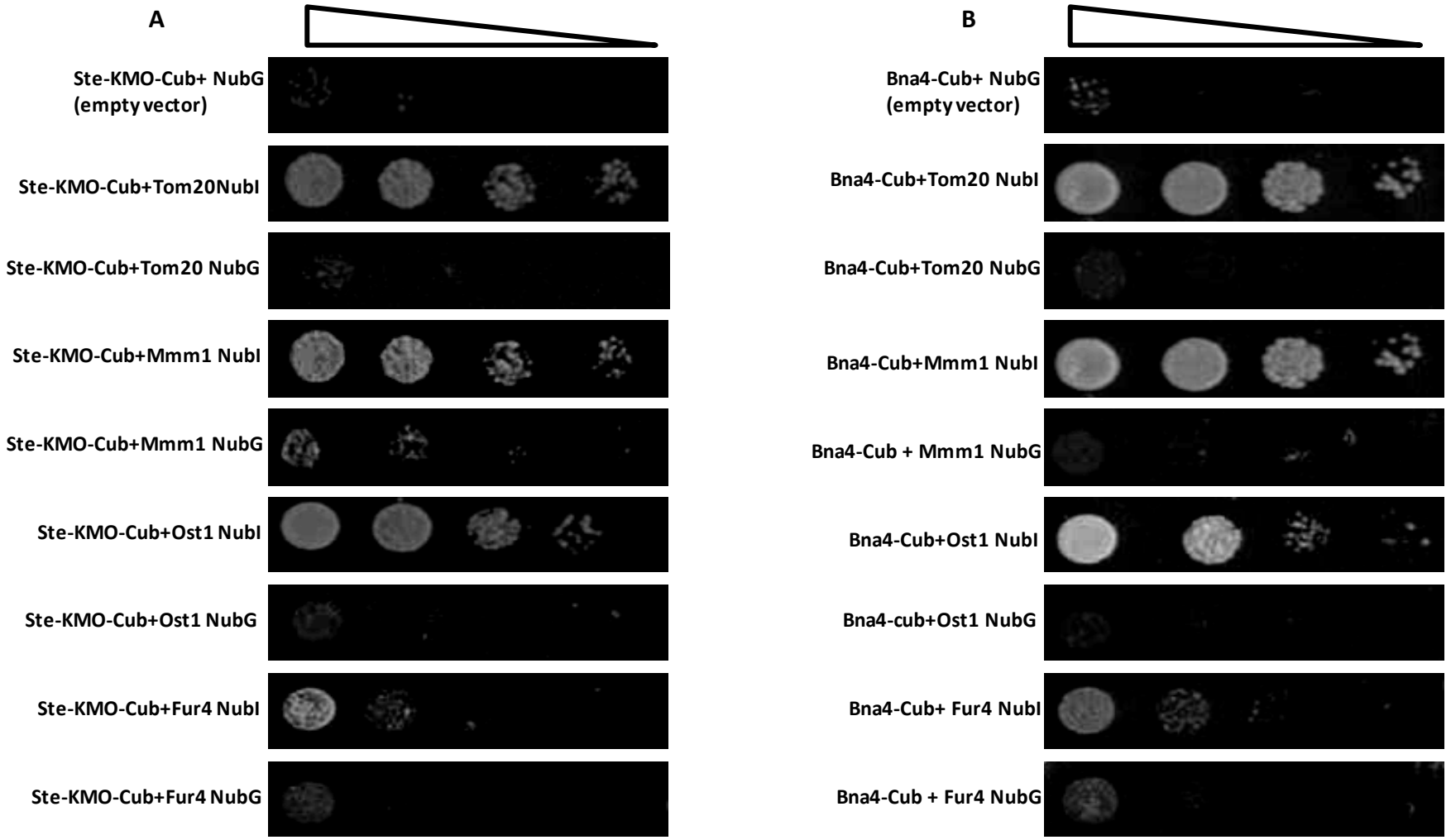
A
Ste-KMO-Cub+ NubG
(empty vector)
Ste-KMO-Cub+Tom20NubI
Ste-KMO-Cub+Tom20 NubG
Ste-KMO-Cub+Mmm1 NubI
Ste-KMO-Cub+Mmm1 NubG
Ste-KMO-Cub+Ost1 NubI
Ste-KMO-Cub+Ost1 NubG
Ste-KMO-Cub+Fur4 NubI
Ste-KMO-Cub+Fur4 NubG
B
Bna4-Cub+ NubG
(empty vector)
Bna4-Cub+Tom20 NubI
Bna4-Cub+Tom20 NubG
Bna4-Cub+Mmm1 NubI
Bna4-Cub + Mmm1 NubG
Bna4-Cub+Ost1 NubI
Bna4-cub+Ost1 NubG
Bna4-Cub+ Fur4 NubI
Bna4-Cub + Fur4 NubG

Figure 3-4: Confirming functionality of KMO and Bna4 bait in MYTH using the NubG/I test

One of the reporters in the MYTH is LacZ. The LacZ activity is measured by assaying for levels of β-galactosidase activity of cells expressing the bait-KMO/Bna4 and prey controls. B-galactosidase levels were assayed for by measuring OD420 of ONPG that gives yellow colour the intensity of which is proportional to concentration of enzyme β-galactosidase. High levels of β-galactosidase activity was observed in yeast expressing KMO/Bna4 + Mmm1 NubI and KMO/Bna4 + Tom20 NubI which are mitochondrial controls and KMO/Bna4+Ost NubI, an ER control. Little or no LacZ activity is seen in yeast expressing KMO/Bna4 + Tom20/Mmm1/Ost1/Fur4 NubG or KMO/Bna4 + NubG (empty vector) The data shown represent the average of at least three independent experiments and the error bars represent the standard deviation.

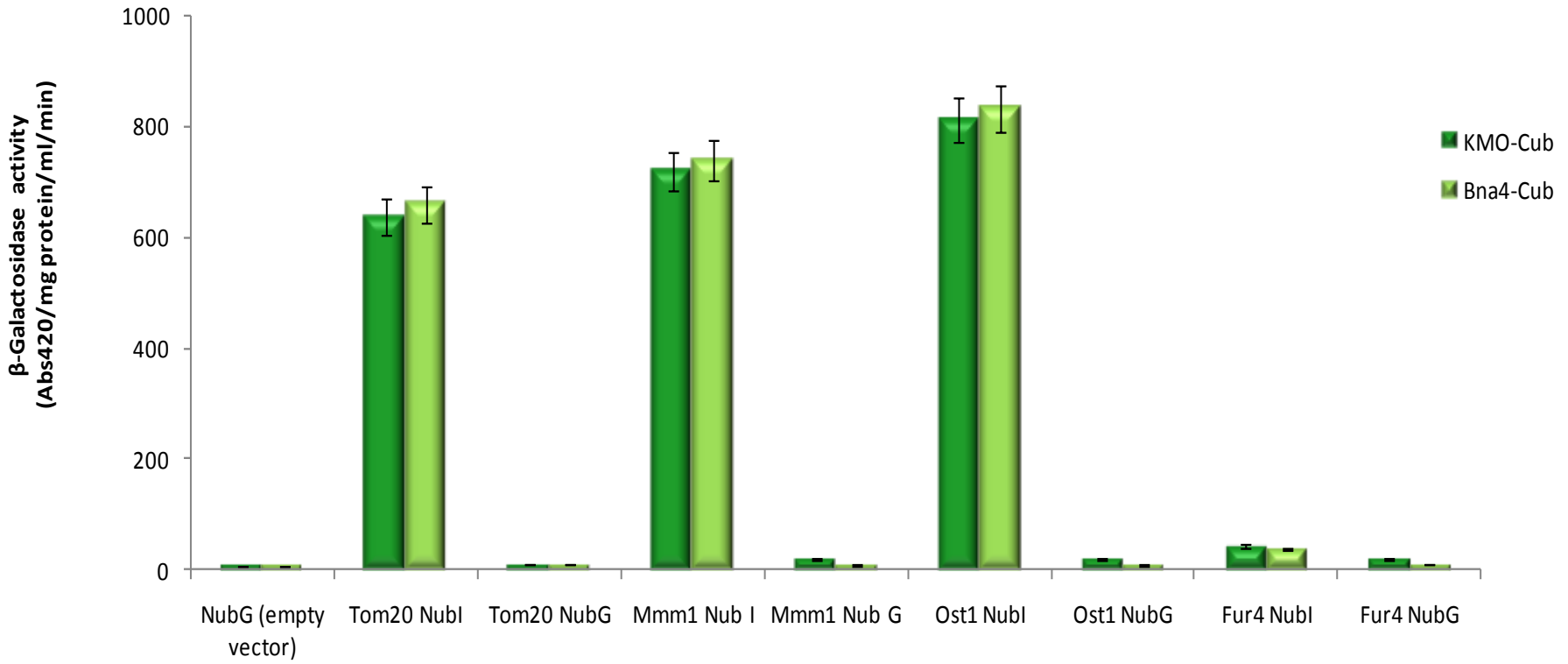
β-Galactosidase activity (Abs420/mg protein/ml/min)
1000
800
600
400
200
0
KMO-Cub
Bna4-Cub
NubG (empty vector)
Tom20 NubI
Tom20 NubG
Mmm1 Nub I
Mmm1 Nub G
Ost1 NubI
Ost1 NubG
Fur4 NubI
Fur4 NubG

is no self-activation by the bait construct. However, an interaction between KMO/Bna4 and Ost1-NubI which is an ER protein was also observed, this is suggestive that some KMO/Bna4 may also be localised to the ER in our system. Subsequent to the above work, Kornmann et al. showed that Mmm1 tethers the mitochondria and the ER (Kornmann et al., 2009), indicating that some of the reporter activity observed in the Mmm1 NubG/NubI test with KMO may be due to ER localization. However, my observations with Tom20 suggested that at least most of the KMO was correctly targeted to the mitochondria, I chose to further explore KMO localization by co-localization studies (see section 3.2.2).

3.2.1.2 Ste2 deletion reduces high background in pBna4-Cub bait

As described in section 2.2.1.1, both Bna4 and KMO were cloned by homologous recombination into the pCCW-Ste vector. The Ste2 sequence immediately upstream to the bait acts as a leader sequence that ensures the correct transcription of DNA to mRNA and ensures optimal expression of the fusion protein (Iyer et al., 2005). Whilst optimising the 3-AT levels such that there is no self-activation of the NubG (empty vector), it was observed that pBna4-Ste-Cub required 180 mM 3-AT concentrations while 120 mM 3-AT concentrations were sufficient for pKMO-Ste-Cub bait (data not shown). Since this optimised concentration would be later used during screening, we had concerns that high levels of 3-AT, while controlling the false positives/background, would also have the potential to mask true protein interactions and thereby increase the rate of false negatives in the screen (Stagljar et al., 1998, Iyer et al., 2005). It has been previously observed that deletion of the Ste2 signal can reduce levels of background in this system (Igor Stagljar, personal communication). Hence the Bna4 bait was redesigned by deleting Ste2 and comparative studies between pBna4-Ste-Cub and pBna4-Cub showed that pBna4-Cub required lower levels of 3-AT-120mM (Figure 3-5) comparable to pCCW-Ste-KMO-Cub.

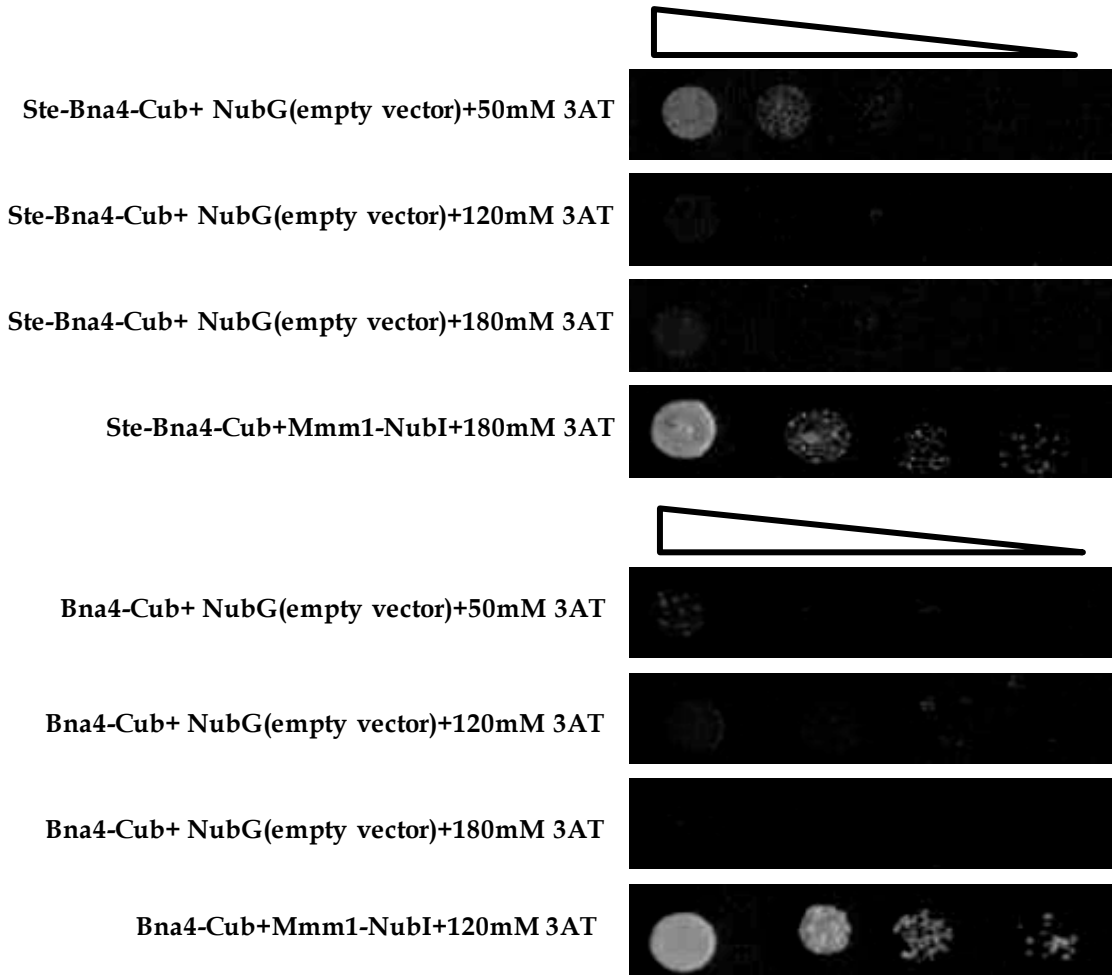

Figure 3-5: Ste2 deletion reduces background with Bna4 bait plasmid

Growth assay for Bna4-Ste-Cub bait (A) and Bna4-Cub (B) with NubG (empty vector) and Mmm1-NubI were carried out to titrate the levels of 3-AT required to reduce background. Overnight cultures of yeast cells bearing the bait and the prey controls were serially diluted and plated on selective media lacking adenine and histidine supplemented with 3AT. The plates were incubated at 30°C for 2-3 days. The growth of colonies observed is directly proportional to the levels of reporter genes activated. A relatively high background is observed with (A) Bna4-Ste-Cub+NubG (empty vector) consequently requiring more 3-AT which in turn affects the growth of cells bearing Bna4-Ste-Cub+Mmm1-NubI. This is overcome when (B) Ste is deleted as Bna4-Cub shows less background and thereby requires less 3-AT.

While producing less background, the NubG/I test with pBna4-Cub showed similar, if not slightly more robust, growth than pBna4-Ste-Cub, further underscoring the optimisation achieved (Figure 3-5).

3.2.2 pKMO-Cub is expressed and localized to the outer mitochondrial membrane

As discussed above, pKMO-Cub localisation to the mitochondria using the NubG/I test was not clear. In order to understand which membrane our bait localised to, indirect immunofluorescence studies with KMO antibody were performed on fixed yeast cells. Cells were pre-stained with a mitochondrial staining dye (MitoTracker red CMXRos (Invitrogen)) as described in section 2.2.18. A z-series of optical sections through the yeast cell shows pKMO-Cub was directed to the mitochondria, which either appear as filamentous or punctuate green spots (Figure 3-6A). Based upon our observations with Ost1 above, we also performed co-localization studies with KMO and Pex3, an ER protein (Tam et al., 2005), tagged with RFP. pKMO-Cub did not co-localise with Pex3-RFP (Figure 3-6E) indicating that that despite the Ost1 NubG/I results, the vast majority of KMO is localised to the OMM.

Since Mmm1 was also designed to be used as a control in the OMM-MYTH system and screen (see section 3.2.3), it was important to verify the localisation of the Mmm1 by microscopy as well. To this end, cells expressing Mmm1-NubG/I-RFP were co-stained with the mitochondrial dye MitoTracker Green (Invitrogen) and co-localisation studies were performed via confocal microscopy. The mitochondria identified by MitoTracker Green presented a characteristic filamentous/punctate staining pattern. RFP fluorescence from the tagged Mmm1-NubG/I-RFP constructs showed a similar pattern of cellular localization, which co-localized with MitoTracker Green (Figure 3-6B), indicating that Mmm1 prey constructs are localized to the mitochondria in the MYTH strain used in our experiments.

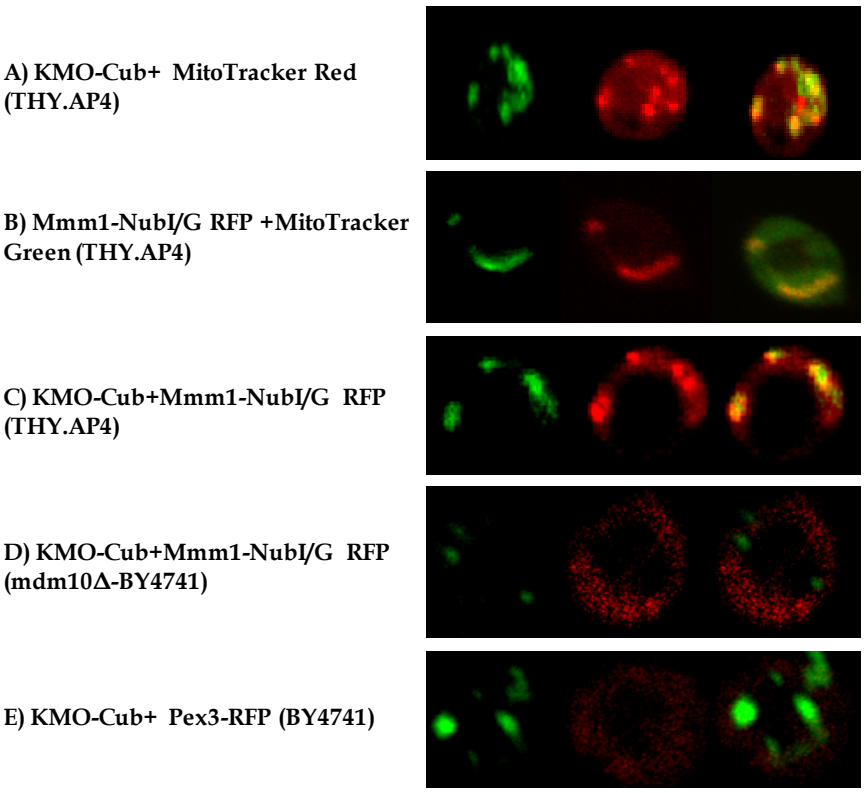

Figure 3-6: Microscopic examination confirms KMO fusion bait localises to the Mitochondria

(A) Shows co-localisation of MitoTracker and KMO bait. Indirect immunofluorescence was performed on yeast bearing KMO. Cells were stained with MitoTracker CMXRos that fluoresces' red and were fixed and incubated with primary antibody followed by Alexa Fluor secondary 488 antibody that fluoresces green. Mitochondrial staining is observed as punctuate spots. (B) Live cells bearing Mmm1-NubI-RFP were stained with 20nm MitoTracker™ Green for 30 minutes and then examined. Overlap between Mmm1-RFP fluorescence and MitoTracker™ Green fluorescence suggests mitochondrial expression. Indirect Immunofluorescence was repeated again with KMO fusion bait and: (C) Mmm1-NubI/G-RFP, co-localisation confirms interaction in the NubG/I test (D)Mmm1-NubI/G-RFP (mdm10Δ) and (E) Pex3-RFP, lack of co-localisation confirms that KMO fusion bait is not mislocalised to ER.

Microscopic studies by Kornmann et al., have shown that the localization of Mmm1 shifts from the mitochondria to the ER in the absence of certain mitochondrial proteins that it interacts with: Mdm10, Mdm12 and Mdm34, which form a complex that tethers the ER and mitochondria, known as the ERMES complex (Kornmann et al., 2009). Hence, we investigated whether in our hands Mmm1 expression (Figure 3-6C&D) in cells lacking Mdm10 showed ER staining pattern. Our data backed the findings by Kornmann et al., where we found a shift in staining pattern of Mmm1 from mitochondria (punctuate spots) to ER (diffused circular stain) in the absence of the mitochondrial protein Mdm10. However, this did not affect the staining pattern of KMO which co-localised with Mmm1-NubG/I-RFP in the presence of Mdm10 (Figure 3-6C) and did not co-localise to Mmm1-NubG/I-RFP when *MDM10* was deleted (Figure 3-6D). These data collectively show that the KMO fusion bait localises to the mitochondria and is not mislocalised to the ER.

3.2.3 pMmm1-Cub is a suitable control bait in the OMM-MYTH for elimination of false positives

Another important control in optimising the MYTH system for OMM proteins is designing a suitable negative control bait. The bait control is used in the MYTH screen to isolate protein interactions specific to the protein of interest and to reduce the rate of false positives (Iyer et al. 2005). Mostly, the control bait is chosen such that it localises to the same membrane as the bait. We chose protein Mmm1 as the control bait, which has the advantage of being ER/mitochondrial protein and in the MYTH screening strain shows mitochondrial staining/localisation. *MMM1* was cloned into the pCCW-Ste bait as described earlier (see section 2.2.1.1). To ensure that Mmm1 was functional as bait in the MYTH, it was subjected to NubG/I test as described in section 3.2.1. As expected from our functional results above, we found the Mmm1-Cub bait localises to the same membranes as Mmm1-NubI (OMM) and Ost1-NubI (ER) based upon the interactions observed in the NubG/I test - both the growth assay and the LacZ assay (Figure 3-7A&B).

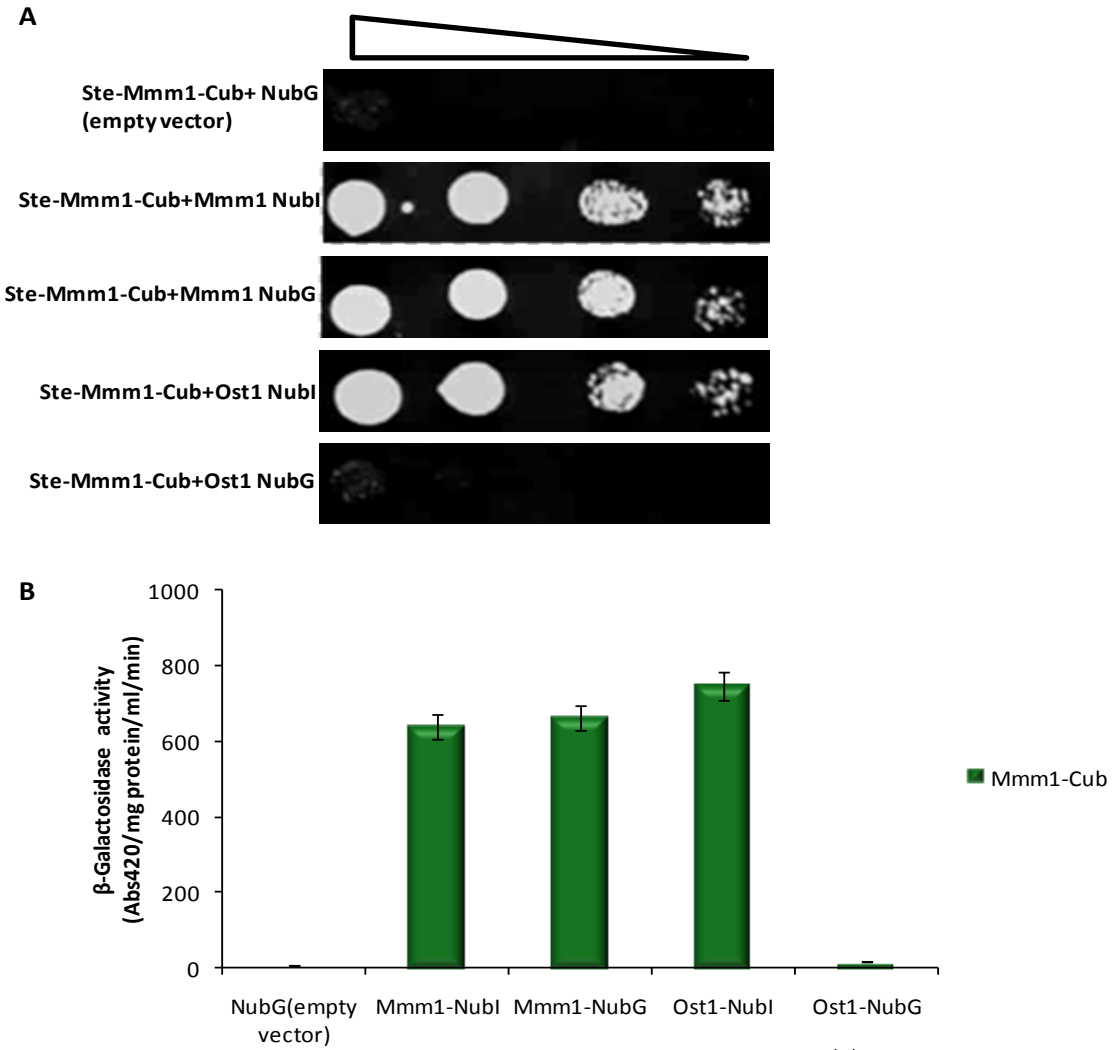

Figure 3-7: Mmm1 fusion (control) bait is functional in the MYTH system

(A)Growth assay for Mmm1 with different prey controls were carried out to verify the expression of reporter genes *ADE2* and *HIS3*. Overnight cultures of yeast cells bearing the bait and the prey controls were serially diluted and plated on selective media lacking adenine and histidine supplemented with 3AT. The plates were incubated at 30°C for 2-3 days. The growth of colonies observed is directly proportional to the levels of reporter genes activated. Higher growth as observed with Mmm1-NubI and Ost1-NubI suggests the bait fusion protein is correctly expressed in the ER. Interaction with Mmm1-NubG indicates that the protein interacts with itself. Very minimal growth is seen in yeast expressing Mmm1 and NubG (empty vector) indicating there is no self activation. (B)To measure LacZ activity β-galactosidase levels were assayed for by measuring OD_{420} of ONPG that gives yellow colour the intensity of which is proportional to concentration of enzyme β-galactosidase. The LacZ assay data confirms the data from growth assay and hence Mmm1 fusion bait is correctly targeted. The data shown represent the average of at least three independent experiments and the error bars represent the standard deviation.

There is no self-activation of the bait since there is very minimal background activity observed with NubG(empty vector) and Ost1-NubG. From literature we know that Mmm1 interacts with itself (Miller et al., 2005) which is confirmed by the NubG/I test where we observe interaction between Mmm1-Cub and Mmm1-NubI/G.

Since our mitochondrial fusion baits-KMO and Bna4 - are correctly expressed, localised, and lack self-activation they can be used for genome-wide screening.

3.3 DISCUSSION

Understanding complex interactions between mitochondria and other cellular components is vital for understanding how mitochondria functions in normal and disease states. The basis of these interactions is characterized by specific protein-protein interactions that mediate communication between the cellular components and mitochondria.

Y2H based approaches have been used widely identify protein interaction partners of proteins of interest. They are relatively simple, efficient and easy to use and the *Saccharomyces cerevisiae* used in Y2H analysis is a well understood organism. Large scale screens can be carried out using the Y2H and the system is sensitive enough to pick up weak or transient protein interactions (Van Criekinge and Beyaert, 1999).

One of the major disadvantages of the original Y2H is that it is not suitable for identifying protein interactions involving membrane proteins (Iyer et al., 2005). Many Y2H based approaches have been devised to make Y2H amenable for identifying protein interactions partners of membrane proteins including the MYTH, reverse RAS recruitment system (rRRS Y2H) and the G-protein fusion system (G-protein Y2H). rRRS Y2H uses the Ras signalling pathway in yeast as a selection mechanism. When localised to the plasma membrane, Ras is activated via GTP-GDP exchange by guanyl exchange factors-*cdc25* in yeast and son of sevenless (SOS) in mammals that through downstream signalling regulates

growth in yeast (Broder et al., 1998). In this system a mutant yeast strain carrying *cdc25-2,* a temperature sensitive allele that grows at 25°C but shows no growth at 36°C is used and the prey's are fused to a constitutively active mutant RAS (mRAS). Upon protein-protein interaction, mRAS is reconstituted to the membrane and overcomes *cdc25-2* mutation deficits to facilitate growth at 36°C (Hubsman et al., 2001). Although this system has been used to identify interactions of membrane proteins, one of the major disadvantages of this system is that when preys that are membrane proteins are fused to mRAS, the Ras signalling is activated in the absence of protein interaction requiring laborious selection processes to overcome false positives (Thaminy et al., 2003, Bruckner et al., 2009). The G-protein Y2H is based on a similar principle to rRRS Y2H and makes use of G-protein signalling. A membrane protein is used as a bait and the preys are fused to γ/β subunit of the heterotrimeric G-protein, protein interaction leads to sequestering of G-protein-β-subunits disrupting G-protein mediated signalling and thereby affecting cell growth (Ehrhard et al., 2000). This technique has not been applied widely and hence little is known of disadvantages associated with this technique.

The MYTH while offering all the advantages of the Y2H, also modifies and makes the Y2H based approach applicable for membrane bound proteins and comparatively less laborious to other membrane Y2H approaches. However, to our knowledge nobody has applied this technique to identify protein interaction partners of mitochondrial proteins in general, or OMM proteins in particular.

To implement the OMM-MYTH, our first step was to construct the baits, Bna4 and KMO, to be used in screening. We confirmed that the baits were cloned correctly into the vector by performing a restriction digestion analysis followed by sequencing of flanking regions. To confirm that the baits were functional, expressed and not self-activating, we performed the NubI/G test including both growth assays and β-galactosidase assays. For these assays

we designed specific OMM based controls: Mmm1-NubI/G and Tom20 NubI/G. In these assays, we observed Mmm1-NubI and Tom20-NubI interacting with the baits, indicating localisation of the baits to the same membrane. This suggests that the bait is expressed and correctly oriented with the Cub domain in cytosol. There is no known interaction between Mmm1 or Tom20 and KMO/Bna4 and hence we were not expecting interactions with Mmm1-NubG or Tom20-NubG (*Saccharomyces cerevisiae* genome database) and no interactions were observed. We also saw that there was no interaction with empty NubG vector indicating that our bait was not self-activating. This satisfies the three main concerns of the membrane two hybrid system: (a) the protein is correctly expressed (b) the protein is correctly oriented in the membrane of interest and (c) the protein is not self activating.

Additionally, in both the growth assays and β-galactosidase assays, we saw that the baits interact with Ost1-NubI in addition to Mmm1-NubI and Tom20-NubI. As discussed previously, for interaction to occur between prey control-NubI and the baits, both proteins must localise to the same cellular compartment. This would indicate that KMO and Bna4 localise to the ER membrane, at least transiently, in addition to the mitochondria. However there is no evidence that KMO is anything other than a mitochondrial protein (Alberati-Giani et al., 1997, SGDdatabase, 2007). This suggests possible mislocalization of our baits to other membranes.

While Mmm1 was annotated as a mitochondrial protein in SGD, work of Kronmann et al., showed that Mmm1 was a tethered to the ER (SGDdatabase, 2007, Kornmann et al., 2009). Therefore KMO interacted strongly with two ER proteins. This might be possible if KMO was being processed via the ER; however since mitochondrial proteins are not believed to be processed via the ER this is unlikely (Pfanner and Geissler, 2001). Therefore, at a cellular level, it rules out the possibility that KMO can interact with Ost1

unless its expression is not restricted to mitochondria alone, or the OMM is in close proximity to the ER. Thus, we further investigated the localisation pattern of KMO by indirect immunofluorescence studies which showed that KMO localised only to the mitochondria and not to any other membrane. Mmm1 in a normal yeast background also showed mitochondrial staining pattern. Thus in a parental yeast screening strain Mmm1 is closely associated with the mitochondria which accounts for the interactions we observed in the NubG/I test between Mmm1-NubI and KMO/Bna4-Cub. Next we explored the close association between mitochondria and the ER as a potential source of positive interactions using the ER specific control Ost1. We monitored the localization of Mmm1-NubI/G in the absence of *MDM10* and observed a dramatic shift to the ER compared with controls suggesting that close proximity might be responsible for the interaction observed between KMO/Bna4-Cub and Ost1-NubI. This observation could be further tested by exploring KMO/Bna4 interactions with Ost1-NubI/G in the *MDM10* deletion background and thus determining if ER based interactions in the OMM-MYTH are due to tethering of mitochondria to the ER. Nonetheless, our localization studies confirm that KMO is localized to the mitochondria, and functional tests with Tom20, further confirm localization to the mitochondria. Thus, using this system, we can screen for protein interaction partners of KMO and Bna4, with these proteins localized to the correct cellular compartment, and thus in their correct physiological state.

The other major concern in the optimisation process was the levels of 3-AT that were required to reduce the background. 3-AT is a competitive inhibitor of the *HIS3* gene product. Leaky expression of *HIS3*, a reporter in MYTH, has been observed and this increases the rate of false positives/background. Growth media supplemented with 3-AT reduces background due to leaky *HIS3* expression (Iyer et al., 2005). High levels of 3-AT in the screen could however mask weak transient interactions, the identification of which is

one of the important advantages of an Y2H based approach. Since the Bna4-Ste-Cub bait required higher levels of 3-AT we redesigned the bait by deleting the Ste2 sequence. The Ste2 sequence is a leader sequence that ensures optimal expression of the DNA (Igor Stagljar-personal communication). We found that deletion of Ste2 reduced background possibly because the presence of Ste2 increases transcription of Bna4 fusion protein which at high levels might be responsible for the background observed. 3-AT levels were re-optimised with this new Bna4 bait which required comparatively lower levels of 3-AT while not affecting the functional assay.

Thus in this chapter we have described creation and validation of new mitochondrial MYTH baits that are functional and ready to be used in the MYTH screen.

CHAPTER 4 IMPLEMENTING THE OMM-MYTH TO IDENTIFY PROTEIN INTERACTION PARTNERS OF KMO AND BNA4

4.1 INTRODUCTION

As discussed earlier (see section 1.2.1), KMO is an OMM enzyme in the KP and is a potential contributor to mHtt toxicity. In order to better understand KMO in health and disease we chose to identify protein interactions involving KMO in humans and yeast. To this end, the MYTH has been optimised to allow identification of protein interaction partners of KMO.

To characterise the protein interaction network of KMO, MYTH fusion baits were constructed for human KMO and its yeast orthologue Bna4. Bna4 bait was used to screen the yeast open reading frame (ORF) library in NubG-HA-X orientation, where X is the inserted ORF. To identify interaction partners of KMO, the KMO bait was used to screen a human fetal cDNA library in the NubG-HA-X orientation (Thaminy et al., 2003). The libraries in NubG-X orientation was chosen because the number of functional fusions between NubG and cDNA in NubG-X is reportedly higher than in X-NubG orientation (Iyer et al., 2005). Although both orientations of the libraries can identify cytoplasmic protein interactors, NubG-X library selectively identifies protein interactions involving type 2 integral proteins over type 1 integral proteins.

In the previous chapter we showed that OMM proteins can be functional as baits in MYTH. In this chapter we use the OMM-MYTH constructs to screen the respective libraries and identify novel protein interaction partners.

4.2 RESULTS

4.2.1 Optimising the OMM-MYTH screen

A small pilot screen was carried out using both KMO and Bna4 to screen their respective libraries. Yeast carrying bait constructs Ste-KMO-Cub and Bna4-Cub were transformed with the appropriate library and the positive interactors were selected by plating cells on selective media supplemented with 3-AT. A total of a million clones was screened in each of these initial screens, where more than 100 clones each were obtained. These numbers were far higher compared to screens conducted before (Thaminy et al., 2003, Pasch et al., 2005). Since it would not be feasible to test all such clones from a large scale screen, we optimised a 96-well plate β-galactosidase assay as a secondary screen to identify robust interactors. In this assay, the levels of β-galactosidase activity of KMO or Bna4 baits with Mmm1-NubI was used as a cut-off such that only putative interactors that had equal or higher β-galactosidase activity were processed further. By employing the 96-well plate β-galactosidase assay we could thus test all the clones that were identified from the primary screen.

4.2.2 OMM-MYTH screen identifies protein interaction partners of KMO and Bna4

The steps involved the OMM-MYTH screen is summarised in Figure 4-1. The human fetal cDNA library was transformed into the yeast strain THYAP4 that expressed KMO-Ste-Cub-TF as the bait and positive interactors were selected by plating cells on selective media supplemented with 3-AT. A total of 2 x 10^7 cDNA clones were screened and 928 initial candidate preys that displayed adenine and histidine prototrophy were selected. These initial preys were subjected to high-throughput β-galactosidase assays that identified 220 preys to be *LacZ*$^+$/*HIS3*$^+$/*ADE2*$^+$.

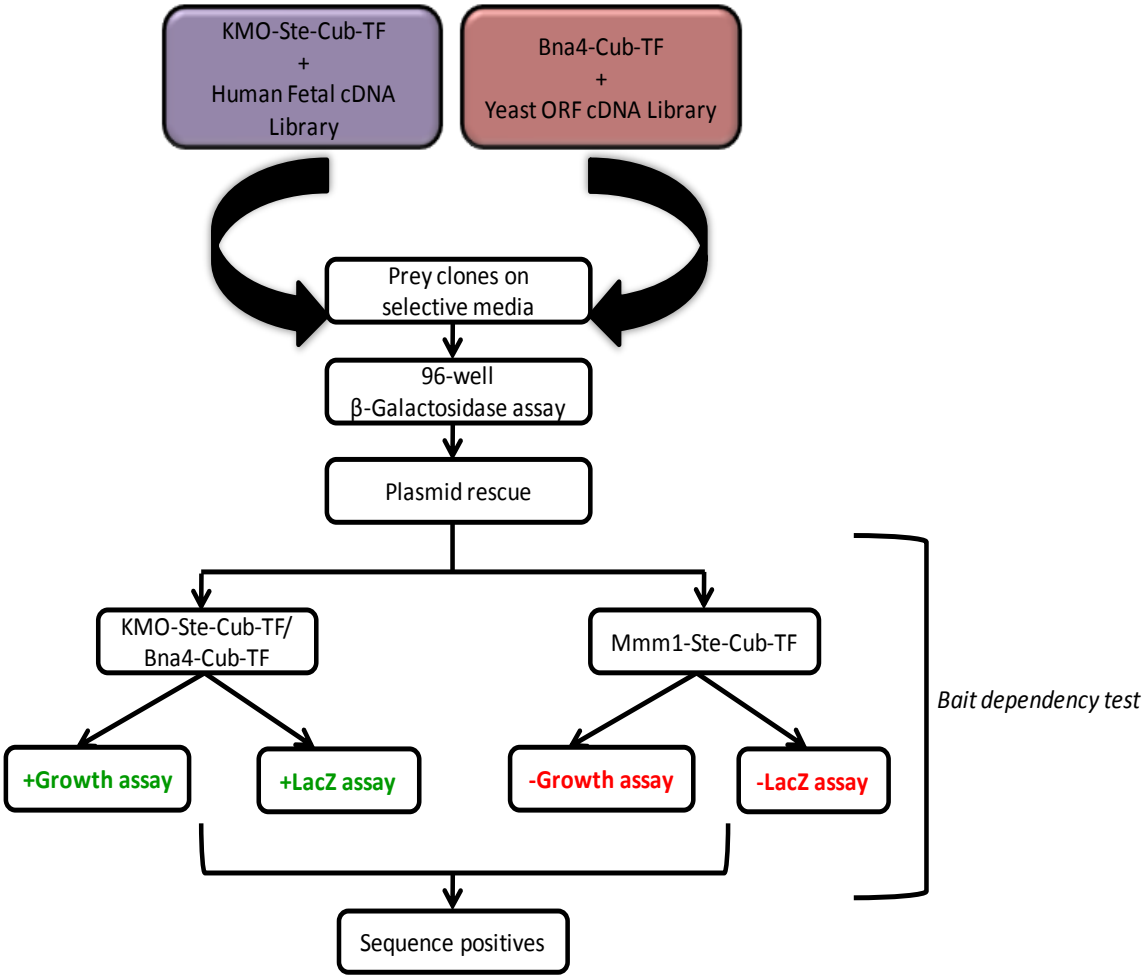

Figure 4-1: Overview of the OMM-MYTH screen

First step in the MYTH screen is a high efficiency transformation of human fetal cDNA into yeast bearing KMO. Plasmid rescue is performed and is re-transformed into yeast bearing (a) Ste-KMO-Cub-TF/Bna4-Cub-TF and (b) control bait which was Mmm1-Cub. Growth assay and LacZ assay were then carried out. Those plasmids that were positive in the growth assay and LacZ assay only with the KMO bait and negative with Mmm1 bait were sequenced. The re-validation of hits with control bait is referred to as bait dependency test.

Following plasmid rescue, the preys were subjected to bait dependency test where the library plasmids for the 220 preys were re-transformed into THYAP4 expressing the Ste-KMO-Cub-TF or Ste-Mmm1-Cub-TF. Growth assays and β-galactosidase assays were repeated. Out of the 220 prey clones, 52 clones showed KMO specific interaction and these putative interacting proteins were selected for DNA sequencing to verify their identity (see Figure 4-2, Table 4-1 & Table 4-2). The Bna4 screen was also carried out as described above. This screen resulted in total of 1430 preys, 290 of which showed robust β-galactosidase activity and were subjected to bait dependency tests. Following the bait dependency test, 32 preys that tested positive were then sequenced (Table 4-1 & Table 4-3).

Interestingly, the KMO interacting proteins identified from the screen included several proteins that are modifiers of mHtt toxicity (e.g. EEFIG) and 4 proteins (DCTN2, DYNC1HI, AP2M1 and GAPDH) that interact with huntingtin (Kaltenbach et al., 2007). Furthermore, proteins identified in the screen correlate to pathways such as endocytosis, signal transduction and energy metabolism that are compromised in HD and in which normal huntingtin protein plays a role. The implications of these protein interactions is briefly discussed later in this chapter and in much further detail in the latter chapters (Chapter 7). Similarly the hits obtained in the Bna4 screen were involved in processes such as energy metabolism, unfolded protein response and exocytosis which are implicated to play a role in HD (Landles and Bates, 2004). These results suggest KMO/Bna4 may a vital role in modulating pathogenecity in HD.

Table 4-1: Overview of the OMM-MYTH screen.

Screening Step	Bait	
OMM-MYTH Screen	KMO	Bna4
Total number of clones screened	2×10^7	2×10^7
Number of HIS3$^+$/ADE2$^+$ clones	928	1430
Number of HIS3+/ADE2+ /LacZ+ clones	220	290
Bait dependency test:		
Number of clones lacking HIS3$^+$/LacZ$^+$	136	240
Number of clones that interact with control bait	32	18
Putative bait specific interactions	52	32
Number of protein interaction partners	30	8

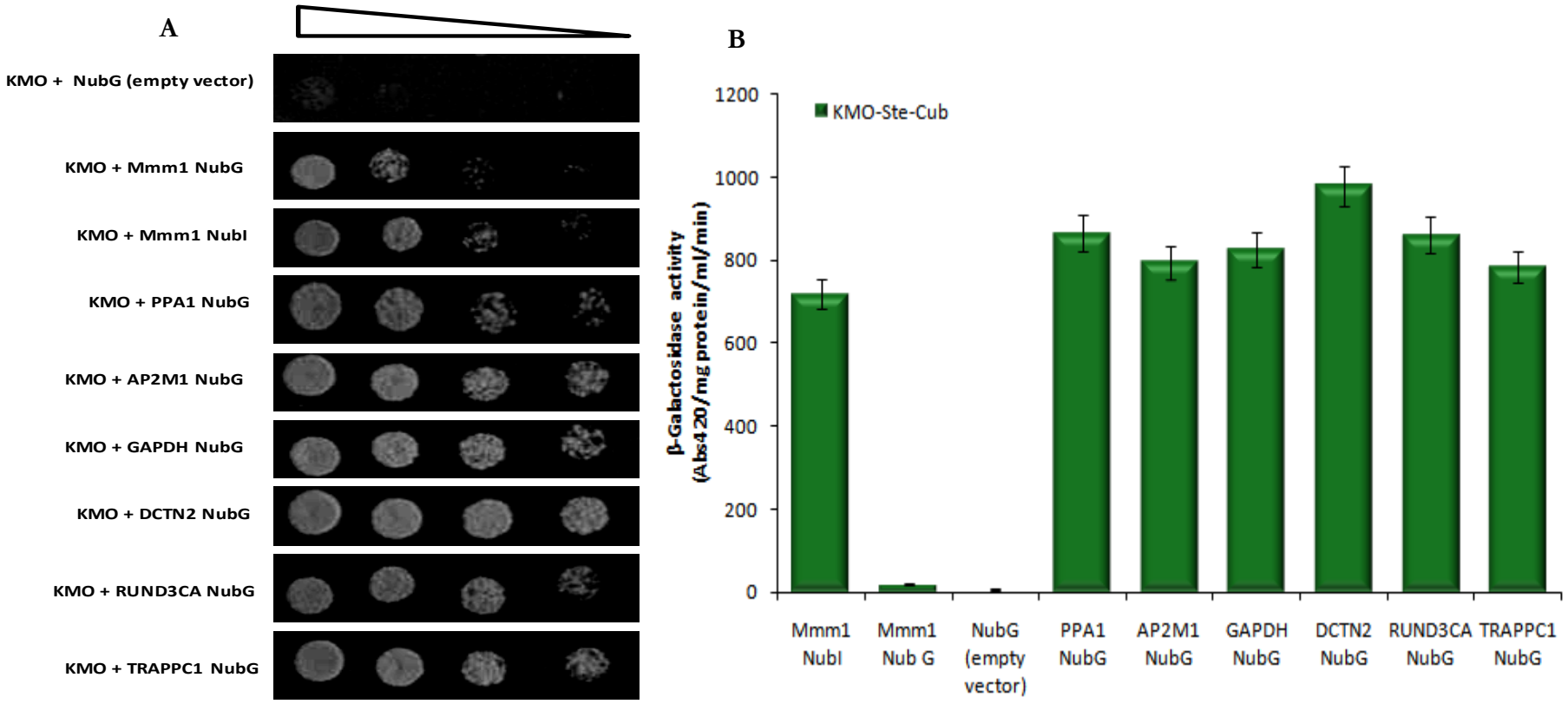

Figure 4-2: Confirmation of reporter gene activity in hits from OMM-MYTH screen

Figure shows reporter gene activity for a subset of hits obtained from the KMO OMM-MYTH screen confirmed by (a) Growth assays to measure for *ADE* and *HIS* reporter activity and (b) β-Galactosidase assays to measure LacZ activity. Yeast cells were co-transformed with hits from the screen and KMO bait and the levels of various reporters was analysed along with prey controls-Mmm1 NubI, Mmm1 NubG and NubG that were used as controls in both the growth assay and LacZ assay. The data shown represent the average of at least three independent experiments and the error bars represent the standard deviation. See Appendix 2 for reporter gene activity of putative KMO interactors from OMM-MYTH.

Table 4-2: Protein interaction partners of KMO from OMM-MYTH screen.

Functional category	Gene ID	Protein name	UNIPROT ID	No.of hits
Metabolism	GAPDH	Glyceraldehyde 3-phosphate	P04406	4
	CKB	Creatine Kinase Brain	P12277	4
	TALDO1	Transaldolase1	P37837	1
	TPI1	Triosephosphate isomerase 1 isoform 2	P60174	4
	PSMB5	Proteasome subunit beta type 5	P28074	1
	PPA1	Inorganic pyrophosphatase	Q15181	1
	ENO2	Gamma Enolase	P09104	1
	PSMA7	proteasome (prosome, macropain) subunit, alpha type, 7	O14818	1
	CBR1	Carbonyl reductase [NADPH] 1	P16152	1
Cytoskeleton organisation and biogenesis	DCTN2	Dynactin 2	Q13561	4
	DYNC1H1	Dynein, cytoplasmic 1, heavy chain 1	Q14204	1
	CFL1	Cofilin 1	P23528	1
	GSN	Gelsolin	P06396	3
Intracellular transport/ endocytosis	TRAPPC1	Trafficking protein particle complex 2	Q9Y5R8	4
	ICA1	Islet cell autoantigen1	Q05084	1
	COL1A1	Collagen alpha-1(I) chain	P02452	1
	BIN1	Myc box-dependent-interacting protein 1	O00449	1
	AP2M1	AP-2 complex subunit mu	Q96CW1	1
	SYNGR3	Synaptogyrin 3	O43761	1

Functional category	Gene ID	Protein name	UNIPROT ID	No.of hits
Signal transduction	RUNDC3A	RUN domain-containing protein 3A	Q59EK9	1
	SUMO2	Small ubiquitin related modifier 2	P61956	1
	PRKAR1B	cAMP-dependent protein kinase type I-beta regulatory subunit	P31321	4
	RAB3A	Ras-related protein Rab-3A	P20336	1
	PARF	Putative GTP-binding protein Parf	Q3YEC7	1
	GABARAPL1	GABA(A) receptor-associated protein like 1	Q9H0R8	1
Translation	RPL27	60S ribosomal protein L27	P61353	1
	EEF1G	Eukaryotic translation elongation factor 1 gamma	P26641	1
Chaperone	CCT7	Chaperonin containing TCP1, subunit 7 (Eta)	Q53HV2	1
Apoptosis	HEBP	Heme binding protein	Q05DB4	2
Transcriptional regulation	CCNC	Cyclin C	Q9UK58	1
Unknown Function	TTC27	Tetratricopeptide repeat domain 27	Q53HV2	1

Table 4-3: Protein interaction partners of Bna4 from the OMM-MYTH screen.

Functional Category	Gene ID	Protein Name	Functional Homologs in humans	No. of Hits
Metabolism	Utr1	ATP-NADH Kinase	NADK (Poly(P))/ATP NADH kinase	10
	Ade8	Phosphoribosyl-glycinamide transformylase	-	3
	Pro2	Gamma glutamyl phosphate reductase	Delta-1-pyrroline-5-carboxylate synthetase(P5C/ALDH18A1)	2
Exocytosis/cytoskeleton maintenance	Rho3	GTP-binding protein RHO3	Rho family GTPase: RND1, RND2 & RND3	4
Unfolded protein binding	Ssz1	Hsp70 protein	Heat shock proteins:72/73	6
Mannosidase activity	Dcw1	Putative mannosidase	-	3
	Pmt2	Protein O-mannosyltransferase	Protein O-mannosyltransferase 2:POMT2	2
Unknown Function	YHL026C	Uncharacterised protein	-	2

4.3 DISCUSSION

In this chapter we have applied the OMM-MYTH to identify protein interaction partners of two mitochondrial proteins: KMO and Bna4. The efficacy of this technique to identify protein interaction partners of mitochondrial proteins is demonstrated by the 31 novel protein interaction partners we have identified for KMO and the 8 unique protein interaction partners identified for Bna4.

As discussed in section 3.3, the split ubiquitin based MYTH approach is more advantageous compared to the classic Y2H. The MYTH offers the prospect of being able to identify protein-protein interactions in an in-vivo environment by using full-length membrane proteins (Van Criekinge and Beyaert, 1999, Iyer et al., 2005). The other advantage of the MYTH is the availability of cDNA libraries in both NubG-X and X-NubG (where X is the insert cDNA) orientations which allows for identification of both type I and type II integral protein interaction partners. The choice of library depends on the nature of protein interactions expected. In MYTH since the Nub and Cub must be in the cytosol for the system to be functional (see Figure 3-1 and Figure 3-2), using NubG-X libraries that tag the NH_2 terminus of a protein will contain only functional fusions with type II integral membrane proteins that have the N-terminus in the cytosol. Consequently, the X-NubG libraries contain functional fusions only with type I integral membrane protein where the COOH-terminal end in the cytosol is tagged with NubG (Iyer et al., 2005). Though ideally it might be ideal to screen using both libraries, in our study we have used the pDSL-Nx libraries that will identify protein interaction partners that include cytoplasmic and soluble membrane proteins as well as type II integral proteins. This was also the library of choice as it contains more functional fusions of proteins in this orientation (Iyer et al., 2005). Additionally, this orientation of the library yields less false

positives due to interaction between N-terminal ubiquitin and bait fused to Cub (Iyer et al., 2005).

3-AT titration and the need for optimising levels of 3-AT have been discussed in detail in Chapter 3 (sections 3.2.1.2 & 3.3). However, despite optimising levels of 3-AT, we observed more colonies on the screening plates than in our test conditions. To overcome this we developed the 96-well plate β-galactosidase assay. This optimised assay enables screening of all the clones and selectively identifying clones that are potentially true interactors based on robust LacZ activity. The clones that do not come through the LacZ screen are potential false positives, although they may include some weak interactors.

While MYTH overcomes some of the disadvantages of the classic Y2H making it more amenable for screening membrane protein interactions, some of the disadvantages of the Y2H such as a high rate of false positives persist in MYTH as well. There are a variety of reasons that can lead to false positives in an Y2H screen. These have been extensively reviewed by Serebriiskii et al (Serebriiskii et al., 2000). One of the reasons why clones that are positive in screening but fail in the LacZ activity has been suggested to be due to self activation of the bait (Iyer et al., 2005). The 3-AT titration potentially rules out false positives that arise due to leaky *HIS3* expression attributed to the self activation of the bait. However, overexpression of MYTH fusion constructs may lead to non-specific *HIS3* activation not dampened by 3-AT. While these overexpression problems might be overcome by endogenously tagging the yeast protein of interest (Paumi et al., 2007), it is not applicable if the bait is a non-yeast protein. Additionally, promoter mutations are another major cause of false positives; these mutations lead to non-specific activation of reporter genes, particularly the auxotrophic markers (Serebriiskii et al., 2000). The LacZ assay therefore helps eliminate these false positives. Some of the transformants that fail to

recapitulate the interaction when re-transformed also may belong to this category of false positives.

The bait dependency test additionally helps remove false positives that arise due to prey protein interacting with ubiquitin, "sticky" proteins (such as some ribosomal and proteasome proteins) or variations in copy number of the library plasmids (Serebriiskii et al., 2000, Thaminy et al., 2003). Thus the control assays that are an integral part of the OMM-MYTH helps overcome most of the false positives.

Following the bait dependency test the prey proteins were sequenced. Interestingly, out of the 31 protein interaction partners of KMO, four proteins are huntingtin interacting proteins. As shown by Kaltenbach et al., DYNC1H1 has been shown to interact with Htt in both pull down experiments and Y2H assay (Kaltenbach et al., 2007). DCTN2 and GAPDH have been shown to interact with Htt by Y2H assay. DCTN2 and DYNC1H2 interact with both normal (23Q) and mHtt (55Q) fragments while GAPDH interacts with mHtt (55Q) (Kaltenbach et al., 2007). In addition to GAPDH, KIPs showed enrichment for proteins involved in energy metabolism which is discussed further in Chapter 7.

Interestingly, the functional categories of KMO interacting proteins (KIPs) are related to pathways involving Htt and pathways that are compromised in HD. One of the major Htt associated functions in the cell is vesicle transport and maintenance of cytoskeleton structure as Htt interacts with components of the cytoskeleton complex such as dynactin, microtubules and β-tubulin (Landles and Bates, 2004). Htt is particularly involved in facilitating dynein/dynactin mediated vesicular transport (Caviston et al., 2007). Overexpression of DCTN2 causes disassociation of the dynein/dynactin complex (Burkhardt et al., 1997) and represses both endosome movement (Valetti et al., 1999) and retrograde transport leading to a late onset neurodegeneration-like phenotype (LaMonte et al., 2002, Perlson et al., 2009). Mutations in DCTN2 and DYNCH1 cause an adult onset

neurodegeneration phenotype characterised by reduced clearance of mHtt aggregates in the cell (Rogers et al., 2001, Ravikumar et al., 2005) suggesting even a slight compromise in functions of these two proteins can impair clearing of mHtt aggregates and affect intracellular transport in the cell. Similarly, Htt interacting protein AP2M1 plays a vital role in clathrin mediated endocytosis (Slepnev and De Camilli, 2000, Blondeau et al., 2004) which is also associated with Htt function (Landles and Bates, 2004) and is associated with recycling of synaptic vesicle membranes at the pre-synaptic surface (Blondeau et al., 2004, McPherson and Ritter, 2005) and is vital for uptake of cargo proteins (Motley et al., 2003). AP2M1 is implicated to play a role in HD and studies have shown that intrastriatal injection of neurotoxic KP metabolite-QUIN selectively reduces the expression of AP2 protein and its association with the membrane thereby impairing the endocytic machinery of the cell (Borgonovo et al., 2009).

Interestingly, apart from the Htt interacting proteins from the screen, other KIPs such as GSN (Qiao et al., 2005, Antequera et al., 2009), CKB (David et al., 1998, Aksenov et al., 2000), CFL1 (Maloney and Bamburg, 2007), may play a vital role in modulating toxicity in neurodegenerative diseases such as Alzheimer's disease apart from HD. The relevance of these interactions with regards to HD pathology and neurodegeneration is discussed in detail in Chapter 7.

Bna4 interacting proteins (BIPs) also fall into three major categories: energy metabolism, unfolded protein response and exocytosis. Although most of these proteins have functional homologs in humans, the functional homologs have not previously been implicated to play a role directly in neurodegeneration. One of these interactors *UTR1* has also been identified as a genetic interactor of *BNA4* (see Chapter 6). The significance of these interactions are further discussed in Chapter 6.

Thus, in this study we have optimised and implemented the OMM-MYTH system to successfully identify protein interaction partners of yeast and human KMO. The protein interaction partners correlate to pathways affected in HD. The potential significance of these interactions following further study is discussed in the forthcoming chapters.

CHAPTER 5 VALIDATING PROTEIN INTERACTION PARTNERS OF BNA4 AND KMO BY CO-IMMUNOPRECIPITATION

5.1 INTRODUCTION

To identify the protein interaction partners of KMO and Bna4, we have optimised and implemented an OMM-MYTH screen which has identified proteins that also interact with huntingtin protein. As discussed in the previous chapter, one of the major disadvantages of applying a Y2H approach to identify protein interactions lies with the high false positive rate associated with Y2H. It has been reported that as many as 50% of initial Y2H hits can be false positives (Serebriiskii et al., 2000). These false positives may arise due to transcriptional activation of the bait, expression levels of the baits, yeast mutations, etc. Hence, there is a requirement to validate hits from Y2H by alternative biochemical methods such as co-immunoprecipitation (Co-IP) experiments in order for them to be considered biologically relevant (Edwards et al., 2002, Dziembowski and Seraphin, 2004). Co-immunoprecipitation experiments have the ability to identify proteins that strongly or stably interact with the protein of interest. Although stringent test controls that are a part of the MYTH system should technically reduce the number of false positives observed, the hits from the MYTH were validated by Co-IP, an in-vitro approach, to further validate the interaction partners, as well as the screen itself.

In this chapter we use epitope tagged KMO and Bna4 constructs optimised for pull down experiments to confirm protein interactions identified from the OMM-MYTH screen by Co-IP analysis in yeast.

5.2 RESULTS

5.2.1 Co-IP analysis with KMO/Bna4-Cub-Myc tagged bait constructs

KMO and Bna4 constructs were used for the OMM-MYTH screen were tagged with 3-Myc by a PCR based approach (see section 2.2.1) to create pCCW-Ste-KMO-Cub-Myc and pCCW-Bna4-Cub-Myc constructs respectively. Yeast cells containing the KMO-Myc/Bna4-Myc construct and each of the HA-tagged preys from the screen were grown exponentially and used to generate protein extracts. The cell lysates were immunoprecipitated with anti-Myc conjugated agarose beads to pull down Myc tagged bait protein and the immunoprecipitates were examined by western blotting using anti-HA antibody. We could not observe any proteins corresponding to the size of HA tagged prey protein other than residual background (data not shown) thus indicating that the protein - protein interactions were not detected either because the tags prevented the expression of the bait/prey protein, the protein-protein interactions are weak/transient (cannot be detected by Co-IP), or were not true interactors and false positives from the OMM-MYTH. We probed for expression of the Myc tagged baits using anti-Myc antibody which could detect KMO (55Kd) and Bna4 (52Kd) at ~100Kd taking into consideration the size of the epitope tag and the Cub half. So clearly the bait fusion protein was expressed (Figure 5-1A). We also verified if the HA expression was detectable in the protein extracts (data not shown).

We reasoned that interactions between the baits and prey proteins could be weak/transient interactions, so we explored chemical crosslinking and UV based crosslinking as a method for "capturing" these transient interactions. Following optimisation of cross-linking conditions, yeast cells containing the KMO-Myc/Bna4-Myc construct and each of the HA-tagged preys from the screen were grown exponentially and treated with formaldehyde or

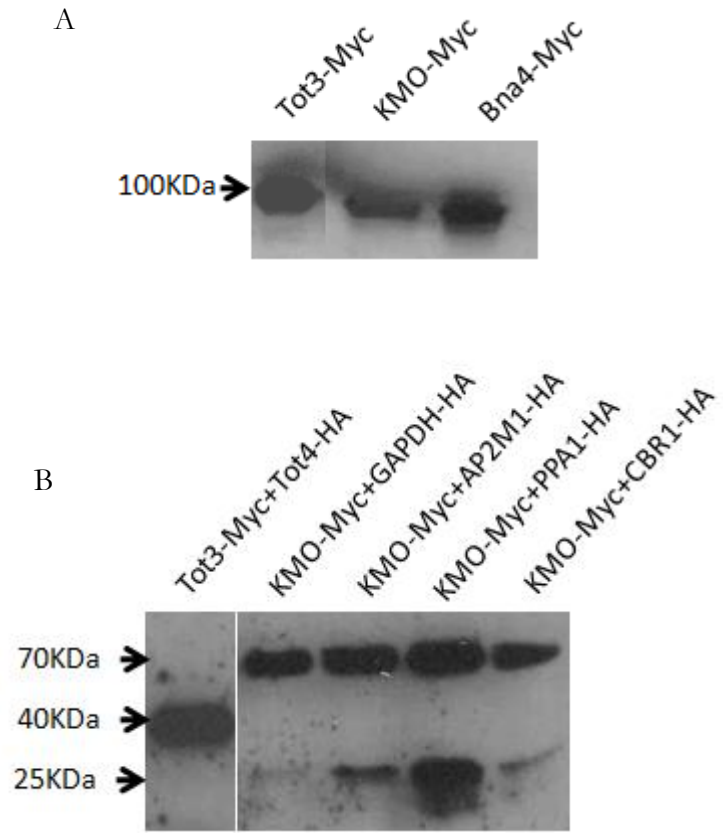

Figure 5-1: Co-Immunoprecipitation analysis using KMO-Myc and Bna4-Myc Baits

Protein interaction partners of KMO and Bna4 were validated by co-immunoprecipitation analysis. (A) The expression of KMO-Myc and Bna4-Myc were confirmed in the cell lysates prepared from yeast cells grown to exponential phase in rich media. (B) Protein lysates from yeast bearing KMO-Myc/Bna4-Myc were cross-linked with formaldehyde (final concentration=1%) before co-immunoprecipitation and western blot analysis using anti-HA antibody to study weak/transient protein interactions. Tot3-Myc and Tot4-HA were used as procedural controls.

subjected to UV-crosslinking before preparation of protein extracts (see section 2.2.13 & 2.2.14). The crosslinked cultures were used to generate protein extracts and the cell lysates were immunoprecipitated with anti-Myc conjugated agarose beads to pull down Myc tagged bait protein and the immunoprecipitates were examined by western blotting using anti-HA antibody (Figure 5-1B). Again no proteins corresponding to the size of HA tagged prey proteins were observed. This suggested that the Co-IP analysis were not failing due to the inability to detect weak/transient protein interactions, and that the tags were affecting interactions.

5.2.2 Co-IP analysis with KMO/Bna4-TAP tagged bait constructs

As it was possible that the Co-IP experiments were failing due to the tags being used, we choose to employ an alternate approach. The bait proteins were amplified and cloned into a vector containing a TAP tag using the Gateway cloning system to generate KMO-TAP and Bna4-TAP constructs (see section 2.2.13). The pull-down experiment was carried out as before: yeast cells containing KMO/Bna4-TAP and each of the protein interactors from the screen were grown exponentially before protein extraction was carried out. The cell lysates were immunoprecipitated with IgG sepharose to pull down TAP tagged bait. The immunoprecipiates were then examined by immunoblotting using anti-HA antibody.

5.2.2.1 Co-IP analysis using KMO-TAP bait

Co-IP experiments with KMO-TAP bait confirmed some of the protein interactions observed in the screen. However, one of the major drawbacks was the high background observed (Figure 5-2A). Different buffers were optimised for the IP but no significant change in the intensity of the background was seen (Figure 5-2B). This background could be attributed to the cleavage of the TAP protein and/or by the cleavage of IgG from the IgG sepharose beads that were used for the pull-down experiments which interfered with

Figure 5-2: Co-Immunoprecipitation analysis using KMO and Bna4 Baits

Protein interaction partners of KMO and Bna4 were validated by co-immunoprecipitation analysis. (A) KMO-TAP construct was used for Co-IP analysis. The cell lysates were immunoprecipitated with IgG sepharose to pull down TAP tagged bait. The immunoprecipiates were then examined by western blotting using anti-HA antibody. (B) To reduce the levels of background observed with the KMO-TAP bait, different buffer conditions were optimised. B60 buffer used for protein extraction was supplemented with 10% sucrose and was used for preparation of cell lysates and co-immunoprecipitation. (C) Co-IP analysis with Bna4-TAP bait showed marked degradation in both cell lysates and immunoprecipitates. Tot3-Myc and Tot4-HA were used as procedural controls.

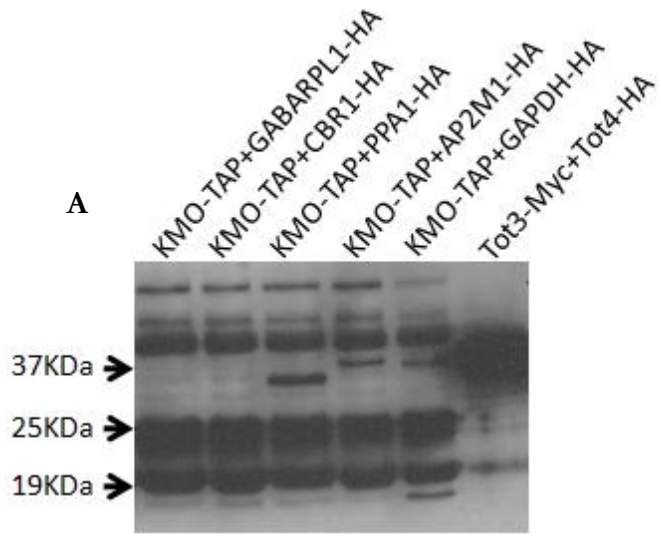
A
KMO-TAP+GABARPL1-HA
KMO-TAP+CBR1-HA
KMO-TAP+PPA1-HA
KMO-TAP+AP2M1-HA
KMO-TAP+GAPDH-HA
Tot3-Myc+Tot4-HA
37KDa
25KDa
19KDa

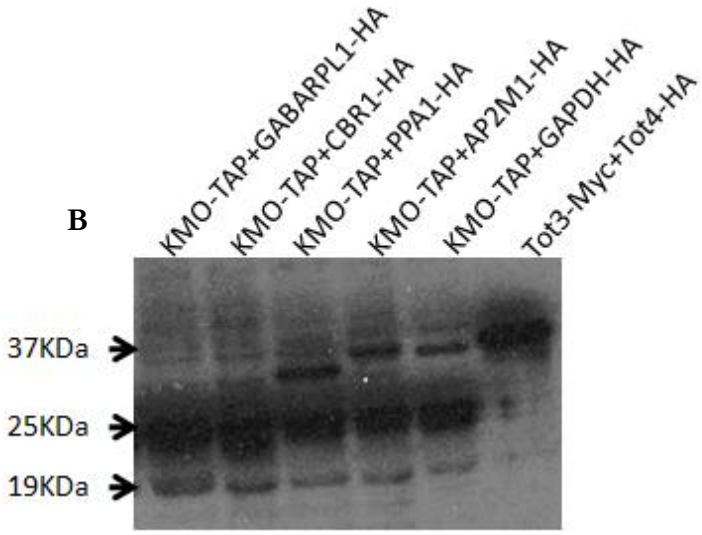
B
KMO-TAP+GABARPL1-HA
KMO-TAP+CBR1-HA
KMO-TAP+PPA1-HA
KMO-TAP+AP2M1-HA
KMO-TAP+GAPDH-HA
Tot3-Myc+Tot4-HA
37KDa
25KDa
19KDa

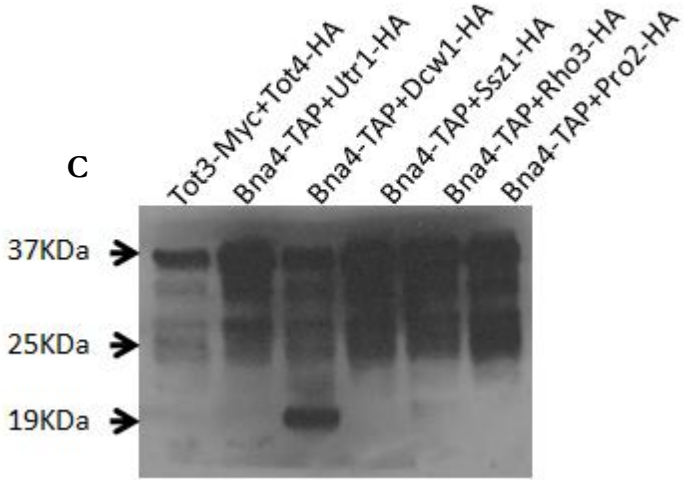
C
Tot3-Myc+Tot4-HA
Bna4-TAP+Utr1-HA
Bna4-TAP+Dcw1-HA
Bna4-TAP+Ssz1-HA
Bna4-TAP+Rho3-HA
Bna4-TAP+Pro2-HA
37KDa
25KDa
19KDa

detection of low molecular weight prey proteins such as GABARPL1(17Kd) and CBR1(26Kd) (Figure 5-2 A&B).

5.2.2.2 Co-IP analysis using Bna4-TAP bait

Co-IP analysis with Bna4-TAP was also not very successful as protein lysates and immunoprecipitates showed marked degradation of the prey protein (Figure 5-2C). Since the Co-IP was carried out in THYAP4 strain background that was used in the screen, we reasoned that the presence of native Bna4 in this yeast strain may result in degradation of Bna4-TAP tagged protein to maintain cellular homeostasis of Bna4. To test this hypothesis the Co-IP was then carried out from protein lysates generated from yeast cells deleted for *BNA4* (BY4741), which also did not show any improvement in the degradation pattern (data not shown). The degradation of proteins observed could be attributed to the large size of the TAP tag (21Kd) which could affect proper folding of the protein thereby leading to their degradation. Since the background from the TAP tag could also interfere with detecting protein interactions of the KMO bait in western blotting, the bait constructs were redesigned with another tag for the Co-IP analysis.

5.2.3 Co-IP analysis with KMO/Bna4-FLAG bait recapitulates protein interactions observed in the OMM-MYTH screen.

As a further attempt to assess protein-protein interactions biochemically, KMO-FLAG and Bna4-FLAG constructs were generated by Gateway cloning (see section 2.2.13). Yeast cells containing the KMO-FLAG construct and each of the HA-tagged preys from the screen were grown exponentially and used to generate protein extracts. The cell lysates were immunoprecipitated with FLAG coated magnetic Dynabeads to pull down FLAG tagged protein and the immunoprecipitates were examined by Western blotting using anti-HA antibody (Figure 5-3A). Using this approach we were able to confirm 17/23 (~75%) of the protein interactions identified by the OMM-MYTH screen, suggesting that the MYTH is a

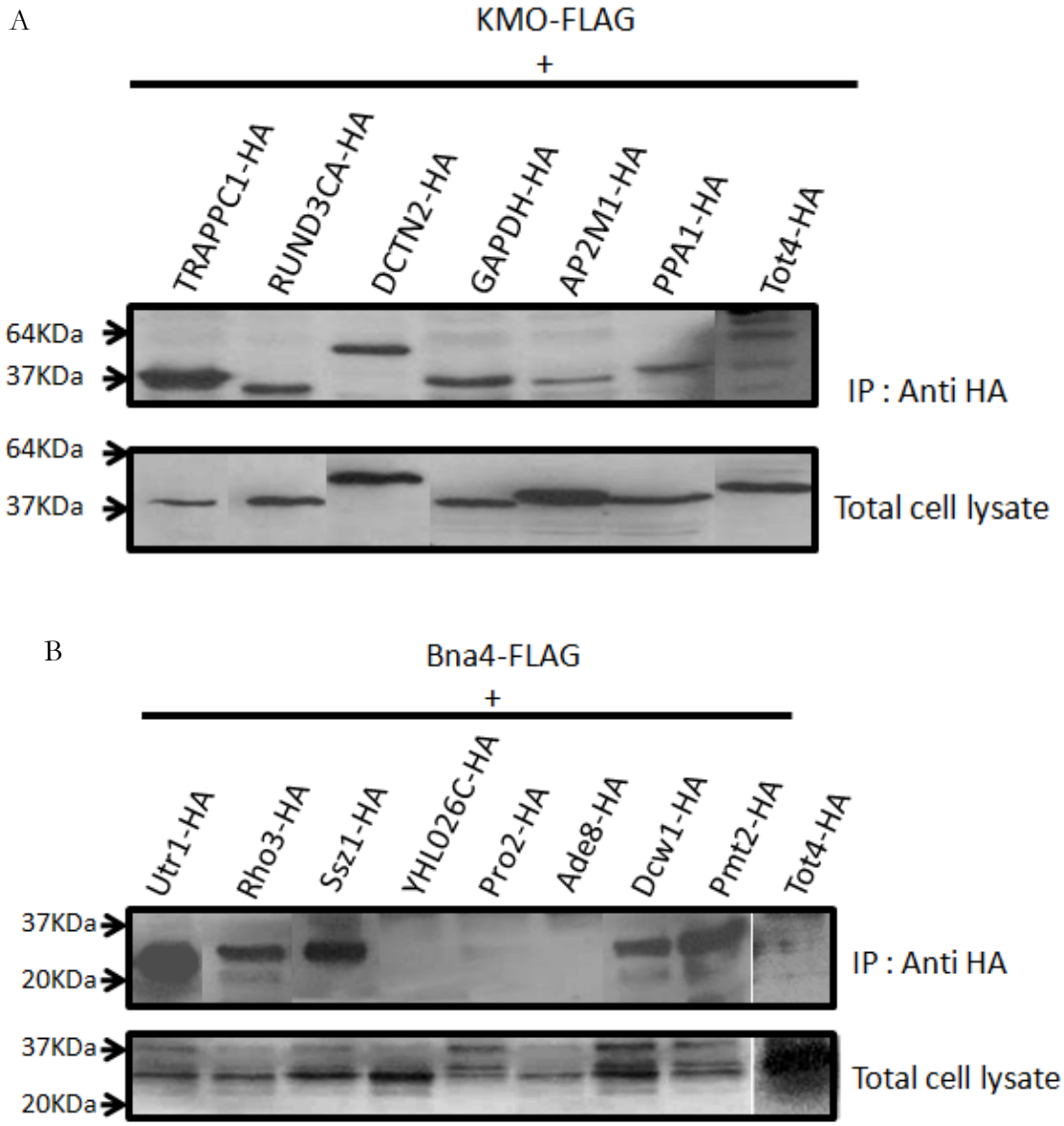

Figure 5-3: Validation of hits from the OMM- MYTH screen by co-immunoprecipitation

Protein interaction partners of (A) KMO and (B) Bna4 were validated by co-immunoprecipitation analysis. The baits were FLAG tagged and the hits from the screen are HA tagged. The hits were co-transformed with the baits. Cell lysates were then immunoprecipitated using magnetic beads coated with anti-FLAG antibody. The immunoprecipiates were then examined by western blotting using anti-HA antibody. The yeast protein Tot4-HA is not known to interact with human KMO and Bna4 was used as negative control. The figure shows a subset of hits from OMM-MYTH that were confirmed by Co-IP.

robust approach for identifying protein partners for OMM proteins with a low rate false-positive rate (Table 5-1). Most interestingly, all of the huntingtin interacting proteins obtained in the screen were validated by co-immunoprecipitation. Appendix 3 shows other putative KMO interactors validated by co-immunoprecipitation.

Similarly for Bna4, the 8 hits obtained from the MYTH screen were tested by Co-IP and 5 of the 8 MYTH protein interactions were confirmed by Co-immunoprecipitation (Figure 5-3B, Table 5-2). One major issue observed with the prey proteins from the yeast ORF NubG library was that the molecular weight of all the proteins were lower than the expected molecular weight. To confirm if the prey proteins were truncated, we re-sequenced the prey ORFs from both ends. We found that the nucleotide sequences were full-length. It remains unclear as to why the molecular weight of these proteins appears lower than expected.

Table 5-1: KMO protein interactions from OMM-MYTH confirmed by Co-Immunoprecipitation.

Functional category	Gene ID	Protein name	UNIPROT ID	No.of hits	Mol. wt	Co-IP
Metabolism	GAPDH	Glyceraldehyde 3-phosphate	P04406	4	36,053	✓
	CKB	Creatine Kinase Brain	P12277	4	38,568	✓
	TALDO1	Transaldolase1	P37837	1	34,270	P/E
	TPI1	Triosephosphate isomerase 1 isoform 2	P60174	4	26,669	x
	PSMB5	Proteasome subunit beta type 5	P28074	1	28,480	P/E
	PPA1	Inorganic pyrophosphatase	Q15181	1	32.659	✓
	ENO2	Gamma Enolase	P09104	1	47,268	P/E
	PSMA7	proteasome (prosome, macropain) subunit, alpha type, 7	O14818	1	21,580	P/E
	CBR1	Carbonyl reductase [NADPH] 1	P16152	1	24,650	✓
Cytoskeleton organisation and biogenesis	DCTN2	Dynactin 2	Q13561	4	34,486	✓
	DYNC1H1	Dynein, cytoplasmic 1, heavy chain 1	Q14204	1	532KDa	✓
	CFL1	Cofilin 1	P23528	1	18,502	x
	GSN	Gelsolin	P06396	3	85,697	✓
Intracellular transport/ endocytosis	TRAPPC1	Trafficking protein particle complex 2	Q9Y5R8	4	16,444	✓
	ICA1	Islet cell autoantigen1	Q05084	1	54,644	P/E
	COL1A1	Collagen alpha-1(I) chain	P02452	1	181,064	x
	BIN1	Myc box-dependent-interacting protein 1	O00449	1	64,669	x
	AP2M1	AP-2 complex subunit mu	Q96CW1	1	49,389	✓
	SYNGR3	Synaptogyrin 3	O43761	1	24,554	✓
Signal transduction	RUNDC3A	RUN domain-containing protein 3A	Q59EK9	1	45,682	✓
	SUMO2	Small ubiquitin related modifier 2	P61956	1	10,000	✓
	PRKAR1B	cAMP-dependent protein kinase type I-beta regulatory subunit	P31321	4	43,072	x
	RAB3A	Ras-related protein Rab-3A	P20336	1	24,983	✓
	PARF	Putative GTP-binding protein Parf	Q3YEC7	1	57,550	x

Functional category	Gene ID	Protein name	UNIPROT ID	No.of hits	Mol. wt	Co-IP
	GABARAPL1	GABA(A) receptor-associated protein like 1	Q9H0R8	1	14,004	✓
Translation	RPL27	60S ribosomal protein L27	P61353	1	15,797	P/E
Chaperone	CCT7	Chaperonin containing TCP1, subunit 7 (Eta)	Q53HV2	1	59,000	P/E
Protein Translation	EEF1G	eukaryotic translation elongation factor 1 gamma	P26641	1	62,000	✓
Apoptosis	HEBP2	Heme binding protein	Q05DB4	2	57,645	✓
Transcriptional regulation	CCNC	Cyclin C	Q9UK58	1	33,242	✓
Unknown Function	TTC27	tetratricopeptide repeat domain 27	Q53HV2	1	96,000	✓

P/E: Indicates proteins whose interaction with KMO could not be detected since the HA-tagged prey protein could not be detected in cell lysates prior to Co-IP.

Table 5-2: Bna4 protein interactions from OMM-MYTH confirmed by co-immunoprecipitation.

Functional Category	Gene ID	Protein Name	Functional Homologs in humans	No. of Hits	Mol.Wt	Co-IP
Metabolism	Utr1	ATP-NADH Kinase	NADK (Poly(P))/ATP NADH kinase	10	59,469	✓
	Ade8	Phosphoribosyl-glycinamide transformylase	~	3	23,540	x
	Pro2	Gamma glutamyl phosphate reductase	Delta-1-pyrroline-5-carboxylate synthetase(P5C/ALDH18A1)	2	49,740	x
Exocytosis/cytoskeleton maintenance	Rho3	GTP-binding protein RHO3	Rho family GTPase: RND1, RND2 & RND3	4	25,312	✓
Unfolded protein binding	Ssz1	Hsp70 protein	Heat shock proteins:72/73	6	58,237	✓
Mannosidase activity	Dcw1	Putative mannosidase	~	3	49,565	✓
	Pmt2	Protein O-mannosyltransferase	Protein O-mannosyltransferase 2:POMT2	2	86,869	✓
Unknown Function	YHL026C	Uncharacterised protein	~	2	35,717	x

5.3 DISCUSSION

In previous chapters we used the OMM-MYTH screen to identify novel protein interactions involving the mitochondrial proteins KMO and Bna4. Despite the multiple advantages that Y2H-based screening approach offers, a major disadvantage of the approach has remained the high false positive rate associated with it. To this end, there is a need to validate protein interactions identified by this system by an alternative approach such as co-immunoprecipitation. In this chapter we have validated the hits obtained from OMM-MYTH system by Co-IP analysis in yeast.

The first step in Co-IP analysis was to design bait constructs with a suitable epitope tag to enable us validate protein interactions by Co-IP. We first attempted using Myc as a tag for Co-IP. However, while both the baits and prey proteins were expressed and could be detected by western blotting, Co-IP analysis showed no protein interaction. It was hypothesised that this could be due to:

(a) All the protein interactions from OMM-MYTH screen being false positives, which seemed unlikely.

(b) As the bait(s) of interest are enzymes, it is possible that many proteins interactions are transient or weak. Since Co-IP detects only stable and strong interactions, it is possible that these interactions were undetected. To test this hypothesis we cross-linked the proteins in the protein extracts by both chemical and UV crosslinking; however we couldn't still detect protein interactions.

(c) The presence of the Myc tag (~49Kd) affected protein folding and thereby affects protein interaction.

To overcome issues caused by reconstitution of ubiquitin or misfolding of the protein that affected Co-IP analysis, the bait was redesigned in a new vector background to generate

KMO-TAP and Bna4-TAP constructs by Gateway cloning and the Co-IP was repeated without any crosslinking. Co-IP analysis with KMO bait recapitulated some of the protein interactions from the OMM-MYTH screen. Interestingly, KIPs that were validated by Co-IP included huntingtin interacting proteins: AP2M1, GAPDH and DCTN2. However, working with TAP also generated background likely caused by the cleavage of IgG from the IgG sepharose beads that were used for the pull-down experiments that interfered with detecting expression of proteins that had similar molecular weight. Different sample handling measures such as altering salt concentration did not alter these background levels.

However, Co-IP analysis with Bna4-TAP tagged showed a lot of protein degradation which remained unaltered even when protein extraction and IP buffers were optimised. It was hypothesised that one of the reasons for this could be that Bna4 levels in the cell are tightly regulated and hence expression of Bna4-TAP increased levels of Bna4 in the cells leading to the degradation of our bait protein. To test this hypothesis, Co-IP analysis were performed from protein extracts generated from a *bna4*Δ background expressing Bna4-TAP and HA tagged prey proteins. There was no change observed in the levels of protein degradation. The other possibility was that the Bna4 protein was more sensitive to TAP tag (~21Kd) which possibly caused misfolding and consequent degradation of the protein.

This in addition to not being able to control background issues with KMO-TAP Co-IP led to the bait being redesigned to include a FLAG tag in place of the TAP tag, the resulting KMO-FLAG and Bna4-FLAG constructs were used for Co-IP analysis. KMO-FLAG overcame the background issues of the KMO-TAP tag.

Interestingly, using the KMO-FLAG we were able to confirm 17/23 protein interactions identified in the OMM-MYTH screen. The 75% re-test rate is higher than reported from most two hybrid screens (Edwards et al., 2002, Dziembowski and Seraphin, 2004). This could be attributed to stringent controls that are a part of the screen that prevented

saturation of false positives. Most interestingly, huntingtin interacting proteins such as DCTN2, AP2M1, and GAPDH were re-confirmed by Co-IP to interact with KMO.

Co-IP analysis with Bna4-FLAG confirmed 5/8 (~62%) protein interactions identified in the OMM-MYTH screen. Interestingly, confirmed BIPs were involved in pathways implicated in HD - such as Ssz1 (a heat shock response protein) Rho3 (GTP mediated signalling protein).

However, Co-IP analysis with Bna4-FLAG showed that the size of all of the prey proteins were smaller than the expected protein size. This was observed in both the protein extracts and Co-IP samples. This problem was particular to the Yeast ORF NubG-X library and not observed with prey proteins from the human fetal cDNA library. The prey proteins from the Bna4 screen were sequenced from both ends to ensure that there was no truncation of the nucleotide sequence. The nucleotide sequence matched the sequence on the *Saccharomyces cerevisiae* genome database. It is unclear what caused the reduction in molecular weight of the prey proteins, but could possibly be attributed to either post-translational modification or cleavage of N-terminal half of the protein (since the epitope tags are C-terminal). With KMO-FLAG, we validated 18/24 protein interactions, as HA expression could not be detected with 7 proteins in the protein extracts (possibly because the prey constructs were not tagged properly when the library was generated). There are several reasons why in some cases protein-protein interactions could not be detected: 1) these are not true interaction partners and thus false positives; 2) the interactions are too transient or weak to detect by this approach. One of the key advantages of the in vivo Y2H based approach is the sensitivity of the technique to identify weak/transient interactions which biochemical approaches such as Co-IP often miss. Therefore it is possible that some of these protein interactions are real although they do not re-test by Co-IP.

Thus in this chapter we have validated protein interactions from the screen using a Co-IP based approach and shown that the OMM-MYTH screen has a low false positive rate. The validated hits are discussed in more detail in Chapter 7.

CHAPTER 6 VALIDATING GENETIC INTERACTION PARTNERS OF *BNA4*

6.1 INTRODUCTION

Genes, like proteins execute and regulate cellular processes through a complex network of genetic interactions. Novel genetic interactions can be established by identifying genes required for viability of the organism in the absence of a gene of interest – this is referred to as synthetic lethality. Synthetic lethality indicates that one gene buffers changes in function of another gene, and thus encoded gene products may be functionally related or play roles in parallel alternative pathways. Such genetic interactions have been studied in various model systems including mammalian cells (Astsaturov et al., 2011), fruit flies (Edgar et al., 2005) and yeast (Bender and Pringle, 1991), and have recently been investigated as an approach for cancer therapeutics (Kaelin, 2005).

Yeast have the advantage that only ~17% of gene deletions affect the viability of the haploid organism (Winzeler et al., 1999) and it is thus possible to measure a phenotypic change for each of these gene deletions in response to genetic, chemical and environmental stimuli (Hillenmeyer et al., 2008). Hence it has been feasible to create a deletion library of ~5000 non-essential yeast genes which wouldn't be possible in a higher eukaryote (Giaever et al., 2002).

This yeast deletion library was used in a high throughput synthetic genetic array (SGA) screen to identify genetic interaction partners of ~75% of the yeast genome, including *BNA4* (Costanzo et al., 2010). The SGA screen identified genes that were synthetic lethal interactors, positive genetic interactors (double mutants which show enhanced fitness) and negative genetic interactors (where fitness of double mutants is highly compromised but

does not necessarily result in lethality) (Tong and Boone, 2006, Costanzo et al., 2010). This genome wide data collection identified several genes that genetically interact with *BNA4*.

Prior to this genome-wide approach, via a collaboration between our group and the labs of Dr. Charlie Boone and Dr. Paul Muchowski, we specifically targeted genes that interact negatively with *BNA4* via synthetic lethal screens. A genome-wide screen with *bna4*Δ was performed twice, yielding a total of 69 hits, with 23 overlapping hits. Due to the high-throughput nature of this screens, it is critical to individually confirm synthetic interactions by individually bringing together the two gene deletions via mating, sporulating this diploid strain, and performing tetrad dissection. Thus, in this chapter, the overlapping hits from the synthetic lethal screens were analysed by tetrad analysis.

The protein interactions of Bna4 and the genetic interactions of *BNA4* were then analysed using bioinformatics tools such as DAVID Bioinformatics Resources 6.7, a functional annotation tool that accesses various public databases, thereby providing information on biological process, molecular function and cellular complexes for the interacting genes and proteins.

6.2 RESULTS

6.2.1 The *bna4*Δ::*NAT* synthetic lethal screen bait strain is not a good sporulator

The *bna4*Δ::*NAT* strain that was used for the synthetic lethal screen (courtesy: Wanda Kwan and Paul Muchowski, UCSF) was crossed to the selected genes (i.e. the overlapping genes from the two synthetic lethal screens) from the yeast *MATa* deletion library and mated, following which the crosses were sporulated (Figure 6-1). However, following both solid and liquid sporulation strategies (for sporulation conditions see section 2.2.19) we were unable to obtain enough healthy tetrads for any of the crosses. A possible explanation

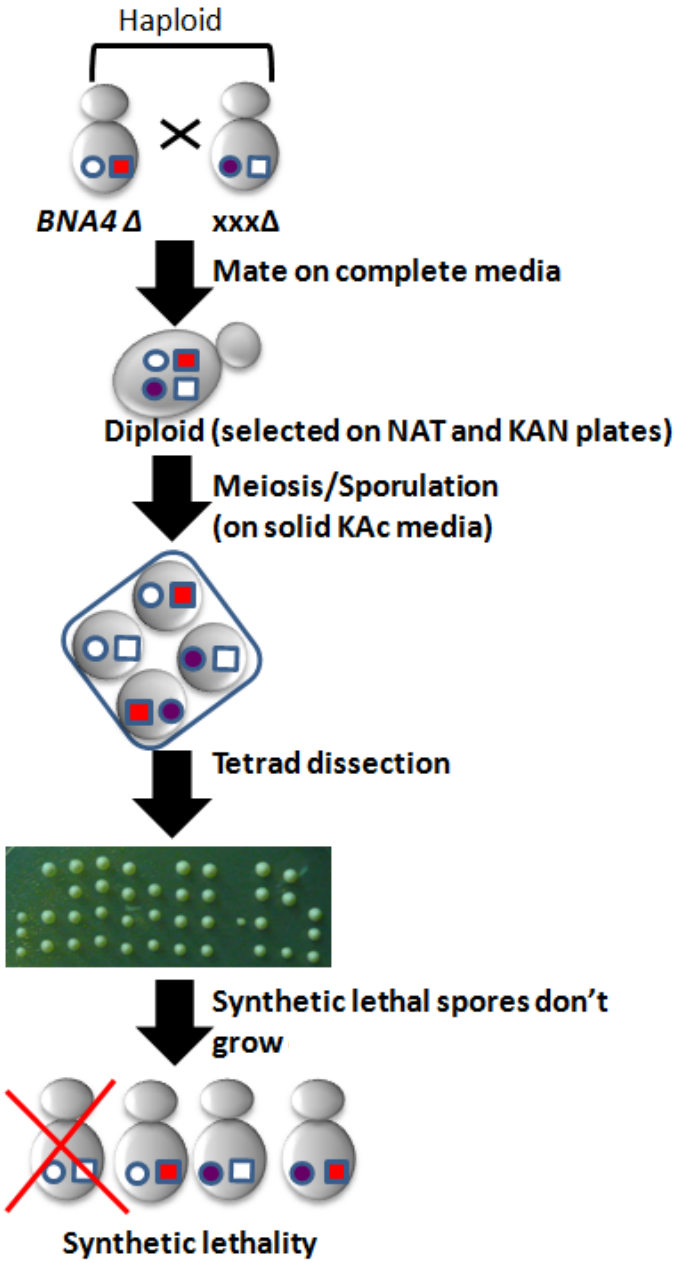

Figure 6-1: Overview of the *BNA4* synthetic lethal screen

Haploid yeast bearing *bna4*Δ (*MAT***α**) was crossed with haploid yeast bearing *yfg*Δ (*MATa*) on YPD overnight. The diploids thus obtained were further selected on double drug ($NAT^{+}KAN^{+}$) plates to obtain pure diploids which were then sporulated on complete KAc plates at 23°C for 7-10days after which the tetrads were processed and dissected on complete media plates. The dissected plate was incubated at 30°C overnight and then replica plated onto double drug ($NAT^{+}KAN^{+}$) plates. Haploid yeast containing both parental gene deletions do not survive if the genes are synthetic lethal.

for this could be that the *bna4*Δ::*NAT* deletion was created in a S288C background which is known to be a poor sporulator (Gerke et al., 2006), and the yeast *MATa* deletion library is in the BY4741 background which is derived from S288C strain (Brachmann et al., 1998). Thus, the combination of these backgrounds could be responsible for the poor sporulating phenotype observed following mating.

To overcome issues with sporulation, *BNA4* was deleted by *NAT* replacement (*bna4*Δ::*NAT*) was created in a modified S288C background that is known to sporulate very well (Deutschbauer and Davis, 2005). Studies by Deutschbauer and Davis, identified three quantitative trait loci (QTL) - *RME1* (a transcription factor), *TAO3* (a putative signalling molecule) and *MKT1* (a putative nuclease) - responsible for sporulation efficiency. Mutations in these genes (an insertion upstream of *RME1* and missense mutations that cause an amino acid change in *TAO3* and *MKT1*) in a pattern genetically similar to the SK1 yeast strain (a highly efficient sporulator), causes an increase in the sporulation efficiency of S288C (Deutschbauer and Davis, 2005). The *bna4*Δ::*NAT* was created in this strain by homologous recombination in yeast (see section 2.2.1.2). A pilot study was carried out with this new *bna4*Δ::*NAT* and it was found that crosses between *bna4*Δ::*NAT MAT***α** and *yfg*Δ::*KAN* MAT**a** sporulated very well.

6.2.2 Tetrad analysis confirms a genetic interaction between *UTR1* and *BNA4*

*bna4*Δ::*NAT MAT***α** was crossed to 23 gene deletions (*yfg*Δ::*KAN MAT***a**) (identified as overlapping hits in the synthetic lethal screen) (Table 6-1), and the crosses were processed as shown in (Figure 6-1). *Bna4*Δ::*NAT* was also crossed with *utr1*Δ which not only emerged from one of the synthetic lethal screens but was also identified as an interactor of Bna4 in the OMM-MYTH screen. Briefly, *bna4*Δ::*NAT* was crossed to each of the 24 gene deletions and mated on YPD. Diploids were selected on double drug media containing Nat and G418 (Kan) and sporulated on KAc at 23°C. Twenty tetrads were analysed for each of

the crosses and the dissected plates were replica plated to double drug media containing both Nat and G418 to check if the haploid double survives (not synthetically lethal) or not (synthetically lethal). The dissected plate was also replica plated onto a plate containing *MATa* cells to determine the mating type and ensure proper gene segregation. The list of genes confirmed by tetrad analysis is shown in Table 6-1. Strikingly, ~80% of the genes from the synthetic lethal screen re-tested with only 5 gene deletions from the 24 tested failing to retest. Interestingly, *UTR1*, which encodes an ATP-NADH kinase that was also identified as a protein interactor of Bna4 (from Chapters 4 & 5) was identified as novel genetic interactor of *BNA4*.

6.2.3 Bioinformatic analysis of genetic and protein interactions of *BNA4*

DAVID Bioinformatics Resources 6.7 consists of integrated biological databases with >20 gene identifiers and >40 functional annotation categories and helps identify enriched biological themes and functionally related gene groups (Huang da et al., 2009a, Huang da et al., 2009b). DAVID was used to analyse protein and genetic interaction data to identify biological processes that are enriched (Table 6-2). Furthermore DAVID was used to collate protein interaction information from other databases such as BIND and MINT to identify common protein interaction partners of genetic and protein interactors of BNA4 (Table 6-3). We found that NADP-related cellular processes were the most enriched group by gene ontology analysis. This finding supported our approach, as KP is involved in the production of NAD+ which is converted to NADP downstream. Interestingly, some of the key biological processes enriched include intracellular signalling, response to oxidative stress, regulation of transcription and chromatin modification. All of these processes have been implicated in HD pathogenesis in various models and are discussed later. Furthermore, these biological processes were also enriched amongst interactors of human KMO (see Chapter 7).

Table 6-1: Genetic interaction partners of *BNA4.*

Biological process	Gene	Segregation Pattern			Phenotype	Synthetic lethality
		3:1	2:2	4:0		
Aromatic amino acid family biosynthetic process	ARO1	17/40	23/40	-	Spore death	✓
	ARO2	19/40	21/40	-	Spore death	✓
	NPT1	24/40	16/40	-	Spore death	✓
Establishment of cell polarity	BEM1	25/40	14/40	1/40	Spore death	✓
Ubiquitin-dependent protein catabolic process	BSD2	23/40	17/40	2/40	Spore death	✓
Histone deacetylase activity	DEP1	22/40	18/40	-	Spore death	✓
Telomere maintenance	FYV4	6/20	14/20	-	Normal growth	x
	RPN4	23/40	17/40	-	Spore death	✓
	PTC1	12/20	8/20	-	Slow growth	x
	SEC66	18/40	22/40	-	Spore death	✓
Transcriptional regulation	HOS2	16/40	24/40	-	Spore death	✓
	MAF1	19/40	21/40	-	Spore death	✓
Chromatin remodelling	NHP10	4/40	36/40	-	Spore death	✓
Cation transport	PMP3	16/40	24/40	-	Spore death	✓
Retrograde transport	RIC1	17/40	23/40	-	Spore death	✓
	YPT6	15/40	25/40	-	Spore death	✓
Cell wall organisation and biogenesis	ROM2	13/20	7/20	-	Normal growth	x
Response to stress	TIM18	23/40	17/40	-	Spore death	✓
Nicotinamide mononucleotide transport	TNA1	14/40	26/40	-	Spore death	✓
Aerobic respiration	OAR1	10/20	10/20	-	Slow growth	x
	UTR1	18/40	22/40	-	Spore death	✓
Unknown function	NKP2	16/40	24/40	-	Spore death	✓
	YGR259C	12/20	8/20	-	Normal growth	x
	YGLO24W	14/40	24/40	2/40	Spore death	✓

The table lists the 23 genes (overlapping hits from two screens) obtained as putative interactors of *BNA4* by SGA analysis. Additionally, Utr1 identified as a protein interactor of Bna4 was also included in the list of genes to be analysed by tetrad dissection. The segregation pattern is represented as x/y; where y=the total number of tetrads dissected and x=the number of tetrads showing a particular segregation pattern.

Table 6-2: Biological process enriched amongst protein and genetic interaction partners of BNA4.

Functional annotation analysis was carried out using DAVID bioinformatics resources 6.7 and included the following annotation categories GOTERM_BP_ALL, GOTERM_CC_ALL, GOTERM_MF_ALL. A p-value ≤0.05 cut-off was used. All hits obtained are listed in decreasing order of significance taking into account the small nature of the dataset (see text).

Table 6-2: Biological process enriched amongst protein and genetic interaction partners of BNA4.

Functional annotation	Genes	P-Value
NADP	*OAR1, ARO1, PRO2, UTR1*	5.30E-03
Small GTPase mediated signal transduction	*BEM1, YPT6, RHO3, ROM2*	9.00E-03
Intracellular signalling cascade	*BEM1, YPT6, RHO3, PTC1, ROM2*	1.20E-02
Phosphorus-oxygen lyase	*ARO1, ARO2*	1.30E-02
Carbon-oxygen lyase activity, acting on phosphates	*ARO1, ARO2*	1.60E-02
Nitrogen compound biosynthetic process	*NPT1, ADE8, ARO1, ARO2, PRO2, UTR1*	2.40E-02
Positive regulation of response to stimulus	*HOS2, RPN4*	2.60E-02
Growth	*SEC66, BEM1, DCW1, ROM2*	3.60E-02
Regulation of cellular response to stress	*HOS2, RPN4*	4.20E-02
Transcription regulation	*HOS2, MAF1, NHP10, RPN4, DEP1, RIC1*	5.00E-02
Plasma membrane part	*YPT6, DCW1, RHO3, TNA1*	5.10E-02
Aromatic amino acid biosynthesis	*ARO1, ARO2*	5.10E-02
Stress response	*BSD2, ARO2, PTC1*	5.10E-02
Cell membrane	*PMP3, YPT6, DCW1, RHO3*	5.20E-02
Response to arsenic	*TIM18, RPN4*	5.70E-02
Organic acid biosynthetic process	*OAR1, ARO1, ARO2, PRO2*	6.20E-02
Carboxylic acid biosynthetic process	*OAR1, ARO1, ARO2, PRO2*	6.20E-02
Chorismate metabolic process	*ARO1, ARO2*	6.20E-02
Aromatic amino acid family biosynthetic process	*ARO1, ARO2*	6.20E-02
Amino-acid biosynthesis	*ARO1, ARO2, PRO2*	6.60E-02
Guanine-nucleotide releasing factor	*ROM2, RIC1*	6.70E-02
Short sequence motif:Effector region	*YPT6, RHO3*	6.70E-02
Transcription	*HOS2, MAF1, NHP10, RPN4, DEP1, RIC1*	6.70E-02
Phenylalanine, tyrosine and tryptophan biosynthesis	*ARO1, ARO2*	6.90E-02
Rpd3L-Expanded complex	*HOS2, DEP1*	8.40E-02
Intracellular protein transport	*SEC66, YPT6, BSD2, TIM18, RIC1*	9.10E-02
Carbon-oxygen lyase	*ARO1, ARO2*	9.10E-02
Nuclear chromatin	*HOS2, NHP10, DEP1*	9.20E-02
Pyridine nucleotide biosynthetic process	*NPT1, UTR1*	9.20E-02
Chromatin remodelling complex	*HOS2, NHP10, DEP1*	9.40E-02

Table 6-3: Common protein interaction partners of protein and genetic interactors of BNA4.

Functional annotation analysis carried out using DAVID bioinformatics resources 6.7 included detection of common protein-protein interaction partners by integrated use of BIND, DIP and MINT databases. An arbitrary p-value cut-off of $2*10^{-2}$ was used for the BIND dataset.

Table 6-3: Common protein interaction partners of protein and genetic interactors of *BNA4*.

Protein Interaction	Genes	P-Value
BIND		
Calcineurin subunit B	*BEM1, YPT6, PMT2, RPN4, RIC1*	6.20E-05
Uncharacterized protein YEL043W	*BEM1, YPT6, RIC1*	2.70E-04
Cell wall assembly regulator Smi1	*BEM1, YPT6, PTC1, ROM2, RIC1*	6.00E-04
cell division control protein 73	*YPT6, NKP2, TIM18, NHP10, RIC1*	2.40E-03
Prefoldin subunit 5	*PMP3, SEC66, BSD2, HOS2, RPN4*	7.80E-03
Prefoldin subunit 6	*PMP3, SEC66, BEM1, HOS2, RPN4*	8.90E-03
Epsin-4	*YPT6, RIC1*	1.10E-02
Epsin-5	*YPT6, RIC2*	1.10E-02
Phosphatase Dcr2	*YPT6, RIC1*	1.10E-02
Protein Rer1	*YPT6, RIC1*	1.10E-02
Mannose 6-phosphate receptor-like protein1	*YPT6, RIC1*	1.10E-02
GPI inositol deacylase	*YPT6, RIC1*	1.10E-02
Heat shock protein Ssa1	*YPT6, BSD2, SSZ1, ARO1*	1.30E-02
NAP1-binding protein 2	*YPT6, PTC1, RIC1*	1.50E-02
Chromatin modification-related protein Eaf7	*YPT6, RIC1*	1.60E-02
Serine/threonine-protein kinase SKY1	*YPT6, RIC2*	1.60E-02
Telomerase reverse transcriptase	*YPT6, RIC3*	1.60E-02
60S ribosomal protein L35	*YPT6, RIC4*	1.60E-02
Oxidation resistance protein 1	*YPT6, RIC5*	1.60E-02
CAAX prenyl protease 2	*YPT6, RIC6*	1.60E-02
1,3-beta-glucanosyltransferase GAS1	*YPT6, PTC1, ROM2, RIC1*	2.00E-02
Similar to APEX nulcease (multifunctional DNA repair enzyme 1:APEX nuclease (multifunctional DNA repair enzyme) 1	*ARO1, ROM2, NHP10, RPN4*	2.00E-02
Heat shock protein Ssb1	*YPT6, BSD2, SSZ1, ARO1*	2.10E-02

Protein Interaction	Genes	P-Value
DIP		
Reduced growth phenotype protein 1	*YPT6, RIC1*	1.10E-02
Secretory component protein Shr3	*PMP3, BSD2, TNA1*	2.60E-02
Inorganic phosphate transporter Pho86	*PMP3, BSD2, TNA1*	2.60E-02
Phosphatidylinositol N-acetylglucosaminyl-transferase GPI2 subunit	*SEC66, BSD2, TNA1*	4.50E-02
Elongation of fatty acids protein 2	*PMP3, BSD2, TNA1*	4.90E-02
MINT		
ATP-dependent molecular chaperone HSC82	*YPT6, SSZ1, ARO1*	5.10E-02
E3 ubiquitin-protein ligase Doa10	*YPT6, NPT1, PRO2*	5.20E-02
Vacuolar membrane protein Pep3	*PTC1, PRO2*	5.50E-02
Phosphatidylinositol N-acetylglucosaminyltransferase GP12 subunit	*SEC66, BSD2*	6.50E-02
GTP-binding protein Ypt6	*SSZ1, RIC1*	6.50E-02
ATP-dependent permease Aus1	*NPT1, PRO2*	8.90E-02

6.3 DISCUSSION

The dissection of genetic interactions is a critical tool which aids in understanding the functional role of gene/pathways/networks in the cell. As described above, the availability of the yeast gene deletion library has facilitated systematic screens for the identification of synthetic lethal interactors. In SGA analysis the deletion library is systematically mated/crossed to an array of query deletion strains through a pinning process. The resulting interactions are classified as negative genetic interactions or positive genetic interactions (Costanzo et al., 2010). The negative genetic interactions typically result in a synthetically sick double mutant, while the single mutants are viable. An extreme case of a negative genetic interaction is synthetic lethality. Synthetic lethality can indicate that the pair of genes 1) regulate an essential cellular process through parallel pathways; 2) regulate the same level of the pathway or act concomitantly in the same pathway or 3) they act in unrelated pathways that interact indirectly.

The major aim of this chapter was to validate synthetic lethal interactors with *BNA4* using tetrad analysis. To this end the *bna4*Δ deletion strain that was used for SGA analysis was mated to selected gene deletions from the BY4741 deletion library. However, we observed that the diploids obtained from such crosses did not sporulate well. A likely reason is the S288C background for *bna4*Δ and the library gene deletions which has poor sporulation efficiency. To test if this was the reason for poor sporulation we recreated the *bna4*Δ in a modified S288C background that showed better sporulation than the native S288C yeast strain (Deutschbauer and Davis, 2005). The crosses were tested for sporulation efficiency with the new strain and were found to show increased sporulation efficiency. The tetrad analysis was repeated and 19/24 genes tested were identified as synthetic lethal interactors of *BNA4*.

Of these genes, *ARO1* and *ARO2* are involved in alternate pathways for metabolising tryptophan(Jones and Fink, 1982). *NPT1* catalyses the conversion of nicotinate to nicotinate ribonucleotide leading to NAD^+ production via an alternate salvage pathway (Anderson et al., 2002). A 2002 study by Panozzo et al., showed that *npt1*Δ was essential for growth of *S. cerevisiae* under anaerobic conditions in yeast and found *npt1*Δ to be co-lethal with *bna4*Δ and deletions of other KP enzymes including *bna2*Δ (tryptophan 2,3-dioxygenase), *bna3*Δ (kynurenine formylase), *bna5*Δ (kynureninase) and *bna6*Δ (quinolate phosphoribosyl transferase), as deletion of these KP enzymes prevents downstream formation of NAD^+ (Panozzo et al., 2002). In our study we have confirmed *npt1*Δ to be synthetically lethal with *bna4*Δ validating our approach and the hits we have confirmed as genetic interactors from the screen.

Interestingly, *UTR1*, which we previously identified as a protein interaction partner of Bna4 was also identified as a genetic interaction partner of *BNA4*. *UTR1*, an ATP-NADH kinase is involved in the formation of NAD+. In double mutants lacking *UTR1* and *BNA4,* NAD+ production could possibly be compromised thereby affecting cell viability. Interestingly, *aro1*Δ and *tna1*Δ (nicotinamide mononucleotide permease) where found to lead to synthetically sick/lethal phenotype in yeast strains that express α-synuclein, a gene implicated to play a role in Parkinson's disease and enhance α-synuclein toxicity (Willingham et al., 2003). The other genetic interaction partners of *BNA4* were interesting as they were associated with pathways that *BNA4* was not known to play a role in. These include pathways such as establishment of cell polarity, telomere maintenance and chromatin remodelling and response to cellular stress. Interestingly, defects in each of these pathways have been implicated to play a role in HD pathology (Giorgini et al., 2008, Cicchetti et al., 2009). One of these genetic interaction partners of *BNA4*, *BSD2* encodes

an ion metal homeostasis protein that detoxifies copper and prevents hyper-accumulation of metalloproteins in the cell. This resonates with recent work exploring copper binding proteins that have been implicated as potential therapeutic target for HD (Hands et al., 2010).

To further understand the nature of the genetic and protein interactions involving Bna4 we carried out gene ontology analysis using DAVID Bioinformatics Resources 6.7 (Huang da et al., 2009a, Huang da et al., 2009b). One of the drawbacks of DAVID is that the program is not as effective in dealing with small gene lists as it is when working with large gene lists such as microarray data (Sleumer et al., 2010). This size of the gene list particularly affects the statistical significance data the program provides, leading to a high rate of false negatives. To obtain results with any significance most genes must fall into specific categories (Sleumer et al., 2010). Inspite of this drawback, many biological processes were significantly enriched when analyzed using this annotation tool.

One of the key processes that was enriched amongst interactors of *BNA4* involved NADP production followed by intracellular signalling and small GTPases that mediate signal transduction. Interestingly, pathways involving intracellular signalling were also enriched amongst physical interactors of KMO (see Chapter 7).

Analysing protein interactions involving interactors of Bna4 revealed that there was significant enrichment of proteins interacting with Calcineurin subunit B (Cnb1) (p-value= 0.000062), the human homolog of which is PPP3R2. This protein is implicated to play a role in several KEGG pathways such as MAPK signalling pathway, calcium signalling pathway, Wnt signalling, apoptosis, axon guidance and VEGF signalling pathway, and is also implicated in neurodegenerative diseases such as Alzheimer's disease and amyotrophic

lateral sclerosis (Kanehisa and Goto, 2000, Kanehisa et al., 2006, Kanehisa et al., 2010). Interactions with chaperone proteins such as prefoldin subunit 5 & 6 are also significantly enriched (p-value >0.05). Most of the other significant protein interactions are mediated by Ypt6 and Ric1. Ypt6 is a Rab family GTPase protein involved in the secretory pathway and is similar to human RAB6 and Ric1 is an exchange factor for Ypt6 (Li and Warner, 1996, Bensen et al., 2001). Studies in our lab have shown the Rab family of mammalian proteins to be modifiers of mHtt toxicity and the activity of Rab proteins have also been shown to be compromised in the presence of mHtt (Li et al., 2009a, Li et al., 2009b, Richards et al., 2011). Additionally, Ypt1p interacts with α-synuclein and consequently increases expression of Rab1p which is found to be protective against dopaminergic neuron loss associated with α-synuclein in animal models of Parkinson's disease(Cooper et al., 2006) The protein interactions mediated by Ypt6 include proteins in vesicle trafficking and transport. In addition to vesicle trafficking, Ric1 is also involved in transcription of rRNA and ribosomal protein genes (Mizuta et al., 1997) and thus plays an important role in translation and is interesting in light of a recent study that has implicated translation defects to play a role in HD pathogenesis (Tauber et al., 2010).

Furthermore some of the (putative) genetic interactors of *BNA4* are also modifiers of mHtt toxicity. In a yeast screen to identify genes that enhance the toxicity caused by the mHtt fragment, *PTC1*, a genetic interactor of *BNA4* was identified as one of the enhancers of mHtt toxicity (Clapp J and Giorgini F, unpublished). Similarly, a deletion of *DEP1* was found to be a suppressor of mHtt toxicity (Clapp J and Giorgini F, unpublished). Moreover, the expression of two other genes: *LYS20* a synthetic lethal interactor of *BNA4* (Deutscher et al., 2006) and *CSE2,* a negative genetic interactor of *BNA4* (Costanzo et al., 2010) levels are found to be altered in the presence of mHtt (Tauber et al., 2010).

Furthermore, overexpression of *CSE2* rescues the toxicity of the mHtt fragment in yeast (Tauber et al., 2010). *LYS20* expression was upregulated in three strains (one of which carries a *bna4*Δ) in which toxicity of mHtt is suppressed (Tauber et al., 2010).

Finally, *BNA4* interacting genes *HOS2* and *DEP1* encode proteins that form part of the Rpd3L HDAC complex (Lamping et al., 1994, Rundlett et al., 1996, Carrozza et al., 2005). As discussed in Chapter 1, dysregulation of the Rpd3-HDAC complex decreases expression of KP genes and metabolites, and ameliorates HD phenotypes in a 3-HK and QUIN dependent manner (Giorgini et al., 2008). In total, the bioinformatic analysis of *BNA4* interacting genes and proteins reveals enrichment in genes and pathways linked to modulation of mHtt toxicity.

CHAPTER 7 ANALYSIS OF KMO PROTEIN INTERACTIONS USING BIOINFORMATIC TOOLS

7.1 INTRODUCTION

The OMM-MYTH screen identified 31 proteins that interact with KMO. Co-immunoprecipitation analysis further confirmed 18 of the 31 protein interactions. These interactors include proteins that directly interact with normal and mHtt (e.g. DCTN2) and modifiers of mHtt toxicity (e.g. EEF1G). To further analyse the significance of these interactions, bioinformatic tools were used to analyse biological processes and pathways that were enriched amongst the protein interaction partners of KMO. This work provides further insight into both the normal physiological role of KMO in the cell as well as its role in HD pathogenesis.

DAVID Bioinformatics Resources 6.7 (described in Chapter 6) was initially used to provide information on enriched biological processes and molecular functions. To provide further insight into protein pathways and to implement pathway analysis, the Ingenuity Pathway Analysis (IPA) software was also implemented. IPA provides functional annotation and also conglomerates published information on molecular interactions, gene expression and modulation, phenotype to gene associations and chemical interactions to graphically generate a network of protein interactions (Ingenuity® systems, www.ingenuity.com(Jimenez-Marin et al., 2009)).

In this chapter, these two bioinformatic tools were used to obtain gene annotation information on the KMO interaction partners and to identify significantly enriched pathways.

7.2 RESULTS

7.2.1 Similarities between interactors of yeast and human KMO

Gene ontology analysis was carried out using DAVID Bioinformatics Resources 6.7 (Huang da et al., 2009a, Huang da et al., 2009b). The functional annotation tool was used to analyse biological processes and molecular functions enriched amongst protein interactors of KMO (for annotation categories included see section 2.2.20). Protein interactors of KMO were found to be enriched in several biological processes (see Table 7-1) out of which 2 processes were found to be enriched amongst interactors of BNA4-NADP metabolism and small GTPase mediated signal transduction and signalling cascade, (Table 6-2). Several molecular function groups were also found to be enriched amongst KIPs, including protein binding and cytoskeletal proteins (Table 7-1). DAVID was also used to collate protein interaction information from other databases such as BIND and MINT to identify common protein interaction partners of KIPs which could provide more information on downstream protein interactions regulated by KIPs (Table 7-2). Strikingly, most of these common protein interactions included proteins involved in cytoskeletal organisation, which was also obtained as the top protein network in IPA analysis (section 7.2.2.2). Using the DAVID, transcription factor binding site analysis was also carried out to identify transcription factors that regulate the expression of KIPs (see Appendix 4). One of the transcription factors that showed a significant enrichment fold change was SP1. SP1 interacts with huntingtin and disruption of SP1 transcription activity is observed at early stages of pathology in HD mouse models (Dunah et al., 2002).

Table 7-1: Biological processes enriched amongst protein interaction partners of KMO.

Functional annotation analysis was carried out using DAVID bioinformatics resources 6.7 and included the following annotation categories GOTERM_BP_ALL, GOTERM_CC_ALL, GOTERM_MF_ALL. A p-value ≤0.05 was considered significant.

Table 7-1: Biological process enriched amongst protein interaction partners of KMO.

Biological process	Genes	P-value
Glucose catabolic process	*TPI1, TALDO1, ENO2, GAPDH*	2.00E-04
Hexose catabolic process	*TPI1, TALDO1, ENO2, GAPDH*	3.40E-04
Monosaccharide catabolic process	*TPI1, TALDO1, ENO2, GAPDH*	3.70E-04
Alcohol catabolic process	*TPI1, TALDO1, ENO2, GAPDH*	5.50E-04
Cellular carbohydrate catabolic process	*TPI1, TALDO1, ENO2, GAPDH*	6.30E-04
Carbohydrate catabolic process	*TPI1, TALDO1, ENO2, GAPDH*	1.30E-03
Glucose metabolic process	*TPI1, TALDO1, ENO2, GAPDH*	3.40E-03
Glycolysis	*TPI1, ENO2, GAPDH*	3.90E-03
Glyceraldehyde-3-phosphate metabolic process	*TPI1, TALDO1*	4.00E-03
Hexose metabolic process	*TPI1, TALDO1, ENO2, GAPDH*	6.40E-03
Monosaccharide metabolic process	*TPI1, TALDO1, ENO2, GAPDH*	9.50E-03
Pentose-phosphate shunt	*TPI1, TALDO1*	1.80E-02
Small GTPase mediated signal transduction	*C9ORF86, RAB3A, CFL1, RUNDC3A*	2.20E-02
Vesicle-mediated transport	*RAB3A, GSN, BIN1, TRAPPC1, AP2M1*	2.60E-02
Synaptic vesicle endocytosis	*RAB3A, BIN1*	2.80E-02
Catabolic process	*SUMO2,TPI1,ENO2,GAPDH,PSMA7 PSMB5,TALDO1*	2.80E-02
Mitotic spindle organisation	*DYNC1H1, DCTN2*	3.00E-02
NADP metabolic process	*TPI1, TALDO1*	3.10E-02
Mitotic cell cycle	*PSMB5, PSMA7, DYNC1H1, DCTN2*	3.70E-02
Cellular carbohydrate metabolic process	*TPI1, TALDO1, ENO2, GAPDH*	3.70E-02
Response to endogenous stimulus	*PRKAR1B, CFL1, ENO2, COL1A1*	4.60E-02
Response to acid	*GSN, CFL1*	4.70E-02
Alcohol metabolic process	*TPI1, TALDO1, ENO2, GAPDH*	4.80E-02
Gluconeogenesis	*TPI1, ENO2*	4.90E-02

Molecular function	***Genes***	**P-Value**
Protein Binding	*GABARAPL1, RAB3A, RUNDC3A, SUMO2,TPI1,AP2M1,BIN1,CBR1,CCT7,C9ORF86,CFL1,COL1A1,CKB,CCNC,DCTN2,DYNC1H1,ENO2,EEF1G,GSN,GAPDH,ICA1,PSMA7,PSMB5, PRKAR1B,PPA1,TTC27,TRAPPC1, TALDO1*	1.10E-04
Identical protein binding	*CCT7, COL1A1, ENO2, PSMA7*	9.10E-02
Threonine type peptidase activity	*PSMA7, PSMB5*	3.20E-02
Threonine type endopeptidase activity	*PSMA7, PSMB6*	3.60E-02
Cytoskeleton protein	*GABARAPL1, GSN, CFL1, EEF1G, DYNC1H1, DCTN2*	1.70E-02

Common protein interaction partners of KIPs (Table 7-2) and BIPs (Table 6-3) were found to be similarly enriched for cytoskeletal proteins, ribosomal proteins and heat shock proteins suggesting that KMO and Bna4 participate in similar processes in the cell though there is no direct overlap between KMO and Bna4 interactors. Moreover, similarities were seen in functional categories of the common protein interaction partners of both KMO and Bna4 (Table 7-2). For detailed information on the protein interactors see Appendix 5.

7.2.2 Network analysis of KMO interacting proteins using IPA

To further validate the results obtained through DAVID functional annotation and to gain insight into protein networks involving KMO IPA was used. A core analysis with IPA was carried out to link genotype to phenotypes and molecular processes. The core analysis identified key molecular and cellular functions, canonical pathways and protein networks involving KMO interacting proteins (Table 7-3 through Table 7-7). We discuss these results at length below.

Table 7-2: Common protein interaction partners of KIPs.

Protein-functional category	No. of genes
Transcription Factors	58
Cytoskeleton proteins-Actin/ tubulin related proteins	46
Ribosomal proteins	23
Heat shock proteins, Chaperones and Histone clusters and apoptosis/cell cycle regulation	15
Energy exchange factors and solute carriers	6
Growth factors	3
Others	42

DAVID analysis was carried out to identify common interaction proteins of KIPs. The table lists the enriched functional categories amongst proteins interacting with KIPs.

*Biological processes and canonical pathways were tested by Fisher exact t-test. A p-value≤0.05 was considered significant. Protein networks were ordered by a score indicative of significance. Canonical pathways were ordered by the ratio value which signifies the number of molecular in a given pathway that meet cut criteria divided by the total number of molecules that make up the pathway.

Table 7-3: Functional characterisation of KMO interacting proteins using IPA.*

Name	P-value	Molecules
Cellular Movement	7.52E-05-4.91E-02	8
Carbohydrate Metabolism	1.06E-04-3.8E-02	7
Cellular assembly and organisation	2.40E-04-4.91E-02	10
Cellular Growth and Proliferation	1.05E-03-1.54E-02	3
Cell Death	1.93E-03-4.84E-02	3

Table 7-4: Physiological role of KMO interacting proteins in development of biological systems using IPA.*

Name	P-value	Molecules
Nervous system development and function	1.05E-03-4.91E-02	8
Embryonic development	1.93E-03-9.62E-03	2
Hematological System Development and Function	1.93E-03-4.35E-02	5
Tissue Morphology	1.93E-03-4.84E-02	3
Connective Tissue Development and Function	3.86E-03-4.35E-02	2

Table 7-5: Key canonical pathways identified using IPA.*

Name	P-Value	Ratio
Glycolysis/Gluconeogenesis	1.01E-03	3/147 (0.02)
Regulation of Actin-based motility by Rho	1.17E-02	2/92 (0.022)
Inositol Metabolism	1.34E-02	1/19 (0.053)
Phenylalanine, Tyrosine and Tryptophan Biosynthesis	3.42E-02	1/67 (0.015)
Maturity Onset Diabetes of Young (MODY) signalling	4.17E-02	1/31 (0.032)

Table 7-6: Top Networks involving KMO interacting proteins using IPA.*

Associated Network Functions	Score
Cellular compromise, Cellular Assembly and Organisation, Post translational Modification	31
Drug metabolism, endocrine system development and function, lipid metabolism	22
Cardiovascular disease, Genetic disorder, Infection mechanism	14
Molecular Transport, Protein trafficking	3

Table 7-7: Toxic role of KMO interacting proteins using IPA.*

Name	P-Value	Ratio
Biogenesis of Mitochondria	5.46E-02	1/29 (0.034)
NRF2-mediated Oxidative stress response	5.92E-02	2/205 (0.01)
Increase transmembrane potential of Mitochondria and mitochondrial membrane	9.23E-02	1/50 (0.02)
PXR/RXR Activation	1.23E-01	1/68 (0.015)
VDR/RXR Activation	1.39E-01	1/77 (0.013)

7.2.2.1 Energy metabolism and Rho-mediated signalling identified as top canonical pathways involving KMO interacting proteins

IPA core analysis identified glycolysis/gluconeogenesis and regulation of actin based motility by Rho as two of the most significant "canonical pathways" (Table 7-5). Three of the proteins identified are implicated to play an important role in energy metabolism (glycolysis and gluconeogenesis): GAPDH (Glyceraldehyde-3-phosphatase dehydrogenase), ENO2 (Enolase) and TPI (triosephosphate isomerise). GAPDH catalyses the conversion of glyceraldehyde 3-phosphate to glycerate 1,3 phosphate; Enolase catalyses the conversion of glycerate 2-phosphate to phosphoenol pyruvate; and TPI converts glyceraldehyde 3-phosphate to glycerone phosphate. These enzymes function in key stages of the pathways and regulate the entry of metabolites into other metabolic pathways such as pentose phosphate pathway and Tricarboxylic acid cycle (TCA) (Figure 7-1).

Regulation of actin via Rho mediated intracellular signalling (Rho is a small GTPase protein that mediates G-protein signalling response that involves actin cytoskeleton reorganisation) was the other pathway of significance and contains two KIPs: GSN (gelsolin) and CFL1 (cofilin1). These two proteins play an important role in actin polymerisation and actin filament stabilisation respectively (Figure 7-2). The KIP-AP2M1 (Adaptor related protein complex 2 mu 1subunit), interacts with huntingtin and huntingtin interacting protein 1 (HIP1) involved in vesicle trafficking plays a vital role in GABA receptor mediated signalling (Figure 7-3). AP2M1 plays a role in endosomal protein sorting, recruitment of clathrin to membranes, recognition of sorting signals in transmembrane cargo proteins and recycling synaptic vesicle membrane from the pre-synaptic surface and plays a vital role in GABA receptor mediated signalling (reviewed in (Bonanomi et al., 2006)).

Figure 7-1: Overview of Glycolysis/gluconeogenesis involving KIPs-GAPDH, ENO2 and TPI.

Schematic illustration of Glycolysis/Gluconeogenesis: KIPs are indicated in dark grey. GAPDH catalyses the conversion of glyceraldehyde 3-phosphate to glycerate 1,3 phosphate; Enolase catalyses the conversion of glycerate 2-phosphate to phosphoenol pyruvate. TPI converts glyceraldehyde 3-phosphate to glycerine phosphate. Enzymes are indicated using IUMMB enzyme nomenclature. 1.2.1.12 =GAPDH; 4.2.1.11=ENO2; 5.3.1.1=TPI.

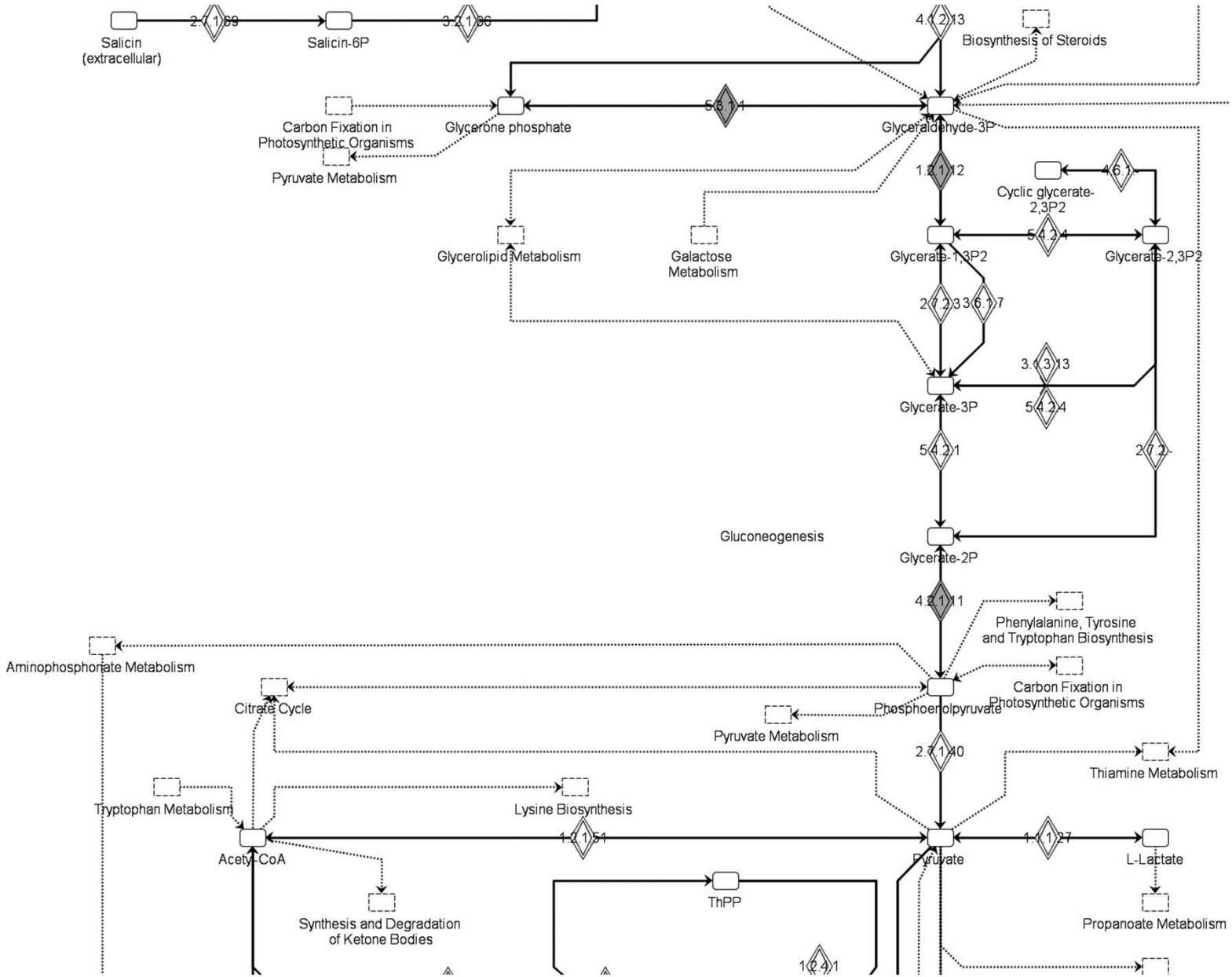
Salicin
(extracellular)
2.7.1.69
Salicin-6P
3.2.1.86
4.1.2.13
Biosynthesis of Steroids
Carbon Fixation in
Photosynthetic Organisms
Pyruvate Metabolism
Glycerone phosphate
5.3.1.1
Glyceraldehyde-3P
1.2.1.12
4.6.1.-
Cyclic glycerate-
2,3P2
5.4.2.4
Glycerolipid Metabolism
Galactose
Metabolism
Glycerate-1,3P2
Glycerate-2,3P2
2.7.2.3
3.6.1.7
3.1.3.13
Glycerate-3P
5.4.2.4
5.4.2.1
2.7.2.-
Gluconeogenesis
Glycerate-2P
4.2.1.11
Phenylalanine, Tyrosine
and Tryptophan Biosynthesis
Aminophosphonate Metabolism
Carbon Fixation in
Photosynthetic Organisms
Citrate Cycle
Phosphoenolpyruvate
Pyruvate Metabolism
2.7.1.40
Thiamine Metabolism
Tryptophan Metabolism
Lysine Biosynthesis
1.2.1.51
1.1.1.27
Acetyl-CoA
Pyruvate
L-Lactate
ThPP
Synthesis and Degradation
of Ketone Bodies
Propanoate Metabolism
1.2.4.1

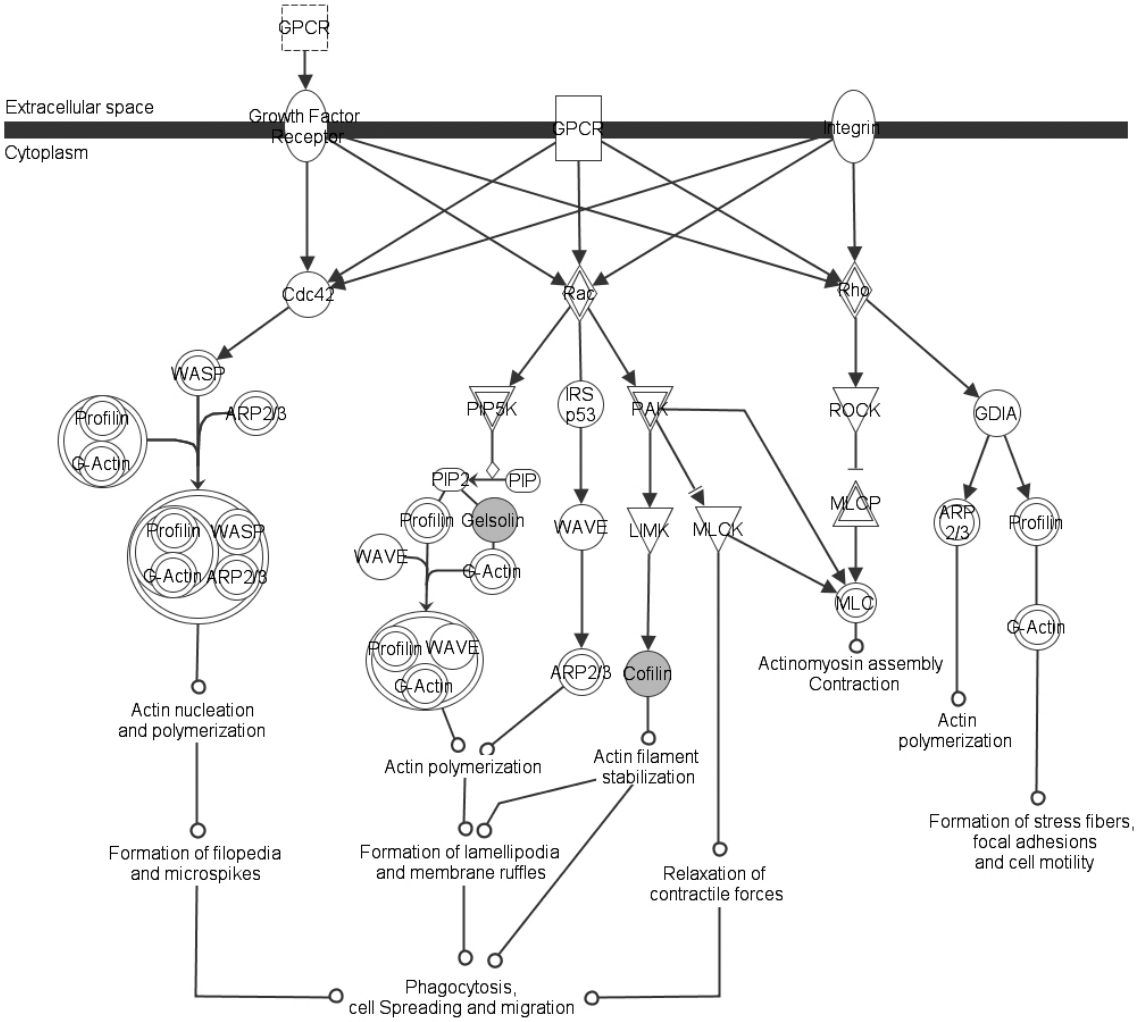

Figure 7-2: Regulation of Actin-based motility by Rho.

The figure illustrates the involvement of KIPs: Gelsolin (GSN), an important regulator of actin assembly and disassembly and Cofilin 1(CFL1), a protein that modulates actin stabilisation in a pH dependent manner in the regulation of Actin based motility.

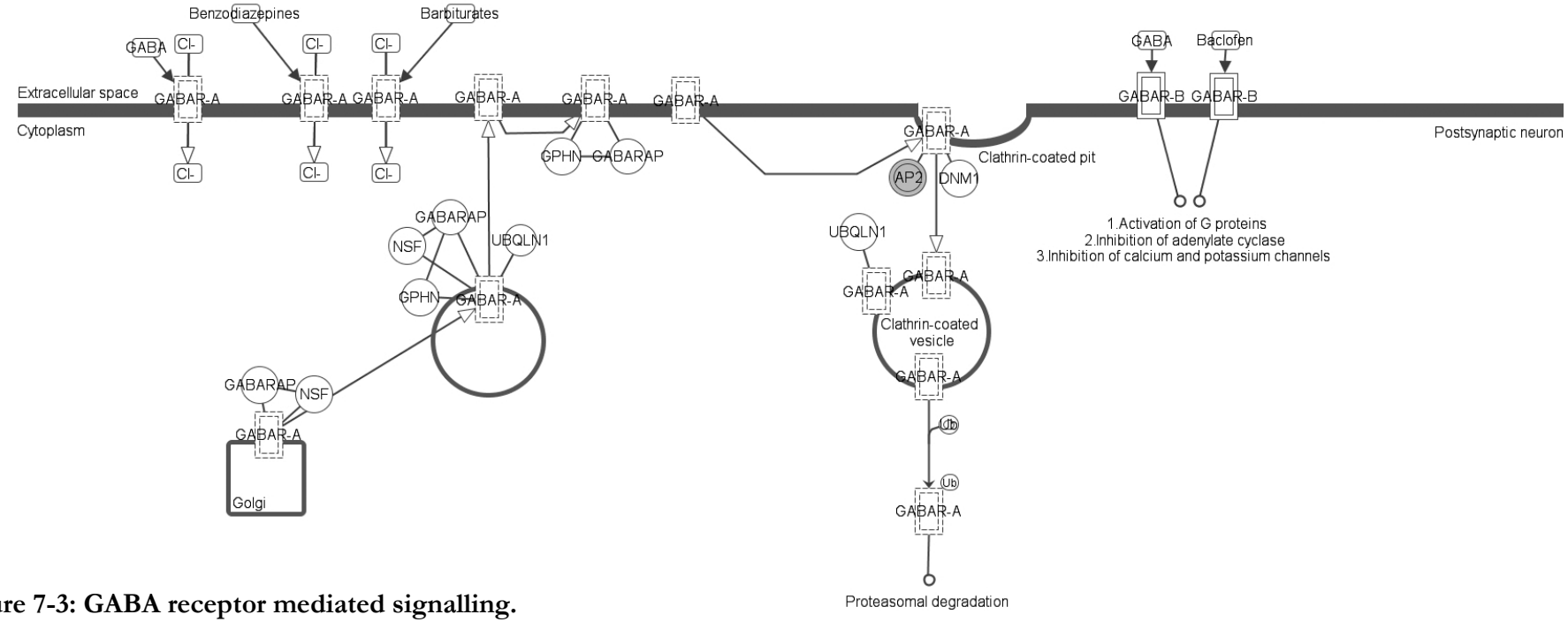

Figure 7-3: GABA receptor mediated signalling.

The figure illustrates the involvement of AP2M1, a KIP in GABA receptor mediated signalling. The GABA receptor mediated signalling plays a vital role in inhibiting neurotransmission. AP2M1 is involved in receptor recycling process and is highlighted in gray.

7.2.2.2 Network analysis reveals that KMO interacting proteins play a key role in cellular assembly and organisation

IPA analysis also revealed important networks involving KIPs (Table 7.6). KIPs were directly or indirectly involved in networks of proteins that play roles in actin mediated cellular assembly and organisation, cellular compromise and post translational modification mediated by actin assembly and disassembly (Figure 7-4). Actin and F-actin (filamentous/polymerised actin) were identified as major nodes in these networks. Four Htt interacting proteins - DCTN2, DYNC1H1, GAPDH and AP2M1 are also involved in this network. Defects in actin treadmilling associated with impaired stress response and reduced ATP levels has been implicated to play a role in HD pathology (Munsie et al., 2011).

The next network that had a significant number of KIPs included proteins that play a role in drug metabolism (i.e.- pathways that modify/regulate activity of drugs in an organism through specific enzyme based biochemical processes) (Figure 7-5). This network contained four key nodes that play a vital role in HD pathology - AKT1 (alpha serine/threonine-protein kinase), TNF, PKA (protein kinase A) and cAMP (cyclic adenosine monophosphate) and 10 KIPs. AKT1, TNF, PKA and cAMP are implicated to play a role in HD pathology and are discussed in further detail later.

KP is shown to be upregulated in response to inflammation and infectious diseases and the next protein network involved 7 KIPs that play a role in cardiovascular disease and infection mechanism; this network predominantly included proteins that play a role in regulating the transcription factor C-Myc (Figure 7-6). The significance of these protein networks are discussed in detail later.

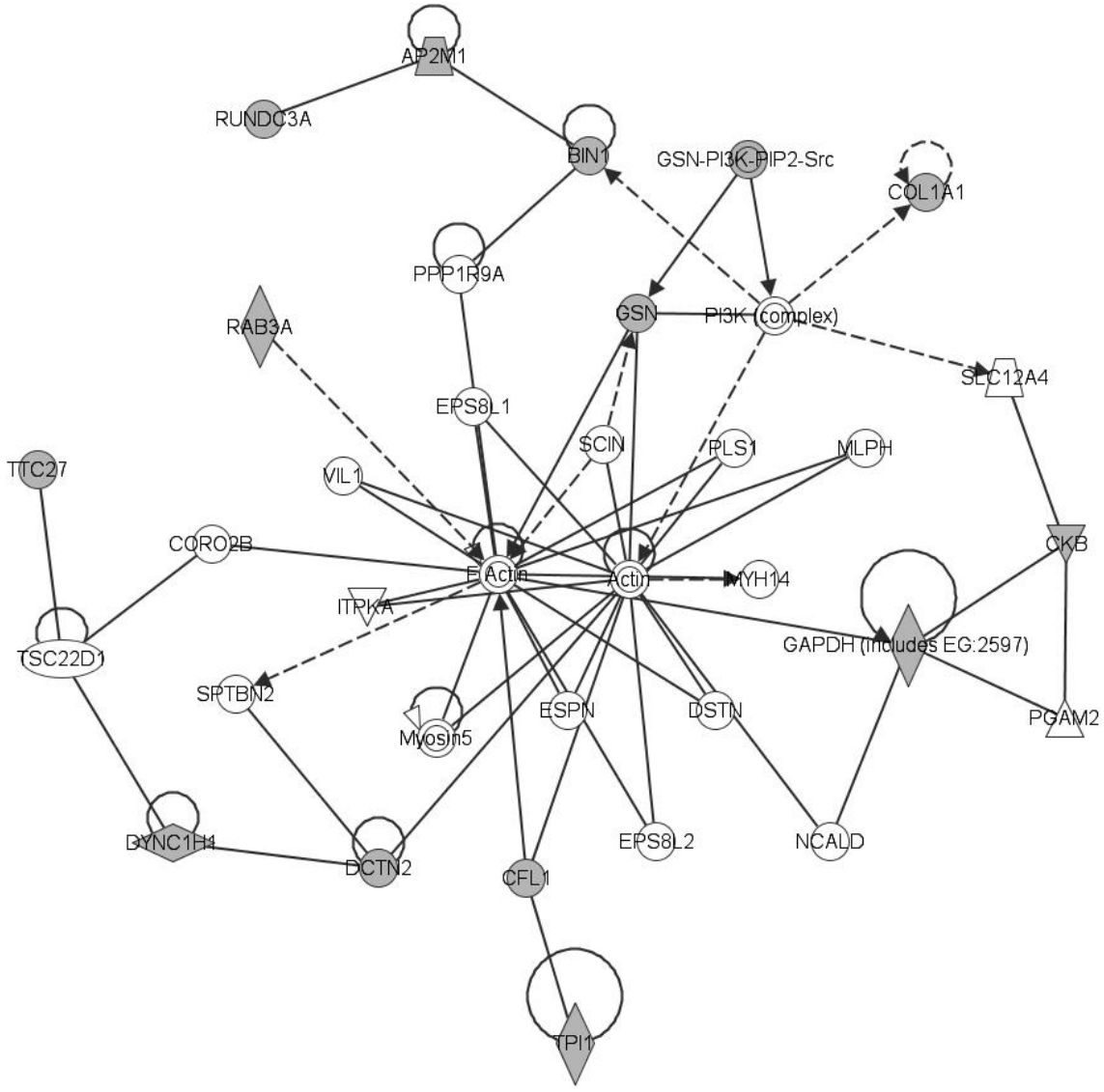

Figure 7-4: Cellular compromise, cellular assembly and organisation and post-translational modification.

Functional network analysis involving KIPs was carried out using IPA which identified this pathway to have the highest score having 14 KIPs. Two nodes [actin and F-actin (filamentous/polymerised actin)] were identified as major nodes. Four Htt interacting proteins are a part of this network. Defective actin cytoskeleton has been implicated in neurodegenerative diseases. KIPs are shown in dark grey.

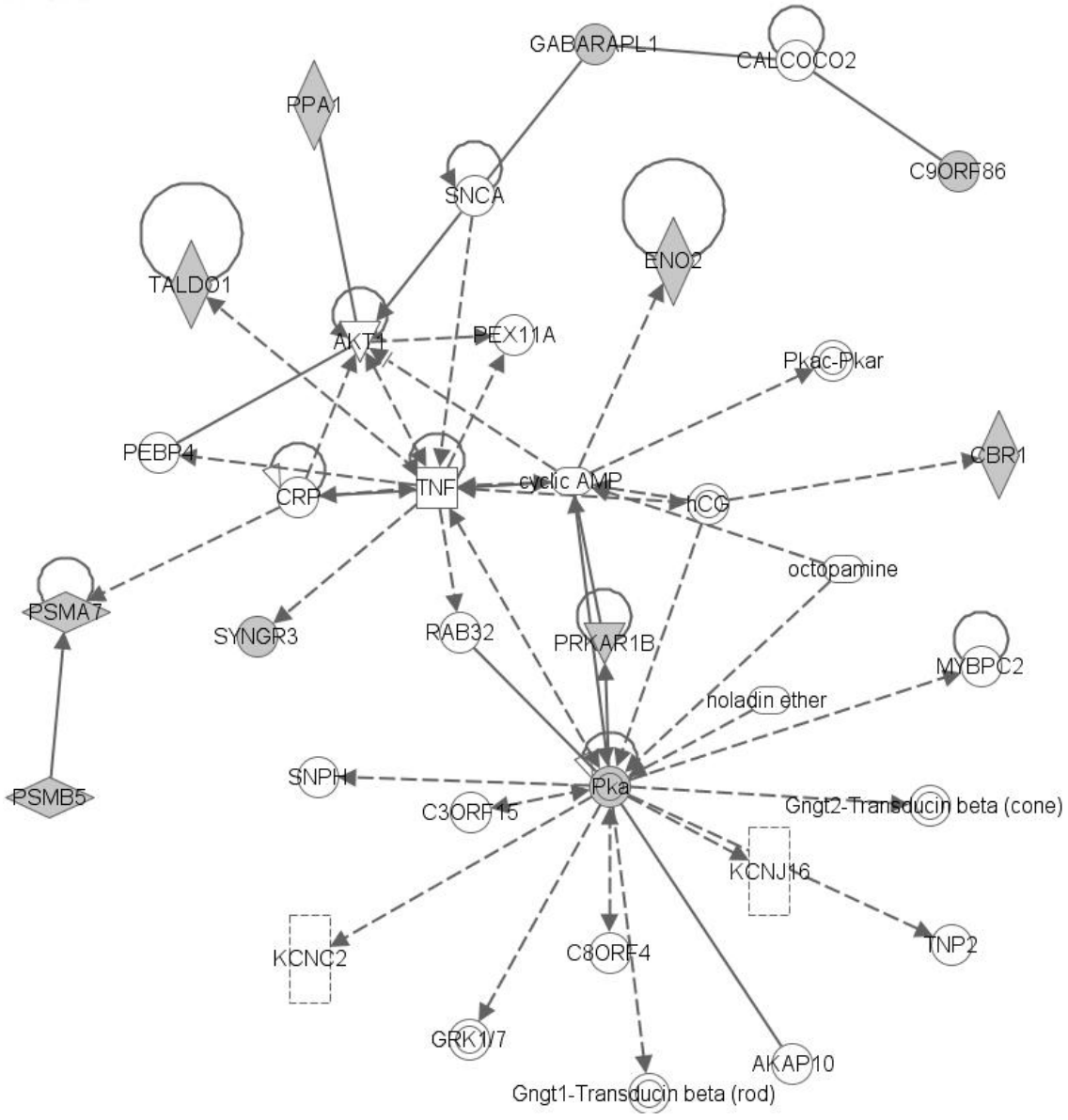

Figure 7-5: Overview of Drug metabolism network involving KIPs

Functional network analysis involving KIPs was carried out using IPA which identified drug metabolism as the second most enriched network containing 10 KIPs. Four key nodes - AKT1, TNF, PKA and cAMP - were identified as major nodes and are also implicated in HD. KIPs are shown in grey.

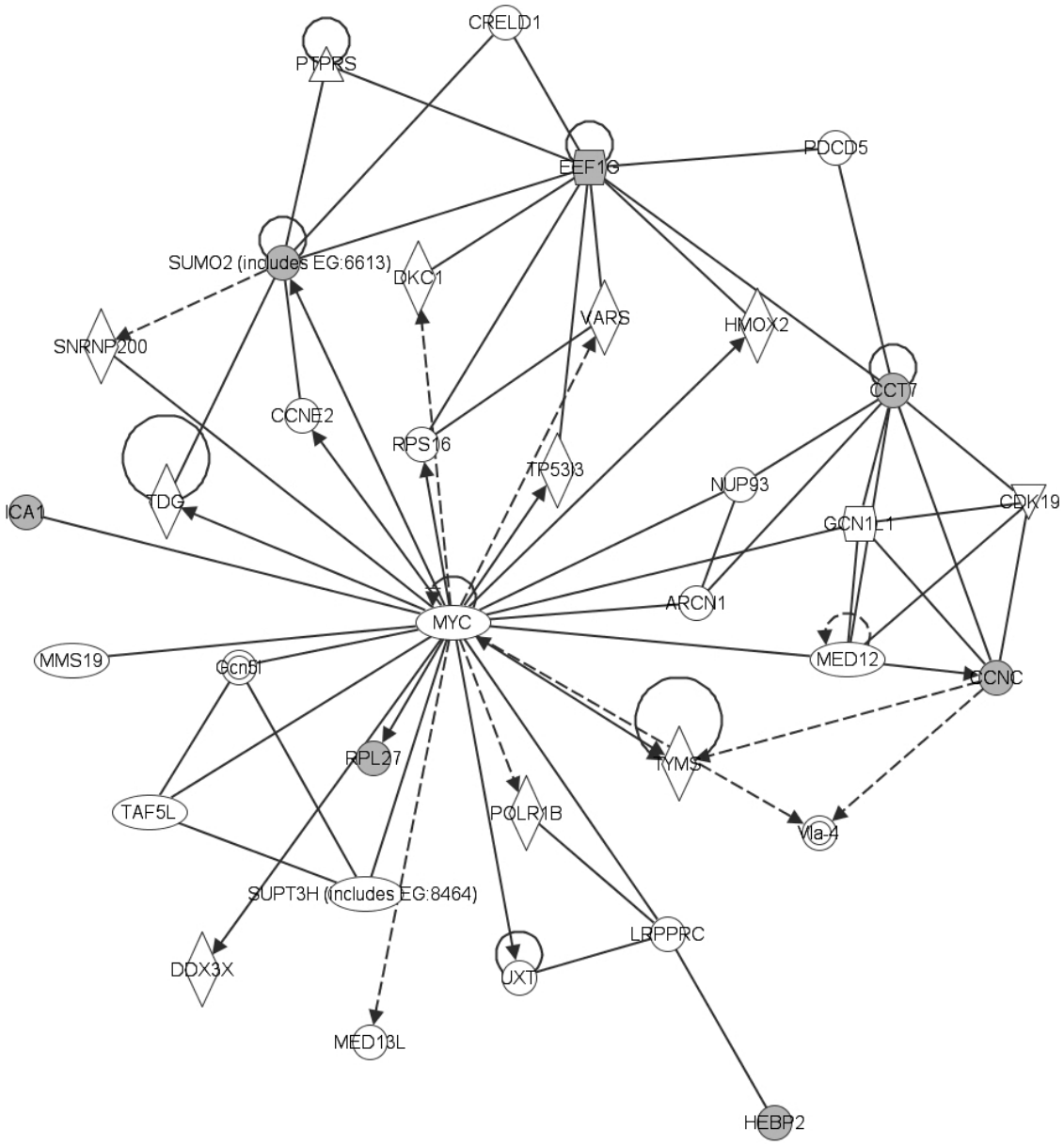

Figure 7-6: KIPs involved in cardiovascular disease, genetic disorder and infection mechanism

IPA functional network analysis was carried out to identify top enriched networks. This network was the 3rd most enriched network, containing 7 KIPs. KMO is known to be upregulated in inflammation and infectious diseases. KIPs are shown in grey.

7.2.3 KMO and huntingtin share common interaction partners

The protein interaction screen for KMO showed enrichment for proteins that interact with Htt or modify mHtt toxicity. Hence following core analysis using IPA, the Ingenuity Knowledgebase was used to query Htt interactions that overlap with KMO protein interaction partners to create a network diagram (Figure 7-7). In addition to 4 known KIPs that interact with Htt (DYNC1H1, DCTN2, AP2M1 and GAPDH), IPA analysis also identified gelsolin (GSN), topoisomerase1 (TPI1), enolase 2 (ENO2) and carbonyl reductase 1 (CBR1) yielding a total of 8 huntingtin interacting proteins. EEF1G (a suppressor of mHtt toxicity in yeast), CKB, CFL1 and SUMO2 have all been implicated to play a role in pathology of HD and other neurodegenerative diseases in addition to the RAB and RPL family of proteins which include RAB3A and RPL27 in this network have been implicated in these processes. The significance of these interactions is discussed in detail later in this chapter. Unexpectedly 14/31 KIPs identified interact with Htt or play a role in HD pathology further underscoring the importance of KMO as a therapeutic target in HD. Existing KMO interaction partners in the Ingenuity Knowledgebase included Tumor necrosis factor (TNF-α) and IFN-γ whose protein interaction partners overlapped with KIPs further validating our approach. IFN-γ, a modulator of immune response is a key regulator of enzyme IDO of the KP and mediates depletion of tryptophan in response to infection and inflammation (Figure 7-8).

Figure 7-7: Network of KMO and Huntingtin interacting proteins

IPA analysis tool was used to integrate KMO protein interactions and huntingtin protein interactions to develop a network of KMO and Huntingtin interacting proteins. 8 /31 KIPs were found to interact with huntingtin. Green lines indicate Htt interacting proteins identified from the screen and grey lines indicate KMO interacting proteins. Grey nodes indicate KIPs identified in the OMM-MYTH screen.

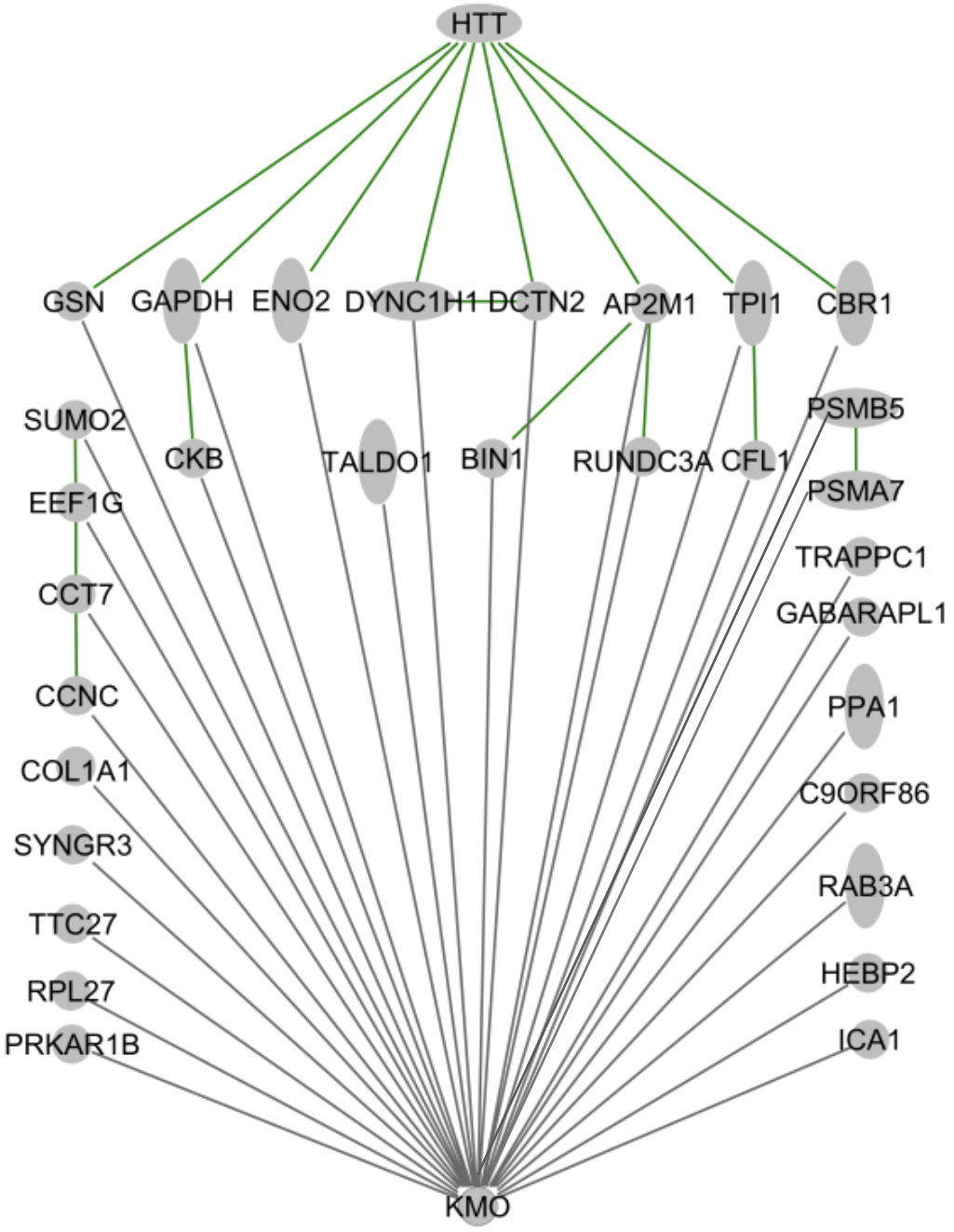
HTT
GSN
GAPDH
ENO2
DYNC1H1
DCTN2
AP2M1
TPI1
CBR1
SUMO2
CKB
TALDO1
BIN1
RUNDC3A
CFL1
PSMB5
PSMA7
EEF1G
TRAPPC1
CCT7
GABARAPL1
CCNC
PPA1
COL1A1
C9ORF86
SYNGR3
RAB3A
TTC27
HEBP2
RPL27
ICA1
PRKAR1B
KMO

Figure 7-8: IPA generated KMO interacting proteins

IPA analysis tool was used to integrate KMO protein interactions from the OMM-MYTH screen and KMO interacting proteins identified by IPA. Orange lines indicate interactions of KMO identified by IPA and interactions amongst KIPs identified by IPA, grey lines signifies protein interaction between KMO and KIPs identified by OMM-MYTH. Proteins are indicated by grey nodes.

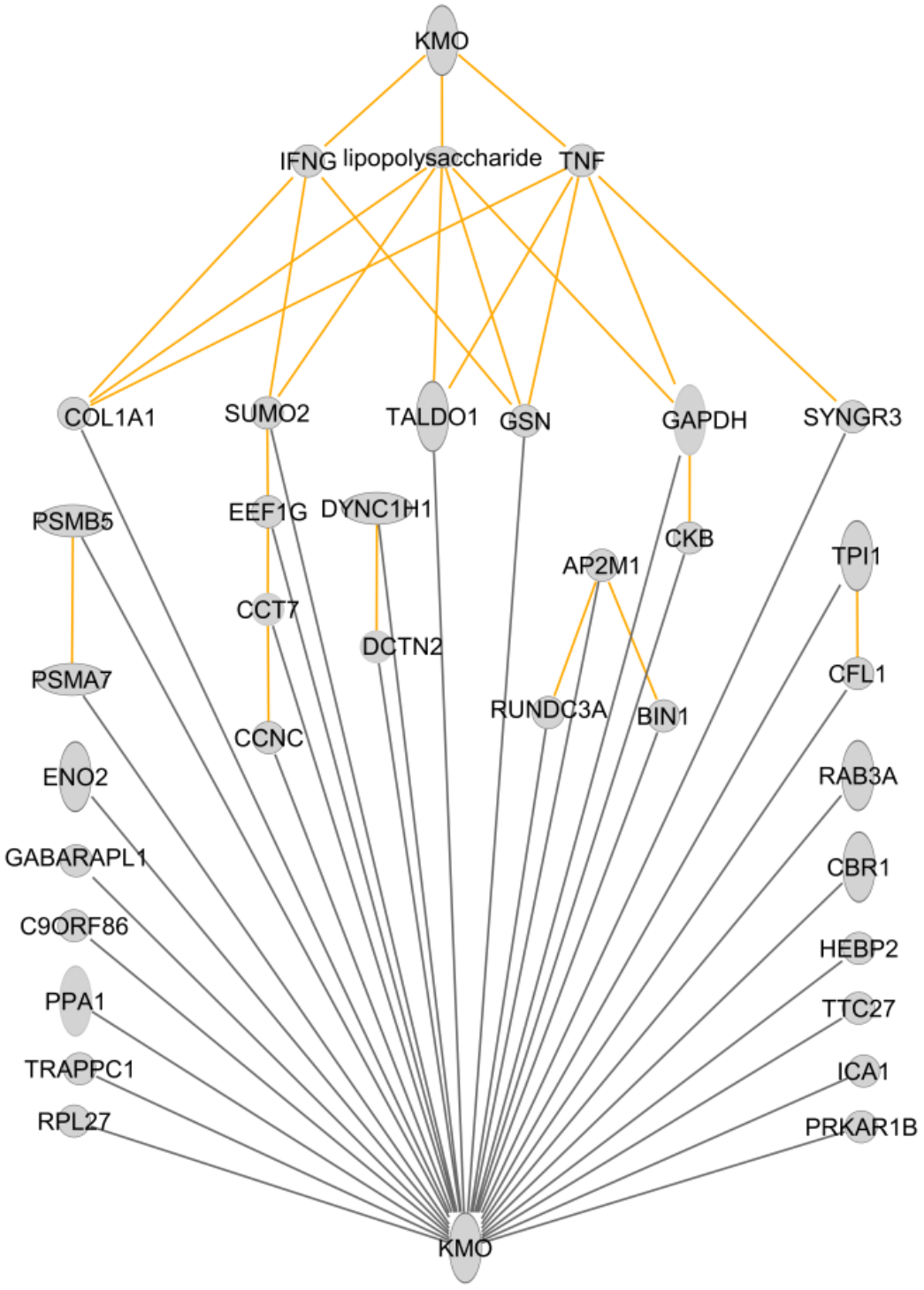
KMO
IFNG
lipopolysaccharide
TNF
COL1A1
SUMO2
TALDO1
GSN
GAPDH
SYNGR3
PSMB5
EEF1G
DYNC1H1
CKB
AP2M1
TPI1
CCT7
DCTN2
CFL1
PSMA7
RUNDC3A
BIN1
CCNC
ENO2
RAB3A
GABARAPL1
CBR1
C9ORF86
HEBP2
PPA1
TTC27
TRAPPC1
ICA1
RPL27
PRKAR1B
KMO

7.3 DISCUSSION

KMO interaction partners identified through the OMM-MYTH screen were subjected to bioinformatic analysis using DAVID bioinformatics database and IPA software. The DAVID bioinformatics resources 6.7, a gene ontology tool (Huang da et al., 2009a, Huang da et al., 2009b) was used to annotate and functionally classify KIPs. The gene ontology tool identified significant enrichment for genes involved in energy metabolism, small GTPase mediated signal transduction, vesicle mediated endocytosis, and NADP metabolic processes. Five of the biological processes involving KIPs were also found to be enriched amongst the Bna4 interactors. These include: NADP metabolism, small GTPase mediated signal transduction, intracellular signalling cascade, response to stimulus (chemical) and pyridine nucleotide biosynthetic process. Interestingly, the common protein interaction partners of KIPs are enriched in the categories that are implicated in HD, which include: transcriptional regulation, cytoskeletal proteins, translation and heat shock proteins (Bates, 2003, Landles and Bates, 2004).

As discussed in Chapter 6, the small gene lists skew the statistical significance of the output in DAVID analysis. Furthermore, for several analyses using DAVID not all genes were incorporated, although present in the database, which further affected the output. To overcome these deficiencies functional annotation analysis with IPA was used, which is optimised to work with small datasets. The functional annotation tool identified carbohydrate metabolism to be an enriched biological process similar to DAVID results. However, carbohydrate metabolism was not the top biological process enriched. IPA identified cellular movement to be the top enriched cellular process followed by carbohydrate metabolism, cellular assembly and organisation, cellular growth and proliferation and cell death. These categories showed significant enrichment with IPA and

were not observed using DAVID analysis. Consequently glycolysis/gluconeogenesis and regulation of actin by Rho proteins were identified as the top canonical pathways followed by inositol metabolism and phenylalanine, tyrosine and tryptophan biosynthesis. Phenylalanine, tyrosine and tryptophan biosynthesis (alternatively aromatic amino acid family biosynthetic process) was also identified as an enriched biological process amongst *BNA4* interactors.

Energy deficiency in HD has been discussed earlier and the top canonical pathway enriched with KIPs included glycolysis/gluconeogenesis, one of the major pathways for glucose metabolism in the brain. GAPDH, an enzyme in the glycolytic pathway has a high affinity for polyQ expanded proteins and interacts with Htt and has a high affinity for mHtt (Kaltenbach et al., 2007). GAPDH is found to be overexpressed in striatum of HD mouse models (Senatorov et al., 2003) and association of GAPDH with mHtt inhibits its enzymatic activity (Mazzola and Sirover, 2001). GAPDH apart from being an enzyme in the glycolytic pathway also plays a major role in apoptosis and membrane trafficking in the early secretory pathway (Chuang et al., 2005). TPI1, another KIP and huntingtin interactor has a key role in glycolysis where it catalyses the conversion of dihydroxyacteone phosphate (DHAP) to glyceraldehyde- 3-phosphate (G3P) which is further acted upon by GAPDH. Missense mutations in TPI1 are associated with adult onset neurodegeneration phenotype characterised by neuromuscular degeneration, motor impairment, susceptibility to infection, haemolytic anaemia and premature death (Orosz et al., 2001). Reduced levels of TPI1 results in accumulation of DHAP and G3P that undergoes non-enzymatic conversion to methylglyoxal leading to advanced glycation end products (AGEs). AGEs cause neuronal dysfunction and neurodegeneration through protein modification and oxidative damage (Ahmed et al., 2003, Gnerer et al., 2006). Inhibition of GAPDH activity

by mHtt can further increase levels of DHAP and G3P and consequently increase levels of AGEs (Gnerer et al., 2006). In HD mice, inhibition of GAPDH and TPI also decreases levels of ATP and causes progressive neuronal death in the striatum and cortex with selective sparing of NADPH diaphorase neurons that is reversible by pyruvate supplementation (the end product of glycolysis) (Sheline and Choi, 1998). AGEs are implicated to play a role in the pathology of Alzheimer's disease and Parkinson's disease (Srikanth et al., 2011). From studies in HD mice, an increase in RAGE (receptor for AGE) has been observed in MSNs and astrocytes and correlates to striatal degeneration (Ma and Nicholson, 2004). Enhanced RAGE expression is postulated to be due to increased AGE levels and not by binding of mHtt (Ma and Nicholson, 2004, Anzilotti et al., 2011). RAGE expression is also associated with increased transcription of genes associated with production of inducible nitric oxide synthetase and pro-inflammatory cytokines (Srikanth et al., 2011). Recent evidence suggests, neuronal injection of QUIN in rodents also causes an increase in RAGE expression (Cuevas et al., 2010) further underscoring that formation of AGE as a consequence of deficient energy metabolism and excitotoxicity.

Levels of both TPI1 and GAPDH are also altered in response to oxidative stress. In yeast, reduction in levels of TPI1 and GAPDH levels is protective under oxidative stress conditions and shifts the metabolic flux from glycolysis to pentose phosphate pathway leading to the production of NADPH which is essential for maintaining reducing environment in the cell (Ralser et al., 2007). Decrease in these metabolites may also trigger other events such as apoptosis eventually leading cell death (Chuang et al., 2005). However, though the re-routing of metabolic flux in response to ROS might be protective, in diseases like HD in which the cells are subject to constant ROS insults, reduced flux through glycolytic pathway may impair neuronal function and plasticity.

ENO2 (neuron specific enolase), another enzyme in the glycolytic pathway, is also an interactor of Htt. In both HD patient samples and mouse models a decrease in ENO2 levels and mRNA expression is observed (Marangos and Paul, 1981, Luthi-Carter et al., 2000, Luthi-Carter et al., 2002). Reduction in ENO2 corresponds to increased levels of excitotoxicity (Haglid et al., 1994) and induction of interleukin 6 (Chang et al., 2005), a marker for microglial activation which is elevated in HD (Dalrymple et al., 2007). Thus the dynamics of interaction between KMO and proteins involved in energy metabolism may play a role in the deficient energy metabolism observed in early HD.

Network analysis also identified cellular compromise, cellular assembly and organisation, and post translational modification as comprising an enriched network. This network is centred on modulation of F-actin (filamentous actin) and actin and contains 14 KIPs as nodes.

Actin is a highly conserved protein that plays a vital role in maintaining cytoskeleton structure, cellular movement, intracellular vesicle trafficking, response to external stimuli and various other cellular functions (Kabsch and Vandekerckhove, 1992). In the brain, actin is involved in neuronal development, synaptogenesis, synaptic vesicle trafficking, maintenance of the synapse and pre- and post-synaptic terminals (Dillon and Goda, 2005). Actin is a monomeric globular protein (G-actin) that is polymerised to F-actin and the polymerisation and depolymerisation of actin plays a key role in implementing the various cellular processes actin is involved in (Kabsch and Vandekerckhove, 1992).

Two of the KIPs identified are actin binding proteins: Gelsolin and Cofilin 1 (also known as actin depolymerisation factor (ADF)) that are involved in actin depolymerisation. Gelsolin is the most potent and the only calcium dependent actin severing protein, causing

the break down of actin filaments such that they cannot re-anneal, ultimately leading to disassembly of actin structure (Silacci et al., 2004). Gelsolin also causes blebbing of the cell membrane in a Ca^{2+} dependent manner in response to apoptotic signals (Silacci et al., 2004), which is mediated by Rho GTPase signalling. Gelsolin function is inhibited by PIP2 (Phosphatidylinositol 4,5-bisphosphate), a signalling molecule that regulates almost all ion channels and transporters (Hilgemann et al., 2001). In mice that are gelsolin null mutants, neurons show increased susceptibility to glutamate mediated excitotoxicity amongst various other defects (Furukawa et al., 1997, Endres et al., 1999). Additionally, in these mouse models, a delay in long term potentiation (LTP), an increase in long term depression (LTD) and an increase in NMDAR currents is observed (Furukawa et al., 1997, Star et al., 2002). Defects in LTP are also noticed in mouse models that are null mutants for Cofilin 1/ADF (Fukazawa et al., 2003). Additionally, gelsolin also plays an important role in apoptosis as a substrate for caspase 3 (Kothakota et al., 1997).

In addition to playing a role in late phase LTP (Fukazawa et al., 2003), Cofilin is critical for normal embryonic tissue development (Bamburg and Bray, 1987) and is involved in pathological conditions such as oxidative stress, ischemia and other stress conditions (Heyworth et al., 1997). Cofilin also plays a role in oxidant mediated apoptosis and oxidation of cofilin leads to its relocation to the mitochondria and triggers apoptosis by opening the MPTP and subsequent release of cytochrome C (Klamt et al., 2009). Cofilin has been implicated to play a role in neurodegeneration with its contribution to Alzheimer's disease progression being well studied. In neurons subjected to stress, cofilin forms rod shaped bundles composed of actin that leads to transport defects in neurites (Minamide et al., 2000). In AD, these sites of actin rods show accumulation of amyloid-β peptide (Davis et al., 2011). Increase in levels of amyloid-β however causes inactivation of

cofilin and causes neuronal dystrophy (Minamide et al., 2000, Maloney et al., 2005, Davis et al., 2011). More recently, it has been shown that like amyloid-β protein, Htt also accumulates to temporary cofilin rods under stress conditions (Munsie et al., 2011). In neurodegenerative conditions, the cofilin rods are protective since they prevent actin treadmilling and thereby make ATP available for other processes (Bernstein et al., 2006). However, the presence of cofilin rods can also affect actin dependent chromatin remodelling and transcriptional regulation, especially in the presence of mHtt which causes the presence of persistent cofilin rods and slower response to stress (Munsie et al., 2011). Cofilin affects synaptic plasticity and under stress conditions the dendritic spines are particularly sensitive. In HD, the dendritic spines of the MSNs are most affected, therefore the inability of the cell to free ATP via defective actin treadmilling may affect spine density leading to axonal atrophy as observed in HD (Munsie et al., 2011). Furthermore, transglutaminase 2 (TG-2), an enzyme involved in cofilin-actin crosslinking, is also found elevated in HD patient samples. Defective calcium signalling causes increases in TG-2 levels leading to more crosslinking between Cofilin and actin that again contributes to the defective neuronal plasticity observed in HD (Munsie et al., 2011). Other characteristics of null mutants of cofilin and gelsolin that affect synaptic plasticity such as: delay in LTP and increase in LTD has also been in observed in HD patients and HD model systems (Hodgson et al., 1999, Usdin et al., 1999, Murphy et al., 2000, Kung et al., 2007) indicating a role for actin mediated dynamics in neurodegeneration.

The other identified networks involving KIPs include drug metabolism and cardiovascular disease. Drug metabolism is a xenobiotic process, where the chemical structure of foreign compounds such as a drug is modified. This metabolism plays a vital role in regulating the efficacy of the drugs in the system and the body's response to it and drug induced

inflammatory reactions (Brodie et al., 1958). Carbonyl reductase (NADPH) 1 (CBR1) a huntingtin interacting protein and a key protein in the drug metabolism network involving 10 KIPs is well characterised for its role in increasing toxicity and decreasing the effectiveness of many drugs, reducing xenobiotic substances like ketones and quinones and buffering toxicity of ROS induced lipid peroxidation moieties (reviewed in (Oppermann, 2007)). CBR1 is highly expressed in the CNS (Wirth and Wermuth, 1992) and studies in Drosophila have demonstrated that CBR1 (*Sniffer*) function is neuroprotective against ROS induced neurodegeneration and apoptosis (Botella et al., 2004). CBR1 knockdown also increases levels of 4-hydroxynonenal (HNE) (Rashid et al., 2010), a toxic by-product of lipid peroxidation that impairs glutamate transport and mitochondrial function in neurons (Keller et al., 1997). HNE is elevated HD brains (Stoy et al., 2005) suggesting that CBR1 levels might be vital for regulating oxidative stress response and might play a role in many neurodegenerative diseases such as HD (Maser, 2006) although further studies are warranted.

The drug metabolism network reveals 4 major nodes involving AKT1, TNF, PKA and cAMP, all of which are implicated in HD pathology. AKT1 levels are found elevated in early stage HD model systems and it is thought to be a pro-survival response that prevents neuronal cell death (Gines et al., 2003). This activation of AKT1 in response to mitochondrial deficits and NMDAR activation is dependent on Ca^{2+} levels and P13 kinase which plays a role in actin-based processes (Figure 7.4) (Gines et al., 2003). Defects in PKA-cAMP signalling cascade have also been observed in presymptomatic HD mouse models (Bibb et al., 2000). TNF, on the other hand, triggers the mitochondrial death cascade apoptotic mechanism associated with microglial activation and is found to be significantly elevated in presymptomatic HD gene carriers (Tai et al., 2007b). Furthermore,

the levels of TNF progressively increase during disease progression (Tai et al., 2007b, Bjorkqvist et al., 2008) and in our study has also been identified as a key node that interacts with 5 other KIPs (see Figure 7-8).

KIPs involved in the cardiovascular disease (CVD) network interact through the Myc signalling pathway, where Myc overexpression leads to p53 dependent apoptosis in response to oxidative stress conditions/hypoxia (Haunstetter and Izumo, 1998). IFNγ mediated activation of the KP enzyme IDO and subsequent tryptophan depletion in vascular smooth muscle cells (VMSC) that make up the blood vessels has been associated with increased cardiovascular risk, especially in artherosclerosis (Wirleitner et al., 2003). Inflammation associated CVD risk is associated with depletion of tryptophan levels than increased levels of toxic metabolites (Cuffy et al., 2007). Upregulation of C-Myc, the key node in CVD and inflammatory disease network is reported to be essential for the development of VMSC (Shi et al., 1993). However increased C-Myc levels following infection or mutation alter VMSC into a progenitor cell whose monoclonal proliferation leads to accumulation of lipid containing plaques as observed in artherosclerotic lesions of the carotid artery (Benditt and Benditt, 1973, Marin et al., 1993). C-Myc expression also contributes to cardiac hypertrophy (thickening of cardiac muscle)(Taketani et al., 1997), angiogenesis (growth of new blood vessels) (Ngo et al., 2000) and other vascular proliferative disorders such as recurring stenosis (narrowing of blood vessels) after aortic injury (Schwartz, 1997).

Thus KMO and its involvement in actin dynamics and related processes may be a part of the KP response to infectious diseases and inflammation, and which involves several actin mediated processes such as phagocytosis, chemokinesis, and response to oxidative stress. However when a misfolded protein such as mHtt acts as stimuli for changes in actin

dynamics, the mutant protein may cause permanent damage to these systems and subsequent accumulation of these defects might be responsible for the pathology observed in neurodegenerative diseases.

KIPs were analysed using the IPA pathway analysis tool, and 8/31 were found to interact with Htt. The common protein interactors include proteins involved in energy metabolism, vesicle transport, oxidative stress and modulators of actin activity. Additionally, from screens carried out in our lab EEF1G overexpression has been identified as a suppressor of mHtt toxicity in yeast (Rob Mason, Ralitsa Kantcheva, Flaviano Giorgini, *unpubl data*). Furthermore, various Rpl and Rab family proteins have also been identified as modulators of mHtt in screens in yeast, mammalian and Drosophila HD models (Rob Mason, Janine Clapp, Susanna Campesan, Charalambos Kyriacou, and Flaviano Giorgini, *unpubl data*).

Thus in this chapter we have explored the biological significance of KIPs, and found a strong link to HD pathogenesis. This work provides further evidence for a mechanistic link between KP and KMO dysfunction and HD, particularly in premanifest individuals and early stage HD patients where activation of microglia and perturbations to KP are observed before the onset of symptoms. Therefore, accumulation of cellular dysfunction caused by changes in KMO biology could contribute to pathological decline in an age dependent manner in HD.

CHAPTER 8 DISCUSSION, FUTURE WORK AND CONCLUSIONS

Excitotoxicity and oxidative stress have been implicated to play a role in HD, and appear to be particularly associated with early neuropathological changes observed (Schwarcz and Kohler, 1983, Schwarcz, 2004). The overactivation/upregulation of the KP appears to be a critical aspect of these pathogenic processes with two enzymes of the KP (KMO and TDO) having been identified as potential therapeutic targets for this disease in HD models (Giorgini et al., 2005 Campesan et al., *in press* and Zwilling et al., *in press*). It is now critical to test inhibitor compounds of these enzymes in patients to ascertain if they can delay the age of onset of symptoms in HD and slow the progression of disease. In particular, targeting the mitochondrial enzyme KMO is currently of great interest to the HD research community.

Although KMO has been at the heart of many studies with regards to HD and other diseases, little is known about its basic role(s) in the cell. In this study, we focussed on KMO with the aim of obtaining a more complete understanding of the physiological role of KMO. This approach will enable a better understanding of the consequences of pharmacological inhibition of KMO and provide further insight into pathological basis of the HD and perhaps other brain diseases.

8.1 OPTIMISING MYTH TO IDENTIFY KMO INTERACTING PROTEINS

We have developed a novel protein-protein interaction system for use with outer mitochondrial membrane proteins (OMM-MYTH). This system is based on the MYTH, which has been used to identify protein interaction partners of membrane proteins in the past (Iyer et al., 2005). To our knowledge, this is the first time a screening methodology has

been developed to identify protein interaction partners of outer mitochondrial membrane proteins.

Apart from the Y2H based approaches discussed earlier (Chapter 3), most identification of protein interactions involving mitochondrial proteins has depended on the use of mass spectrometry for analysis of components obtained after affinity purification of complexes following bait presentation (Rabilloud et al., 1998, Danial et al., 2003). One of the technical challenges that mitochondrial proteins present is associated with the hydrophobic nature of most mitochondrial proteins. To this end, sucrose gradient fractionation and blue native electrophoresis have been used to elucidate protein interactions of mitochondrial proteins (Lin et al., 2002, Nijtmans et al., 2002). For example, Taylor et al. used this approach to identify the subunits of oxidative phosphorylation machinery in the heart (Taylor et al., 2002, Taylor et al., 2003). However, most of these studies involve targeted proteins that occur in complexes with a protein of interest. These approaches are not well-suited for screening approaches where either the protein interactions do not occur as part of a complex or where the interaction partners are unknown.

OMM-MYTH, a Y2H-based approach is relatively simple, easy to use and efficient. *Saccharomyces cerevisiae*, the eukaryotic organism used in the system is well understood biologically and can be readily manipulated. Importantly, the Y2H system allows for screening of thousands of possible interactions with the protein of interest in an *in vivo* setting. Another major advantage of this system is the sensitivity of the system in detecting weak or transient interactions between proteins (Van Criekinge and Beyaert, 1999). One limitation of the classic Y2H system is the dependence upon reconstitution of a transcription factor in the nucleus, which does not permit testing of protein interactions involving membrane proteins (Iyer et al., 2005). MYTH overcomes this disadvantage,

making Y2H possible for membrane bound proteins. However, prior to our study, this system had never been used with an OMM protein as bait and thus the MYTH had to be optimised to be used with OMM proteins. The most challenging part of optimising the OMM-MYTH was designing the appropriate controls to ensure correct localisation and expression of the bait. Specifically for this study we created two mitochondrial prey controls, Tom20 and Mmm1, which are both targeted to the mitochondria (Pfanner and Neupert, 1990, Burgess et al., 1994, Pfanner et al., 2004) and whose interaction with KMO/Bna4 baits confirmed the mitochondrial localisation of our proteins of interest. However, Mmm1 was later shown to be tethered to the ER as a part of a complex (Kornmann et al., 2009) showing a mitochondrial staining pattern under normal cellular conditions and an ER staining pattern when any genes of the ERMES were deleted (e.g. *mdm10*Δ) (Kornmann et al., 2009). Since our bait was found to interact with both Mmm1-NubI and Ost1-NubI, we verified if there was any mislocalisation of our protein by conducting indirect immunofluorescence studies with KMO that confirmed the localisation of KMO to the mitochondria and not to the ER. We were also able to reproduce the results observed by Kornmann et al., where we observed mitochondrial staining pattern with Mmm1-RFP under normal conditions and a ER staining pattern in a *mdm10*Δ (a member of the ERMES complex) background. This underscores the importance having multiple prey controls and the need to verify the membrane localisation of the prey controls before they are used to confirm the correct localisation of the bait. In our study we also found that there was a need to control the amount of fusion protein expressed. Studies with yeast Bna4 bait showed that in the presence of the Ste2 sequence in the bait, increased levels of 3AT were required to reduce false positive interactions associated with

the amount of fusion protein expressed. This issue was eliminated by deleting the Ste2 sequence.

Once optimised, this system has enabled us perform large scale screens to identify protein interaction partners for both human KMO and yeast Bna4. As a means to validate both the OMM-MYTH and the hits from the KMO screen itself, we also interrogated these hits by Co-IP analysis.

Additionally, we have also confirmed genetic interaction partners of yeast KMO-*BNA4* using the powerful tool of tetrad dissection. A synthetic lethal genetic screen was carried out twice in collaboration between our group and the labs of Charlie Boone and Paul Muchowski and 69 potential genetic interactors of *BNA4* were identified, of which 23 interactors were found to overlap between the two screens. The 23 candidate genes and *UTR1* (whose protein product - Utr1 is also an interactor of Bna4) were analysed by dissecting the asci (a by-product of meiosis in yeast) of diploid yeast carrying deletion for *BNA4* and each of the candidate genes. The genetic interaction data and protein interaction data were integrated in bioinformatic analysis to understand KMO/Bna4 associated function in the cell.

8.2 IDENTIFYING THE CELLULAR ROLE OF KMO

Aside from its enzymatic role in the KP, the cellular role of KMO is not well studied. In my study, the protein interaction data and genetic interaction data of KMO and Bna4 were used to understand the physiological role of KMO. KIPs from the physical interaction screen fell predominantly into four main categories: metabolism, cytoskeleton organisation, intracellular transport and signal transduction. Although there were no overlapping proteins between Bna4 and KMO interacting proteins, the proteins identified were

enriched for overlapping functional groups. In addition, the hits from the *BNA4* synthetic lethal screen were also enriched in the same functional categories as BIPs and KIPs. Bioinformatic analysis also identified similar processes (glycolysis and gluconeogenesis, regulation of actin based motility by Rho, synthesis of aromatic amino acids) as top enriched canonical pathways and actin mediated cytoskeleton organisation emerged as the top protein network involving the highest number of KIPs. The other two protein networks enriched with KIPs include drug metabolism and cardiovascular disease and, quite interestingly, infectious mechanisms.

Perturbations of KP and accumulation of KP metabolites are characteristic pathological changes observed in acute inflammatory and infectious diseases (especially diseases that affect the CNS) such as cerebral malaria and acute septicaemia (Heyes and Lackner, 1990, Clark et al., 2005). A key well studied KP enzyme – IDO, a key regulator of the KP, is activated by IFNγ, causing a depletion of tryptophan levels which inhibits growth of viral cells during infection (Takikawa et al., 1999) though depletion of tryptophan during chronic infection compromises immune T-cell function (Takikawa et al., 1999, Chiarugi et al., 2001b). IDO activation and upregulation of KP also causes serotonin depletion which in turn leads to psychosomatic and depressive symptoms (Leonard, 2007). As discussed earlier IFNγ mediated IDO activation and upregulation of KP also contributes to artherosclerotic cardiovascular disease (Pawlak et al., 2010) (Chapter 7) and involves KIPs that play a role in c-Myc signalling, mediating vascular development and proliferation. Additionally, another KP metabolite KYNA is also known to modulate cardiovascular function by regulating the rostral ventrolateral medulla of CNS, thereby regulating blood pressure (Colombari et al., 2001). In spontaneously hypertensive rats, a missense mutation in kynurenine aminotransferase I leading to low levels of KYNA and in the region of brain

controlling blood pressure contributes to pathology (Kwok et al., 2002). This suggests a role for the KP and KMO in maintaining cardiovascular function and for KMO as well.

IDO likely is involved in actin mediated dynamics via its role in phagocytosis (Chimini and Chavrier, 2000) , which forms a part of host response to infection. This suggests that KMO through actin treadmilling and cytoskeleton associated functions may also contribute to immune response in infectious diseases. Further studies are required to understand exactly how KMO is involved response in infectious disease.

8.3 ROLE OF KMO IN HD PATHOLOGY AND MITOCHONDRIAL FUNCTION

Notably, protein interaction partners of KMO included proteins that interact with huntingtin and known modifiers of mHtt toxicity in various model systems such as yeast, fruit flies, and mammalian cell lines. This indicates that inhibition of KMO may be an interesting therapeutic target not only because it increases KYNA relative to QUIN and 3-HK, but also because upregulation of KMO on its own could possibly contribute to toxicity of mHtt by perturbation of its cellular interactions, although further studies are required to understand the relationship between KMO mediated protein interactions and mHtt toxicity. For example, lipopolysaccharide treatment causes CNS inflammation and induction of IFNγ/TNF-α consequently induces IDO and KMO expression and depletion of tryptophan via KP (Connor et al., 2008), suggesting that regulation of both KMO and IDO is vital for KP regulation.

Another interesting aspect of KMO and its contribution to HD pathology lies in the cellular localisation of KMO to the OMM. The proteins of the outer mitochondrial membrane include key proteins such as VDAC proteins that regulate the opening and

closing ion channels in the mitochondria (Hoogenboom et al., 2007), and the TOM proteins which are a part of the protein translocation complex that is involved in the transport of mitochondrial pre-proteins from the cytoplasm to their requisite location within the mitochondria (Pfanner and Meijer, 1997). As evinced above, directly or indirectly proteins in the mitochondrial outer membrane contribute to the maintenance of functional and healthy mitochondria that is essential for various mitochondrial processes involving energy metabolism, reducing damage by free radicals and maintaining the correct redox environment in the cell. This suggests that KMO, by virtue of its localisation may contribute in hitherto unknown ways to maintaining functional and healthy mitochondria. Alterations in KMO function could affect mitochondrial biology, ultimately contributing to the mitochondrial dysfunction phenotype observed in HD. Interestingly, enzymes of different energy metabolic pathways such as GAPDH, TPI1, ENO2, TALDO1, CKB identified been identified as KIPs in our study which further suggests a possible role for KMO in mitochondrial function and deficient energy metabolism observed in HD. Also, there are four KATs reported so far, of which KATIV, or mitochondrial aspartate aminotransferase, is targeted to the mitochondria (Han et al., 2010). Studies with other KATs have shown that KATI and KATIII also have isoforms that are targeted to the mitochondria and KATII may also be a mitochondrial protein (Han et al., 2010). KATIV plays a major role in KYNA synthesis in the brain and is required for the synthesis of neurotransmitter glutamate and in the synthesis of α-ketoglutarate through which it regulates glutamate recycling via the TCA cycle (Schousboe et al., 1993, McKenna et al., 1996a, McKenna et al., 1996b). KATIV also plays a vital role in the malate-aspartate shuttle in the brain, through which reducing equivalents such as NAD+ and NADH are transported from the cytosol to the mitochondria (McKenna et al., 2006). The presence of

multiple KP enzymes in the mitochondria suggests that mitochondrial localisation is critical to KP function and that KMO is important in mitochondrial function. Thus, it is clear that further studies are required to clarify the role of KMO in mitochondrial function.

As highlighted earlier, targeting the KP by inhibition of either TDO or KMO clearly reduces the 3HK/KYNA ratio is neuroprotective in HD model flies (Campesan et al., 2011). This work has been translated into mice, where the KMO inhibitor JM6 was found to ameliorate neurodegeneration in Alzheimer's disease and HD mouse models (Zwilling et al., 2011). These studies strongly underscore the importance of KP perturbations in neurodegenerative diseases and suggest that targeting the KP could be widely applied to treat/delay the onset of symptoms in neurodegenerative disorders in general.

8.4 KMO AND SCHIZOPHRENIA

Perturbation of the KP has also been implicated in schizophrenia, a complex mental disorder characterised by psychotic symptoms, cognitive impairment and dysfunction of the neurotransmitters glutamate, dopamine and acetylcholine in the prefrontal cortex (Sarter et al., 2005, Lewis and Moghaddam, 2006). KYNA antagonises both NMDA (Birch et al., 1988) and α7-nicotinic acetylcholine receptors (Hilmas et al., 2001) and thereby indirectly regulates the levels of all three neurotransmitters. Increased KYNA levels has been observed in the plasma and the cerebrospinal fluid of schizophrenic patients, as well as in the prefrontal cortex, which is causally associated with neuropathology and cognitive defects observed in this disorder (Wonodi and Schwarcz, 2010).

Interestingly, the chromosomal region containing KMO (1q42-44) has been associated with aetiology of schizophrenia (Blackwood et al., 2001). A study in a Japanese population identified a SNP (rs2275163) in KMO associated with susceptibility to schizophrenia, but

could not initially be replicated by the authors (Aoyama et al., 2006) However, the same SNP in KMO was found to be associated with schizophrenia endophenotypes in a more recent study (Wonodi and Schwarcz, 2010). Subsequent analysis also recorded a decrease in metabolites in the KMO branch of the pathway (Sathyasaikumar et al., 2010) and specifically in KMO activity and KMO gene expression in prefrontal cortex in schizophrenic patients (Wonodi and Schwarcz, 2010), suggesting that increased KYNA production driven by a decrease in KMO activity may contribute to cognitive deficits in schizophrenic patients. Another non-synonymous polymorphism in KMO causing an increase in KYNA levels in both healthy and schizophrenic controls has been identified (Linderholm et al., 2010). Furthermore, another KMO polymorphism (rs2065799) was found to be associated with psychotic disorders in the Norwegian population (Holtze et al., 2011), suggesting that KMO polymorphisms may play a role in a wide variety of mental illnesses in which KP perturbations have already been implicated. It is of interest that proteome analysis of post-mortem prefrontal cortex samples from schizophrenic patients showed a significant change in expression of proteins involved in cytoskeleton assembly, energy metabolism, calcium homeostasis (involving calmoudulin and calcineurin) and maintenance of the immune system (Martins-de-Souza et al., 2009), all functional processes involving KIPs.

8.5 FUTURE WORK

One of the first steps for future analysis would be the validation of interesting hits from the OMM-MYTH screen in higher model systems such as mammalian cell lines. An established method in the lab that we plan to use for this purpose is bimolecular fluorescence complementation (BiFC), also known as the split-GFP system. In this system, two molecules that are interactors from the yeast screens could be fused to two halves of a

fluorescent protein (GFP, Venus, etc.) such that an interaction between the two proteins results in fluorescence where the intensity of interaction may be measured by the strength of fluorescence (Kerppola, 2006a, Kerppola, 2006b). One of the major advantages of this system is that it allows visualisation of protein interactions in living mammalian cells, and does not require lysis of cells as required in biochemical approaches. Furthermore, this technique provides information on the localization of the interacting proteins, which is critical as KMO is a membrane protein. This system can be used to detect weak transient interactions and interactions of proteins that are expressed at low levels (Kerppola, 2006a). Additionally, if cell-lines are used that contain inducible mHtt constructs, this system will aid in understanding alteration in protein interactions dynamics involving KMO in the presence of mHtt fragment and shed further light on how cellular dynamics may be altered. Such experiments could provide the launching pad for further analysis of a subset of the KIPs and their interactions with KMO in the context of HD. Parallel experiments with other cell models of disease involving KMO could also be undertaken.

While the current studies aid in understanding the cellular role of KMO via their protein and genetic interactions, there is a limitation on how much information protein interaction can provide about the cellular role of KMO. Another powerful tool that will aid in further characterising the role of KMO in vivo is gene expression analysis. Microarray analysis on several tissues from homozygous and heterozygous KMO knockout mice (Giorgini et al., *in preparation*) available in our lab will help identify genes that are differentially expressed versus wild-type controls. Identifying differentially expressed genes will provide vital information on how KMO modulates the activity of these genes, and aid in understanding KMO biology and its contribution to pathology in both neurodegenerative disease and

infection. Additionally, primary tissues from KMO knockout mice will also aid in understand the role of KMO in mitochondrial function.

Similar studies with other KP genes/enzymes will also aid in generating a complete KP network that will aid in further characterising the role of KP in the cell. Understanding how different KP genes/enzymes are regulated in disease conditions will further our understanding about the role of KP in normal and disease states.

8.6 CONCLUSIONS

Thus in conclusion, KP plays a vital role in many diseases that affect the CNS through processes such as excitotoxicity, oxidative stress and deficient energy metabolism. KMO is critical enzyme in this pathway that regulates the formation of neuroactive metabolites and is a potential therapeutic target for neurodegenerative diseases such as HD. The primary focus of this work has been the identification of protein interaction partners of KMO which include proteins involved in a wide array of cellular processes. Interestingly, several of these processes are altered in HD, and many huntingtin interacting proteins and HD modifiers are among the proteins identified. Thus, it appears that KMO may play additional roles in HD pathophysiology, in addition to its central role in modulation of neuroactive KP metabolites, further supporting KMO as a central therapeutic target for this disease. It is now critical to explore the new avenues generated by this study, both in the context of normal cellular biology, as well as in disease pathogenesis.

BIBLIOGRAPHY

ABDULLAH, M. F. & BORTS, R. H. (2001) Meiotic recombination frequencies are affected by nutritional states in Saccharomycescerevisiae. *Proc Natl Acad Sci U S A,* 98**,** 14524-9.

AHMED, N., BATTAH, S., KARACHALIAS, N., BABAEI-JADIDI, R., HORANYI, M., BAROTI, K., HOLLAN, S. & THORNALLEY, P. J. (2003) Increased formation of methylglyoxal and protein glycation, oxidation and nitrosation in triosephosphate isomerase deficiency. *Biochim Biophys Acta,* 1639**,** 121-32.

AKSENOV, M., AKSENOVA, M., BUTTERFIELD, D. A. & MARKESBERY, W. R. (2000) Oxidative modification of creatine kinase BB in Alzheimer's disease brain. *J Neurochem,* 74**,** 2520-7.

ALBERATI-GIANI, D., CESURA, A. M., BROGER, C., WARREN, W. D., ROVER, S. & MALHERBE, P. (1997) Cloning and functional expression of human kynurenine 3-monooxygenase. *FEBS Lett,* 410**,** 407-12.

ALBERTI, S., GITLER, A. D. & LINDQUIST, S. (2007) A suite of Gateway cloning vectors for high-throughput genetic analysis in Saccharomyces cerevisiae. *Yeast,* 24**,** 913-9.

ANDERSON, R. M., BITTERMAN, K. J., WOOD, J. G., MEDVEDIK, O., COHEN, H., LIN, S. S., MANCHESTER, J. K., GORDON, J. I. & SINCLAIR, D. A. (2002) Manipulation of a nuclear NAD+ salvage pathway delays aging without altering steady-state NAD+ levels. *J Biol Chem,* 277**,** 18881-90.

ANTEQUERA, D., VARGAS, T., UGALDE, C., SPUCH, C., MOLINA, J. A., FERRER, I., BERMEJO-PAREJA, F. & CARRO, E. (2009) Cytoplasmic gelsolin increases mitochondrial activity and reduces A beta burden in a mouse model of Alzheimer's disease. *Neurobiology of Disease,* 36**,** 42-50.

ANZILOTTI, S., GIAMPA, C., LAURENTI, D., PERRONE, L., BERNARDI, G., MELONE, M. A. & FUSCO, F. R. (2011) Immunohistochemical localization of receptor for advanced glycation end (RAGE) products in the R6/2 mouse model of Huntington's disease. *Brain Res Bull.*

AOYAMA, N., TAKAHASHI, N., SAITO, S., MAENO, N., ISHIHARA, R., JI, X., MIURA, H., IKEDA, M., SUZUKI, T., KITAJIMA, T., YAMANOUCHI, Y., KINOSHITA, Y., YOSHIDA, K., IWATA, N., INADA, T. & OZAKI, N. (2006) Association study between kynurenine 3-monooxygenase gene and schizophrenia in the Japanese population. *Genes Brain Behav,* 5**,** 364-8.

ARNING, L., KRAUS, P. H., VALENTIN, S., SAFT, C., ANDRICH, J. & EPPLEN, J. T. (2005) NR2A and NR2B receptor gene variations modify age at onset in Huntington disease. *Neurogenetics,* 6**,** 25-8.

ASTSATUROV, I., RATUSHNY, V., SUKHANOVA, A., EINARSON, M. B., BAGNYUKOVA, T., ZHOU, Y., DEVARAJAN, K., SILVERMAN, J. S., TIKHMYANOVA, N., SKOBELEVA, N., PECHERSKAYA, A., NASTO, R. E., SHARMA, C., JABLONSKI, S. A., SEREBRIISKII, I. G., WEINER, L. M. & GOLEMIS, E. A. (2011) Synthetic lethal screen of an EGFR-centered network to improve targeted therapies. *Sci Signal,* 3**,** ra67.

BALAKIREV, M., KHRAMTSOV, V. V. & ZIMMER, G. (1997) Modulation of the mitochondrial permeability transition by nitric oxide. *Eur J Biochem,* 246**,** 710-8.

BALL, H. J., SANCHEZ-PEREZ, A., WEISER, S., AUSTIN, C. J., ASTELBAUER, F., MIU, J., MCQUILLAN, J. A., STOCKER, R., JERMIIN, L. S. & HUNT, N. H. (2007) Characterization of an indoleamine 2,3-dioxygenase-like protein found in humans and mice. *Gene,* 396**,** 203-13.

BAMBURG, J. R. & BRAY, D. (1987) Distribution and cellular localization of actin depolymerizing factor. *J Cell Biol,* 105**,** 2817-25.

BATES, G. (2003) Huntingtin aggregation and toxicity in Huntington's disease. *Lancet,* 361**,** 1642-4.

BEAL, M. F., MATSON, W. R., STOREY, E., MILBURY, P., RYAN, E. A., OGAWA, T. & BIRD, E. D. (1992) Kynurenic acid concentrations are reduced in Huntington's disease cerebral cortex. *J Neurol Sci,* 108**,** 80-7.

BEAL, M. F., SWARTZ, K. J., HYMAN, B. T., STOREY, E., FINN, S. F. & KOROSHETZ, W. (1991) Aminooxyacetic acid results in excitotoxin lesions by a novel indirect mechanism. *J Neurochem,* 57**,** 1068-73.

BECKMAN, J. S., BECKMAN, T. W., CHEN, J., MARSHALL, P. A. & FREEMAN, B. A. (1990) Apparent hydroxyl radical production by peroxynitrite: implications for endothelial injury from nitric oxide and superoxide. *Proc Natl Acad Sci U S A,* 87**,** 1620-4.

BENDER, A. & PRINGLE, J. R. (1991) Use of a screen for synthetic lethal and multicopy suppressee mutants to identify two new genes involved in morphogenesis in Saccharomyces cerevisiae. *Mol Cell Biol,* 11**,** 1295-1305.

BENDER, D. A. & MCCREANOR, G. M. (1982) The preferred route of kynurenine metabolism in the rat. *Biochim Biophys Acta,* 717**,** 56-60.

BENDITT, E. P. & BENDITT, J. M. (1973) Evidence for a monoclonal origin of human atherosclerotic plaque. *Proc Natl Acad Sci USA,* 70**,** 1753–1756.

BENSEN, E. S., YEUNG, B. G. & PAYNE, G. S. (2001) Ric1p and the Ypt6p GTPase function in a common pathway required for localization of trans-Golgi network membrane proteins. *Mol Biol Cell,* 12**,** 13-26.

BERLIOCCHI, L., BANO, D. & NICOTERA, P. (2005) Ca2+ signals and death programmes in neurons. *Philos Trans R Soc Lond B Biol Sci,* 360**,** 2255-8.

BERNSTEIN, B. W., CHEN, H., BOYLE, J. A. & BAMBURG, J. R. (2006) Formation of actin-ADF/cofilin rods transiently retards decline of mitochondrial potential and ATP in stressed neurons. *Am J Physiol Cell Physiol,* 291**,** C828-39.

BERTOLINO, M., VICINI, S. & COSTA, E. (1989) Kynurenic acid inhibits the activation of kainic and N-methyl-D-aspartic acid-sensitive ionotropic receptors by a different mechanism. *Neuropharmacology,* 28**,** 453-7.

BIBB, J. A., YAN, Z., SVENNINGSSON, P., SNYDER, G. L., PIERIBONE, V. A., HORIUCHI, A., NAIRN, A. C., MESSER, A. & GREENGARD, P. (2000) Severe deficiencies in dopamine signaling in presymptomatic Huntington's disease mice. *Proc Natl Acad Sci U S A,* 97**,** 6809-14.

BIRCH, P. J., GROSSMAN, C. J. & HAYES, A. G. (1988) Kynurenic acid antagonises responses to NMDA via an action at the strychnine-insensitive glycine receptor. *Eur J Pharmacol,* 154**,** 85-7.

BJORKQVIST, M., WILD, E. J., THIELE, J., SILVESTRONI, A., ANDRE, R., LAHIRI, N., RAIBON, E., LEE, R. V., BENN, C. L., SOULET, D., MAGNUSSON, A., WOODMAN, B., LANDLES, C., POULADI, M. A., HAYDEN, M. R., KHALILI-SHIRAZI, A., LOWDELL, M. W., BRUNDIN, P., BATES, G. P., LEAVITT, B. R., MOLLER, T. & TABRIZI, S. J. (2008) A novel pathogenic pathway of immune activation detectable before clinical onset in Huntington's disease. *J Exp Med,* 205**,** 1869-77.

BLACKWOOD, D. H., FORDYCE, A., WALKER, M. T., ST CLAIR, D. M., PORTEOUS, D. J. & MUIR, W. J. (2001) Schizophrenia and affective disorders--cosegregation with a translocation at chromosome 1q42 that directly disrupts brain-expressed genes: clinical and P300 findings in a family. *Am J Hum Genet,* 69**,** 428-33.

BLOCK, M. L., ZECCA, L. & HONG, J. S. (2007) Microglia-mediated neurotoxicity: uncovering the molecular mechanisms. *Nat Rev Neurosci,* 8**,** 57-69.

BLONDEAU, F., RITTER, B., ALLAIRE, P. D., WASIAK, S., GIRARD, M., HUSSAIN, N. K., ANGERS, A., LEGENDRE-GUILLEMIN, V., ROY, L., BOISMENU, D., KEARNEY, R. E., BELL, A. W., BERGERON, J. J. & MCPHERSON, P. S. (2004) Tandem MS analysis of brain clathrin-coated vesicles reveals their critical involvement in synaptic vesicle recycling. *Proc Natl Acad Sci U S A,* 101**,** 3833-8.

BONANOMI, D., BENFENATI, F. & VALTORTA, F. (2006) Protein sorting in the synaptic vesicle life cycle. *Prog Neurobiol,* 80**,** 177-217.

BORGONOVO, J., SELTZER, A. & SOSA, M. A. (2009) Acute intrastriatal administration of quinolinic acid affects the expression of the coat protein AP-2 and its interaction with membranes. *J Neural Transm,* 116**,** 1201-8.

BOTELLA, J. A., ULSCHMID, J. K., GRUENEWALD, C., MOEHLE, C., KRETZSCHMAR, D., BECKER, K. & SCHNEUWLY, S. (2004) The Drosophila carbonyl reductase sniffer prevents oxidative stress-induced neurodegeneration. *Curr Biol,* 14**,** 782-6.

BRACHMANN, C. B., DAVIES, A., COST, G. J., CAPUTO, E., LI, J., HIETER, P. & BOEKE, J. D. (1998) Designer deletion strains derived from Saccharomyces cerevisiae S288C: a useful set of strains and plasmids for PCR-mediated gene disruption and other applications. *Yeast,* 14**,** 115-32.

BRODER, Y. C., KATZ, S. & ARONHEIM, A. (1998) The ras recruitment system, a novel approach to the study of protein-protein interactions. *Curr Biol,* 8**,** 1121-4.

BRODIE, B. B., GILLETTE, J. R. & LA DU, B. N. (1958) Enzymatic metabolism of drugs and other foreign compounds. *Annu Rev Biochem,* 27**,** 427-54.

BRUCKNER, A., POLGE, C., LENTZE, N., AUERBACH, D. & SCHLATTNER, U. (2009) Yeast two-hybrid, a powerful tool for systems biology. *Int J Mol Sci,* 10**,** 2763-88.

BURGESS, S. M., DELANNOY, M. & JENSEN, R. E. (1994) MMM1 encodes a mitochondrial outer membrane protein essential for establishing and maintaining the structure of yeast mitochondria. *J Cell Biol,* 126**,** 1375-91.

BURKHARDT, J. K., ECHEVERRI, C. J., NILSSON, T. & VALLEE, R. B. (1997) Overexpression of the dynamitin (p50) subunit of the dynactin complex disrupts dynein-dependent maintenance of membrane organelle distribution. *J Cell Biol,* 139**,** 469-84.

CARPENEDO, R., PITTALUGA, A., COZZI, A., ATTUCCI, S., GALLI, A., RAITERI, M. & MORONI, F. (2001) Presynaptic kynurenate-sensitive receptors inhibit glutamate release. *Eur J Neurosci,* 13**,** 2141-7.

CARRERAS, M. C., FRANCO, M. C., PERALTA, J. G. & PODEROSO, J. J. (2004) Nitric oxide, complex I, and the modulation of mitochondrial reactive species in biology and disease. *Mol Aspects Med,* 25**,** 125-39.

CARROZZA, M. J., FLORENS, L., SWANSON, S. K., SHIA, W. J., ANDERSON, S., YATES, J., WASHBURN, M. P. & WORKMAN, J. L. (2005) Stable incorporation of sequence specific repressors Ash1 and Ume6 into the Rpd3L complex. *Biochim Biophys Acta,* 1731**,** 77-87; discussion 75-6.

CASCINO, A., CANGIANO, C., CECI, F., FRANCHI, F., MINEO, T., MULIERI, M., MUSCARITOLI, M. & ROSSI FANELLI, F. (1991) Increased plasma free tryptophan levels in human cancer: a tumor related effect? *Anticancer Res,* 11**,** 1313-6.

CAVISTON, J. P., ROSS, J. L., ANTONY, S. M., TOKITO, M. & HOLZBAUR, E. L. F. (2007) Huntingtin facilitates dynein/dynactin-mediated vesicle transport. *Proceedings of the National Academy of Sciences of the United States of America,* 104**,** 10045-10050.

CEPEDA, C., HURST, R. S., CALVERT, C. R., HERNANDEZ-ECHEAGARAY, E., NGUYEN, O. K., JOCOY, E., CHRISTIAN, L. J., ARIANO, M. A. & LEVINE, M. S. (2003) Transient and progressive electrophysiological alterations in the corticostriatal pathway in a mouse model of Huntington's disease. *J Neurosci,* 23**,** 961-9.

CERESOLI-BORRONI, G., GUIDETTI, P., AMORI, L., PELLICCIARI, R. & SCHWARCZ, R. (2007) Perinatal kynurenine 3-hydroxylase inhibition in rodents: pathophysiological implications. *J Neurosci Res,* 85**,** 845-54.

CHANG, K. T., TSAI, C. M., CHIOU, Y. C., CHIU, C. H., JENG, K. S. & HUANG, C. Y. (2005) IL-6 induces neuroendocrine dedifferentiation and cell proliferation in non-small cell lung cancer cells. *Am J Physiol Lung Cell Mol Physiol,* 289**,** L446-53.

CHAVEZ, E., MELENDEZ, E., ZAZUETA, C., REYES-VIVAS, H. & PERALES, S. G. (1997) Membrane permeability transition as induced by dysfunction of the electron transport chain. *Biochem Mol Biol Int,* 41**,** 961-8.

CHEN, D. C., YANG, B. C. & KUO, T. T. (1992) One-step transformation of yeast in stationary phase. *Curr Genet,* 21**,** 83-4.

CHEN, S., BERTHELIER, V., YANG, W. & WETZEL, R. (2001) Polyglutamine aggregation behavior in vitro supports a recruitment mechanism of cytotoxicity. *J Mol Biol,* 311**,** 173-82.
CHEVALLIER, M. R. & LACROUTE, F. (1982) Expression of the cloned uracil permease gene of Saccharomyces cerevisiae in a heterologous membrane. *EMBO J,* 1**,** 375-7.
CHIARUGI, A., CALVANI, M., MELI, E., TRAGGIAI, E. & MORONI, F. (2001a) Synthesis and release of neurotoxic kynurenine metabolites by human monocyte-derived macrophages. *J Neuroimmunol,* 120**,** 190-8.
CHIARUGI, A., MELI, E. & MORONI, F. (2001b) Similarities and differences in the neuronal death processes activated by 3OH-kynurenine and quinolinic acid. *J Neurochem,* 77**,** 1310-8.
CHIARUGI, A. & MORONI, F. (1999) Quinolinic acid formation in immune-activated mice: studies with (m-nitrobenzoyl)-alanine (mNBA) and 3,4-dimethoxy-[-N-4-(-3-nitrophenyl)thiazol-2yl]-benzenesul fonamide (Ro 61-8048), two potent and selective inhibitors of kynurenine hydroxylase. *Neuropharmacology,* 38**,** 1225-33.
CHIMINI, G. & CHAVRIER, P. (2000) Function of Rho family proteins in actin dynamics during phagocytosis and engulfment. *Nat Cell Biol,* 2**,** E191-6.
CHOU, S. Y., WENG, J. Y., LAI, H. L., LIAO, F., SUN, S. H., TU, P. H., DICKSON, D. W. & CHERN, Y. (2008) Expanded-polyglutamine huntingtin protein suppresses the secretion and production of a chemokine (CCL5/RANTES) by astrocytes. *J Neurosci,* 28**,** 3277-90.
CHUANG, D. M., HOUGH, C. & SENATOROV, V. V. (2005) Glyceraldehyde-3-phosphate dehydrogenase, apoptosis, and neurodegenerative diseases. *Annu Rev Pharmacol Toxicol,* 45**,** 269-90.
CICCHETTI, F., SAPORTA, S., HAUSER, R. A., PARENT, M., SAINT-PIERRE, M., SANBERG, P. R., LI, X. J., PARKER, J. R., CHU, Y., MUFSON, E. J., KORDOWER, J. H. & FREEMAN, T. B. (2009) Neural transplants in patients with Huntington's disease undergo disease-like neuronal degeneration. *Proc Natl Acad Sci U S A,* 106**,** 12483-8.
CLARK, C. J., MACKAY, G. M., SMYTHE, G. A., BUSTAMANTE, S., STONE, T. W. & PHILLIPS, R. S. (2005) Prolonged survival of a murine model of cerebral malaria by kynurenine pathway inhibition. *Infect Immun,* 73**,** 5249-51.
COLOMBARI, E., SATO, M. A., CRAVO, S. L., BERGAMASCHI, C. T., CAMPOS, R. R., JR. & LOPES, O. U. (2001) Role of the medulla oblongata in hypertension. *Hypertension,* 38**,** 549-54.
COLOWICK, S. P., KAPLAN, N. O., GUTHRIE, C. & FINK, G. R. (2002) *Methods in enzymology. Vol.350, Guide to yeast genetics and molecular and cell biology. Part B,* San Diego, Calif. ; London, Academic Press.
CONNOR, T. J., STARR, N., O'SULLIVAN, J. B. & HARKIN, A. (2008) Induction of indolamine 2,3-dioxygenase and kynurenine 3-monooxygenase in rat brain following a systemic inflammatory challenge: a role for IFN-gamma? *Neurosci Lett,* 441**,** 29-34.
COOPER, A. A., GITLER, A. D., CASHIKAR, A., HAYNES, C. M., HILL, K. J., BHULLAR, B., LIU, K., XU, K., STRATHEARN, K. E., LIU, F., CAO, S., CALDWELL, K. A., CALDWELL, G. A., MARSISCHKY, G., KOLODNER, R. D., LABAER, J., ROCHET, J. C., BONINI, N. M. & LINDQUIST, S. (2006) Alpha-synuclein blocks ER-Golgi traffic and Rab1 rescues neuron loss in Parkinson's models. *Science,* 313**,** 324-8.
COSTANZO, M., BARYSHNIKOVA, A., BELLAY, J., KIM, Y., SPEAR, E. D., SEVIER, C. S., DING, H., KOH, J. L., TOUFIGHI, K., MOSTAFAVI, S., PRINZ, J., ST ONGE, R. P., VANDERSLUIS, B., MAKHNEVYCH, T., VIZEACOUMAR, F. J., ALIZADEH, S., BAHR, S., BROST, R. L., CHEN, Y., COKOL, M., DESHPANDE, R., LI, Z., LIN, Z. Y., LIANG, W., MARBACK, M., PAW, J., SAN LUIS, B. J., SHUTERIQI, E., TONG, A. H., VAN DYK, N., WALLACE, I. M., WHITNEY, J. A., WEIRAUCH, M. T., ZHONG, G., ZHU, H., HOURY, W. A., BRUDNO, M., RAGIBIZADEH, S., PAPP, B., PAL, C., ROTH, F. P., GIAEVER, G., NISLOW, C., TROYANSKAYA, O. G., BUSSEY, H., BADER, G. D., GINGRAS, A. C., MORRIS, Q. D., KIM, P. M., KAISER, C. A., MYERS, C. L., ANDREWS, B. J. & BOONE, C. (2010) The genetic landscape of a cell. *Science,* 327**,** 425-31.

CUEVAS, E., LANTZ, S., NEWPORT, G., DIVINE, B., WU, Q., PAULE, M. G., TOBON-VELASCO, J. C., ALI, S. F. & SANTAMARIA, A. (2010) On the early toxic effect of quinolinic acid: involvement of RAGE. *Neurosci Lett,* 474**,** 74-8.

CUFFY, M. C., SILVERIO, A. M., QIN, L., WANG, Y., EID, R., BRANDACHER, G., LAKKIS, F. G., FUCHS, D., POBER, J. S. & TELLIDES, G. (2007) Induction of indoleamine 2,3-dioxygenase in vascular smooth muscle cells by interferon-gamma contributes to medial immunoprivilege. *J Immunol,* 179**,** 5246-54.

DALRYMPLE, A., WILD, E. J., JOUBERT, R., SATHASIVAM, K., BJORKQVIST, M., PETERSEN, A., JACKSON, G. S., ISAACS, J. D., KRISTIANSEN, M., BATES, G. P., LEAVITT, B. R., KEIR, G., WARD, M. & TABRIZI, S. J. (2007) Proteomic profiling of plasma in Huntington's disease reveals neuroinflammatory activation and biomarker candidates. *J Proteome Res,* 6**,** 2833-40.

DANIAL, N. N., GRAMM, C. F., SCORRANO, L., ZHANG, C. Y., KRAUSS, S., RANGER, A. M., DATTA, S. R., GREENBERG, M. E., LICKLIDER, L. J., LOWELL, B. B., GYGI, S. P. & KORSMEYER, S. J. (2003) BAD and glucokinase reside in a mitochondrial complex that integrates glycolysis and apoptosis. *Nature,* 424**,** 952-6.

DARLINGTON, L. G., MACKAY, G. M., FORREST, C. M., STOY, N., GEORGE, C. & STONE, T. W. (2007) Altered kynurenine metabolism correlates with infarct volume in stroke. *Eur J Neurosci,* 26**,** 2211-21.

DAVID, S., SHOEMAKER, M. & HALEY, B. E. (1998) Abnormal properties of creatine kinase in Alzheimer's disease brain: correlation of reduced enzyme activity and active site photolabeling with aberrant cytosol-membrane partitioning. *Brain Res Mol Brain Res,* 54**,** 276-87.

DAVIS, R. C., MARSDEN, I. T., MALONEY, M. T., MINAMIDE, L. S., PODLISNY, M., SELKOE, D. J. & BAMBURG, J. R. (2011) Amyloid beta dimers/trimers potently induce cofilin-actin rods that are inhibited by maintaining cofilin-phosphorylation. *Mol Neurodegener,* 6**,** 10.

DEUTSCHBAUER, A. M. & DAVIS, R. W. (2005) Quantitative trait loci mapped to single-nucleotide resolution in yeast. *Nat Genet,* 37**,** 1333-40.

DEUTSCHER, D., MEILIJSON, I., KUPIEC, M. & RUPPIN, E. (2006) Multiple knockout analysis of genetic robustness in the yeast metabolic network. *Nat Genet,* 38**,** 993-8.

DILLON, C. & GODA, Y. (2005) The actin cytoskeleton: integrating form and function at the synapse. *Annu Rev Neurosci,* 28**,** 25-55.

DINGLEDINE, R., BORGES, K., BOWIE, D. & TRAYNELIS, S. F. (1999) The glutamate receptor ion channels. *Pharmacol Rev,* 51**,** 7-61.

DUNAH, A. W., JEONG, H., GRIFFIN, A., KIM, Y. M., STANDAERT, D. G., HERSCH, S. M., MOURADIAN, M. M., YOUNG, A. B., TANESE, N. & KRAINC, D. (2002) Sp1 and TAFII130 transcriptional activity disrupted in early Huntington's disease. *Science,* 296**,** 2238-43.

DUYAO, M., AMBROSE, C., MYERS, R., NOVELLETTO, A., PERSICHETTI, F., FRONTALI, M., FOLSTEIN, S., ROSS, C., FRANZ, M., ABBOTT, M. & ET AL. (1993) Trinucleotide repeat length instability and age of onset in Huntington's disease. *Nat Genet,* 4**,** 387-92.

DZIEMBOWSKI, A. & SERAPHIN, B. (2004) Recent developments in the analysis of protein complexes. *FEBS Lett,* 556**,** 1-6.

EDGAR, K. A., BELVIN, M., PARKS, A. L., WHITTAKER, K., MAHONEY, M. B., NICOLL, M., PARK, C. C., WINTER, C. G., CHEN, F., LICKTEIG, K., AHMAD, F., ESENGIL, H., LORENZI, M. V., NORTON, A., RUPNOW, B. A., SHAYESTEH, L., TABIOS, M., YOUNG, L. M., CARROLL, P. M., KOPCZYNSKI, C., PLOWMAN, G. D., FRIEDMAN, L. S. & FRANCIS-LANG, H. L. (2005) Synthetic lethality of retinoblastoma mutant cells in the Drosophila eye by mutation of a novel peptidyl prolyl isomerase gene. *Genetics,* 170**,** 161-71.

EDWARDS, A. M., KUS, B., JANSEN, R., GREENBAUM, D., GREENBLATT, J. & GERSTEIN, M. (2002) Bridging structural biology and genomics: assessing protein interaction data with known complexes. *Trends Genet,* 18**,** 529-36.

EHRHARD, K. N., JACOBY, J. J., FU, X. Y., JAHN, R. & DOHLMAN, H. G. (2000) Use of G-protein fusions to monitor integral membrane protein-protein interactions in yeast. *Nat Biotechnol,* 18**,** 1075-9.

ENDRES, M., FINK, K., ZHU, J., STAGLIANO, N. E., BONDADA, V., GEDDES, J. W., AZUMA, T., MATTSON, M. P., KWIATKOWSKI, D. J. & MOSKOWITZ, M. A. (1999) Neuroprotective effects of gelsolin during murine stroke. *J Clin Invest,* 103**,** 347-54.

ERHARDT, S., BLENNOW, K., NORDIN, C., SKOGH, E., LINDSTROM, L. H. & ENGBERG, G. (2001) Kynurenic acid levels are elevated in the cerebrospinal fluid of patients with schizophrenia. *Neurosci Lett,* 313**,** 96-8.

FAN, M. M. & RAYMOND, L. A. (2007) N-methyl-D-aspartate (NMDA) receptor function and excitotoxicity in Huntington's disease. *Prog Neurobiol,* 81**,** 272-93.

FAULL, R. L., WALDVOGEL, H. J., NICHOLSON, L. F. & SYNEK, B. J. (1993) The distribution of GABAA-benzodiazepine receptors in the basal ganglia in Huntington's disease and in the quinolinic acid-lesioned rat. *Prog Brain Res,* 99**,** 105-23.

FIELDS, S. & SONG, O. (1989) A novel genetic system to detect protein-protein interactions. *Nature,* 340**,** 245-6.

FISCHER, M., HAASE, I., SIMMETH, E., GERISCH, G. & MULLER-TAUBENBERGER, A. (2004) A brilliant monomeric red fluorescent protein to visualize cytoskeleton dynamics in Dictyostelium. *FEBS Lett,* 577**,** 227-32.

FOSTER, A. C., MILLER, L. P., OLDENDORF, W. H. & SCHWARCZ, R. (1984a) Studies on the disposition of quinolinic acid after intracerebral or systemic administration in the rat. *Exp Neurol,* 84**,** 428-40.

FOSTER, A. C., VEZZANI, A., FRENCH, E. D. & SCHWARCZ, R. (1984b) Kynurenic acid blocks neurotoxicity and seizures induced in rats by the related brain metabolite quinolinic acid. *Neurosci Lett,* 48**,** 273-8.

FUCHS, D., MOLLER, A. A., REIBNEGGER, G., WERNER, E. R., WERNER-FELMAYER, G., DIERICH, M. P. & WACHTER, H. (1991) Increased endogenous interferon-gamma and neopterin correlate with increased degradation of tryptophan in human immunodeficiency virus type 1 infection. *Immunol Lett,* 28**,** 207-11.

FUKAZAWA, Y., SAITOH, Y., OZAWA, F., OHTA, Y., MIZUNO, K. & INOKUCHI, K. (2003) Hippocampal LTP is accompanied by enhanced F-actin content within the dendritic spine that is essential for late LTP maintenance in vivo. *Neuron,* 38**,** 447-60.

FURUKAWA, K., FU, W., LI, Y., WITKE, W., KWIATKOWSKI, D. J. & MATTSON, M. P. (1997) The actin-severing protein gelsolin modulates calcium channel and NMDA receptor activities and vulnerability to excitotoxicity in hippocampal neurons. *J Neurosci,* 17**,** 8178-86.

GERKE, J. P., CHEN, C. T. & COHEN, B. A. (2006) Natural isolates of Saccharomyces cerevisiae display complex genetic variation in sporulation efficiency. *Genetics,* 174**,** 985-97.

GIAEVER, G., CHU, A. M., NI, L., CONNELLY, C., RILES, L., VERONNEAU, S., DOW, S., LUCAU-DANILA, A., ANDERSON, K., ANDRE, B., ARKIN, A. P., ASTROMOFF, A., EL-BAKKOURY, M., BANGHAM, R., BENITO, R., BRACHAT, S., CAMPANARO, S., CURTISS, M., DAVIS, K., DEUTSCHBAUER, A., ENTIAN, K. D., FLAHERTY, P., FOURY, F., GARFINKEL, D. J., GERSTEIN, M., GOTTE, D., GULDENER, U., HEGEMANN, J. H., HEMPEL, S., HERMAN, Z., JARAMILLO, D. F., KELLY, D. E., KELLY, S. L., KOTTER, P., LABONTE, D., LAMB, D. C., LAN, N., LIANG, H., LIAO, H., LIU, L., LUO, C., LUSSIER, M., MAO, R., MENARD, P., OOI, S. L., REVUELTA, J. L., ROBERTS, C. J., ROSE, M., ROSS-MACDONALD, P., SCHERENS, B., SCHIMMACK, G., SHAFER, B., SHOEMAKER, D. D., SOOKHAI-MAHADEO, S., STORMS, R. K., STRATHERN, J. N., VALLE, G., VOET, M., VOLCKAERT, G., WANG, C. Y., WARD, T. R., WILHELMY, J., WINZELER, E. A., YANG, Y., YEN, G., YOUNGMAN, E., YU, K., BUSSEY, H., BOEKE, J. D.,

SNYDER, M., PHILIPPSEN, P., DAVIS, R. W. & JOHNSTON, M. (2002) Functional profiling of the Saccharomyces cerevisiae genome. *Nature,* 418**,** 387-91.
GINES, S., IVANOVA, E., SEONG, I. S., SAURA, C. A. & MACDONALD, M. E. (2003) Enhanced Akt signaling is an early pro-survival response that reflects N-methyl-D-aspartate receptor activation in Huntington's disease knock-in striatal cells. *J Biol Chem,* 278**,** 50514-22.
GIORGINI, F., GUIDETTI, P., NGUYEN, Q., BENNETT, S. C. & MUCHOWSKI, P. J. (2005) A genomic screen in yeast implicates kynurenine 3-monooxygenase as a therapeutic target for Huntington disease. *Nat Genet,* 37**,** 526-31.
GIORGINI, F., MOLLER, T., KWAN, W., ZWILLING, D., WACKER, J. L., HONG, S., TSAI, L. C., CHEAH, C. S., SCHWARCZ, R., GUIDETTI, P. & MUCHOWSKI, P. J. (2008) Histone deacetylase inhibition modulates kynurenine pathway activation in yeast, microglia, and mice expressing a mutant huntingtin fragment. *J Biol Chem,* 283**,** 7390-400.
GIORGINI, F. & MUCHOWSKI, P. J. (2006) Screening for genetic modifiers of amyloid toxicity in yeast. *Methods Enzymol,* 412**,** 201-22.
GNERER, J. P., KREBER, R. A. & GANETZKY, B. (2006) wasted away, a Drosophila mutation in triosephosphate isomerase, causes paralysis, neurodegeneration, and early death. *Proc Natl Acad Sci U S A,* 103**,** 14987-93.
GOLDSTEIN, A. L. & MCCUSKER, J. H. (1999) Three new dominant drug resistance cassettes for gene disruption in Saccharomyces cerevisiae. *Yeast,* 15**,** 1541-53.
GOULD, D. H. & GUSTINE, D. L. (1982) Basal ganglia degeneration, myelin alterations, and enzyme inhibition induced in mice by the plant toxin 3-nitropropanoic acid. *Neuropathol Appl Neurobiol,* 8**,** 377-93.
GRIFFITH, K. L. & WOLF, R. E., JR. (2002) Measuring beta-galactosidase activity in bacteria: cell growth, permeabilization, and enzyme assays in 96-well arrays. *Biochem Biophys Res Commun,* 290**,** 397-402.
GUIDETTI, P., AMORI, L., SAPKO, M. T., OKUNO, E. & SCHWARCZ, R. (2007) Mitochondrial aspartate aminotransferase: a third kynurenate-producing enzyme in the mammalian brain. *J Neurochem,* 102**,** 103-11.
GUIDETTI, P., BATES, G. P., GRAHAM, R. K., HAYDEN, M. R., LEAVITT, B. R., MACDONALD, M. E., SLOW, E. J., WHEELER, V. C., WOODMAN, B. & SCHWARCZ, R. (2006) Elevated brain 3-hydroxykynurenine and quinolinate levels in Huntington disease mice. *Neurobiol Dis,* 23**,** 190-7.
GUIDETTI, P., LUTHI-CARTER, R. E., AUGOOD, S. J. & SCHWARCZ, R. (2004) Neostriatal and cortical quinolinate levels are increased in early grade Huntington's disease. *Neurobiol Dis,* 17**,** 455-61.
GUIDETTI, P., REDDY, P. H., TAGLE, D. A. & SCHWARCZ, R. (2000) Early kynurenergic impairment in Huntington's disease and in a transgenic animal model. *Neurosci Lett,* 283**,** 233-5.
GUIDETTI, P. & SCHWARCZ, R. (1999) 3-Hydroxykynurenine potentiates quinolinate but not NMDA toxicity in the rat striatum. *Eur J Neurosci,* 11**,** 3857-63.
GUIDETTI, P. & SCHWARCZ, R. (2003) 3-Hydroxykynurenine and quinolinate: pathogenic synergism in early grade Huntington's disease? *Adv Exp Med Biol,* 527**,** 137-45.
GUILLEMIN, G. J., KERR, S. J., SMYTHE, G. A., SMITH, D. G., KAPOOR, V., ARMATI, P. J., CROITORU, J. & BREW, B. J. (2001) Kynurenine pathway metabolism in human astrocytes: a paradox for neuronal protection. *J Neurochem,* 78**,** 842-53.
GUSELLA, J. F. & MACDONALD, M. E. (2009) Huntington's disease: the case for genetic modifiers. *Genome Med,* 1**,** 80.
GUTEKUNST, C. A., NORFLUS, F. & HERSCH, S. M. (2002) The neuropathology of Huntington's disease. IN BATES, G., HARPER, P. S. & JONES, L. (Eds.) *Huntington's disease.* 3rd ed. Oxford, Oxford University Press.

H.D.C.R.G (1993) A novel gene containing a trinucleotide repeat that is expanded and unstable on Huntington's disease chromosomes. The Huntington's Disease Collaborative Research Group. *Cell,* 72**,** 971-83.

HAGLID, K. G., WANG, S., QINER, Y. & HAMBERGER, A. (1994) Excitotoxicity. Experimental correlates to human epilepsy. *Mol Neurobiol,* 9**,** 259-63.

HAMILTON, B. F. & GOULD, D. H. (1987) Nature and distribution of brain lesions in rats intoxicated with 3-nitropropionic acid: a type of hypoxic (energy deficient) brain damage. *Acta Neuropathol,* 72**,** 286-97.

HAN, Q., CAI, T., TAGLE, D. A. & LI, J. (2010) Structure, expression, and function of kynurenine aminotransferases in human and rodent brains. *Cell Mol Life Sci,* 67**,** 353-68.

HANDS, S. L., MASON, R., SAJJAD, M. U., GIORGINI, F. & WYTTENBACH, A. (2010) Metallothioneins and copper metabolism are candidate therapeutic targets in Huntington's disease. *Biochem Soc Trans,* 38**,** 552-8.

HARTAI, Z., JUHASZ, A., RIMANOCZY, A., JANAKY, T., DONKO, T., DUX, L., PENKE, B., TOTH, G. K., JANKA, Z. & KALMAN, J. (2007) Decreased serum and red blood cell kynurenic acid levels in Alzheimer's disease. *Neurochem Int,* 50**,** 308-13.

HAUNSTETTER, A. & IZUMO, S. (1998) Apoptosis: basic mechanisms and implications for cardiovascular disease. *Circ Res,* 82**,** 1111-29.

HEYES, M. P. & LACKNER, A. (1990) Increased cerebrospinal fluid quinolinic acid, kynurenic acid, and L-kynurenine in acute septicemia. *J Neurochem,* 55**,** 338-41.

HEYES, M. P., SAITO, K., DEVINSKY, O. & NADI, N. S. (1994) Kynurenine pathway metabolites in cerebrospinal fluid and serum in complex partial seizures. *Epilepsia,* 35**,** 251-7.

HEYES, M. P., SAITO, K., MAJOR, E. O., MILSTIEN, S., MARKEY, S. P. & VICKERS, J. H. (1993) A mechanism of quinolinic acid formation by brain in inflammatory neurological disease. Attenuation of synthesis from L-tryptophan by 6-chlorotryptophan and 4-chloro-3-hydroxyanthranilate. *Brain,* 116 (Pt 6)**,** 1425-50.

HEYES, M. P., SWARTZ, K. J., MARKEY, S. P. & BEAL, M. F. (1991) Regional brain and cerebrospinal fluid quinolinic acid concentrations in Huntington's disease. *Neurosci Lett,* 122**,** 265-9.

HEYWORTH, P. G., ROBINSON, J. M., DING, J., ELLIS, B. A. & BADWEY, J. A. (1997) Cofilin undergoes rapid dephosphorylation in stimulated neutrophils and translocates to ruffled membranes enriched in products of the NADPH oxidase complex. Evidence for a novel cycle of phosphorylation and dephosphorylation. *Histochem Cell Biol,* 108**,** 221-33.

HILGEMANN, D. W., FENG, S. & NASUHOGLU, C. (2001) The complex and intriguing lives of PIP2 with ion channels and transporters. *Sci STKE,* 2001**,** re19.

HILLENMEYER, M. E., FUNG, E., WILDENHAIN, J., PIERCE, S. E., HOON, S., LEE, W., PROCTOR, M., ST ONGE, R. P., TYERS, M., KOLLER, D., ALTMAN, R. B., DAVIS, R. W., NISLOW, C. & GIAEVER, G. (2008) The chemical genomic portrait of yeast: uncovering a phenotype for all genes. *Science,* 320**,** 362-5.

HILMAS, C., PEREIRA, E. F., ALKONDON, M., RASSOULPOUR, A., SCHWARCZ, R. & ALBUQUERQUE, E. X. (2001) The brain metabolite kynurenic acid inhibits alpha7 nicotinic receptor activity and increases non-alpha7 nicotinic receptor expression: physiopathological implications. *J Neurosci,* 21**,** 7463-73.

HODGSON, J. G., AGOPYAN, N., GUTEKUNST, C. A., LEAVITT, B. R., LEPIANE, F., SINGARAJA, R., SMITH, D. J., BISSADA, N., MCCUTCHEON, K., NASIR, J., JAMOT, L., LI, X. J., STEVENS, M. E., ROSEMOND, E., RODER, J. C., PHILLIPS, A. G., RUBIN, E. M., HERSCH, S. M. & HAYDEN, M. R. (1999) A YAC mouse model for Huntington's disease with full-length mutant huntingtin, cytoplasmic toxicity, and selective striatal neurodegeneration. *Neuron,* 23**,** 181-92.

HOLTZE, M., SAETRE, P., ERHARDT, S., SCHWIELER, L., WERGE, T., HANSEN, T., NIELSEN, J., DJUROVIC, S., MELLE, I., ANDREASSEN, O. A., HALL, H., TERENIUS, L., AGARTZ, I., ENGBERG, G., JONSSON, E. G. & SCHALLING, M.

(2011) Kynurenine 3-monooxygenase (KMO) polymorphisms in schizophrenia: An association study. *Schizophr Res.*

HOOGENBOOM, B. W., SUDA, K., ENGEL, A. & FOTIADIS, D. (2007) The supramolecular assemblies of voltage-dependent anion channels in the native membrane. *J Mol Biol,* 370**,** 246-55.

HUANG, A., FUCHS, D., WIDNER, B., GLOVER, C., HENDERSON, D. C. & ALLEN-MERSH, T. G. (2002) Serum tryptophan decrease correlates with immune activation and impaired quality of life in colorectal cancer. *Br J Cancer,* 86**,** 1691-6.

HUANG DA, W., SHERMAN, B. T. & LEMPICKI, R. A. (2009a) Bioinformatics enrichment tools: paths toward the comprehensive functional analysis of large gene lists. *Nucleic Acids Res,* 37**,** 1-13.

HUANG DA, W., SHERMAN, B. T. & LEMPICKI, R. A. (2009b) Systematic and integrative analysis of large gene lists using DAVID bioinformatics resources. *Nat Protoc,* 4**,** 44-57.

HUBSMAN, M., YUDKOVSKY, G. & ARONHEIM, A. (2001) A novel approach for the identification of protein-protein interaction with integral membrane proteins. *Nucleic Acids Res,* 29**,** E18.

ILZECKA, J., KOCKI, T., STELMASIAK, Z. & TURSKI, W. A. (2003) Endogenous protectant kynurenic acid in amyotrophic lateral sclerosis. *Acta Neurol Scand,* 107**,** 412-8.

IYER, K., BURKLE, L., AUERBACH, D., THAMINY, S., DINKEL, M., ENGELS, K. & STAGLJAR, I. (2005) Utilizing the split-ubiquitin membrane yeast two-hybrid system to identify protein-protein interactions of integral membrane proteins. *Sci STKE,* 2005**,** pl3.

JACOBSON, J. & DUCHEN, M. R. (2002) Mitochondrial oxidative stress and cell death in astrocytes--requirement for stored Ca2+ and sustained opening of the permeability transition pore. *J Cell Sci,* 115**,** 1175-88.

JIMENEZ-MARIN, A., COLLADO-ROMERO, M., RAMIREZ-BOO, M., ARCE, C. & GARRIDO, J. J. (2009) Biological pathway analysis by ArrayUnlock and Ingenuity Pathway Analysis. *BMC Proc,* 3 Suppl 4**,** S6.

JONES, E. W. & FINK, G. R. (Eds.) (1982) *Regulation of amino acid and nucleotide biosynthesis in yeast,* Cold Spring Harbor, NY, Cold Spring Harbor Laboratory Press.

KABSCH, W. & VANDEKERCKHOVE, J. (1992) Structure and function of actin. *Annu Rev Biophys Biomol Struct,* 21**,** 49-76.

KAELIN, W. G., JR. (2005) The concept of synthetic lethality in the context of anticancer therapy. *Nat Rev Cancer,* 5**,** 689-98.

KALTENBACH, L. S., ROMERO, E., BECKLIN, R. R., CHETTIER, R., BELL, R., PHANSALKAR, A., STRAND, A., TORCASSI, C., SAVAGE, J., HURLBURT, A., CHA, G. H., UKANI, L., CHEPANOSKE, C. L., ZHEN, Y., SAHASRABUDHE, S., OLSON, J., KURSCHNER, C., ELLERBY, L. M., PELTIER, J. M., BOTAS, J. & HUGHES, R. E. (2007) Huntingtin interacting proteins are genetic modifiers of neurodegeneration. *PLoS Genet,* 3**,** e82.

KANEHISA, M. & GOTO, S. (2000) KEGG: kyoto encyclopedia of genes and genomes. *Nucleic Acids Res,* 28**,** 27-30.

KANEHISA, M., GOTO, S., FURUMICHI, M., TANABE, M. & HIRAKAWA, M. (2010) KEGG for representation and analysis of molecular networks involving diseases and drugs. *Nucleic Acids Res,* 38**,** D355-60.

KANEHISA, M., GOTO, S., HATTORI, M., AOKI-KINOSHITA, K. F., ITOH, M., KAWASHIMA, S., KATAYAMA, T., ARAKI, M. & HIRAKAWA, M. (2006) From genomics to chemical genomics: new developments in KEGG. *Nucleic Acids Res,* 34**,** D354-7.

KELLER, J. N., MARK, R. J., BRUCE, A. J., BLANC, E., ROTHSTEIN, J. D., UCHIDA, K., WAEG, G. & MATTSON, M. P. (1997) 4-Hydroxynonenal, an aldehydic product of membrane lipid peroxidation, impairs glutamate transport and mitochondrial function in synaptosomes. *Neuroscience,* 80**,** 685-96.

KERPPOLA, T. K. (2006a) Complementary methods for studies of protein interactions in living cells. *Nat Methods,* 3**,** 969-71.
KERPPOLA, T. K. (2006b) Design and implementation of bimolecular fluorescence complementation (BiFC) assays for the visualization of protein interactions in living cells. *Nat Protoc,* 1**,** 1278-86.
KIRKWOOD, S. C., SU, J. L., CONNEALLY, P. & FOROUD, T. (2001) Progression of symptoms in the early and middle stages of Huntington disease. *Arch Neurol,* 58**,** 273-8.
KISS, C., CERESOLI-BORRONI, G., GUIDETTI, P., ZIELKE, C. L., ZIELKE, H. R. & SCHWARCZ, R. (2003) Kynurenate production by cultured human astrocytes. *J Neural Transm,* 110**,** 1-14.
KITA, T., MORRISON, P. F., HEYES, M. P. & MARKEY, S. P. (2002) Effects of systemic and central nervous system localized inflammation on the contributions of metabolic precursors to the L-kynurenine and quinolinic acid pools in brain. *J Neurochem,* 82**,** 258-68.
KLAMT, F., ZDANOV, S., LEVINE, R. L., PARISER, A., ZHANG, Y., ZHANG, B., YU, L. R., VEENSTRA, T. D. & SHACTER, E. (2009) Oxidant-induced apoptosis is mediated by oxidation of the actin-regulatory protein cofilin. *Nat Cell Biol,* 11**,** 1241-6.
KNOP, M., SIEGERS, K., PEREIRA, G., ZACHARIAE, W., WINSOR, B., NASMYTH, K. & SCHIEBEL, E. (1999) Epitope tagging of yeast genes using a PCR-based strategy: more tags and improved practical routines. *Yeast,* 15**,** 963-72.
KORNITZER, D. & CIECHANOVER, A. (2000) Modes of regulation of ubiquitin-mediated protein degradation. *J Cell Physiol,* 182**,** 1-11.
KORNMANN, B., CURRIE, E., COLLINS, S. R., SCHULDINER, M., NUNNARI, J., WEISSMAN, J. S. & WALTER, P. (2009) An ER-mitochondria tethering complex revealed by a synthetic biology screen. *Science,* 325**,** 477-81.
KOTHAKOTA, S., AZUMA, T., REINHARD, C., KLIPPEL, A., TANG, J., CHU, K., MCGARRY, T. J., KIRSCHNER, M. W., KOTHS, K., KWIATKOWSKI, D. J. & WILLIAMS, L. T. (1997) Caspase-3-generated fragment of gelsolin: effector of morphological change in apoptosis. *Science,* 278**,** 294-8.
KUNG, V. W., HASSAM, R., MORTON, A. J. & JONES, S. (2007) Dopamine-dependent long term potentiation in the dorsal striatum is reduced in the R6/2 mouse model of Huntington's disease. *Neuroscience,* 146**,** 1571-80.
KWOK, J. B., KAPOOR, R., GOTODA, T., IWAMOTO, Y., IIZUKA, Y., YAMADA, N., ISAACS, K. E., KUSHWAHA, V. V., CHURCH, W. B., SCHOFIELD, P. R. & KAPOOR, V. (2002) A missense mutation in kynurenine aminotransferase-1 in spontaneously hypertensive rats. *J Biol Chem,* 277**,** 35779-82.
LAMONTE, B. H., WALLACE, K. E., HOLLOWAY, B. A., SHELLY, S. S., ASCANO, J., TOKITO, M., VAN WINKLE, T., HOWLAND, D. S. & HOLZBAUR, E. L. (2002) Disruption of dynein/dynactin inhibits axonal transport in motor neurons causing late-onset progressive degeneration. *Neuron,* 34**,** 715-27.
LAMPING, E., LUCKL, J., PALTAUF, F., HENRY, S. A. & KOHLWEIN, S. D. (1994) Isolation and characterization of a mutant of Saccharomyces cerevisiae with pleiotropic deficiencies in transcriptional activation and repression. *Genetics,* 137**,** 55-65.
LANDLES, C. & BATES, G. P. (2004) Huntingtin and the molecular pathogenesis of Huntington's disease. Fourth in molecular medicine review series. *EMBO Rep,* 5**,** 958-63.
LEONARD, B. E. (2007) Inflammation, depression and dementia: are they connected? *Neurochem Res,* 32**,** 1749-56.
LEWIS, D. A. & MOGHADDAM, B. (2006) Cognitive dysfunction in schizophrenia: convergence of gamma-aminobutyric acid and glutamate alterations. *Arch Neurol,* 63**,** 1372-6.
LI, B. & WARNER, J. R. (1996) Mutation of the Rab6 homologue of Saccharomyces cerevisiae, YPT6, inhibits both early Golgi function and ribosome biosynthesis. *J Biol Chem,* 271**,** 16813-9.
LI, X., SAPP, E., CHASE, K., COMER-TIERNEY, L. A., MASSO, N., ALEXANDER, J., REEVES, P., KEGEL, K. B., VALENCIA, A., ESTEVES, M., ARONIN, N. &

DIFIGLIA, M. (2009a) Disruption of Rab11 activity in a knock-in mouse model of Huntington's disease. *Neurobiol Dis,* 36**,** 374-83.

LI, X., STANDLEY, C., SAPP, E., VALENCIA, A., QIN, Z. H., KEGEL, K. B., YODER, J., COMER-TIERNEY, L. A., ESTEVES, M., CHASE, K., ALEXANDER, J., MASSO, N., SOBIN, L., BELLVE, K., TUFT, R., LIFSHITZ, L., FOGARTY, K., ARONIN, N. & DIFIGLIA, M. (2009b) Mutant huntingtin impairs vesicle formation from recycling endosomes by interfering with Rab11 activity. *Mol Cell Biol,* 29**,** 6106-16.

LIN, T. K., HUGHES, G., MURATOVSKA, A., BLAIKIE, F. H., BROOKES, P. S., DARLEY-USMAR, V., SMITH, R. A. & MURPHY, M. P. (2002) Specific modification of mitochondrial protein thiols in response to oxidative stress: a proteomics approach. *J Biol Chem,* 277**,** 17048-56.

LINDERHOLM, K. R., SKOGH, E., OLSSON, S. K., DAHL, M. L., HOLTZE, M., ENGBERG, G., SAMUELSSON, M. & ERHARDT, S. (2010) Increased Levels of Kynurenine and Kynurenic Acid in the CSF of Patients With Schizophrenia. *Schizophr Bull.*

LUTHI-CARTER, R., HANSON, S. A., STRAND, A. D., BERGSTROM, D. A., CHUN, W., PETERS, N. L., WOODS, A. M., CHAN, E. Y., KOOPERBERG, C., KRAINC, D., YOUNG, A. B., TAPSCOTT, S. J. & OLSON, J. M. (2002) Dysregulation of gene expression in the R6/2 model of polyglutamine disease: parallel changes in muscle and brain. *Hum Mol Genet,* 11**,** 1911-26.

LUTHI-CARTER, R., STRAND, A., PETERS, N. L., SOLANO, S. M., HOLLINGSWORTH, Z. R., MENON, A. S., FREY, A. S., SPEKTOR, B. S., PENNEY, E. B., SCHILLING, G., ROSS, C. A., BORCHELT, D. R., TAPSCOTT, S. J., YOUNG, A. B., CHA, J. H. & OLSON, J. M. (2000) Decreased expression of striatal signaling genes in a mouse model of Huntington's disease. *Hum Mol Genet,* 9**,** 1259-71.

MA, H., KUNES, S., SCHATZ, P. J. & BOTSTEIN, D. (1987) Plasmid construction by homologous recombination in yeast. *Gene,* 58**,** 201-16.

MA, L. & NICHOLSON, L. F. (2004) Expression of the receptor for advanced glycation end products in Huntington's disease caudate nucleus. *Brain Res,* 1018**,** 10-7.

MACKAY, G. M., FORREST, C. M., STOY, N., CHRISTOFIDES, J., EGERTON, M., STONE, T. W. & DARLINGTON, L. G. (2006) Tryptophan metabolism and oxidative stress in patients with chronic brain injury. *Eur J Neurol,* 13**,** 30-42.

MALONEY, M. T. & BAMBURG, J. R. (2007) Cofilin-mediated neurodegeneration in Alzheimer's disease and other amyloidopathies. *Mol Neurobiol,* 35**,** 21-44.

MALONEY, M. T., MINAMIDE, L. S., KINLEY, A. W., BOYLE, J. A. & BAMBURG, J. R. (2005) Beta-secretase-cleaved amyloid precursor protein accumulates at actin inclusions induced in neurons by stress or amyloid beta: a feedforward mechanism for Alzheimer's disease. *J Neurosci,* 25**,** 11313-21.

MARANGOS, P. J. & PAUL, S. M. (1981) Brain levels of neuron-specific and nonneuronal enolase in Huntington's disease. *J Neurochem,* 37**,** 1338-40.

MARIN, M. L., GORDON, R. E., VEITH, F. J., TULCHIN, N. & PANETTA, T. F. (1993) Distribution of c-myc oncoprotein in healthy and atherosclerotic human carotid arteries. *J Vasc Surg,* 18**,** 170-6; discussion 176-7.

MARTINEZ-VICENTE, M., SOVAK, G. & CUERVO, A. M. (2005) Protein degradation and aging. *Exp Gerontol,* 40**,** 622-33.

MARTINS-DE-SOUZA, D., GATTAZ, W. F., SCHMITT, A., REWERTS, C., MACCARRONE, G., DIAS-NETO, E. & TURCK, C. W. (2009) Prefrontal cortex shotgun proteome analysis reveals altered calcium homeostasis and immune system imbalance in schizophrenia. *Eur Arch Psychiatry Clin Neurosci,* 259**,** 151-63.

MASER, E. (2006) Neuroprotective role for carbonyl reductase? *Biochem Biophys Res Commun,* 340**,** 1019-22.

MAZZIOTTA, J. C., PHELPS, M. E., PAHL, J. J., HUANG, S. C., BAXTER, L. R., RIEGE, W. H., HOFFMAN, J. M., KUHL, D. E., LANTO, A. B., WAPENSKI, J. A. & ET AL.

(1987) Reduced cerebral glucose metabolism in asymptomatic subjects at risk for Huntington's disease. *N Engl J Med,* 316**,** 357-62.

MAZZOLA, J. L. & SIROVER, M. A. (2001) Reduction of glyceraldehyde-3-phosphate dehydrogenase activity in Alzheimer's disease and in Huntington's disease fibroblasts. *J Neurochem,* 76**,** 442-9.

MCGEER, E. G. & MCGEER, P. L. (1978) Some factors influencing the neurotoxicity of intrastriatal injections of kainic acid. *Neurochem Res,* 3**,** 501-17.

MCKENNA, M. C., SONNEWALD, U., HUANG, X., STEVENSON, J. & ZIELKE, H. R. (1996a) Exogenous glutamate concentration regulates the metabolic fate of glutamate in astrocytes. *J Neurochem,* 66**,** 386-93.

MCKENNA, M. C., TILDON, J. T., STEVENSON, J. H. & HUANG, X. (1996b) New insights into the compartmentation of glutamate and glutamine in cultured rat brain astrocytes. *Dev Neurosci,* 18**,** 380-90.

MCKENNA, M. C., WAAGEPETERSEN, H. S., SCHOUSBOE, A. & SONNEWALD, U. (2006) Neuronal and astrocytic shuttle mechanisms for cytosolic-mitochondrial transfer of reducing equivalents: current evidence and pharmacological tools. *Biochem Pharmacol,* 71**,** 399-407.

MCPHERSON, P. S. & RITTER, B. (2005) Peptide motifs: building the clathrin machinery. *Mol Neurobiol,* 32**,** 73-87.

MEDANA, I. M., HIEN, T. T., DAY, N. P., PHU, N. H., MAI, N. T., CHU'ONG, L. V., CHAU, T. T., TAYLOR, A., SALAHIFAR, H., STOCKER, R., SMYTHE, G., TURNER, G. D., FARRAR, J., WHITE, N. J. & HUNT, N. H. (2002) The clinical significance of cerebrospinal fluid levels of kynurenine pathway metabolites and lactate in severe malaria. *J Infect Dis,* 185**,** 650-6.

METZGER, S., RONG, J., NGUYEN, H. P., CAPE, A., TOMIUK, J., SOEHN, A. S., PROPPING, P., FREUDENBERG-HUA, Y., FREUDENBERG, J., TONG, L., LI, S. H., LI, X. J. & RIESS, O. (2008) Huntingtin-associated protein-1 is a modifier of the age-at-onset of Huntington's disease. *Hum Mol Genet,* 17**,** 1137-46.

MILLER, J. P., LO, R. S., BEN-HUR, A., DESMARAIS, C., STAGLJAR, I., NOBLE, W. S. & FIELDS, S. (2005) Large-scale identification of yeast integral membrane protein interactions. *Proc Natl Acad Sci U S A,* 102**,** 12123-8.

MINAMIDE, L. S., STRIEGL, A. M., BOYLE, J. A., MEBERG, P. J. & BAMBURG, J. R. (2000) Neurodegenerative stimuli induce persistent ADF/cofilin-actin rods that disrupt distal neurite function. *Nat Cell Biol,* 2**,** 628-36.

MIU, J., BALL, H. J., MELLOR, A. L. & HUNT, N. H. (2009) Effect of indoleamine dioxygenase-1 deficiency and kynurenine pathway inhibition on murine cerebral malaria. *Int J Parasitol,* 39**,** 363-70.

MIZUTA, K., PARK, J. S., SUGIYAMA, M., NISHIYAMA, M. & WARNER, J. R. (1997) RIC1, a novel gene required for ribosome synthesis in Saccharomyces cerevisiae. *Gene,* 187**,** 171-8.

MOTLEY, A., BRIGHT, N. A., SEAMAN, M. N. & ROBINSON, M. S. (2003) Clathrin-mediated endocytosis in AP-2-depleted cells. *J Cell Biol,* 162**,** 909-18.

MUNSIE, L., CARON, N., ATWAL, R. S., MARSDEN, I., WILD, E. J., BAMBURG, J. R., TABRIZI, S. J. & TRUANT, R. (2011) Mutant Huntingtin Causes Defective Actin Remodeling During Stress: Defining a New Role for Transglutaminase 2 in Neurodegenerative Disease. *Hum Mol Genet.*

MURPHY, K. P., CARTER, R. J., LIONE, L. A., MANGIARINI, L., MAHAL, A., BATES, G. P., DUNNETT, S. B. & MORTON, A. J. (2000) Abnormal synaptic plasticity and impaired spatial cognition in mice transgenic for exon 1 of the human Huntington's disease mutation. *J Neurosci,* 20**,** 5115-23.

MYERS, R. H., SAX, D. S., KOROSHETZ, W. J., MASTROMAURO, C., CUPPLES, L. A., KIELY, D. K., PETTENGILL, F. K. & BIRD, E. D. (1991) Factors associated with slow progression in Huntington's disease. *Arch Neurol,* 48**,** 800-4.

NGO, C. V., GEE, M., AKHTAR, N., YU, D., VOLPERT, O., AUERBACH, R. & THOMAS-TIKHONENKO, A. (2000) An in vivo function for the transforming Myc protein: elicitation of the angiogenic phenotype. *Cell Growth Differ,* 11**,** 201-10.

NICHOLLS, D. G. & WARD, M. W. (2000) Mitochondrial membrane potential and neuronal glutamate excitotoxicity: mortality and millivolts. *Trends Neurosci,* 23**,** 166-74.

NIJTMANS, L. G., HENDERSON, N. S. & HOLT, I. J. (2002) Blue Native electrophoresis to study mitochondrial and other protein complexes. *Methods,* 26**,** 327-34.

NILSSON, L. K., LINDERHOLM, K. R., ENGBERG, G., PAULSON, L., BLENNOW, K., LINDSTROM, L. H., NORDIN, C., KARANTI, A., PERSSON, P. & ERHARDT, S. (2005) Elevated levels of kynurenic acid in the cerebrospinal fluid of male patients with schizophrenia. *Schizophr Res,* 80**,** 315-22.

NISIMOTO, Y., TAKEUCHI, F. & SHIBATA, Y. (1977) Molecular properties of L-kynurenine 3-hydroxylase from rat liver mitochondria. *J Biochem,* 81**,** 1413-25.

O'BRIEN, C. F., MILLER, C., GOLDBLATT, D., WELLE, S., FORBES, G., LIPINSKI, B., PANZIK, J., PECK, R., PLUMB, S., OAKES, D., KURLAN, R. & SHOULSON, I. (1990) Extraneural metabolism in early Huntington's disease. *Annals of neurology,* 28**,** 300-301.

OKUDA, S., NISHIYAMA, N., SAITO, H. & KATSUKI, H. (1996) Hydrogen peroxide-mediated neuronal cell death induced by an endogenous neurotoxin, 3-hydroxykynurenine. *Proc Natl Acad Sci U S A,* 93**,** 12553-8.

OPPERMANN, U. (2007) Carbonyl reductases: the complex relationships of mammalian carbonyl- and quinone-reducing enzymes and their role in physiology. *Annu Rev Pharmacol Toxicol,* 47**,** 293-322.

ORLANDO, L. R., ALSDORF, S. A., PENNEY, J. B., JR. & YOUNG, A. B. (2001) The role of group I and group II metabotropic glutamate receptors in modulation of striatal NMDA and quinolinic acid toxicity. *Exp Neurol,* 167**,** 196-204.

ORLIKOV, A. B., PRAKHYE, I. B. & RYZOV, I. V. (1994) Kynurenine in blood plasma and DST in patients with endogenous anxiety and endogenous depression. *Biol Psychiatry,* 36**,** 97-102.

OROSZ, F., OLAH, J., ALVAREZ, M., KESERU, G. M., SZABO, B., WAGNER, G., KOVARI, Z., HORANYI, M., BAROTI, K., MARTIAL, J. A., HOLLAN, S. & OVADI, J. (2001) Distinct behavior of mutant triosephosphate isomerase in hemolysate and in isolated form: molecular basis of enzyme deficiency. *Blood,* 98**,** 3106-12.

PANOZZO, C., NAWARA, M., SUSKI, C., KUCHARCZYKA, R., SKONECZNY, M., BECAM, A. M., RYTKA, J. & HERBERT, C. J. (2002) Aerobic and anaerobic NAD+ metabolism in Saccharomyces cerevisiae. *FEBS Lett,* 517**,** 97-102.

PASCH, J. C., NICKELSEN, J. & SCHUNEMANN, D. (2005) The yeast split-ubiquitin system to study chloroplast membrane protein interactions. *Appl Microbiol Biotechnol,* 69**,** 440-7.

PATHAK, R., PARKER, C. S. & IMPERIALI, B. (1995) The essential yeast NLT1 gene encodes the 64 kDa glycoprotein subunit of the oligosaccharyl transferase. *FEBS Lett,* 362**,** 229-34.

PAUMI, C. M., MENENDEZ, J., ARNOLDO, A., ENGELS, K., IYER, K. R., THAMINY, S., GEORGIEV, O., BARRAL, Y., MICHAELIS, S. & STAGLJAR, I. (2007) Mapping protein-protein interactions for the yeast ABC transporter Ycf1p by integrated split-ubiquitin membrane yeast two-hybrid analysis. *Mol Cell,* 26**,** 15-25.

PAVESE, N., GERHARD, A., TAI, Y. F., HO, A. K., TURKHEIMER, F., BARKER, R. A., BROOKS, D. J. & PICCINI, P. (2006) Microglial activation correlates with severity in Huntington disease: a clinical and PET study. *Neurology,* 66**,** 1638-43.

PAWLAK, K., MYSLIWIEC, M. & PAWLAK, D. (2010) Haemostatic system, biochemical profiles, kynurenines and the prevalence of cardiovascular disease in peritoneally dialyzed patients. *Thromb Res,* 125**,** e40-5.

PEARSON, S. J. & REYNOLDS, G. P. (1992) Increased brain concentrations of a neurotoxin, 3-hydroxykynurenine, in Huntington's disease. *Neurosci Lett,* 144**,** 199-201.

PELLICCIARI, R., NATALINI, B., COSTANTINO, G., MAHMOUD, M. R., MATTOLI, L., SADEGHPOUR, B. M., MORONI, F., CHIARUGI, A. & CARPENEDO, R. (1994) Modulation of the kynurenine pathway in search for new neuroprotective agents. Synthesis and preliminary evaluation of (m-nitrobenzoyl)alanine, a potent inhibitor of kynurenine-3-hydroxylase. *J Med Chem,* 37**,** 647-55.

PERKINS, M. N. & STONE, T. W. (1983) Pharmacology and regional variations of quinolinic acid-evoked excitations in the rat central nervous system. *J Pharmacol Exp Ther,* 226**,** 551-7.

PERLSON, E., JEONG, G. B., ROSS, J. L., DIXIT, R., WALLACE, K. E., KALB, R. G. & HOLZBAUR, E. L. (2009) A switch in retrograde signaling from survival to stress in rapid-onset neurodegeneration. *J Neurosci,* 29**,** 9903-17.

PFANNER, N. & GEISSLER, A. (2001) Versatility of the mitochondrial protein import machinery. *Nat Rev Mol Cell Biol,* 2**,** 339-49.

PFANNER, N. & MEIJER, M. (1997) The Tom and Tim machine. *Curr Biol,* 7**,** R100-3.

PFANNER, N. & NEUPERT, W. (1990) The mitochondrial protein import apparatus. *Annu Rev Biochem,* 59**,** 331-53.

PFANNER, N., WIEDEMANN, N., MEISINGER, C. & LITHGOW, T. (2004) Assembling the mitochondrial outer membrane. *Nat Struct Mol Biol,* 11**,** 1044-8.

PHIZICKY, E. M. & FIELDS, S. (1995) Protein-protein interactions: methods for detection and analysis. *Microbiol Rev,* 59**,** 94-123.

POEGGELER, B., RASSOULPOUR, A., WU, H. Q., GUIDETTI, P., ROBERTS, R. C. & SCHWARCZ, R. (2007) Dopamine receptor activation reveals a novel, kynurenate-sensitive component of striatal N-methyl-D-aspartate neurotoxicity. *Neuroscience,* 148**,** 188-97.

POWERS, W. J., HAAS, R. H., LE, T., VIDEEN, T. O., HERSHEY, T., MCGEE-MINNICH, L. & PERLMUTTER, J. S. (2007) Normal platelet mitochondrial complex I activity in Huntington's disease. *Neurobiol Dis,* 27**,** 99-101.

QIAO, H. J., KOYA, R. C., NAKAGAWA, K., TANAKA, H., FUJITA, H., TAKIMOTO, M. & KUZUMAKI, N. (2005) Inhibition of Alzheimer's amyloid-beta peptide-induced reduction of mitochondrial membrane potential and neurotoxicity by gelsolin. *Neurobiology of Aging,* 26**,** 849-855.

RABILLOUD, T., KIEFFER, S., PROCACCIO, V., LOUWAGIE, M., COURCHESNE, P. L., PATTERSON, S. D., MARTINEZ, P., GARIN, J. & LUNARDI, J. (1998) Two-dimensional electrophoresis of human placental mitochondria and protein identification by mass spectrometry: toward a human mitochondrial proteome. *Electrophoresis,* 19**,** 1006-14.

RALSER, M., ZAMELINK, M. M., KOWALD, A., GERISCH, B., HEEREN, G., STRUYS, E. A., KLIPP, E., JAKOBS, C., BREITENBACH, M., LEHRACH, H. & KROBITSCH, S. (2007) Dynamic rerouting of the carbohydrate flux is key to counteracting oxidative stress. *Journal of biology,* 6.

RASHID, M. A., LEE, S., TAK, E., LEE, J., CHOI, T. G., LEE, J. W., KIM, J. B., YOUN, J. H., KANG, I., HA, J. & KIM, S. S. (2010) Carbonyl reductase 1 protects pancreatic beta-cells against oxidative stress-induced apoptosis in glucotoxicity and glucolipotoxicity. *Free Radic Biol Med,* 49**,** 1522-33.

RAVIKUMAR, B., ACEVEDO-AROZENA, A., IMARISIO, S., BERGER, Z., VACHER, C., O'KANE, C. J., BROWN, S. D. & RUBINSZTEIN, D. C. (2005) Dynein mutations impair autophagic clearance of aggregate-prone proteins. *Nat Genet,* 37**,** 771-6.

REYNOLDS, G. P., PEARSON, S. J., HALKET, J. & SANDLER, M. (1988) Brain quinolinic acid in Huntington's disease. *J Neurochem,* 50**,** 1959-60.

RICHARDS, P., DIDSZUN, C., CAMPESAN, S., SIMPSON, A., HORLEY, B., YOUNG, K. W., GLYNN, P., CAIN, K., KYRIACOU, C. P., GIORGINI, F. & NICOTERA, P. (2011) Dendritic spine loss and neurodegeneration is rescued by Rab11 in models of Huntington's disease. *Cell Death Differ,* 18**,** 914.

RODGERS, J., STONE, T. W., BARRETT, M. P., BRADLEY, B. & KENNEDY, P. G. (2009) Kynurenine pathway inhibition reduces central nervous system inflammation in a model of human African trypanosomiasis. *Brain,* 132**,** 1259-67.

ROGERS, D. C., PETERS, J., MARTIN, J. E., BALL, S., NICHOLSON, S. J., WITHERDEN, A. S., HAFEZPARAST, M., LATCHAM, J., ROBINSON, T. L., QUILTER, C. A. & FISHER, E. M. (2001) SHIRPA, a protocol for behavioral assessment: validation for longitudinal study of neurological dysfunction in mice. *Neurosci Lett,* 306**,** 89-92.

RONGVAUX, A., ANDRIS, F., VAN GOOL, F. & LEO, O. (2003) Reconstructing eukaryotic NAD metabolism. *Bioessays,* 25**,** 683-90.

ROSS, C. A., BECHER, M. W., COLOMER, V., ENGELENDER, S., WOOD, J. D. & SHARP, A. H. (1997) Huntington's disease and dentatorubral-pallidoluysian atrophy: proteins, pathogenesis and pathology. *Brain Pathol,* 7**,** 1003-16.

RUNDLETT, S. E., CARMEN, A. A., KOBAYASHI, R., BAVYKIN, S., TURNER, B. M. & GRUNSTEIN, M. (1996) HDA1 and RPD3 are members of distinct yeast histone deacetylase complexes that regulate silencing and transcription. *Proc Natl Acad Sci U S A,* 93**,** 14503-8.

SANTAMARIA, A., FLORES-ESCARTIN, A., MARTINEZ, J. C., OSORIO, L., GALVAN-ARZATE, S., PEDRAZA-CHAVERRI, J., MALDONADO, P. D., MEDINA-CAMPOS, O. N., JIMENEZ-CAPDEVILLE, M. E., MANJARREZ, J. & RIOS, C. (2003) Copper blocks quinolinic acid neurotoxicity in rats: contribution of antioxidant systems. *Free Radic Biol Med,* 35**,** 418-27.

SAPKO, M. T., GUIDETTI, P., YU, P., TAGLE, D. A., PELLICCIARI, R. & SCHWARCZ, R. (2006) Endogenous kynurenate controls the vulnerability of striatal neurons to quinolinate: Implications for Huntington's disease. *Exp Neurol,* 197**,** 31-40.

SAPP, E., KEGEL, K. B., ARONIN, N., HASHIKAWA, T., UCHIYAMA, Y., TOHYAMA, K., BHIDE, P. G., VONSATTEL, J. P. & DIFIGLIA, M. (2001) Early and progressive accumulation of reactive microglia in the Huntington disease brain. *J Neuropathol Exp Neurol,* 60**,** 161-72.

SARDAR, A. M. & REYNOLDS, G. P. (1995) Frontal cortex indoleamine-2,3-dioxygenase activity is increased in HIV-1-associated dementia. *Neurosci Lett,* 187**,** 9-12.

SARTER, M., NELSON, C. L. & BRUNO, J. P. (2005) Cortical cholinergic transmission and cortical information processing in schizophrenia. *Schizophr Bull,* 31**,** 117-38.

SAS, K., ROBOTKA, H., TOLDI, J. & VECSEI, L. (2007) Mitochondria, metabolic disturbances, oxidative stress and the kynurenine system, with focus on neurodegenerative disorders. *J Neurol Sci,* 257**,** 221-39.

SATHYASAIKUMAR, K. V., STACHOWSKI, E. K., WONODI, I., ROBERTS, R. C., RASSOULPOUR, A., MCMAHON, R. P. & SCHWARCZ, R. (2010) Impaired Kynurenine Pathway Metabolism in The Prefrontal Cortex of Individuals With Schizophrenia. *Schizophr Bull.*

SCHERZINGER, E., SITTLER, A., SCHWEIGER, K., HEISER, V., LURZ, R., HASENBANK, R., BATES, G. P., LEHRACH, H. & WANKER, E. E. (1999) Self-assembly of polyglutamine-containing huntingtin fragments into amyloid-like fibrils: implications for Huntington's disease pathology. *Proc Natl Acad Sci U S A,* 96**,** 4604-9.

SCHOUSBOE, A., WESTERGAARD, N., SONNEWALD, U., PETERSEN, S. B., HUANG, R., PENG, L. & HERTZ, L. (1993) Glutamate and glutamine metabolism and compartmentation in astrocytes. *Dev Neurosci,* 15**,** 359-66.

SCHUTZ, G., CHOW, E. & FEIGELSON, P. (1972) Regulatory properties of hepatic tryptophan oxygenase. *J Biol Chem,* 247**,** 5333-7.

SCHUTZ, G. & FEIGELSON, P. (1972) Purification and properties of rat liver tryptophan oxygenase. *J Biol Chem,* 247**,** 5327-32.

SCHWARCZ, R. (2004) The kynurenine pathway of tryptophan degradation as a drug target. *Curr Opin Pharmacol,* 4**,** 12-7.

SCHWARCZ, R. & KOHLER, C. (1983) Differential vulnerability of central neurons of the rat to quinolinic acid. *Neurosci Lett,* 38**,** 85-90.
SCHWARCZ, R., OKUNO, E., WHITE, R. J., BIRD, E. D. & WHETSELL, W. O., JR. (1988) 3-Hydroxyanthranilate oxygenase activity is increased in the brains of Huntington disease victims. *Proc Natl Acad Sci U S A,* 85**,** 4079-81.
SCHWARCZ, R., WHETSELL, W. O., JR. & MANGANO, R. M. (1983) Quinolinic acid: an endogenous metabolite that produces axon-sparing lesions in rat brain. *Science,* 219**,** 316-8.
SCHWARTZ, R. S. (1997) The vessel wall reaction in restenosis. *Semin Interv Cardiol,* 2**,** 83-8.
SENATOROV, V. V., CHARLES, V., REDDY, P. H., TAGLE, D. A. & CHUANG, D. M. (2003) Overexpression and nuclear accumulation of glyceraldehyde-3-phosphate dehydrogenase in a transgenic mouse model of Huntington's disease. *Mol Cell Neurosci,* 22**,** 285-97.
SEREBRIISKII, I., ESTOJAK, J., BERMAN, M. & GOLEMIS, E. A. (2000) Approaches to detecting false positives in yeast two-hybrid systems. *Biotechniques,* 28**,** 328-30, 332-6.
SGDDATABASE (2007).
SHELINE, C. T. & CHOI, D. W. (1998) Neuronal death in cultured murine cortical cells is induced by inhibition of GAPDH and triosephosphate isomerase. *Neurobiol Dis,* 5**,** 47-54.
SHI, Y., HUTCHINSON, H. G., HALL, D. J. & ZALEWSKI, A. (1993) Downregulation of c-myc expression by antisense oligonucleotides inhibits proliferation of human smooth muscle cells. *Circulation,* 88**,** 1190-5.
SHIN, J. Y., FANG, Z. H., YU, Z. X., WANG, C. E., LI, S. H. & LI, X. J. (2005) Expression of mutant huntingtin in glial cells contributes to neuronal excitotoxicity. *J Cell Biol,* 171**,** 1001-12.
SILACCI, P., MAZZOLAI, L., GAUCI, C., STERGIOPULOS, N., YIN, H. L. & HAYOZ, D. (2004) Gelsolin superfamily proteins: key regulators of cellular functions. *Cell Mol Life Sci,* 61**,** 2614-23.
SILVE, S., VOLLAND, C., GARNIER, C., JUND, R., CHEVALLIER, M. R. & HAGUENAUER-TSAPIS, R. (1991) Membrane insertion of uracil permease, a polytopic yeast plasma membrane protein. *Mol Cell Biol,* 11**,** 1114-24.
SLEPNEV, V. I. & DE CAMILLI, P. (2000) Accessory factors in clathrin-dependent synaptic vesicle endocytosis. *Nat Rev Neurosci,* 1**,** 161-72.
SLEUMER, M. C., MAH, A. K., BAILLIE, D. L. & JONES, S. J. (2010) Conserved elements associated with ribosomal genes and their trans-splice acceptor sites in Caenorhabditis elegans. *Nucleic Acids Res,* 38**,** 2990-3004.
SRIKANTH, B., MACZUREK, A., PHAN, T., STEELE, M., WESTCOTT, B., JUSKIW, D. & MÜNCH, G. (2011) Advanced glycation endproducts and their receptor RAGE in Alzheimer's disease. *Neurobiology of Aging,* 32**,** 763-777.
STAGLJAR, I., KOROSTENSKY, C., JOHNSSON, N. & TE HEESEN, S. (1998) A genetic system based on split-ubiquitin for the analysis of interactions between membrane proteins in vivo. *Proc Natl Acad Sci U S A,* 95**,** 5187-92.
STAR, E. N., KWIATKOWSKI, D. J. & MURTHY, V. N. (2002) Rapid turnover of actin in dendritic spines and its regulation by activity. *Nat Neurosci,* 5**,** 239-46.
STONE, T. W. (1993) Neuropharmacology of quinolinic and kynurenic acids. *Pharmacol Rev,* 45**,** 309-79.
STOREY, E., CIPOLLONI, P. B., FERRANTE, R. J., KOWALL, N. W. & BEAL, M. F. (1994) Movement disorder following excitotoxin lesions in primates. *Neuroreport,* 5**,** 1259-61.
STOY, N., MACKAY, G. M., FORREST, C. M., CHRISTOFIDES, J., EGERTON, M., STONE, T. W. & DARLINGTON, L. G. (2005) Tryptophan metabolism and oxidative stress in patients with Huntington's disease. *J Neurochem,* 93**,** 611-23.
TAI, Y. F., PAVESE, N., GERHARD, A., TABRIZI, S. J., BARKER, R. A., BROOKS, D. J. & PICCINI, P. (2007a) Imaging microglial activation in Huntington's disease. *Brain Res Bull,* 72**,** 148-51.

TAI, Y. F., PAVESE, N., GERHARD, A., TABRIZI, S. J., BARKER, R. A., BROOKS, D. J. & PICCINI, P. (2007b) Microglial activation in presymptomatic Huntington's disease gene carriers. *Brain,* 130**,** 1759-66.

TAKETANI, S., SAWA, Y., TANIGUCHI, K., MITSUNO, M., KAWAGUCHI, N., ONISHI, S. & MATSUDA, H. (1997) C-Myc expression and its role in patients with chronic aortic regurgitation. *Circulation,* 96**,** II-83-7; discussion II-87-9.

TAKIKAWA, O., TAGAWA, Y., IWAKURA, Y., YOSHIDA, R. & TRUSCOTT, R. J. (1999) Interferon-gamma-dependent/independent expression of indoleamine 2,3-dioxygenase. Studies with interferon-gamma-knockout mice. *Adv Exp Med Biol,* 467**,** 553-7.

TAM, Y. Y., FAGARASANU, A., FAGARASANU, M. & RACHUBINSKI, R. A. (2005) Pex3p initiates the formation of a preperoxisomal compartment from a subdomain of the endoplasmic reticulum in Saccharomyces cerevisiae. *J Biol Chem,* 280**,** 34933-9.

TATTER, S. B., GALPERN, W. R., HOOGEVEEN, A. T. & ISACSON, O. (1995) Effects of striatal excitotoxicity on huntingtin-like immunoreactivity. *Neuroreport,* 6**,** 1125-9.

TAUBER, E., MILLER-FLEMING, L., MASON, R. P., KWAN, W., CLAPP, J., BUTLER, N. J., OUTEIRO, T. F., MUCHOWSKI, P. J. & GIORGINI, F. (2010) Functional gene expression profiling in yeast implicates translational dysfunction in mutant huntingtin toxicity. *J Biol Chem,* 286**,** 410-9.

TAYLOR, S. W., FAHY, E., ZHANG, B., GLENN, G. M., WARNOCK, D. E., WILEY, S., MURPHY, A. N., GAUCHER, S. P., CAPALDI, R. A., GIBSON, B. W. & GHOSH, S. S. (2003) Characterization of the human heart mitochondrial proteome. *Nat Biotechnol,* 21**,** 281-6.

TAYLOR, S. W., WARNOCK, D. E., GLENN, G. M., ZHANG, B., FAHY, E., GAUCHER, S. P., CAPALDI, R. A., GIBSON, B. W. & GHOSH, S. S. (2002) An alternative strategy to determine the mitochondrial proteome using sucrose gradient fractionation and 1D PAGE on highly purified human heart mitochondria. *J Proteome Res,* 1**,** 451-8.

THAMINY, S., AUERBACH, D., ARNOLDO, A. & STAGLJAR, I. (2003) Identification of novel ErbB3-interacting factors using the split-ubiquitin membrane yeast two-hybrid system. *Genome Res,* 13**,** 1744-53.

THEVANDAVAKKAM, M. A., SCHWARCZ, R., MUCHOWSKI, P. J. & GIORGINI, F. (2010) Targeting Kynurenine 3-Monooxygenase (KMO): Implications for Therapy in Huntington's Disease. *CNS Neurol Disord Drug Targets,* 9**,** 791-800.

TONG, A. H. & BOONE, C. (2006) Synthetic genetic array analysis in Saccharomyces cerevisiae. *Methods Mol Biol,* 313**,** 171-92.

UEMURA, T. & HIRAI, K. (1998) L-kynurenine 3-monooxygenase from mitochondrial outer membrane of pig liver: purification, some properties, and monoclonal antibodies directed to the enzyme. *J Biochem,* 123**,** 253-62.

USDIN, M. T., SHELBOURNE, P. F., MYERS, R. M. & MADISON, D. V. (1999) Impaired synaptic plasticity in mice carrying the Huntington's disease mutation. *Hum Mol Genet,* 8**,** 839-46.

VALETTI, C., WETZEL, D. M., SCHRADER, M., HASBANI, M. J., GILL, S. R., KREIS, T. E. & SCHROER, T. A. (1999) Role of dynactin in endocytic traffic: effects of dynamitin overexpression and colocalization with CLIP-170. *Mol Biol Cell,* 10**,** 4107-20.

VAN CRIEKINGE, W. & BEYAERT, R. (1999) Yeast Two-Hybrid: State of the Art. *Biol Proced Online,* 2**,** 1-38.

VECSEI, L. & BEAL, M. F. (1990) Intracerebroventricular injection of kynurenic acid, but not kynurenine, induces ataxia and stereotyped behavior in rats. *Brain Res Bull,* 25**,** 623-7.

WELLINGTON, C. L., ELLERBY, L.M., LEAVITT, B.R., ROY,S., NICHOLSON, D.W., HAYDEN, M.R. (2003) Huntingtin proteolysis in huntington disease. *Clinical neuroscience research,* 3**,** 10.

WERNER, E. R., FUCHS, D., HAUSEN, A., JAEGER, H., REIBNEGGER, G., WERNER-FELMAYER, G., DIERICH, M. P. & WACHTER, H. (1988) Tryptophan degradation in patients infected by human immunodeficiency virus. *Biol Chem Hoppe Seyler,* 369**,** 337-40.

WEXLER, N. S., LORIMER, J., PORTER, J., GOMEZ, F., MOSKOWITZ, C., SHACKELL, E., MARDER, K., PENCHASZADEH, G., ROBERTS, S. A., GAYAN, J., BROCKLEBANK, D., CHERNY, S. S., CARDON, L. R., GRAY, J., DLOUHY, S. R., WIKTORSKI, S., HODES, M. E., CONNEALLY, P. M., PENNEY, J. B., GUSELLA, J., CHA, J. H., IRIZARRY, M., ROSAS, D., HERSCH, S., HOLLINGSWORTH, Z., MACDONALD, M., YOUNG, A. B., ANDRESEN, J. M., HOUSMAN, D. E., DE YOUNG, M. M., BONILLA, E., STILLINGS, T., NEGRETTE, A., SNODGRASS, S. R., MARTINEZ-JAURRIETA, M. D., RAMOS-ARROYO, M. A., BICKHAM, J., RAMOS, J. S., MARSHALL, F., SHOULSON, I., REY, G. J., FEIGIN, A., ARNHEIM, N., ACEVEDO-CRUZ, A., ACOSTA, L., ALVIR, J., FISCHBECK, K., THOMPSON, L. M., YOUNG, A., DURE, L., O'BRIEN, C. J., PAULSEN, J., BRICKMAN, A., KRCH, D., PEERY, S., HOGARTH, P., HIGGINS, D. S., JR. & LANDWEHRMEYER, B. (2004) Venezuelan kindreds reveal that genetic and environmental factors modulate Huntington's disease age of onset. *Proc Natl Acad Sci U S A,* 101**,** 3498-503.

WILLINGHAM, S., OUTEIRO, T. F., DEVIT, M. J., LINDQUIST, S. L. & MUCHOWSKI, P. J. (2003) Yeast genes that enhance the toxicity of a mutant huntingtin fragment or alpha-synuclein. *Science,* 302**,** 1769-72.

WINZELER, E. A., SHOEMAKER, D. D., ASTROMOFF, A., LIANG, H., ANDERSON, K., ANDRE, B., BANGHAM, R., BENITO, R., BOEKE, J. D., BUSSEY, H., CHU, A. M., CONNELLY, C., DAVIS, K., DIETRICH, F., DOW, S. W., EL BAKKOURY, M., FOURY, F., FRIEND, S. H., GENTALEN, E., GIAEVER, G., HEGEMANN, J. H., JONES, T., LAUB, M., LIAO, H., LIEBUNDGUTH, N., LOCKHART, D. J., LUCAU-DANILA, A., LUSSIER, M., M'RABET, N., MENARD, P., MITTMANN, M., PAI, C., REBISCHUNG, C., REVUELTA, J. L., RILES, L., ROBERTS, C. J., ROSS-MACDONALD, P., SCHERENS, B., SNYDER, M., SOOKHAI-MAHADEO, S., STORMS, R. K., VERONNEAU, S., VOET, M., VOLCKAERT, G., WARD, T. R., WYSOCKI, R., YEN, G. S., YU, K., ZIMMERMANN, K., PHILIPPSEN, P., JOHNSTON, M. & DAVIS, R. W. (1999) Functional characterization of the S. cerevisiae genome by gene deletion and parallel analysis. *Science,* 285**,** 901-6.

WIRLEITNER, B., RUDZITE, V., NEURAUTER, G., MURR, C., KALNINS, U., ERGLIS, A., TRUSINSKIS, K. & FUCHS, D. (2003) Immune activation and degradation of tryptophan in coronary heart disease. *Eur J Clin Invest,* 33**,** 550-4.

WIRTH, H. & WERMUTH, B. (1992) Immunohistochemical localization of carbonyl reductase in human tissues. *J Histochem Cytochem,* 40**,** 1857-63.

WONODI, I. & SCHWARCZ, R. (2010) Cortical kynurenine pathway metabolism: a novel target for cognitive enhancement in Schizophrenia. *Schizophr Bull,* 36**,** 211-8.

YAMAZAKI, F., KUROIWA, T., TAKIKAWA, O. & KIDO, R. (1985) Human indolylamine 2,3-dioxygenase. Its tissue distribution, and characterization of the placental enzyme. *Biochem J,* 230**,** 635-8.

YU, P., DI PROSPERO, N. A., SAPKO, M. T., CAI, T., CHEN, A., MELENDEZ-FERRO, M., DU, F., WHETSELL, W. O., JR., GUIDETTI, P., SCHWARCZ, R. & TAGLE, D. A. (2004) Biochemical and phenotypic abnormalities in kynurenine aminotransferase II-deficient mice. *Mol Cell Biol,* 24**,** 6919-30.

ZERON, M. M., HANSSON, O., CHEN, N., WELLINGTON, C. L., LEAVITT, B. R., BRUNDIN, P., HAYDEN, M. R. & RAYMOND, L. A. (2002) Increased sensitivity to N-methyl-D-aspartate receptor-mediated excitotoxicity in a mouse model of Huntington's disease. *Neuron,* 33**,** 849-60.

ZUHLKE, C., RIESS, O., BOCKEL, B., LANGE, H. & THIES, U. (1993) Mitotic stability and meiotic variability of the (CAG)n repeat in the Huntington disease gene. *Hum Mol Genet,* 2**,** 2063-7.

APPENDICES

APPENDIX 1: MAPS OF PLASMIDS USED IN THE STUDY

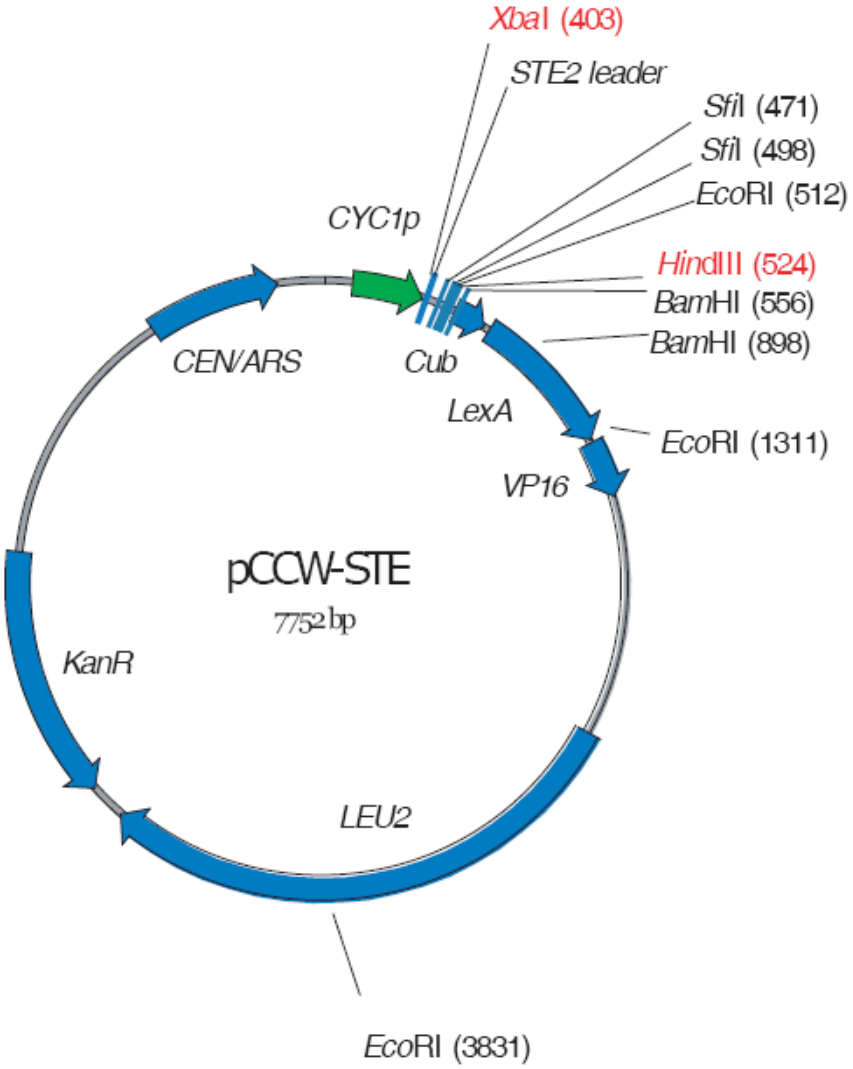

Figure A1-1: Vector used for cloning the Baits in OMM-MYTH (Iyer et al., 2005)

The baits were amplified and cloned into the *E.coli*-yeast shuttle vector pCCW-Ste vector containing the leader sequence Ste and the Cub domain enabling C-terminal tagging of the protein of interest. It also contains KanR and *LEU2* for selection in *E.coli* and yeast.

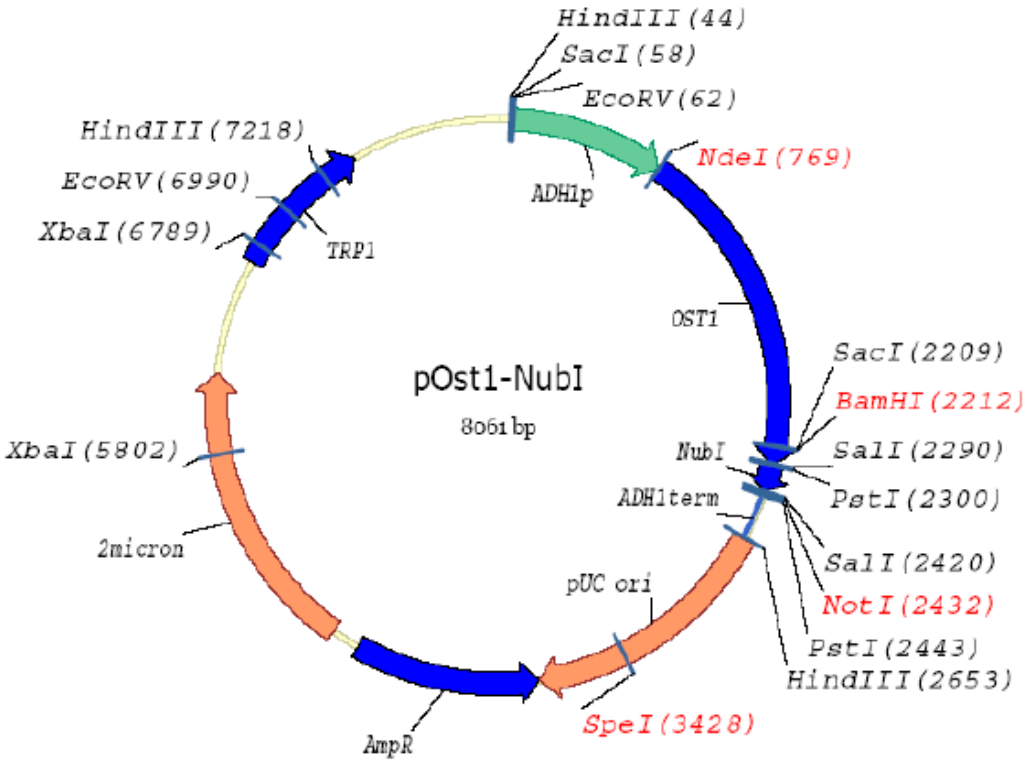

Figure A1-2: Vector used for cloning the prey proteins in OMM-MYTH (Iyer et al., 2005)

The prey proteins were amplified and cloned into the *E.coli*-yeast shuttle vector pOst1-NubI vector and prey specific protein sequences replaced Ost1p sequence. The vector contain the NubI domain and enables C-terminal tagging of proteins of interest. It also contains AmpR and *TRP1* for selection in *E.coli* and yeast.

Figure A2: **Confirmation of reporter gene activity in hits from the OMM-MYTH screen.**

Figure shows reporter gene activity of hits obtained from the KMO OMM-MYTH screen confirmed by (a) Growth assays to measure for *ADE* and *HIS* reporter activity and (b) β-Galactosidase assays to measure LacZ activity. Yeast cells were co-transformed with hits from the screen and the KMO bait, and the levels of various reporters was analysed along with prey controls-Mmm1 NubI, Mmm1 NubG and NubG that were used as controls in both the growth assay and LacZ assay. The data shown represent the average of at least three independent experiments and the error bars represent the standard deviation.

APPENDIX 2: CONFIRMATION OF REPORTER GENE ACTIVITY OF HITS FROM THE OMM-MYTH SCREEN BY GROWTH ASSAY AND B-GALACTOSIDASE ASSAYS

Figure A2 (A)

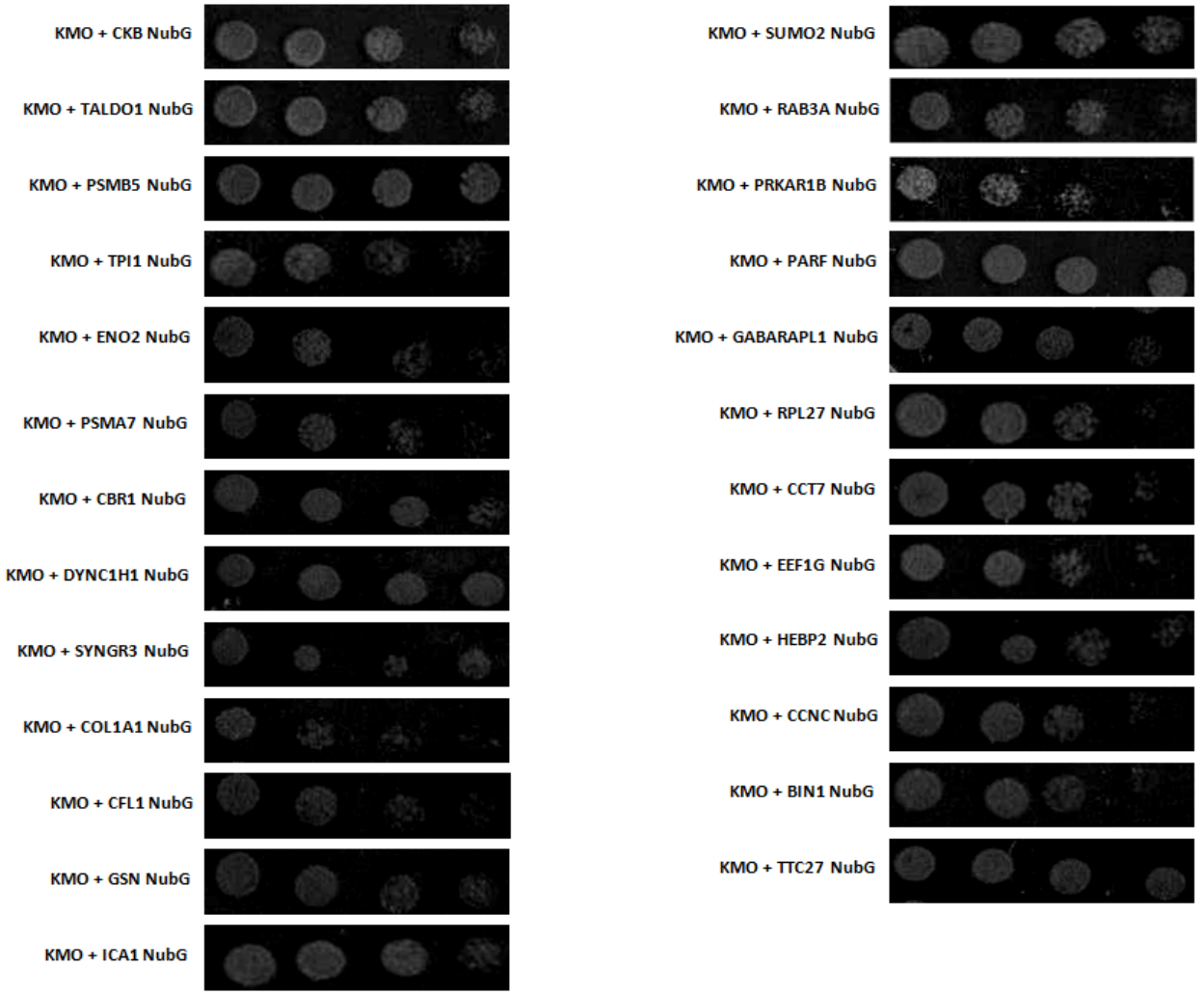

Figure A2 (B)

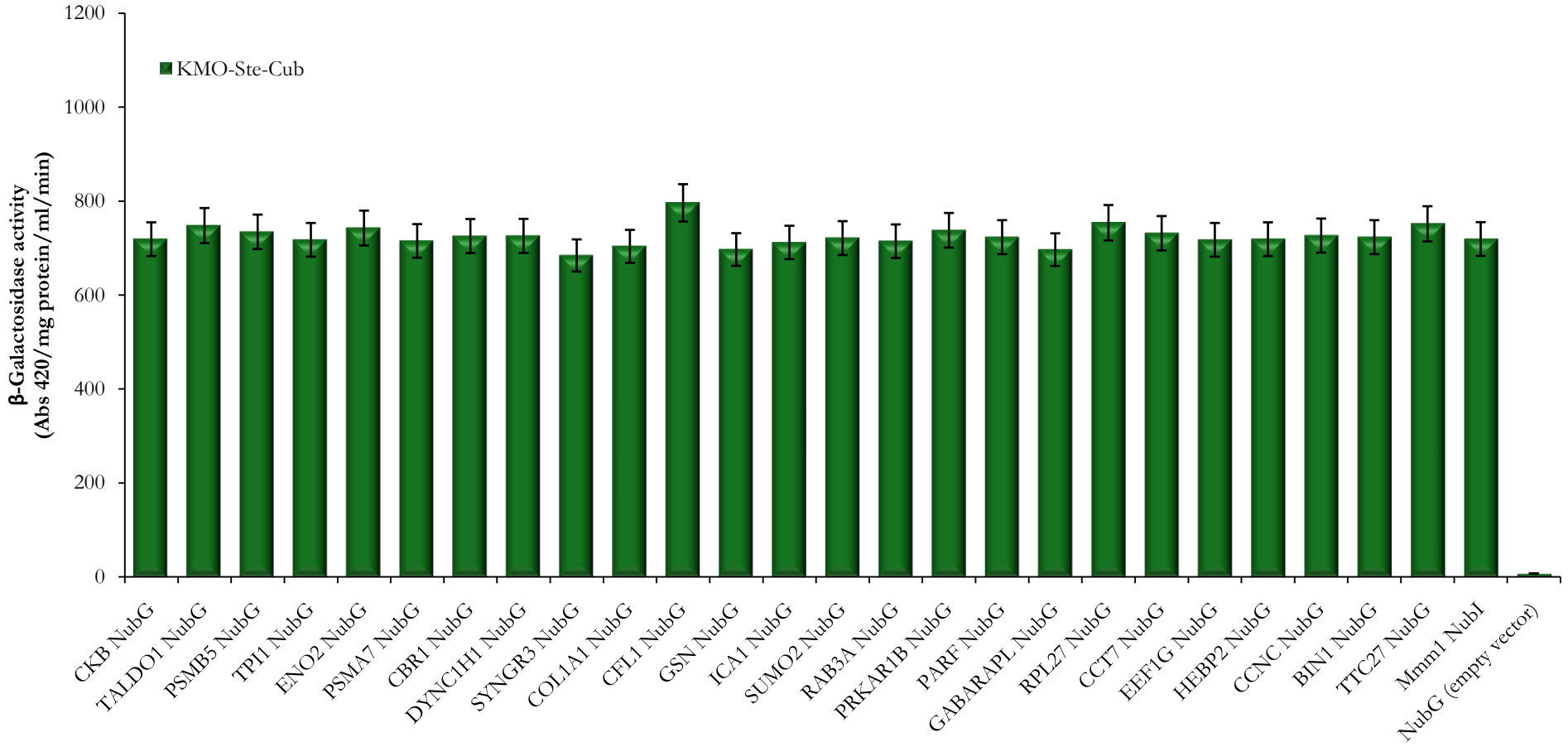
KMO-Ste-Cub
β-Galactosidase activity
(Abs 420/mg protein/ml/min)
1200
1000
800
600
400
200
0
CKB NubG
TALDO1 NubG
PSMB5 NubG
TPI1 NubG
ENO2 NubG
PSMA7 NubG
CBR1 NubG
DYNC1H1 NubG
SYNGR3 NubG
COL1A1 NubG
CFL1 NubG
GSN NubG
ICA1 NubG
SUMO2 NubG
RAB3A NubG
PRKAR1B NubG
PARF NubG
GABARAPL NubG
RPL27 NubG
CCT7 NubG
EEF1G NubG
HEBP2 NubG
CCNC NubG
BIN1 NubG
TTC27 NubG
Mmm1 NubI
NubG (empty vector)

Figure A3: Validation of hits from the OMM- MYTH screen by co-immunoprecipitation

Protein interaction partners of KMO were validated by co-immunoprecipitation analysis. The bait was FLAG tagged and the hits from the screen are HA tagged. The hits were co-transformed with the baits. Cell lysates were then immunoprecipitated using magnetic beads coated with anti-FLAG antibody. The immunoprecipiates were then examined by western blotting using anti-HA antibody. The figure shows a subset of hits from OMM-MYTH that were confirmed by Co-IP.

APPENDIX 3: VALIDATION OF PUTATIVE KMO INTERACTORS BY CO-IMMUNOPRECIPITATION

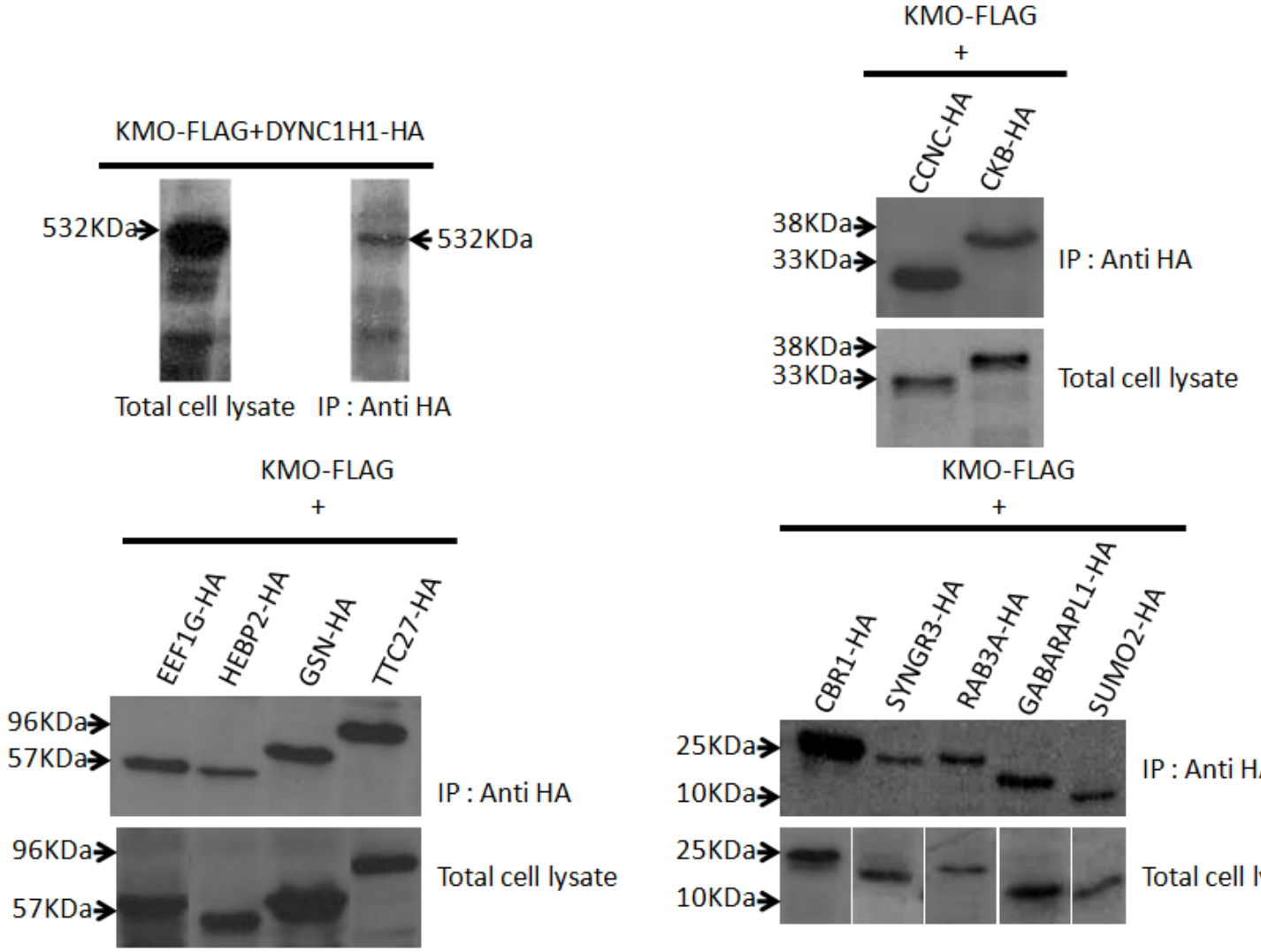

Table A4: Common transcription factors that interact with KIPs.

Functional annotation analysis was carried out using DAVID bioinformatics resources 6.7 and included the annotation category UCSC_TFBS. A p-value ≤0.05 cut-off was used.

APPENDIX 4 COMMON TRANSCRIPTION FACTORS THAT INTERACT WITH KIPs

Common interacting genes	Genes	% fold change	P-Value
PAX2	*RAB3A, TALDO1, RUNDC3A, PSMA7, CKB, PSMB5, TPI1, CBR1, GSN, ENO2, DYNC1H1, GAPDH, AP2M1, C9ORF86, ICA1, RPL27, CCNC, SYNGR3, DCTN2, PPA1, HEBP2, PRKAR1B, CFL1, EEF1G, COL1A1, TRAPPC1*	83.9	1.40E-04
HNF4	*C9ORF86, ICA1, GABARAPL1, RPL27, RUNDC3A, CCNC, SYNGR3, PPA1, DCTN2, CCT7, TPI1, CBR1, GSN, PRKAR1B, CFL1, ENO2, EEF1G, COL1A1, BIN1, DYNC1H1, TRAPPC1, GAPDH, AP2M1*	74.2	2.50E-04
OLF1/EBF1	*C9ORF86, ICA1, TALDO1, RPL27, RUNDC3A, SYNGR3, CKB, DCTN2, CCT7, TPI1, CBR1, GSN, HEBP2, PRKAR1B, CFL1, ENO2, EEF1G, COL1A1, BIN1, DYNC1H1, TRAPPC1, AP2M1*	71	3.60E-04
ELK1	*C9ORF86, RAB3A, GABARAPL1, TALDO1, RPL27, RUNDC3A, CCNC, TTC27, SYNGR3, CKB, DCTN2, PSMB5, CCT7, SUMO2, TPI1, HEBP2, CFL1, ENO2, EEF1G, COL1A1, BIN1, TRAPPC1, GAPDH*	74.2	4.70E-04
USF	*RAB3A, TALDO1, RUNDC3A, PSMA7, CKB, SUMO2, TPI1, GSN, ENO2, DYNC1H1, GAPDH, AP2M1, C9ORF86, ICA1, RPL27, SYNGR3, DCTN2, PPA1, CCT7, HEBP2, PRKAR1B, CFL1, COL1A1, BIN1, TRAPPC1*	80.6	6.60E-04
AP4	*RAB3A, TALDO1, RUNDC3A, TTC27, CKB, PSMB5, SUMO2, TPI1, CBR1, GSN, ENO2, GAPDH, C9ORF86, ICA1, GABARAPL1, RPL27, SYNGR3, DCTN2, CCT7, HEBP2, PRKAR1B, CFL1, EEF1G, COL1A1, BIN1, TRAPPC1*	83.9	1.10E-03
PAX5	*C9ORF86, RAB3A, ICA1, TALDO1, RUNDC3A, TTC27, PSMA7, SYNGR3, CKB, DCTN2, PSMB5, CCT7, TPI1, GSN, PRKAR1B, HEBP2, CFL1, ENO2, EEF1G, COL1A1, DYNC1H1, TRAPPC1, GAPDH, AP2M1*	77.4	1.20E-03
NMYC	*ICA1, RUNDC3A, SYNGR3, PPA1, DCTN2, CKB, CCT7, GSN, HEBP2, PRKAR1B, COL1A1, BIN1, TRAPPC1, DYNC1H1, GAPDH, AP2M1*	54.8	1.20E-03
MYCMAX	*RAB3A, TALDO1, RUNDC3A, CKB, PSMB5, SUMO2, TPI1, CBR1, GSN, DYNC1H1, GAPDH, AP2M1, C9ORF86, ICA1, SYNGR3, DCTN2, PPA1, CCT7, HEBP2, PRKAR1B, CFL1, EEF1G, COL1A1, BIN1, TRAPPC1*	80.6	2.30E-03

Common interacting genes	Genes	% fold change	P-Value
BRACH	*C9ORF86, RAB3A, ICA1, RPL27, RUNDC3A, TTC27, SYNGR3, CKB, DCTN2, PSMB5, SUMO2, TPI1, GSN, HEBP2, PRKAR1B, CFL1, ENO2, COL1A1, BIN1, DYNC1H1, TRAPPC1, GAPDH, AP2M1*	74.2	2.70E-03
TCF11MAFG	*C9ORF86, RAB3A, ICA1, GABARAPL1, TALDO1, RPL27, RUNDC3A, TTC27, CCNC, SYNGR3, DCTN2, CCT7, GSN, HEBP2, CFL1, ENO2, EEF1G, COL1A1, BIN1, DYNC1H1, GAPDH, AP2M1*	71	3.90E-03
E47	*C9ORF86, RAB3A, ICA1, GABARAPL1, TALDO1, RUNDC3A, TTC27, SYNGR3, CKB, DCTN2, PSMB5, CCT7, SUMO2, TPI1, GSN, PRKAR1B, CFL1, ENO2, EEF1G, COL1A1, BIN1, DYNC1H1, GAPDH, AP2M1*	77.4	4.70E-03
SPZ1	*GABARAPL1, ICA1, RUNDC3A, RPL27, SYNGR3, DCTN2, TPI1, GSN, CFL1, ENO2, EEF1G, COL1A1, BIN1, TRAPPC1, DYNC1H1, AP2M1*	51.6	4.80E-03
GCNF	*C9ORF86, RAB3A, ICA1, GABARAPL1, RPL27, TTC27, CCNC, PSMA7, SYNGR3, DCTN2, CCT7, SUMO2, TPI1, GSN, PRKAR1B, CFL1, ENO2, EEF1G, COL1A1, BIN1, DYNC1H1, GAPDH, AP2M1*	74.2	4.90E-03
TAXCREB	*C9ORF86, ICA1, RUNDC3A, TTC27, PSMA7, SYNGR3, CKB, DCTN2, PSMB5, CCT7, TPI1, GSN, PRKAR1B, CFL1, ENO2, EEF1G, COL1A1, BIN1, DYNC1H1, TRAPPC1, GAPDH, AP2M1*	71	6.10E-03
ER	*C9ORF86, ICA1, GABARAPL1, RUNDC3A, TTC27, CCNC, SYNGR3, CKB, DCTN2, CCT7, TPI1, GSN, HEBP2, CFL1, ENO2, EEF1G, COL1A1, BIN1, DYNC1H1, TRAPPC1, GAPDH*	67.7	7.20E-03
ARNT/HIF-A	*C9ORF86, ICA1, RUNDC3A, TTC27, PSMA7, SYNGR3, PPA1, CKB, DCTN2, CCT7, GSN, HEBP2, PRKAR1B, CFL1, ENO2, COL1A1, BIN1, DYNC1H1, GAPDH, AP2M1*	64.5	7.60E-03
HOX13	*C9ORF86, RAB3A, ICA1, TALDO1, RPL27, TTC27, PSMA7, SYNGR3, DCTN2, CKB, SUMO2, TPI1, CFL1, ENO2, EEF1G, COL1A1, DYNC1H1, TRAPPC1, AP2M1*	61.3	1.20E-02
HTF	*GABARAPL1, RPL27, TTC27, CCNC, PSMA7, CKB, DCTN2, PSMB5, CCT7, TPI1, CBR1, GSN, CFL1, ENO2, EEF1G, COL1A1, BIN1, DYNC1H1, TRAPPC1, GAPDH, AP2M1*	67.7	1.40E-02
NRSF	*C9ORF86, RAB3A, TALDO1, RPL27, RUNDC3A, TTC27, CKB, DCTN2, PSMB5, CCT7, CBR1, GSN, HEBP2, CFL1, ENO2, EEF1G, COL1A1, DYNC1H1, TRAPPC1, GAPDH, AP2M1*	67.7	1.40E-02
PAX4	*RAB3A, RUNDC3A, TTC27, PSMA7, CKB, PSMB5, SUMO2, TPI1, GSN, ENO2, DYNC1H1, GAPDH, AP2M1, C9ORF86, ICA1, RPL27, CCNC, SYNGR3, PPA1, DCTN2, CCT7, PRKAR1B, CFL1, EEF1G, COL1A1, BIN1, TRAPPC1*	87.1	1.50E-02

Common interacting genes	Genes	% fold change	P-Value
CREB	*RAB3A, ICA1, RUNDC3A, DCTN2, CKB, PSMB5, CCT7, SUMO2, TPI1, GSN, CFL1, COL1A1, BIN1, DYNC1H1, TRAPPC1, GAPDH, AP2M1*	58.1	1.50E-02
CP2	*C9ORF86, TALDO1, SYNGR3, PPA1, DCTN2, PSMB5, CCT7, SUMO2, TPI1, HEBP2, PRKAR1B, CFL1, EEF1G, BIN1, TRAPPC1, DYNC1H1, AP2M1*	54.8	1.50E-02
P53	*C9ORF86, ICA1, GABARAPL1, RUNDC3A, CCNC, PSMA7, SYNGR3, CKB, DCTN2, PSMB5, CCT7, SUMO2, TPI1, GSN, HEBP2, PRKAR1B, CFL1, ENO2, EEF1G, COL1A1, BIN1, DYNC1H1, TRAPPC1, AP2M1*	77.4	1.70E-02
YY1	*RAB3A, TALDO1, RUNDC3A, PSMA7, CKB, PSMB5, SUMO2, GSN, ENO2, DYNC1H1, GAPDH, AP2M1, C9ORF86, ICA1, CCNC, SYNGR3, DCTN2, PPA1, CCT7, PRKAR1B, CFL1, EEF1G, COL1A1, BIN1, TRAPPC1*	80.6	1.70E-02
NGFIC	*GABARAPL1, ICA1, RUNDC3A, CCT7, GSN, HEBP2, PRKAR1B, CFL1, EEF1G, BIN1, TRAPPC1, DYNC1H1, GAPDH, AP2M1*	45.2	1.70E-02
MZF1	*C9ORF86, GABARAPL1, RUNDC3A, RPL27, PSMA7, SYNGR3, DCTN2, CCT7, SUMO2, TPI1, HEBP2, CFL1, ENO2, EEF1G, COL1A1, BIN1, DYNC1H1, GAPDH, AP2M1*	61.3	2.50E-02
MYOD	*C9ORF86, RAB3A, ICA1, RUNDC3A, RPL27, TTC27, PSMA7, SYNGR3, CKB, DCTN2, CCT7, SUMO2, TPI1, PRKAR1B, CFL1, ENO2, EEF1G, BIN1, DYNC1H1, GAPDH, AP2M1*	67.7	2.60E-02
SP1	*C9ORF86, CCT7, RAB3A, ICA1, CFL1, ENO2, RUNDC3A, COL1A1, TRAPPC1, GAPDH, CKB, DCTN2*	38.7	2.80E-02
HSF2	*C9ORF86, RAB3A, ICA1, TALDO1, CCNC, SYNGR3, DCTN2, PSMB5, CCT7, GSN, EEF1G, COL1A1, BIN1, DYNC1H1, TRAPPC1, GAPDH, AP2M1*	54.8	2.80E-02
ROAZ	*C9ORF86, RAB3A, RUNDC3A, RPL27, PSMA7, SYNGR3, CKB, DCTN2, CCT7, TPI1, GSN, HEBP2, CFL1, ENO2, EEF1G, COL1A1, DYNC1H1, AP2M1*	58.1	3.00E-02
HMX1	*C9ORF86, GABARAPL1, RUNDC3A, TTC27, PSMA7, DCTN2, PSMB5, TPI1, GSN, HEBP2, PRKAR1B, ENO2, EEF1G, COL1A1, DYNC1H1, TRAPPC1, GAPDH, AP2M1*	58.1	3.10E-02
AP2	*C9ORF86, CCT7, ICA1, CFL1, ENO2, EEF1G, RPL27, COL1A1, PSMA7, TRAPPC1, SYNGR3, AP2M1*	38.7	3.20E-02
EN1	*C9ORF86, ICA1, GABARAPL1, TALDO1, RUNDC3A, RPL27, TTC27, PSMA7, SYNGR3, CKB, DCTN2, GSN, HEBP2, CFL1, ENO2, EEF1G, DYNC1H1, TRAPPC1, GAPDH, AP2M1*	64.5	3.40E-02

Common interacting genes	Genes	% fold change	P-Value
BACH1	*ICA1, GABARAPL1, RUNDC3A, RPL27, TTC27, CCNC, DCTN2, PSMB5, CCT7, SUMO2, GSN, PRKAR1B, ENO2, EEF1G, COL1A1, BIN1, DYNC1H1, GAPDH, AP2M1*	61.3	3.70E-02
BACH2	*ICA1, GABARAPL1, RUNDC3A, TTC27, PSMA7, PSMB5, SUMO2, TPI1, GSN, PRKAR1B, ENO2, EEF1G, COL1A1, TRAPPC1, DYNC1H1, GAPDH, AP2M1*	54.8	3.90E-02
RORA2	*C9ORF86, ICA1, GABARAPL1, RUNDC3A, CCNC, SYNGR3, DCTN2, SUMO2, TPI1, GSN, HEBP2, PRKAR1B, ENO2, COL1A1, BIN1, TRAPPC1, DYNC1H1, AP2M1*	58.1	4.30E-02
AP2REP	*C9ORF86, GABARAPL1, ICA1, RUNDC3A, DCTN2, CKB, CCT7, TPI1, GSN, PRKAR1B, ENO2, EEF1G, COL1A1, BIN1, TRAPPC1, DYNC1H1, AP2M1*	54.8	5.50E-02
GATA2	*C9ORF86, RAB3A, RUNDC3A, SYNGR3, DCTN2, TPI1, GSN, CFL1, ENO2, EEF1G, TRAPPC1, DYNC1H1, GAPDH, AP2M1*	45.2	5.80E-02
AP1	*C9ORF86, ICA1, GABARAPL1, RUNDC3A, RPL27, TTC27, CCNC, SYNGR3, CKB, DCTN2, TPI1, GSN, PRKAR1B, CFL1, ENO2, EEF1G, COL1A1, DYNC1H1, TRAPPC1, GAPDH, AP2M1*	67.7	6.10E-02
RREB1	*C9ORF86, ICA1, RUNDC3A, RPL27, DCTN2, CKB, CCT7, CFL1, ENO2, EEF1G, COL1A1, BIN1, DYNC1H1, GAPDH, AP2M1*	48.4	6.60E-02
ATF	*C9ORF86, RAB3A, ICA1, RUNDC3A, PSMA7, SYNGR3, CKB, PSMB5, GSN, HEBP2, COL1A1, TRAPPC1, BIN1*	41.9	6.80E-02
NFKB	*C9ORF86, ICA1, GABARAPL1, RUNDC3A, RPL27, TTC27, SYNGR3, PPA1, DCTN2, PSMB5, CCT7, GSN, ENO2, EEF1G, COL1A1, DYNC1H1, TRAPPC1, AP2M1*	58.1	7.20E-02
NFKAPPAB	*ICA1, RUNDC3A, RPL27, SYNGR3, DCTN2, PSMB5, GSN, PRKAR1B, CFL1, EEF1G, BIN1, DYNC1H1, GAPDH, AP2M1*	45.2	7.20E-02
CMYB	*C9ORF86, RAB3A, ICA1, RUNDC3A, RPL27, SYNGR3, DCTN2, CCT7, TPI1, GSN, CFL1, EEF1G, COL1A1, BIN1, DYNC1H1, GAPDH*	51.6	7.20E-02
AREB6	*RAB3A, TALDO1, RUNDC3A, TTC27, PSMA7, CKB, PSMB5, SUMO2, TPI1, GSN, ENO2, DYNC1H1, GAPDH, AP2M1, C9ORF86, ICA1, RPL27, SYNGR3, DCTN2, CCT7, HEBP2, PRKAR1B, CFL1, EEF1G, COL1A1, BIN1, TRAPPC1*	87.1	7.20E-02
CDPCR1	*C9ORF86, RAB3A, TALDO1, RUNDC3A, RPL27, CCNC, DCTN2, CKB, PSMB5, PRKAR1B, CFL1, ENO2, COL1A1, TRAPPC1, AP2M1*	48.4	7.30E-02
LUN1	*C9ORF86, RAB3A, ICA1, RUNDC3A, CCNC, PSMB5, SUMO2, TPI1, GSN, HEBP2, CFL1, ENO2, EEF1G, COL1A1, BIN1, DYNC1H1, TRAPPC1, GAPDH*	58.1	7.40E-02

Common interacting genes	Genes	% fold change	P-Value
MEIS1	*C9ORF86, ICA1, TALDO1, RPL27, TTC27, CKB, DCTN2, PSMB5, CCT7, PRKAR1B, CFL1, EEF1G, COL1A1, DYNC1H1, TRAPPC1, GAPDH, AP2M1*	54.8	7.80E-02
RFX1	*C9ORF86, ICA1, TALDO1, RPL27, PSMA7, SYNGR3, CKB, DCTN2, CCT7, TPI1, CBR1, GSN, PRKAR1B, CFL1, ENO2, EEF1G, COL1A1, BIN1, DYNC1H1, GAPDH, AP2M1*	67.7	8.10E-02
PAX6	*C9ORF86, RAB3A, ICA1, TALDO1, RUNDC3A, TTC27, SYNGR3, DCTN2, CCT7, SUMO2, TPI1, GSN, HEBP2, CFL1, ENO2, COL1A1, BIN1, DYNC1H1, AP2M1*	61.3	8.20E-02
STAT1	*ICA1, CCNC, SYNGR3, DCTN2, PSMB5, CCT7, SUMO2, TPI1, GSN, HEBP2, CFL1, EEF1G, COL1A1, BIN1, GAPDH*	48.4	8.30E-02
NFKAPPAB50	*C9ORF86, GABARAPL1, TPI1, ENO2, TTC27, BIN1, DYNC1H1, GAPDH, CKB, DCTN2*	32.3	8.40E-02
CREBP1CJUN	*RAB3A, GABARAPL1, GSN, CCNC, TRAPPC1, SYNGR3, CKB*	22.6	8.90E-02
NRF2	*CCT7, GABARAPL1, CFL1, ENO2, RPL27, BIN1, TRAPPC1, GAPDH, SYNGR3, AP2M1, CKB, DCTN2*	38.7	9.20E-02
ARP1	*C9ORF86, RUNDC3A, TTC27, SYNGR3, DCTN2, CCT7, TPI1, CBR1, GSN, HEBP2, PRKAR1B, CFL1, ENO2, EEF1G, COL1A1, DYNC1H1, AP2M1*	54.8	9.30E-02
LMO2COM	*C9ORF86, ICA1, GABARAPL1, RUNDC3A, RPL27, PSMA7, SYNGR3, PPA1, CKB, DCTN2, TPI1, CBR1, PRKAR1B, CFL1, ENO2, COL1A1, BIN1, DYNC1H1, TRAPPC1, GAPDH*	64.5	9.80E-02
AHR	*C9ORF86, ICA1, SYNGR3, PSMB5, SUMO2, HEBP2, PRKAR1B, CFL1, ENO2, EEF1G, COL1A1, DYNC1H1, GAPDH*	41.9	9.90E-02

Table A5: Common interaction partners of KIPs.

Functional annotation analysis was carried out using DAVID bioinformatics resources 6.7 and included the following annotation categories GOTERM_BP_ALL, GOTERM_CC_ALL, GOTERM_MF_ALL. A p-value ≤0.05 cut-off was used.

APPENDIX 5: COMMON PROTEIN INTERACTION PARTNERS OF KIPs

Protein interactions	Genes	% fold change	P-value
adaptor-related protein complex 2, beta 1 subunit	*CBR1, GSN, CFL1, EEF1G, RPL27, AP2M1*	19.4	1.00E-04
actin related protein 2/3 complex, subunit 1A, 41kDa	*CBR1, GSN, CFL1, EEF1G, RPL27*	16.1	1.10E-03
tropomyosin 2 (beta)	*CBR1, GSN, CFL1, EEF1G, RPL27*	16.1	1.10E-03
leucine zipper protein 1	*CBR1, GSN, CFL1, EEF1G, RPL27*	16.1	1.10E-03
coronin, actin binding protein, 1B	*CBR1, GSN, CFL1, EEF1G, RPL27*	16.1	1.10E-03
glutathione S-transferase mu 1	*CBR1, GSN, CFL1, EEF1G, RPL27*	16.1	1.10E-03
keratin 17; keratin 17 pseudogene 3	*CBR1, GSN, CFL1, EEF1G, RPL27*	16.1	1.10E-03
myosin, heavy chain 9, non-muscle	*CBR1, GSN, CFL1, EEF1G, RPL27*	16.1	1.10E-03
ribosomal protein L21 pseudogene 134/80/20/46/45/131/16/53/120/37/93/39/29/28/14/98/105/87/128/69/97/119/125	*CBR1, GSN, CFL1, EEF1G, RPL27*	16.1	1.10E-03
ribosomal protein S16 pseudogene 1; ribosomal protein S16 pseudogene 10; ribosomal protein S16	*CBR1, GSN, CFL1, EEF1G, RPL27*	16.1	1.10E-03
ribosomal protein L36a pseudogene 51; ribosomal protein L36a pseudogene 37; ribosomal protein L36a pseudogene 49; heterogeneous nuclear ribonucleoprotein H2 (H'); ribosomal protein L36a	*CBR1, GSN, CFL1, EEF1G, RPL27*	16.1	1.10E-03
synaptopodin	*CBR1, GSN, CFL1, EEF1G, RPL27*	16.1	1.10E-03
vav 3 guanine nucleotide exchange factor	*CBR1, GSN, CFL1, EEF1G, RPL27*	16.1	1.10E-03
tropomodulin 3 (ubiquitous)	*CBR1, GSN, CFL1, EEF1G, RPL27*	16.1	1.10E-03
histone cluster 1, H2bh	*CBR1, GSN, CFL1, EEF1G, RPL27*	16.1	1.10E-03
tubulin, beta 2C	*CBR1, GSN, CFL1, EEF1G, RPL27*	16.1	1.10E-03
SAPS domain family, member 3	*CBR1, GSN, CFL1, EEF1G, RPL27*	16.1	1.10E-03

Protein interactions	Genes	% fold change	P-value
ribosomal protein, large, P2 pseudogene 3; ribosomal protein, large, P2	*CBR1, GSN, CFL1, EEF1G, RPL27*	16.1	1.10E-03
WD repeat domain 1	*CBR1, GSN, CFL1, EEF1G, RPL27*	16.1	1.10E-03
deoxyuridine triphosphatase	*CBR1, GSN, CFL1, EEF1G, RPL27*	16.1	1.10E-03
matrin 3	*CBR1, GSN, CFL1, EEF1G, RPL27*	16.1	1.10E-03
heterogeneous nuclear ribonucleoprotein F	*CBR1, GSN, CFL1, EEF1G, RPL27*	16.1	1.10E-03
flightless I homolog (Drosophila)	*CBR1, GSN, CFL1, EEF1G, RPL27*	16.1	1.10E-03
ATP synthase, H+ transporting, mitochondrial F1 complex, alpha subunit 1, cardiac muscle	*CBR1, GSN, CFL1, EEF1G, RPL27*	16.1	1.10E-03
protein phosphatase 1, catalytic subunit, beta isoform; speedy homolog A (Xenopus laevis)	*CBR1, GSN, CFL1, EEF1G, RPL27*	16.1	1.10E-03
similar to Plectin 1 (PLTN) (PCN) (Hemidesmosomal protein 1) (HD1); plectin 1, intermediate filament binding protein 500kDa	*CBR1, GSN, CFL1, EEF1G, RPL27*	16.1	1.10E-03
myosin IB	*CBR1, GSN, CFL1, EEF1G, RPL27*	16.1	1.10E-03
coronin, actin binding protein, 1C	*CBR1, GSN, CFL1, EEF1G, RPL27*	16.1	1.10E-03
ribosomal protein L3; similar to 60S ribosomal protein L3 (L4)	*CBR1, GSN, CFL1, EEF1G, RPL27*	16.1	1.10E-03
glia maturation factor, beta	*CBR1, GSN, CFL1, EEF1G, RPL27*	16.1	1.10E-03
Rac GTPase activating protein 1 pseudogene; Rac GTPase activating protein 1	*CBR1, GSN, CFL1, EEF1G, RPL27*	16.1	1.10E-03
tubulin, alpha 4a	*CBR1, GSN, CFL1, EEF1G, RPL27*	16.1	1.10E-03
ribosomal protein S8; ribosomal protein S8 pseudogene 8; ribosomal protein S8 pseudogene 10	*CBR1, GSN, CFL1, EEF1G, RPL27*	16.1	1.10E-03
ribosomal protein S14	*CBR1, GSN, CFL1, EEF1G, RPL27*	16.1	1.10E-03
importin 7	*CBR1, GSN, CFL1, EEF1G, RPL27*	16.1	1.10E-03
ribosomal protein S28 pseudogene 6; ribosomal protein S28 pseudogene 9; ribosomal protein S28	*CBR1, GSN, CFL1, EEF1G, RPL27*	16.1	1.10E-03
family with sequence similarity 55, member B	*CBR1, GSN, CFL1, EEF1G, RPL27*	16.1	1.10E-03
ribosomal protein L23a pseudogene 63; ribosomal protein L23a pseudogene 75; ribosomal protein L23a pseudogene 37; ribosomal protein L23a pseudogene 65; ribosomal protein L23a pseudogene 43; ribosomal protein L23a pseudogene 44; ribosomal	*CBR1, GSN, CFL1, EEF1G, RPL27*	16.1	1.10E-03

Protein interactions	Genes	% fold change	P-value
protein L23a			
fascin homolog 1, actin-bundling protein (Strongylocentrotus purpuratus)	*CBR1, GSN, CFL1, EEF1G, RPL27*	16.1	1.10E-03
S100 calcium binding protein A6	*CBR1, GSN, CFL1, EEF1G, RPL27*	16.1	1.10E-03
retinoic acid induced 14	*CBR1, GSN, CFL1, EEF1G, RPL27*	16.1	1.10E-03
ribosomal protein S5	*CBR1, GSN, CFL1, EEF1G, RPL27*	16.1	1.10E-03
scaffold attachment factor B2	*CBR1, GSN, CFL1, EEF1G, RPL27*	16.1	1.10E-03
ribosomal protein S3 pseudogene 3; ribosomal protein S3	*CBR1, GSN, CFL1, EEF1G, RPL27*	16.1	1.10E-03
ribosomal protein L36; ribosomal protein L36 pseudogene 14	*CBR1, GSN, CFL1, EEF1G, RPL27*	16.1	1.10E-03
tubulin, beta 3; melanocortin 1 receptor (alpha melanocyte stimulating hormone receptor)	*CBR1, GSN, CFL1, EEF1G, RPL27*	16.1	1.10E-03
myosin, heavy chain 14	*CBR1, GSN, CFL1, EEF1G, RPL27*	16.1	1.10E-03
serpin peptidase inhibitor, clade H (heat shock protein 47), member 1, (collagen binding protein 1)	*CBR1, GSN, CFL1, EEF1G, RPL27*	16.1	1.10E-03
ribosomal protein S23	*CBR1, GSN, CFL1, EEF1G, RPL27*	16.1	1.10E-03
myosin, light chain 12B, regulatory	*CBR1, GSN, CFL1, EEF1G, RPL27*	16.1	1.10E-03
aryl-hydrocarbon receptor repressor; programmed cell death 6	*CBR1, GSN, CFL1, EEF1G, RPL27*	16.1	1.10E-03
TAO kinase 2	*CBR1, GSN, CFL1, EEF1G, RPL27*	16.1	1.10E-03
solute carrier family 25 (mitochondrial carrier; phosphate carrier), member 3	*CBR1, GSN, CFL1, EEF1G, RPL27*	16.1	1.10E-03
HtrA serine peptidase 1	*CBR1, GSN, CFL1, EEF1G, RPL27*	16.1	1.10E-03
poly(A) binding protein, cytoplasmic pseudogene 5; poly(A) binding protein, cytoplasmic 1	*CBR1, GSN, CFL1, EEF1G, RPL27*	16.1	1.10E-03
ribosomal protein S9; ribosomal protein S9 pseudogene 4	*CBR1, GSN, CFL1, EEF1G, RPL27*	16.1	1.10E-03
ribosomal protein S3A pseudogene 5; ribosomal protein S3a pseudogene 47; ribosomal protein S3a pseudogene 49; ribosomal protein S3A; hypothetical LOC100131699; hypothetical LOC100130107	*CBR1, GSN, CFL1, EEF1G, RPL27*	16.1	1.10E-03

Protein interactions	Genes	% fold change	P-value
supervillin	*CBR1, GSN, CFL1, EEF1G, RPL27*	16.1	1.10E-03
myosin phosphatase Rho interacting protein; similar to Myosin phosphatase Rho-interacting protein (Rho-interacting protein 3) (M-RIP) (RIP3) (p116Rip)	*CBR1, GSN, CFL1, EEF1G, RPL27*	16.1	1.10E-03
serine hydroxymethyltransferase 2 (mitochondrial)	*CBR1, GSN, CFL1, EEF1G, RPL27*	16.1	1.10E-03
LIM domain 7	*CBR1, GSN, CFL1, EEF1G, RPL27*	16.1	1.10E-03
nexilin (F actin binding protein)	*CBR1, GSN, CFL1, EEF1G, RPL27*	16.1	1.10E-03
death-associated protein kinase 3	*CBR1, GSN, CFL1, EEF1G, RPL27*	16.1	1.10E-03
plastin 3 (T isoform)	*CBR1, GSN, CFL1, EEF1G, RPL27*	16.1	1.10E-03
dystonin	*CBR1, GSN, CFL1, EEF1G, RPL27*	16.1	1.10E-03
UDP-glucose dehydrogenase	*CBR1, GSN, CFL1, EEF1G, RPL27*	16.1	1.10E-03
regulator of chromosome condensation 2	*CBR1, GSN, CFL1, EEF1G, RPL27*	16.1	1.10E-03
LIM domain and actin binding 1	*CBR1, GSN, CFL1, EEF1G, RPL27*	16.1	1.10E-03
ribosomal protein S15a pseudogene 17; ribosomal protein S15a pseudogene 19; ribosomal protein S15a pseudogene 12; ribosomal protein S15a pseudogene 24; ribosomal protein S15a pseudogene 11; ribosomal protein S15a	*CBR1, GSN, CFL1, EEF1G, RPL27*	16.1	1.10E-03
actin related protein 2/3 complex, subunit 2, 34kDa	*CBR1, GSN, CFL1, EEF1G, RPL27*	16.1	1.20E-03
ARP2 actin-related protein 2 homolog (yeast)	*CBR1, GSN, CFL1, EEF1G, RPL27*	16.1	1.20E-03
ribosomal protein L12 pseudogene 2; ribosomal protein L12 pseudogene 32; ribosomal protein L12 pseudogene 35; ribosomal protein L12 pseudogene 19; ribosomal protein L12 pseudogene 6; ribosomal protein L12; ribosomal protein L12 pseudogene 14	*CBR1, GSN, CFL1, EEF1G, RPL27*	16.1	1.20E-03
myosin IA	*CBR1, GSN, CFL1, EEF1G, RPL27*	16.1	1.20E-03
annexin A2 pseudogene 3; annexin A2; annexin A2 pseudogene 1	*CBR1, GSN, CFL1, EEF1G, RPL27*	16.1	1.20E-03
dihydrolipoamide S-succinyltransferase (E2 component of 2-oxo-glutarate complex); dihydrolipoamide S-succinyltransferase pseudogene (E2 component of 2-oxo-glutarate complex)	*CBR1, GSN, CFL1, EEF1G, RPL27*	16.1	1.20E-03
cofilin 2 (muscle)	*CBR1, GSN, CFL1, EEF1G, RPL27*	16.1	1.20E-03

Protein interactions	Genes	% fold change	P-value
protein-L-isoaspartate (D-aspartate) O-methyltransferase	*CBR1, GSN, CFL1, EEF1G, RPL27*	16.1	1.20E-03
actin, alpha, cardiac muscle 1	*CBR1, GSN, CFL1, EEF1G, RPL27*	16.1	1.20E-03
DnaJ (Hsp40) homolog, subfamily A, member 2	*CBR1, GSN, CFL1, EEF1G, RPL27*	16.1	1.20E-03
glutathione S-transferase mu 3 (brain)	*CBR1, GSN, CFL1, EEF1G, RPL27*	16.1	1.20E-03
hydroxyacyl-Coenzyme A dehydrogenase/3-ketoacyl-Coenzyme A thiolase/enoyl-Coenzyme A hydratase (trifunctional protein), beta subunit	*CBR1, GSN, CFL1, EEF1G, RPL27*	16.1	1.20E-03
heat shock 70kDa protein 8	*CBR1, GSN, CFL1, EEF1G, RPL27*	16.1	1.20E-03
similar to actin related protein 2/3 complex subunit 3; hypothetical LOC729841; actin related protein 2/3 complex, subunit 3, 21kDa	*CBR1, GSN, CFL1, EEF1G, RPL27*	16.1	1.20E-03
ribosomal protein L31 pseudogene 49; ribosomal protein L31 pseudogene 17; ribosomal protein L31	*CBR1, GSN, CFL1, EEF1G, RPL27*	16.1	1.20E-03
ribosomal protein L7 pseudogene 26; ribosomal protein L7 pseudogene 16; ribosomal protein L7; ribosomal protein L7 pseudogene 32; ribosomal protein L7 pseudogene 23; ribosomal protein L7 pseudogene 24; ribosomal protein L7 pseudogene 20	*CBR1, GSN, CFL1, EEF1G, RPL27*	16.1	1.20E-03
histone cluster 2, H2aa3; histone cluster 2, H2aa4	*CBR1, GSN, CFL1, EEF1G, RPL27*	16.1	1.20E-03
similar to Bcl-2-associated transcription factor 1 (Btf); BCL2-associated transcription factor 1	*CBR1, GSN, CFL1, EEF1G, RPL27*	16.1	1.20E-03
protein phosphatase 1, regulatory (inhibitor) subunit 12A	*CBR1, GSN, CFL1, EEF1G, RPL27*	16.1	1.20E-03
ribosomal protein L18	*CBR1, GSN, CFL1, EEF1G, RPL27*	16.1	1.20E-03
actin, gamma 1	*CBR1, GSN, CFL1, EEF1G, RPL27*	16.1	1.20E-03
predicted gene 10027; hypothetical protein LOC674425; predicted gene 6794; predicted gene 9175; similar to ribosomal protein S18; similar to ribosomal protein; ribosomal protein S18; predicted gene 11230; predicted gene 5321; predicted gene 10260; predicted gene 8599; predicted gene 8268	*CBR1, GSN, CFL1, EEF1G, RPL27*	16.1	1.20E-03
tubulin tyrosine ligase-like family, member 3; actin related protein 2/3 complex, subunit 4, 20kDa	*CBR1, GSN, CFL1, EEF1G, RPL27*	16.1	1.20E-03
ribosomal protein L24; ribosomal protein L24 pseudogene 6	*CBR1, GSN, CFL1, EEF1G, RPL27*	16.1	1.20E-03
IQ motif containing GTPase activating protein 1	*CBR1, GSN, CFL1, EEF1G, RPL27*	16.1	1.20E-03

Protein interactions	Genes	% fold change	P-value
ribosomal protein L26 pseudogene 33; ribosomal protein L26; ribosomal protein L26 pseudogene 16; ribosomal protein L26 pseudogene 19; ribosomal protein L26 pseudogene 6	*CBR1, GSN, CFL1, EEF1G, RPL27*	16.1	1.20E-03
ARP3 actin-related protein 3 homolog (yeast)	*CBR1, GSN, CFL1, EEF1G, RPL27*	16.1	1.20E-03
FUS interacting protein (serine/arginine-rich) 1; similar to FUS interacting protein (serine-arginine rich) 1	*CBR1, GSN, CFL1, EEF1G, RPL27*	16.1	1.20E-03
adaptor-related protein complex 2, alpha 1 subunit	*CBR1, GSN, CFL1, EEF1G, RPL27*	16.1	1.20E-03
hypothetical gene supported by AF216292; NM_005347; heat shock 70kDa protein 5 (glucose-regulated protein, 78kDa)	*CBR1, GSN, CFL1, EEF1G, RPL27*	16.1	1.20E-03
ribosomal protein S25 pseudogene 8; ribosomal protein S25	*CBR1, GSN, CFL1, EEF1G, RPL27*	16.1	1.20E-03
heat shock 27kDa protein-like 2 pseudogene; heat shock 27kDa protein 1	*CBR1, GSN, CFL1, EEF1G, RPL27*	16.1	1.20E-03
spectrin, alpha, non-erythrocytic 1 (alpha-fodrin)	*CBR1, GSN, CFL1, EEF1G, RPL27*	16.1	1.20E-03
peroxiredoxin 1	*CBR1, GSN, CFL1, EEF1G, RPL27*	16.1	1.20E-03
ribosomal protein S20	*CBR1, GSN, CFL1, EEF1G, RPL27*	16.1	1.20E-03
similar to TRIMCyp; peptidylprolyl isomerase A (cyclophilin A); peptidylprolyl isomerase A (cyclophilin A)-like 3	*CBR1, GSN, CFL1, EEF1G, RPL27*	16.1	1.20E-03
actin related protein 2/3 complex, subunit 5, 16kDa	*CBR1, GSN, CFL1, EEF1G, RPL27*	16.1	1.20E-03
keratin 18; keratin 18 pseudogene 26; keratin 18 pseudogene 19	*CBR1, GSN, CFL1, EEF1G, RPL27*	16.1	1.20E-03
protein phosphatase 3 (formerly 2B), catalytic subunit, alpha isoform	*CBR1, GSN, CFL1, EEF1G, RPL27*	16.1	1.20E-03
actinin, alpha 4	*CBR1, GSN, CFL1, EEF1G, RPL27*	16.1	1.30E-03
actinin, alpha 1	*CBR1, GSN, CFL1, EEF1G, RPL27*	16.1	1.30E-03
ribosomal protein S11 pseudogene 5; ribosomal protein S11	*CBR1, GSN, CFL1, EEF1G, RPL27*	16.1	1.40E-03
small nuclear ribonucleoprotein D2 polypeptide 16.5kDa; similar to hCG2040270	*CBR1, GSN, CFL1, EEF1G, RPL27*	16.1	1.40E-03
dynein, light chain, LC8-type 1	*CBR1, GSN, CFL1, EEF1G, RPL27*	16.1	1.40E-03
ribosomal protein L4; ribosomal protein L4 pseudogene 5; ribosomal protein L4 pseudogene 4	*CBR1, GSN, CFL1, EEF1G, RPL27*	16.1	1.40E-03

Protein interactions	Genes	% fold change	P-value
histone cluster 1, H3j; histone cluster 1, H3i; histone cluster 1, H3h; histone cluster 1, H3g; histone cluster 1, H3f; histone cluster 1, H3e; histone cluster 1, H3d; histone cluster 1, H3c; histone cluster 1, H3b; histone cluster 1, H3a; histone cluster 1, H2ad; histone cluster 2, H3a; histone cluster 2, H3c; histone cluster 2, H3d	*CBR1, GSN, CFL1, EEF1G, RPL27*	16.1	1.50E-03
SWI/SNF related, matrix associated, actin dependent regulator of chromatin, subfamily a, member 5	*CBR1, GSN, CFL1, EEF1G, RPL27*	16.1	1.50E-03
heterogeneous nuclear ribonucleoprotein H1 (H)	*CBR1, GSN, CFL1, EEF1G, RPL27*	16.1	1.50E-03
X-ray repair complementing defective repair in Chinese hamster cells 6; similar to ATP-dependent DNA helicase II, 70 kDa subunit	*CBR1, GSN, CFL1, EEF1G, RPL27*	16.1	1.50E-03
histone cluster 1, H4l; histone cluster 1, H4k; histone cluster 4, H4; histone cluster 1, H4h; histone cluster 1, H4j; histone cluster 1, H4i; histone cluster 1, H4d; histone cluster 1, H4c; histone cluster 1, H4f; histone cluster 1, H4e; histone cluster 1, H4b; histone cluster 1, H4a; histone cluster 2, H4a; histone cluster 2, H4b	*CBR1, GSN, CFL1, EEF1G, RPL27*	16.1	1.50E-03
DEAD (Asp-Glu-Ala-Asp) box polypeptide 5	*CBR1, GSN, CFL1, EEF1G, RPL27*	16.1	1.50E-03
ribosomal protein S13 pseudogene 8; ribosomal protein S13; ribosomal protein S13 pseudogene 2	*CBR1, GSN, CFL1, EEF1G, RPL27*	16.1	1.60E-03
ribosomal protein L30	*CBR1, GSN, CFL1, EEF1G, RPL27*	16.1	1.60E-03
epidermal growth factor receptor (erythroblastic leukemia viral (v-erb-b) oncogene homolog, avian)	*CBR1, GSN, CFL1, EEF1G, RPL27*	16.1	1.80E-03
growth factor receptor-bound protein 2	*CBR1, GSN, CFL1, EEF1G, RPL27*	16.1	2.20E-03
eukaryotic translation elongation factor 2	*CBR1, GSN, CFL1, EEF1G, RPL27*	16.1	2.20E-03
capping protein (actin filament) muscle Z-line, beta	*CBR1, GSN, CFL1, EEF1G, RPL27*	16.1	2.20E-03
actin, gamma 2, smooth muscle, enteric	*CBR1, GSN, CFL1, EEF1G, RPL27*	16.1	2.30E-03
heterogeneous nuclear ribonucleoprotein A1-like 3; similar to heterogeneous nuclear ribonucleoprotein A1; heterogeneous nuclear ribonucleoprotein A1 pseudogene 2; heterogeneous nuclear ribonucleoprotein A1; heterogeneous nuclear ribonucleoprotein A1 pseudogene	*CBR1, GSN, CFL1, EEF1G, RPL27*	16.1	2.50E-03
interleukin enhancer binding factor 3, 90kDa	*CBR1, GSN, CFL1, EEF1G, RPL27*	16.1	2.60E-03
retinoblastoma binding protein 7	*CBR1, GSN, CFL1, EEF1G, RPL27*	16.1	3.70E-03

Protein interactions	Genes	% fold change	P-value
lamin A/C	*CBR1, GSN, CFL1, EEF1G, RPL27*	16.1	5.30E-03
heat shock 60kDa protein 1 (chaperonin) pseudogene 5; heat shock 60kDa protein 1 (chaperonin) pseudogene 6; heat shock 60kDa protein 1 (chaperonin) pseudogene 1; heat shock 60kDa protein 1 (chaperonin) pseudogene 4; heat shock 60kDa protein 1 (chaperonin)	*CBR1, GSN, CFL1, EEF1G, RPL27*	16.1	5.80E-03
polypyrimidine tract binding protein 1	*CBR1, GSN, CFL1, EEF1G, RPL27*	16.1	6.30E-03
similar to eukaryotic translation initiation factor 4A; small nucleolar RNA, H/ACA box 67; eukaryotic translation initiation factor 4A, isoform 1	*CBR1, GSN, CFL1, EEF1G, RPL27*	16.1	6.40E-03
RuvB-like 2 (E. coli)	*CBR1, GSN, CFL1, EEF1G, RPL27*	16.1	6.50E-03
HLA-B associated transcript 1	*CBR1, GSN, CFL1, EEF1G, RPL27*	16.1	6.60E-03
nucleophosmin 1 (nucleolar phosphoprotein B23, numatrin) pseudogene 21; hypothetical LOC100131044; similar to nucleophosmin 1; nucleophosmin (nucleolar phosphoprotein B23, numatrin)	*CBR1, GSN, CFL1, EEF1G, RPL27*	16.1	9.80E-03
eukaryotic translation elongation factor 1 alpha-like 7; eukaryotic translation elongation factor 1 alpha-like 3; similar to eukaryotic translation elongation factor 1 alpha 1; eukaryotic translation elongation factor 1 alpha 1	*CBR1, GSN, CFL1, EEF1G, RPL27*	16.1	1.00E-02
heterogeneous nuclear ribonucleoprotein M	*CBR1, GSN, CFL1, EEF1G, RPL27*	16.1	1.10E-02
carbonyl reductase 1	*GSN, CFL1, EEF1G, RPL27*	12.9	1.20E-02
cofilin 1 (non-muscle)	*CBR1, GSN,EEF1G, RPL27*	12.9	1.20E-02
ribosomal protein L27	*CBR1, GSN, CFL1, EEF1G,*	12.9	1.20E-02
eukaryotic translation elongation factor 1 gamma	*CBR1, GSN, CFL1,RPL27*	12.9	1.20E-02
gelsolin (amyloidosis, Finnish type)	*CBR1,CFL1, EEF1G, RPL27*	12.9	1.20E-02
MINT			
proteasome (prosome, macropain) subunit, beta type, 4	*PSMB5, PSMA7*	6.5	2.30E-02
tyrosine 3-monooxygenase/tryptophan 5-monooxygenase activation protein, zeta polypeptide	*CCT7, TPI1, CFL1, DYNC1H1, GAPDH*	16.1	2.40E-02
proteasome (prosome, macropain) subunit, beta type, 3	*PSMB5, PSMA7*	6.5	2.70E-02

Protein interactions	Genes	% fold change	P-value
proteasome (prosome, macropain) subunit, beta type, 7	*PSMB5, PSMA7*	6.5	3.40E-02
proteasome maturation protein	*PSMB5, PSMA7*	6.5	4.90E-02
proteasome (prosome, macropain) subunit, alpha type, 6	*PSMB5, PSMA7*	6.5	6.7E-02
nuclear factor of kappa light polypeptide gene enhancer in B-cells 2 (p49/p100)	*PSMB5, DYNC1H1, CKB*	9.7	9.8E-02

NOTES